PhD Dissertation

Development of brain electrophysiological activity in relation to the emergence of executive attention from infancy to early childhood

Josué Rico Picó

DOCTORAL DISSERTATION

Development of brain electrophysiological activity in relation to the emergence of executive attention from infancy to early childhood: A longitudinal study

PhD CANDIDATE

Josué Rico Picó

SUPERVISOR

Dra. M.ª Rosario Rueda Cuerva

Developmental Cognitive Neuroscience Lab

Department of Experimental Psychology

Mind, Brain and Behavior Research Center (CIMCYC)

Doctoral Program in Psychology

International Doctorate

January 2024

UNIVERSIDAD
DE GRANADA

Editor: Universidad de Granada. Tesis Doctorales
Autor: Josué Rico Picó
ISBN: 978-84-1195-256-9
URI: https://hdl.handle.net/10481/90835

The studies conducted in the current doctoral dissertation were funded by the Spanish State Agency grants (Ref. PSI2017–82670-P & Ref: PID2020–113996GB-100) awarded to M. Rosario Rueda, and a predoctoral fellowship in Neuroscience (2019) awarded to Josué Rico Picó.

Front and back cover images, and those of the cover of each chapter, were generated using AI (Midjourney).

Living here day by day, you think it's the center of the world. You believe nothing will ever change. Then you leave: a year, two years. When you come back, everything's changed. The thread's broken. What you came to find isn't there. What was yours is gone. You have to go away for a long time... many years... before you can come back and find your people. The land where you were born.

Cinema Paradiso

Al iaio y la iaia

AGRADEMIENTOS / ACKNOWLEDGEMENTS

TABLE OF CONTENTS

Chapter 1: Introduction **27**

1.1. The Human Attentional System *30*

1.1.1. Alerting *30*

1.1.2. Orienting *30*

1.1.3. Executive *32*

1.2. Early Development of Attention Networks *33*

1.2.1. Alertness development *34*

1.2.2. Orienting development *34*

1.3. Brain Development from Infancy to Early Childhood and its Correlates with Cognition *43*

1.3.1. Structural brain development *43*

Chapter 2: Aims and General Method **61**

2.1. Aims *63*

2.1.1. Brain function development *63*

2.1.2. Flexibility and inhibitory control development *65*

2.1.3. Bain function correlates of cognitive development *65*

2.2. The BEXAT and EDEXAT Projects *65*

2.3. Demographical Information *66*

2.2. Apparatus, Questionnaires and Experimental Task *67*

2.2.1. General structure of the sessions *67*

2.3. Electroencephalography *73*

2.3.1. EEG recording *73*

2.3.2. EEG preprocessing *74*

2.3.3. Power variables: aperiodic and oscillatory/relative power *76*

2.3.4. Network construction and graph variables *78*

2.4. Analysis Plan *81*

2.4.1. Longitudinal development of brain function and behavior *81*

2.4.2. Stability analysis *82*

2.4.3. Relationship Analysis *82*

Chapter 3A: Early Development of the EEG power: Oscillatory and Aperiodic Contributions **85**

3A.2. Results *90*

3A.2.1. Early development of rs-EEG power *90*
3A.2.2. Spatial and within-participant stability *100*
3A.2.3. Aperiodic and oscillatory contributions to the relative power *103*
3A.3. Discussion *105*
3A.3.1. EEG power development *105*
3A.3.2. EEG power stability *107*
3A.3.3. Contributions of aperiodic and oscillatory activity to relative power *108*
3A.3.4. Limitations *108*
3A.4. Conclusion *109*

Chapter 3B: Development of the EEG connectome 111
3B.2. Results *115*
3B.2.1. Development of electrophysiological brain network: a multiverse approach *118*
3B.2.2. Network efficiency, centrality, and small-world topology development *118*
3B.2.3. Modularity development *125*
3B.2.4. Brain Networks Topologic Stability *129*
3B.3. Discussion *131*
3B.3.1. Multiverse Analysis *131*
3B.3.2. Brain Network Development *132*
3B.3.3. Limitations and future directions *134*

Chapter 4: Executive Attention Development and Stability from Infancy to Early Childhood 137
4.2. Results *142*
4.2.1. Longitudinal development of inhibitory control and stability in the ECITT task *142*
4.2.2. Bee attentive task: behavioral results *144*
4.2.3. Relationship between the Bee-Attentive and ECITT tasks *147*
4.3. Discussion *149*
4.3.1. Bee-Attentive Performance *150*
4.3.3. Executive attention stability *152*
4.3.4. Limitations and future studies *153*
4.4. Conclusion *154*

Chapter 5A: Oscillatory and Aperiodic contribution to Executive Attention Development 157

5A.2. Results 161

5A.2.1. Aperiodic and oscillatory power correlates of the ECITT task 162

5A.2.2. Aperiodic and oscillatory power correlates of the Bee-Attentive task 166

..... 168

5A.3. Discussion 169

5A.3.1. Alpha and theta oscillatory activity 169

5A.3.2. Aperiodic activity 171

5A.3.3. Different associations between ECITT and Bee-Attentive .. 172

5A.3.3. Limitations and Future Directions 172

5A.4. Conclusion 173

Chapter 5B: Functional Connectome and Executive Attention 175

5B.2. Results 179

5B.2.1. Functional network topology and ECITT performance 181

5B.2.2. Functional network topology and Bee-Attentive performance 185

5B.3 Discussion 186

5B.3.1. Functional connectivity and cognitive capacity 186

5.3.2. Alpha and theta bands connectivity and cognition 188

5B.3.4 Limitations and future directions 190

5B.4. Conclusion 191

Chapter 6: General Discussion 193

6.1. Brain Maturation Comes with Oscillatory, Aperiodic, and Communication Changes 195

6.2. Age-related Gains in EA 201

6.3. Developing Oscillations for a Rhythmically Sampled World 204

6.4. Developmental In(stability): Key Factors in Open Systems 209

6.5. Conclusion 213

General Summary 215

English 217

Español 225

References 235

Appendix **293**
Appendix of Chapter 2 ..... *295*
A2.1. Time Spent with the Children *295*
A2.2. Socioeconomic indicators *296*
A2.2. Early Childhood Schooling *297*
A2.2. Maternal Mental Health *298*
Appendix of Chapter 3A *301*
A3A. Burst and Rhythms Development *307*
Appendix of Chapter 3B *322*
Appendix of Chapter 4 ..... *329*
A4.1. ECITT original indices *334*
Appendix of Chapter 5A *337*
Appendix of Chapter 5B *341*

INDEX OF FIGURES

Fig. 1.1. Graphical representation of the main brain nodes of the activation, orientation, and executive attention networks. 31
Fig. 1.2. Periodic and aperiodic power spectrum components. 46
Fig. 1.3. Network topology measures. 54
Fig. 1.4. Topological network development in infancy and early childhood 55
Fig. 2.1. Schematic summary of the BEXAT and EDEXAT projects. 66
Fig. 2.3. Bee-Attentive task protocol. 73
Fig. 2.4. Geodesic EGI layout employed in the EEG recordings. 75
Fig. 2.5. Pipeline of the network constructions steps. 79
Fig. 3A.1. Slope and offset aperiodic component development. 92
Fig. 3A.2. Topological development of the slope and offset aperiodic components. 93
Fig. 3A.3. Peak frequency and oscillatory power development. 95
Fig. 3A.4. Oscillatory power development per frequency band. 97
Fig. 3A.5. Topological development of oscillatory power. 96
Fig. 3A.6. Relative power development per frequency band. 98
Fig. 3A.7. Topological development of relative power. 98
Fig. 3B.1. Multiverse analysis of network development. 117
Fig. 3B.2. Network topology development. 119
Fig. 3B.3. Node degree and betweenness centrality. 119
Fig. 3B.4. Network global and local efficiency development. 121
Fig. 3B.5. Development of network efficiency topology. 122
Fig. 3B.6. Small-world topology and centrality development. 124
Fig. 3B.7. Development of betweenness centrality topology. 124
Fig. 3B.8. Node roles per session and frequency band. 126
Fig. 3B.9. Topological development of participation coefficient. 128
Fig. 3B.10. Network modularity and participation segregation coefficient development. 128
Fig. 4.1. ECITT performance development. 144
Fig. 4.2. Bee-Attentive task performance. 145
Fig. 4.3. Performance after committing an error in the Bee-Attentive task. 147
Fig. 4.4. Performance per block in the Bee-Attentive task. 147
Fig. 5A.1. EEG layout and power decomposition. 162
Fig. 5A.2. Regression plots of significant EEG power variables related to ECITT performance. 166

Fig. 5B.1. Schematic diagram of direct and indirect paths in the PLS analysis. 180
Fig. 5B.2. PLS analysis for predicting PS/PNS performance based on functional network properties 183
Fig. 5B.3. PLS analysis for predicting IS performance based on functional network properties 184

INDEX OF TABLES

Table 3A.1. Demographic information of the children included in the EEG power longitudinal analysis. 91
Table 3A.2. Descriptive statistics of the aperiodic parameters. 92
Table 3A.3. Descriptive statistics of the power peaks per age 94
Table 3A.4. Descriptive statistics of oscillatory power per session and band**. 99**
Table 3A.1. Demographic information of the children included in the EEG power longitudinal analysis. 99
Table 3A.5. Descriptive statistics of the participants included in the stability analysis 101
Table 3A.6. Spatial stability in the relative and oscillatory power 102
Table 3A.7. Spatial stability of the aperiodic components 102
Table 3A.8. Within-participant stability in relative and oscillatory power. 104
Table 3A.9. Within-participant stability in aperiodic components. 104
Table 3B.1. Demographic information of the sample included in the analysis of the development of functional network 116
Table 3B.2. Demographic information of the sample included in the stability analysis 129
Table 3B.3. Spatial stability of functional network properties. 130
Table 4.2. Demographic information of the sample included in the longitudinal analysis of the ECITT task. 142
Table 4.2. Mean (standard deviation) performance in the ECITT task at 9 and 16 months of age. 143
Table 4.3. Linear regression models predicting the ECITT performance at 16mo based on 9mo results. 144
Table 4.4. Demographic information of the sample included in the Bee-Attentive task analysis 145
Table 4.5. Descriptive statistics of performance in the Bee-Attentive task 146
Table 4.6. Demographic descriptives of the participants behavioral stability analysis between the ECITT and Bee-Attentive tasks. 148
Table 4.7. Spearman's Rank Correlation between the ECITT performance at 16 mo. and the Bee-Attentive at 36 mo. 148
Table 5A.1, Demographic information of the participants included the regression models between rs-EEG power and behavioral performance in the ECITT task. 163

Table 5A.2, Linear regression models predicting concurrent performance in the ECITT task and aperiodic and oscillatory power. 165
Table 5A.3, Demographic information of the participants included in the regression models between rs-EEG power and Bee-Attentive performance.. 167
Table 5A.4. Linear regression models predicting concurrent performance of the Bee Attentive task at 36-mo. session..... 168
Table 5B.1 Demographic information of the sample included in the relationship analysis between ECITT and functional network properties. 181
Table 5B.2 Mean number of trials (SD) in each session of the EEG and ECITT at 16-mo..... 181
Table 5B.3 Mean number of trials (SD) in each session of the EEG and Bee-Attentive at 36 months..... 185
Table 5B.4 Demographic information of the sample included in the relationship analysis between Bee-Attentive and functional network properties 185

INDEX OF APPENDIX FIGURES

Fig. A2.1. Time spent with the children divided by the caregiver. 296
Fig. A2.2. Socioeconomic indicators of the families included in the study. 298
Fig. A2.3. Maternal depression scores by session 299
Fig. A2.4. Pipeline of the EEG preprocessing 300
Fig. A3A.1. Within-participant spatial stability 304
Fig. A3A.2. Within-participant spatial stability in the relative and oscillatory power. 306
Fig. RA3A.1. Lagged coherence values at 6-mo 310
Fig. RA3A.2 Burst properties in the theta and alpha at 6-mo. 311
Fig. RA3A.3. Lagged coherence in the alpha band at 6-mo. 311
Fig. RA3A.4. Spatial correlation between oscillatory power and burst and rhythmic properties at 6-mo 314
Fig. RA3A.5. Burst property development in theta band 315
Fig. RA3A.6. Lagged coherence development 316
Fig. RA3A.8. Burst amplitude development in the beta band. 319
Fig. A3B.1. Diagram of participants included in the longitudinal analysis exploring network development. 322
Fig. A3B.2. Descriptive representation of multiverse network trajectories. 323
Fig. A3B.3. Distribution of Spearman's rho values in within-participant spatial stability for each variable, band, and pair of sessions. 326
Fig. A4.1. Development of switching and inhibition cost indices in the ECITT. 329
Fig. RA4.1. Development of ECITT performance based on the original indices. 335
Fig. RA4.2. Inhibitory cost development according to the original index. 336
Fig. A5A.1. Topographical representation of the goodness of fit in the participants included in the analysis relating EEG and Bee-Attentive task. 338
Fig. A5A.2. Descriptive figure of oscillatory and aperiodic parameters included in the regression analysis predicting ECITT performance. 339
Fig. A5A.3. Descriptive figure of the peak frequency of alpha and theta bands included in the regression analysis predicting ECITT performance. 339

Fig. A5A.4. Topographical representation of the goodness of fit in the participants included in the analysis related to EEG and Bee-Attentive tasks. 340
Fig. A5B.1. PLS analysis predicting Go Accuracy performance from functional network properties. 343
Fig. A5B.2. PLS analysis predicting NoGo Accuracy performance from functional network properties. 343
Fig. A5B.3. PLS analysis predicting median RT performance from functional network properties. 343
Fig. A5B.4. PLS analysis predicting RT SD performance from functional network properties. 343
Fig. A5B.5. PLS analysis predicting RT cost from functional network properties. 343

INDEX OF APPENDIX TABLES

Table A3A.1. Goodness of fit of the power specparam toolbox divided by cluster and session age. 301
Table A3A.2. Oscillatory power per cluster, band, and session age. 302
Table A3A.3. Relative power per cluster, band, and session age. 303
Table A3A.4. Within-participant spatial stability of the aperiodic components 304
Table A3A.5. Within participant spatial stability in the relative and oscillatory power 305
Table RA3A.1. Descriptive statistics of burst and lagged coherence properties in electrodes with and without an oscillatory peak at 6-mo. 312
Table RA3A.2. Spearman's rho correlation between oscillatory power and lagged coherence and burst properties 314
Table RA3A.3. Alpha lagged coherence development 317
Table RA3A.4. Descriptive statistics of burst properties in each session and frequency band 319
Table 3B.1. Socio-economic information of the sample included in development of functional networks analysis. 322
Table 3B.3. Descriptive statistics of the iCoh weighted (density: .25) network for each session, band, and sex. It displays the mean (SD) for Newman's Q modularity (Q) and the participation coefficient (P) 324
Table 3B.2. Descriptive statistics of the iCoh weighted (density: .25) network for each session, band, and sex. It displays the mean (SD) for global efficiency (Geff), local efficiency (Leff), and betweenness centrality (Bet.) and small-world propensity score (SWP) 324
Table 3B.4. Within-participant spatial stability in the functional networks properties. 325
Table 3B.5. Within-participants stability in the functional networks properties. 327
Table A4.1. Multiple linear regression models predicting Inhibitory Switch at 16-mo based on performance at 9-mo. 329
Table A4.2 Spearman rho correlations between session age (in days) and performance on the ECITT task. 330
Table A4.3 Descriptive statistics of the Bee-Attentive Task after the commission of an error or a hit. 331
Table A4.4. Descriptive statistics of the accuracy in the Bee-Attentive Task per block and trial type 332

Table A4.5. Descriptive statistics of the RT in the Bee-Attentive Task per block and trial type. 332
Table A4.6. Descriptive statistics of ECITT and Bee Attentive tasks included in the correlation analysis..... 333
Table RA4.1. Mean (standard deviation) performance on the ECITT task at 9 and 16 months of age using the original indices..... 335
Table RA4.2 Linear regression models predicting the ECITT performance at 16-mo based on 9-mo results employing the original indices..... 336
Table A5A.1. Descriptive statistics of the goodness of fit (R2) and percentage of electrodes were included in the analysis..... 337
Table A5A.2. Descriptives of the oscillatory and aperiodic EEG parameters of the participants included in the regression models predicting ECITT performance. 337
Table A5A.3. Descriptives of the ECITT performance of the participants included in the regression models between the EEG and ECITT..... 338
Table A5A.4. Descriptives of the oscillatory and aperiodic EEG parameters of the participants included in the regression models predicting Bee-Attentive performance at 36-mo..... 340
Table A5B.1. Descriptives of the ECITT performance at 16-mo. of the participants included in the PLS analysis..... 341
Table A5B.2. Descriptives of the network parameters divided by cluster and frequency band of the participants included in the PLS predicting ECITT performance..... 341
Table A5B.3. Descriptives of the Bee-Attentive performance at 36-mo. in the participants included in the PLS analysis. 342
Table A5B.4. Descriptives of networks parameters divided by cluster and frequency band of the participants included in the PLS analysis predicting Bee-Attentive performance. 342

Chapter 1: Introduction

Chapter 1: Introduction

Humans are in constant interaction with their surrounding environment that is filled with stimulation. Every moment we are immersed in an immeasurable amount of information from our surroundings. Our eye receptors receive the light contrast of a vast landscape, our ears are filled with sounds, and our skin detects temperature and pressure. If we were to focus on every piece, we would be overwhelmed. A clear illustration of this is that the nice music you were listening to only a few moments ago becomes disturbing when confronted with a difficult task, such as parking in a very narrow spot. You might also find it difficult to read while other people are chitchatting nearby, or even a laundry machine can interfere with your thoughts if you are attempting a challenging test.

Given the limitations of human cognitive system, we must select and retain the key aspects of the environment, which also contains irrelevant details. This requests an optimal level of activation, filtering the crucial elements, and guiding and adapting our behavior. It would be impossible to achieve our goals if we were in a drowsy state, as this impedes us from detecting the important stimuli of our surroundings, and our behavior would not be well planned if our arousal level is too high. When we have an optimal level of activation, not too low or too high, we can optimize the processing of surrounding information. However, we do not need to pay attention to every tree branch while walking, but we need to be able to detect the moving cars crossing the street. Therefore, we must select relevant elements throughout a constant interplay between what is useful and salient. Then, we will be ready to respond appropriately in a particular context according to our goals. Importantly, our behaviors must be changed when they are ineffective. For instance, if we have missed the train three times in a row, it may be time to change the alarm, or if we have pushed the same button more than those in a vending machine without the results, we should look for what is going on. Accordingly, acting in a self-regulated volitional manner requires several orchestrated processes, among which attentional processes play a crucial role (Rueda et al., 2021).

The three functions we referred to, namely alerting, selection, and control, are supported by different structural and functional brain networks

in constant interaction according to Posner's model of attention (1990; Petersen & Posner, 2012), and are immature at birth. The maturation of the volitional control of attention has its roots in the first years of life, underpinned by the development of functional brain activity. For this reason, age-related changes in attention and its relationship with brain function development will be the goal of this thesis. We aimed to further delineate electrophysiological activity changes and the maturation of executive attention (EA) in the first three years of life. To that end, in this introductory chapter, we will describe in further detail the attentional model of Posner and colleagues to then introduce the emergence of attentional capabilities from infancy to early childhood. Finally, we discuss the progress that brain function has in the same period, linking it to the emergence of attention.

1.1. The Human Attentional System

According to Petersen and Posner's (2012) model, five different networks are the biological substrates of alerting, orientation, and executive processes. Each has its own role but works interconnectedly to achieve our objectives (Fig. 1.1.).

1.1.1. Alerting

The alerting network involves brainstem areas that modulate arousal levels via noradrenergic neurotransmitter activity (Aston-Jones et al., 1994; Coull et al., 2001; Usher et al., 1999). It controls our alerting level in both phasic (elicited by a stimulus) and tonic (sustained activation) manners. Its activity is modulated by high-order control networks to adjust the alertness level to the task demands.

1.1.2. Orienting

Neuroimaging research has shown that attentional orientation involves two functional networks (Corbetta & Shulman, 2002; Fox et al., 2006). The dorsal attention network (DAN) has a general role in the control of attention, being related to voluntary orientation towards a stimulus, either endogenous or exogenous, and comprises bilateral regions of the superior parietal lobule (SLP), frontal eye field (FEF), and intraparietal sulcus (IPS). In

contrast, the ventral attention network (VAN) is involved in bottom-up or stimulus-driven attention. The VAN is deactivated during prolonged attention periods but is transiently triggered along with the DAN when the attentional focus is reoriented, especially when the target is salient (Corbetta et al., 2008; Spadone et al., 2015; Tosoni et al., 2023). It involves the ventral frontal cortex (VFC) and temporoparietal junction (TPJ).

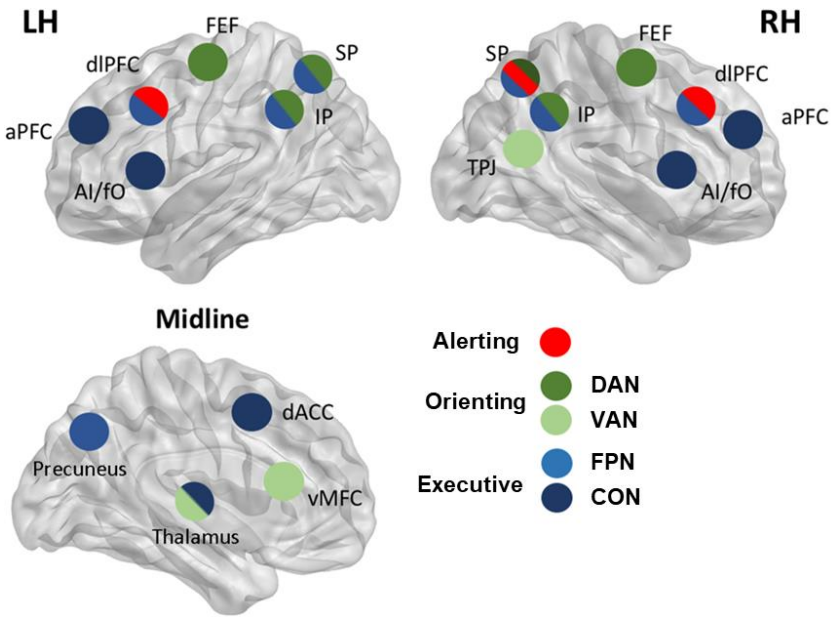

Fig. 1.1. Graphical representation of the main brain nodes of the activation, orientation, and executive attention networks. DAN = Dorsal Attention Network, VAN = Ventral Attention Network, FPN = Frontoparietal Netwok, CON = Cingulo-opercular Network. aPFC = anterior Prefrontal Cortex, dlPFC = dorsolateral Prefrontal Cortex, FEF = Frontal Eye Field, aI/fO = anterior insula/ frontal operculum, SP = Superior Parietal lobe, IP = Intraparietal Sulcus, dACC = dorsal Anterior Cingulate Cortex, vMFC = ventromedial Frontal Cortex, TPJ = Temporoparietal Junction. Adapted with the permission of Rueda et al. (2021).

DAN has a crucial role moving the attentional "spotlight", and its activation can be both tonic and sustained (Tosoni et al., 2023). VAN presents a dynamic pattern, being triggered when a relevant stimulus is detected, especially if it is unexpected, but being desynchronized when we voluntarily

shift our attentional focus (Shulman et al., 2003; Stevens et al., 2005). VAN is sensitive to relevant and/or salient features of the environment (Fockert et al., 2004) and it shows low spatial selectivity and slow triggering (Corbetta et al., 2008). Therefore, the interplay between DAN and VAN provides a flexible toolkit to efficiently select relevant information, sustain attentional focus, and adjust it according to endogenous goals or intentions.

1.1.3. Executive

Controlling our behavior requires several intertwined processes. We must create a mental set with our objectives and the necessary information to guide our behavior. Within this context, we need to detect whether our actions have brought us closer to our goal and adjust our plain if it fails or the environment changes. Consequently, controlling our behavior requires selecting the most appropriate answer, implementing it, and evaluating whether our current situation is incongruent with our goals to flexibly change subsequent responses. Therefore, it involves, at least, three core mechanisms: 1) context monitoring, 2) cognitive flexibility (CF), 3) inhibitory control (IC).

There is evidence showing that these processes involved in goal-driven behavior are supported by two distinct brain networks: the cinguloopercular (CON) and frontoparietal (FPN) (Dosenbach et al., 2008). CON is involved in maintaining a stable mental representation within a task, whereas short-term adjustment relies on FPN activation. According to Posner's model, the dorsal anterior cingulate cortex (dACC) is the main core of the CON network because of its relevance in conflict monitoring (Botvinick et al., 2001) in connection with the anterior Prefrontal Cortex (aPFC), the anterior Insula (aI) and frontal operculum (fO). On the other hand, the dorsolateral Prefrontal Cortex (dlPFC), which is involved in inhibition, updating, and task-set reconfiguration (Badre & Nee, 2018; Marek & Dosenbach, 2018), is considered the main node of the FPN, and is connected to the precuneus, superior parietal lobe (SP) and intraparietal sulcus (IP).

Both CON and FPN contribute to volitional behavior by supervising and adapting the activities of other attentional systems (Rueda et al., 2015).

When our goals are pursued, the CON and FPN will procure an optimal level of alertness and monitor the orientation process. Notice that the control of our behavior may also rely on automatic processes when they have been largely practiced or are implicit (D'Angelo et al., 2013). This is beneficial when the context is stable because it has a lower demand for adjustment processes as it triggers to lesser extend the executive networks. However, it results in a more rigid umbrella of actions as they are mostly driven by the environment. In these cases, executive networks will monitor the results and change to conscious control when an error occurs.

The concept of EA (Engle & Kane, 2003; Petersen & Posner, 2012) is very similar to that of executive functions (Diamond, 2013; Friedman & Miyake, 2017; Miyake & Friedman, 2012). The different names are mostly due to them being originated in different research backgrounds. While both EA and executive control involve mechanisms of conflict monitoring, error detection, and cognitive control, executive functions definition add working memory (WM). However, the principal components of flexible adaptation to the situation (CF) and inhibiting responses (IC) are common processes of executive control. In this thesis, which is mostly focused on cognitive flexibility (CF) and inhibitory control (IC), we use the definition proposed by Diamond (2013). She refers to CF as the capacity to flexibly switch between answers/task sets and defines IC as the ability to withhold a prepotent answer.

1.2. Early Development of Attention Networks

At birth, attentional processes are immature. Infants spend most of their time sleeping, do not maintain their attentional focus, and are unable to self-regulate their behavior. Consequently, most of their actions are driven by external stimulation or automatic drives. However, these processes mature rapidly in the first years of life. From a developmental perspective, the maturation of attention is protracted when compared to other processes. Additionally, it is thought that the maturation of attentional processes occurs in two axes: within and between processes (Hendry et al., 2016, 2019; Posner et al., 2014). Every process will quantitatively augment its capacity with age; however, given the slower maturation of executive systems, their functions

seem to be undertaken by the other attentional systems that mature earlier (Posner et al., 2014). As a result, attentional control transitions from bottom-up to top-down from early infancy to childhood, and both sustained attention (alerting) and endogenous selection (orienting) have been proposed as the founding blocks of EA (Conejero & Rueda, 2017; Hendry et al., 2016; Posner et al., 2014).

1.2.1. Alertness development

The time a newborn spends in an alert state is very restricted. At birth, infants spend approximately 25% of their time awake (Colombo & Degen Horowitz, 1987). However, by the twelfth week of life, infants display regular cycles of alertness and sleep, and reduce the time sleeping until the second year of life (Dias & Figueiredo, 2020; Figueiredo et al., 2016; Paavonen et al., 2020). In addition, alerting is primarily caused by external stimulation in the first months, but with age they ability to sustain the attentional focus improves steadily (Colombo, 2001; Lawson & Ruff, 2004; Richards, 1985; Ruff & Lawson, 1990). This improvement in the ability to regulate arousal allows increasing the time babies interact with their environment, which is crucial for exploring and learning about the world.

1.2.2. Orienting development

Similar to the arousal level, selecting the relevant elements and orienting the attentional focus rely on external stimulation at birth. The first few months of life are characterized by infants' inability to endogenously shift their attentional focus when something has attracted it (a phenomenon named *sticky fixation*). Therefore, babies remain fixated in the object or event up until something captures their attention again (Stechler & Latz, 1966). Starting at about the third month of life, infants start to move their gaze voluntarily, as shown in their newly acquired capacity to disengage and anticipate (Hendry et al., 2019; Johnson et al., 1991).

Regarding the ability to disengage attention from an object or event, most studies have employed gap overlap and fixation shift protocols to study its development. Both tasks present a central stimulus and, when the infants

are looking at it, a peripheral stimulus is displayed. In these tasks, disengaging capacity is measured by considering the number of times that infants can move their gaze to look at the peripheral stimulus, as well as the latency of that movement. For instance, the gap overlap task consists of two conditions: gap (the central stimulus disappears when the peripheral one is presented) and overlap (the central stimulus remains when the peripheral one is presented). The gap condition is easier because it does not require inhibition of the foveated stimulus to move the gaze, and even the disappearance of the central stimulus may serve as an alerting cue (Csibra et al., 2001; Ellis et al., 2021).

Before the third month of life, infants rarely disengage in overlap conditions in the gap overlap task (Atkinson et al., 1992). This rapidly change after that age (Atkinson et al., 1992; Papageorgiou et al., 2014), despite of presenting the general cost of latency in overlap (vs. gap) condition (Holmboe et al., 2018; Johnson et al., 1991; A. Nakagawa & Sukigara, 2019). Beyond the third month, the time needed to foveate the peripheral stimulus in gap trials steadily diminishes (Moyano et al., 2023; Siqueiros Sanchez et al., 2021), but the development of the overlap is less clear, as latency appears not to vary with age or even increase (Moyano et al., 2023; Nakagawa & Sukigara, 2013, 2019). Instead, longer explorations of the central stimulus are shown to be related to self-regulation in toddlerhood (Nakagawa & Sukigara, 2019). In fact, in the case of the gap/overlap task the central stimulus is usually more salient than the one in the periphery (Holmboe et al., 2008; Kwon et al., 2016). This suggests that with age also increases the capacity to inhibit peripheral stimuli when a foveated stimuli causes interest (Holmboe et al., 2018).

The capacity to endogenously orienting is also studied by means of anticipatory and sequence paradigms. For example, the Visual Expectation Paradigm (VExP; Canfield & Haith, 1991), Visual Sequence Learning (VSL; Clohessy et al., 2001), and shifting tasks (Kovacs & Mehler, 2009; Shinya et al., 2022) present sequences of stimuli that follow a spatial pattern combining both simple and complex transitions. In the first, it is not necessary to monitor the context to anticipate as the following stimulus is always certain, but in complex transitions context monitoring is necessary to properly move the attentional focus to upcoming events due to its probabilistic nature. Previous

studies has shown that despite of the ability to detect regularities being present in newborns (Bulf et al., 2011), at this age infants cannot displace their gaze to search for stimuli (Colombo, 2001; Hendry et al., 2019). The capacity to anticipate simple transitions appears from the third month of life but predicting complex sequences does not appear until some months later (Clohessy et al., 2001; Sheese et al., 2008). The percentage of reactive (vs. anticipatory) looks is reduced from infancy to the fourth year of life (Moyano et al., 2022; Rothbart et al., 2003; Sheese et al., 2008), which unveils a more proactive approach with age instead of relying on bottom-up search (Chatham et al., 2009).

1.2.3. Executive attention development

The transition from exogenous- to endogenously driven orienting is not sufficient to self-regulate our behavior. Nonadaptive patterns of behavior must flexibly change when the outcome is not desired. These processes have even more protracted development, but their roots are already present in the second half of the first years of life (Conejero & Rueda, 2017; Hendry et al., 2016) supported by the parallel and rapid development of frontal brain areas and executive networks (Diamond, 2013; Fiske & Holmboe, 2019).

Conflict monitoring appears relatively early. Paradigms exploring this process usually present an object/situation that violates infants' expectative (vs. non-violation). For example, we can resolve incorrectly mathematical equations (e.g., 2 – 1 = 2) and compare it when the equations were correct (e.g., 2 – 1 = 1). Starting at 6 to 9 months of age, infants interact and pay more attention to the situations that violated their expectations and remarkably their behavior is biased by the unexpected event (Berger & Posner, 2023; Stahl & Feigenson, 2015). This has been shown in behavioral and neuroimaging protocols, with different stimulus and error types causes, such as mathematical errors, physical laws, and semantical alterations (Berger et al., 2006; Conejero et al., 2016; Köster et al., 2019, 2021; Stahl & Feigenson, 2015). The appearance of this mechanism in the first years of life supposes that, even if it is still immature (Davies et al., 2004; Segalowitz & Davies, 2004), infants are ready to detect the incongruences found in the environment to then adapt their behavior.

Behavioral development of IC and CF has been studied mostly using the A-not-B task in the first months of life (Piaget, 1954). In this task, a researcher presents a toy to infants and hides it in one of two locations (A). Then, the infant is encouraged to retrieve the object after a short delay. This procedure is repeated a fixed number of times or until looking/reaching the object at location A becomes prepotent. Subsequently, the object is shown but hiding it the other place (B). Thus, infants must inhibit their previous answer to search for the object in the newest location and the performance is evaluated by the perseverative looks or behaviors conducted in that block. Due to its simplicity, it has been used from the fifth month of life in both behavioral (Clearfield et al., 2006; Diamond, 1985) and looking (Bell & Adams, 1999) versions.

Previous studies employing the A-not-B task in longitudinal studies has found that infants younger than 7 to 8 months of life do not persevere in behavioral protocols. At this age, infants are equally accurate in both A and B trials, probably because the immaturity of both motor and memory systems (Clearfield et al., 2006). After an initial increase in perseverative behaviors, those are steadily reduced and children perform more accurate even when the delay between the hiding and retrieval is increased (Cuevas & Bell, 2010; Diamond, 1985; Diamond & Doar, 1989; Espy et al., 1999; Marcovitch & Zelazo, 1999). For example, the performance increases between 15 and 30 months of age with 5s of delay (Diamond et al., 1995) and so does between 24 and 66 months of age when the delay last for 10s (Espy et al., 1999). This pattern of results also occurs in eye-tracking versions of the A-not-B (Bell & Adams, 1999) although infants perform better than in the reaching one arguably probably because of the gradual development of motor capacity (Cuevas & Bell, 2010; Marcovitch & Zelazo, 1999).

Further studies have provided evidence of a developmental trajectory similar to that of A-not-B using other eye-tracking paradigms that measure perseverative looking, such as the shifting task (Kovacs & Mehler, 2009). This task consists of two blocks of trials. In the first block, a stimulus always appears on the same side of the screen until infants can anticipate where it will appear. In the second block, the location of the stimulus is shifted to the opposite side of the screen. CF is measured by the number of

perseverations in the second block (i.e., times anticipating the location of the first block). By the eighth month, infants gradually stop persevering in the second block (Kovacs & Mehler, 2009) and the number of anticipations increases from 6 to 9 months, and then decreases at 18 months of age (Moyano et al. In prep).

One limitation of the A-not-B and shifting tasks is that they rely on memory processes (Holmboe et al., 2018). Prove of this is the lack of perseveration found in younger infants in the A-not-B task (Clearfield et al., 2006). Additionally, recent research of our laboratory shows an inverted "u" shaped trajectory of the perseverations in the shifting task (Moyano et al. In prep.). It is unlikely that infants' capacity to adjust their behavior/gaze decrease. Therefore, the development of other necessary processes for the task are probably influencing the results (Hendry et al., 2016). In the case of these tasks, both require the maintenance of the location in the memory to build a prepotent tendency. Given the rapid maturation of working memory in this period (Courage & Cowan, 2022), a stronger representation of the pre-switch blocks may account for the initial increase in perseverative behaviors (Clearfield et al., 2006). In fact, the relationship between WM and IC found with this task in 2 to 5 years old children supports this idea (Espy et al., 1999).

To address the limitations of A-not-B and shifting-task, recent authors has developed the freeze-frame and the early childhood inhibitory touchscreen tasks (ECITT; Holmboe et al., 2008, 2021). The freeze-frame task consists of the presentation of a static or dynamic central stimulus and tests infants' capacity to suppress peripheral images. In this task, 6-month-old (-mo.) infants present lower interference when the central stimulus is dynamic (vs. static). Additionally, their capacity to inhibit the peripheral stimuli increases from 6 to 9 months of age, suggesting that the IC capacity matures in this period independently of the memory. This is corroborated in wider age range in the ECITT task. This task consists of displaying two blue rectangles on both sides of the tablet, with one containing a smiley face (target). When infants touch the target, positive feedback appears with sound and animation. The target appears most of the time on one side of the screen (prepotent trials), and less frequently on the opposite side (inhibitory trials). Thus, it creates prepotency based on contingency-learning, without requiring

memorization, and permits the evaluation of IC and CF when the target changes its location. This task is doable in 10 months old infants (Fiske et al., 2022; Hendry et al., 2021). Additionally, both cross-sectional and longitudinal studies have shown the improvement in inhibitory trials. For instance, Holmboe et al. (2021) shown an increase in inhibitory trials accuracy from 18 months onward, while Hendry et al. (2021) found reduced switching cost, but not inhibitory cost, from 10 to 16 months of age. Importantly, both the freeze-frame task and the ECITT were related to the performance in A-not-B (Hendry et al., 2021; Holmboe et al., 2018). For instance, the accuracy of inhibitory trials and switching trials at 16-mo. was negatively correlated with perseverations in the A-not-B, although this relationship was not significant at 10-mo. (Hendry et al., 2021).

From about the second year of life on, children can comprehend more complex instructions, which permits the evaluation of executive processes with paradigms that are more similar to those used with adults. However, longitudinal research during this period is scarce. Most studies have not employed the same task systematically in part because of the rapid maturation of IC and CF. Consequently, several authors have labelled this period as "resolving conflict" maturation (see Hendry et al., 2016) because of the difference in tasks employed with similar rationale.

When it comes to CF, one of the most employed task designs consist of evaluating children's capacity to shift between sets of rules. For example, the dimensional change card sorting (DCCS) test (Zelazo et al., 2003) and the reverse categorization task (Carlson, 2005; Hongwanishkul et al., 2005) follow this logic. In the DCCS, children must sort cards according to an unknown rule, and after several correct trials, the sorting principle changes to other criteria. CF is measured by the number of incorrectly sorted cards used before following the new rule. This task is not suited for children below four years in the standard version (Zelazo et al., 2003); however, it is doable before that age if simplified to reduce conflict (Blakey et al., 2016; Garon et al., 2014). For instance, 36-mo. children can correctly sort the cards according to one rule but fail to sort the cards when the rule is changed (Zelazo, 2003). However, if we remove the conflict elicited by removing the switching between the set tasks 18-mo. toddlers can accurately change their behavior

(Garon et al., 2014). In reverse categorization task children are asked to sort the object following an initial rule, and then the experimenter tell them to classify it in the opposite way. For example, the researcher can instruct the children to introduce small objects into a tiny box and then change the rules and ask them to introduce small objects into a big box. This task is less demanding than the DCCS (Carlson, 2005); however, children are not accurate until the second and a half year approximately (Carlson, 2005; Conejero et al., 2023), although this may be related to the cost of retaining and updating the information in the WM (Carlson, 2005). This aligns with the protracted emergence of conflict in incongruent-like tasks, as toddlers seem to response at random until approximately 30 months of age (Garon et al., 2014; Blackey et al., 2016).

The development of IC between toddlerhood and early childhood has been assessed using different paradigms, including spatial conflict (Gerardi-Caulton, 2000), strop-like modifications (Kochanska et al., 2000), and Go/NoGo (Casey et al., 1997) tasks. These protocols either create an incongruency that must be resolved to produce the appropriate response (e.g., the target appears on the contralateral side with respect to the answering key) or build a tendency that must be withheld.

In the spatial conflict task two houses appear on the screen. Each one of the houses corresponds with a specific animal. To guide the animal to its house, children must press a key that is ipsilateral (congruent) or contralateral (incongruent) with respect to the house. In this task, infants answer above chance approximately at 30 months of age and children become more accurate and faster in incongruent trials between that age and the 48 months of life (Gerardi-Caulton, 2000; Jones et al., 2003; Rothbart et al., 2003). Similarly, in the child-version of the Stroop task the incongruency is elicited either by semantic or size incongruencies. For example, we can ask the children to speak out the small fruits nested in bigger ones, such as a small apple that is contained in a big pineapple (Kochanska et al., 2000). Children's capacity to resolve incongruent trials improves in this task between 2 and 3 years of life, even in different versions of the task (Carlson, 2005).

The Go/NoGo paradigm is suitable for children from about three years of age on (Clark et al., 2023). This task usually presents two stimuli. One of them appear in a larger proportion of trials (Go) and require that children press a key. On a few occasions another stimulus appears (NoGo), and children must withhold their behavior to correctly answer it. In this task, IC is measured by the number of commission errors in NoGo trials. The performance in this task increases with age because of the number of commission errors is reduced between early and middle childhood (Clark et al., 2023; Howard & Melhuish, 2017; Johnstone et al., 2005; Mehnert et al., 2013). In addition, children's incapacity to conduct other protocols that involve larger demands of IC also accounts for its development. For example, in the stoop signal task infants must answer all the time to the target but stop their behavior if a warning sound is presented (Logan & Cowan, 1984). This task will not be doable until the fifth year and present a more protracted development than the Go/NoGo task (Bedard et al., 2002; Carver et al., 2001), signaling the constant maturation of IC.

Finally, other protocols that aim to capture several attentional mechanisms cannot be implemented until three and a half years owing to the complexity of their instructions. For example, the child version of the Attentional network test (ANT; Fan et al., 2002) developed by Rueda et al. (2004) combines a Eriksen's flanker task with alerting and orienting cues. In the Child ANT a row of fishes is displayed on the screen and children are instructed to "feed" the fish in the middle of the row by pressing a key according to the side the fish is pointing to (either left or right key). To "feed" the middle fish properly, they must ignore the peripheral fishes that can either look to the same side (congruent) or the opposite side (incongruent) of the target fish. In their original study, Rueda et al. (2004) found an increase in conflict resolution capacity in the incongruent trials between the fourth and the sixth year of life. Additionally, a recently developed variant of this task, substituting directionality with colors, was developed by Casagrande et al. (2022). This task is doable starting at approximately 40 months of life and previous experiments has shown the improvement of conflict resolution and orienting that takes place between the third and the fourth, fifth, and sixth years of life.

Taken together, previous studies have shown that in the first two years of life attentional processes go through a dramatic maturation. Infants' attention will be exogenously driven by the external stimulation in the first months until they become able to endogenously guide their attentional focus. This first milestone in the development of volitional control emerges at around three months, when infants can disengage and displace their gaze voluntarily to explore and anticipate their surrounding (Johnson et al., 1991). The increase in sustained attention, tonic alertness, and orienting will derive in the exploration of the environment volitionally, increasing its opportunities to interact with their surroundings (Hendry et al., 2020; Posner et al., 2014; Colombo, 2001).

Some months later, around the 6 month of life, infants start to detect the incongruences of the environment (Berger & Posner, 2023; Köster et al., 2021). They behave differently when face with objects that present unexpected outcomes; thus, being able to monitor and adapt their behavior to them (Berger et al., 2006; Stahl & Feigenson, 2015). Also, around 6 to 8 months of life, infants' behavior become more flexible (Hendry et al., 2016; Conejero & Rueda, 2017). At this age, infants are able to modify an action that no longer provides the desired results (e.g., Kovacs et al., 2009). The ability to withhold and modify the previous answer rapidly changes from infancy to toddlerhood, as with age children commit less perseveration when face inhibitory/shift trials (Holmboe et al., 2021; Hendry et al., 2021).

Beyond the second year of life, alertness and sustained attention keeps improving (Paavonen et al., 2020; Ruff & Lawson, 1990) and so does orienting capacity (Hendry et al., 2019; Moyano et al., 2022). In this period, executive attention development has measured based on the feasibility of the tasks and performance indicators of conflict-based tasks. Among the task used, most of them can not be performed below two years and a half because children respond mostly at random (e.g., spatial conflict) or with very poor performance (e.g., DCCS). However, starting at that age, children start to resolve the conflict elicited, improving their performance in the following months. For example, between the third and fourth year of life they will pass the DCCS without adaptation or the accuracy in conflict tasks will increase (Zelazo et al., 2003; Gauron et al., 2000). This development will continue in

the following years which speaks for the protracted development of executive functions.

1.3. Brain Development from Infancy to Early Childhood and its Correlates with Cognition

The brain changes that take place in the first three years of life are the most drastic and rapid of the entire lifespan (Bethlehem et al., 2022). Newborns' brains are relatively large, complex, and metabolically active compared to those of adults (Gilmore et al., 2018). Although some neuronal processes, such as neuronal migration, are completed by birth, the brains of infants continue to be refined both structurally and functionally (Dubois, 2014; Ouyang et al., 2019; Vértes & Bullmore, 2015).

1.3.1. Structural brain development

One of the most marked changes between infancy and early childhood is an increase in brain volume. The newborn's brain has one-third of the volume of an adult, and reaches ~80% of the adult volume on the third birthday (Knickmeyer, 2008). By that time, both gray and white matter had undergone several changes with different maturation rates (Gilmore et al., 2018). The gray matter volume increases on average by 100% in the first year of life and about 15% on average in the second year, whereas the white matter volume increases on average by 15% per year until the second birthday to then slow down the maturation rate (Groeschel et al., 2010). Other parameters, such as the brain surface area and cortical thickness greatly increase from the prenatal period, showing an extraordinary growth during the first years of life (Bethlehem et al., 2022; Vasung et al., 2019).

The development of gray and white matter is not equivalent across all brain regions. The posterior areas mature before the associative and frontotemporal areas (Bethlehem et al., 2022). For example, the peak volume of gray matter is reached at about 5 years of age in the occipital areas, whereas peak volume in most of the prefrontal cortex and the anterior cingulate is not reached until puberty (Bethlehem et al. 2022). This pattern of growth is related to the hierarchy of cognitive control processes in the first years of life (Amso & Scerif, 2015).

A similar developmental pattern is also observed with white matter. Although most of the white matter tracts are present at birth (Qiu et al., 2015), only sensory connections are myelinated (Dubois, 2014). For example, by the fourth month of life, sensory areas are mostly myelinated, while fibers that connect parietal and frontal areas begin their myelination process around the sixth month of life (Dean et al., 2014; Ouyang et al., 2019). This myelination process is the fastest of all lifespan between infancy and early childhood, which suggests that beyond this point, there is a period of reorganization and fine-tuning of the already present brain circuits (Gilmore et al., 2018).

1.3.2. Functional brain development

1.3.2.1. Electrophysiological brain function development

Parallel to structural changes, brain function rapidly evolves in the first three years of life. Given the low tolerance to neuroimaging protocols of awake infants and toddlers, most studies investigating functional brain development have employed electroencephalography (EEG). EEG recordings provide information about the extracellular postsynaptic potentials of large groups of neurons, mostly pyramidal parallel to the cortex, which synchronously fire and create large electric dipoles (Buzsáki et al., 2012). As EEG records electrical activity with sensors located in the surface of the head, it offers functional information with high temporal precision, but low spatial resolution. This permits the exploration brain of brain activity divided by several brain rhythms: (e.g., alpha) each of one linked to different yet complementary cognitive processes in developing samples (Anderson & Perone, 2018; Cuevas & Bell, 2022; Saby & Marshall, 2012).

Both evoked and baseline/resting-state (rs-EEG) protocols have been used in very young participants. In evoked tasks, brain function is related to the appearance of an auditory/visual stimulus, whereas rs-EEG usually involves presenting images and sounds to engage children's attention and help them to remain soothed during the recording period. Although both are applied in young children, rs-EEG has been widely used in infancy and toddlerhood because it does not require to pay attention to the stimuli (Cuevas & Bell, 2022; Saby & Marshall, 2012). In rs-EEG, the gold-standard

measurement is the power of the signal divided into canonical bands, which include theta (3 – 5 Hz), alpha (6 – 9 Hz), and beta (9 – 30 Hz) activity. This power can be considered in its absolute value, or as a relative value when the power of a specific frequency band is divided by the added power of all frequency ranges (e.g., alpha power/theta + alpha + beta power).

The rs-EEG undergoes profound reconfiguration during the first decades of life (Anderson & Perone, 2018). Pioneering studies have demonstrated that the dominant rhythm (alpha) gradually emerges during infancy and moves from lower to higher frequencies (Smith, 1939). An increase in alpha peak frequency has been repetitively reported and is considered a marker of brain function development (Freschl et al., 2022; Miskovic et al., 2015; Stroganova et al., 1999). Similarly, alpha power appears to increase in the first years of life and along childhood (Marshall et al., 2002; Perone et al., 2018). Findings on other frequency bands have yielded mixed results, particularly when considering the absolute (vs. relative) distinction. Some studies have reported an increase in absolute power in all frequency bands followed by a decrease in middle childhood (Dustman et al., 1999; Gasser et al., 1988; Jing et al., 2010; Wilkinson et al., 2023). In contrast, when relative power is considered, the power is redistributed from lower (e.g., theta) to higher (e.g., alpha and beta) frequency bands (Anderson & Perone, 2018; Brandes-Aitken et al., 2023; Clarke et al., 2001; Marshall et al., 2002).

A recent reconceptualization of electrophysiological activity, which considers the power spectrum as a mixture of aperiodic and oscillatory activity, may reconcile the mixed pattern of results (Donoghue, Haller, et al., 2020). That is, previous studies have considered absolute/relative power as oscillatory activity. However, oscillatory activity is narrowband and limited (He, 2014), whereas scale-free or aperiodic activity accounts for most of the power spectrum energy (Voytek & Knight, 2015). This aperiodic activity corresponded to the decaying background curve obtained from the power spectrum (Fig. 1.2A). It follows a power-law distribution (1/*f*-like) with less energy at higher frequencies because of the low-pass filter properties of the neurons and shorter integration time window (Buzsáki et al.,. 2012; Voytek & Knight, 2015). This aperiodic activity is independent of the presence (or absence) of oscillatory activity. In fact, its broadband power (offset of the

background curve) is related to the spiking rate of the neurons (Miller et al., 2009), whereas the decay rate (slope or exponent of the background curve) is determined by the balance between excitatory and inhibitory currents (Gao et al., 2017).

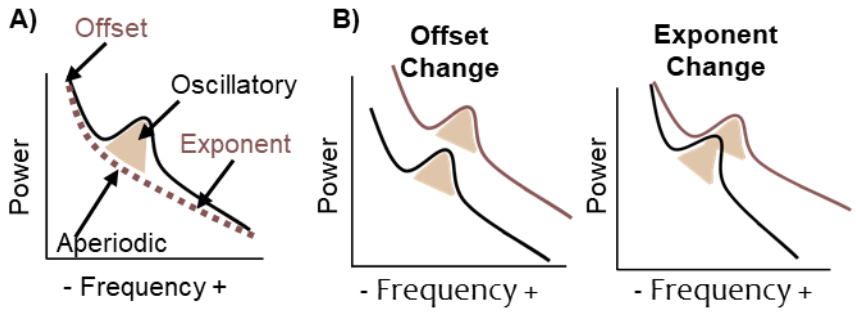

Fig. 1.2. Periodic and aperiodic power spectrum components. (A) Decomposition of power spectra. The aperiodic background curve is defined by the offset (energy at the lowest frequency) and exponent (1/*f* decay rate). (B) Changes in aperiodic components may cause changes in relative and absolute power but not in oscillatory activity. Offset changes affect absolute power, while exponent changes drive a change in both absolute and relative power.

The aperiodic background curve is already present in newborns (Fransson et al., 2013) and flattens in the first two years of life (Brandes-Aitken et al., 2023; Schaworonkow & Voytek, 2021). This reduction also occurs from childhood to adulthood and from adulthood to old age (Tröndle et al., 2022; Voytek et al., 2015). This suggests an increase in the excitatory currents in the excitatory/inhibitory balance throughout life (Perica et al., 2022).

Given the systematic changes in aperiodic activity, previous developmental results of absolute/relative power may have been mislead (Ostlund et al., 2022). Changes in the offset or exponent are sufficient to alter the power ratios between the bands or absolute energy (Donoghue et al., 2020; see Fig. 1.2B). For example, a flatter curve would result in less relative power in the theta band, even when oscillatory activity does not change. Additionally, recent studies have explored the development of alpha and

theta oscillatory activity (Hill et al., 2022; McSweeney et al., 2021; Schaworonkow & Voytek, 2021). These studies have replicated the steady increase in alpha peak frequency, and some have found an increase in alpha presence or energy from birth to the seventh month of life, and from early childhood to adulthood (Donoghue et al., 2020b; Tröndle et al., 2022; Schaworonkow and Voytek, 2021; but see Cellier et al., 2021; Hill et al., 2022), which speaks for the constant changes of alpha band even when the aperiodic component is removed from the signal. Nonetheless, classic power ratios in children are more related to the aperiodic component than to the absolute power, except when alpha band is included (Donoghue et al., 2020).

1.3.2.2. Brain oscillations and cognitive processes in the first years of life

Oscillatory activity has been related to cognition in both evoked and rs-EEG protocols in infancy and childhood, especially over frontal areas (Cuevas & Bell, 2022). To achieve this, three approaches (baseline, evoked, and baseline vs. evoked) have been used to understand how brain function relates to cognition and individual differences of efficacy in particular cognitive processes.

To date, most studies have explored alpha and/or theta bands in developing samples. These bands has shown their sensitivity to context stimuli, differentiating between social and non-social, play vs. static, and room illumination (Anderson et al., 2022; St. John et al., 2016; Stroganova et al., 1999). Both have been also associated with the cognitive processes targeted with evoked paradigms, suggesting similar roles for adult oscillations, albeit at lower frequencies, as described below.

Theta Band

The theta band has been considered an index of cognitive control, resource allocation, memory, and sustained attention across several paradigms (Barwick et al., 2012; Cavanagh & Frank, 2014; Fiebelkorn & Kastner, 2019; Klimesch, 1999; Sauseng et al., 2010). Memory maintenance and item manipulation triggers theta activity (Klimesch, 1999; Klimesch et al., 2007), and the allocation of cognitive resources promotes theta

synchronization (Sauseng, Klimesch, Schabus, et al., 2005; Sauseng, Klimesch, Stadler, et al., 2005). In addition, observing an error or unexpected event increases theta power over the frontal-medial areas (Cohen & Donner, 2013; Fu et al., 2023; Ito et al., 2003). Thus, theta plays a central role in EA processes (Botvinick et al., 2001; Cavanagh & Frank, 2014; Cohen, 2016) as it has been shown to modulate cognitive control tasks (Cooper et al., 2015; Eschmann et al., 2018).

Theta band power has had similar functional roles in early development. In infants, theta power is triggered in anticipatory attention protocols (Orekhova et al., 1999) and while infants present a sustained attention state (Stroganova et al., 1998). In addition, recent studies by Xie et al. (2018) and Brandes-Aitken et al. (2023) provided further evidence of higher theta power in frontal areas during sustained (vs. inattention) periods starting from the third month of age. Similarly, theta power increases when infants watch a dynamic video before 1 year of age (Braithwaite et al., 2020; Jones et al., 2020) suggesting its early involvement in cognitive resource allocation. Theta power also increases when infants and children manipulate objects in either experimental or naturalistic contexts. Remarkably, this is related to the posterior recognition of the objects, suggesting its involvement in memory (Begus et al., 2015; Wass et al., 2018). Finally, protocols that involved error-detection or violation of expectations induce larger theta power (Berger et al., 2006; Conejero & Rueda, 2018; Köster et al., 2021) speaking for its role in early conflict monitoring.

At rest, the theta band has been generally related to individual differences in high-order cognitive processes. However, although a relationship between cognition and performance has been found, to date the results have been mixed. In evoked and modulation protocols, higher theta power appears to be a positive predictor of children's performance in memory, EA processes, and intelligence (Begus et al., 2015; Braithwaite et al., 2020; Jones et al., 2020). On the contrary, studies measuring the absolute and relative powers in rs-EEG protocols have found an association in the opposite direction (Cai et al., 2021; Perone et al., 2018; Tan et al., 2023). For instance, a larger power at rest in early childhood and infancy has been linked to poorer intelligence at age 18 years (Tan et al., 2023), lower EA performance (Cai

et al., 2021; Perone & Gartstein, 2019), and worse WM capacity (Maguire & Schneider, 2019), although this relationship is not always found (Brito et al., 2016; Maguire & Schneider, 2019; Troller-Renfree et al., 2020).

Alpha band

The alpha band is considered multifaceted owing to its several roles, and because it is generated in different brain areas (Clayton et al., 2018; Wang, 2010). Its roles mainly involve processes related to attention and perception (Klimesch, 2012) by inhibiting the non-relevant brain areas while guiding the attentional focus (Klimesch et al., 2007) and communicating between brain areas to modulate the activity of other zones (Palva & Palva, 2011; Sadaghiani & Kleinschmidt, 2016). The modulation of perception and attention via adjusting the activity of other brain areas occur through long-range connections (Sadaghiani & Kleinschmidt, 2016) and is key in filtering and inhibition processes (Jensen & Mazaheri, 2010).

In infancy, the power of alpha band is modulated by the cognitive demands of the paradigm (Bell & Fox, 1997; Cuevas et al., 2012). For instance, alpha power increases over frontal areas when WM and executive control are required to complete a task (Cuevas et al., 2012; Wolfe & Bell, 2004). Additionally, alpha band is desynchronized in sustained (vs. inattentive) states, suggesting an online modulation of alpha functional activity during the task period (Xie et al., 2018). Posterior alpha has similar roles with respect to adult alpha, as its power attenuates when there is illumination in a room (vs. a dark room) (Stroganova et al., 1999), and it is triggered in anticipatory attention paradigms, albeit in the opposite direction with respect to adults (Cuevas & Bell, 2022; Orekhova et al., 2001). These results account for the early involvement of alpha in attentional processes and suggest a similar role than adult alpha.

Several studies have linked baseline and task-evoked alpha to cognitive performance. In general, greater alpha power is a positive predictor of individual differences in EA (Cuevas & Bell, 2022; Hofstee et al., 2022). For example, in her studies Bell (2001, 2002) found larger differences between task-evoked (versus baseline) and better IC performance in infancy. Also, a

larger alpha at baseline is associated with improved performance in large cross-sectional and longitudinal analyses (Cuevas et al., 2012; Marcovitch et al., 2016; Morasch & Bell, 2011; but see Perone & Gartstein, 2019), although this relationship interacts with the type of task and the effect size is greater in older children (Hofstee et al., 2022). Additionally, age-related changes in baseline alpha are positively related to IC in early childhood (Whedon et al. 2020). In fact, given the marked trajectory of the alpha band and its early involvement in high-order cognitive processes some authors claim that alpha band is one of the candidates for measuring brain maturation (Cuevas & Bell, 2022).

Beta and gamma frequency bands

Beta and gamma frequency bands have also been related to high-order cognitive processes, including, but not limited to, WM and EA (e.g., Bastos et al., 2020; Lundqvist et al., 2016). These bands have been less studied in infants because of their sensitivity to motor artifacts. However, previous studies have linked these bands to children's cognitive capacity (Saby & Marshall, 2012). Gamma power over frontal areas seems to be positively associated with EA (Perone et al., 2018; Tarullo et al., 2017) and language acquisition (Benasich et al., 2008; Cantiani et al., 2019) in infancy and childhood. For example, larger gamma power over frontal electrodes (eyes open) appears to be related to the scores of the Minnesota Executive Function Scale in childhood (Perone et al., 2018), and gamma power at birth predicts cognitive outcomes several months later (Brito et al., 2016). Additionally, both gamma and beta (frontal right) seem to predict better orientation obtained via part-reported questionnaires (Perone & Garstein, 2019).

Aperiodic activity

Even though studies incorporating the measurement of aperiodic (vs. oscillatory) activity are still scarce, this activity has been linked to cognitive performance in both offline and online paradigms. For example, aperiodic activity has been associated with executive functions (Donoghue et al., 2020) and processing speed (Pathania et al., 2022). In addition, some studies have suggested the existence of alterations in the aperiodic exponent in attention

deficit and hyperactivity disorder (ADHD; Karalunas et al., 2021; Ostlund et al., 2021). However, the results are somewhat inconsistent when treatment and age is considered. For instance, Robertson et al. (2019) found larger and equal slopes in non-medicated and medicated ADHD children (vs. controls), respectively. On the contrary, other studies has reported reduced slope (Arnett et al., 2021; Ostlund et al., 2021). Additionally, infants at risk of autism spectrum disorder (ASD) at 10-mo. presented flatter background curve in a recent study (Carter Leno et al., 2022). Remarkably, in the same study the symptomatology was mediated through EA capacity. Larger EA scores were a protective factor of ASD behaviors. These results suggest the link between aperiodic activity and cognition in both neurotypical and children at risk or diagnosed with a neurodevelopmental disorder. Indeed, as absolute power and power ratios conflate both aperiodic and oscillatory activity, it is possible that part of the previous results may be explained by the contribution of aperiodic components.

1.3.2.2. Functional networks development

Brain regions coordinate their activity to flexibly orchestrate cognitive processes (Buzsáki, 2006; Fries, 2015; Petersen & Posner, 2012), Therefore, effective communication between brain regions is crucial for development of attentional mechanisms as this synchronous activity permits integration between both proximal and distal areas (Buzsáki, 2006; Fries, 2015). However, brain communication is immature at birth, especially in frontal-parietal circuits that support executive processes (Gilmore et al., 2018; Vértes & Bullmore, 2015), albeit some recent studies have shown the involvement of frontal areas in fMRI/fNIRS studies in infancy (Ellis et al., 2021; Fiske et al., 2022) despite their immaturity (Dehaene-Lambertz & Spelke, 2015).

Most studies have employed fMRI in asleep infants to study the development of functional networks because its good spatial resolution and the possibility to measure metabolic (i.e. BOLD signal) changes over time in precise brain regions. In addition, in the last decade, graph theory has been implemented as a reference choice because of the richness of the data it provides to explore the functional organization of the brain. This framework

extends the information of direct connectivity by considering all the brain as a set of nodes interconnected by edges, which permits a more comprehensive characterization of the human connectome. Nodes can be voxels of gray matter, regions of interest, or electrodes, whereas the edges refer to their synchronization (e.g., BOLD correlation or EEG coherence). Thus, graph theory provides a common mathematical principle, independent of neuroimaging techniques, that offers an opportunity to describe functional network development across studies undertaking a similar framework.

Human functional brain networks present a balance between short- and long-range communication to integrate proximal and distal areas (Bassett & Bullmore, 2006, 2017). This topological configuration, called small-word, optimizes the information flow and reduces the wiring cost of the network (Achard & Bullmore, 2007). Thus, it presents a trade-off between the cost of integrating the network and its adaptability (Bullmore & Sporns, 2012). In addition, brain networks nodes group into specialized modules. Those comprise a group of areas that are highly interconnected to ease the short-range communication while promoting brain segregation (Alexander-Bloch et al., 2013). Importantly, modules are interconnected with the other modules through long-range edges (Salvador et al., 2005). This permits the efficient integration between specialized zones and helps to orchestrate the information across the brain (Bullmore & Sporns, 2012). Additionally, the degree of connections is not evenly distributed. A handful of nodes, denominated hubs, accounts for a large proportion of the connections (Guimera & Amaral, 2005). Hubs are crucial to optimize information flow within- and between- modules (Heuvel & Sporns, 2013) because the existence of highly interconnected nodes promotes the local and global efficiency of brain networks (Bullmore & Sporns, 2012).

Several measures can be computed to determine the topological characteristics of brain networks (Rubinov & Sporns, 2010; see Fig. 1.3.). These can be mostly divided into segregation and integration properties. Segregation has been largely evaluated using the clustering coefficient, which represents the number of triangular connections between three neighbor nodes (Watts & Strogatz, 1998), while the participation coefficient represents the percentage of connections within- (vs. between-) modules. The capacity

to integrate brain information has been measured using the characteristic path length. It represents the cost of integrating each pair of nodes considering all the intermediate steps. If we average the path length of every pairwise connection we obtain the characteristic path length of the network, and the global efficiency is the inverse of this value (Latora & Marchiori, 2001). Integration and segregation characteristics can be combined to obtain a single index of the topological properties of the network, the so-called small-world index (SWI), and small-word propensity (SWP) scores. They result from normalizing the original clustering and path length values with random networks (SWI) or random and lattice networks (SWP) to provide a summary measure. That is, we compare the real distribution of edges to a network with the edges randomly distributed (random) or placed to promote the maximum segregation of the net (lattice).

When the network approach has been applied to development, studies has shown synchronous fluctuations in BOLD activity in preterm infants, mainly in the primary and sensorimotor areas (Cao et al., 2016; Fransson et al., 2007; Smyser et al., 2010). At birth, visual and sensorimotor networks show a great degree of maturation, with a distribution similar to that of homologous networks in the adult brain (Doria et al., 2010; Fransson et al., 2011). In contrast, higher-order networks, such as visual orientation and executive progress, are present at birth, but their connectivity patterns are scarce and fragmented (Gao et al., 2011; Gao, Alcauter, Elton, et al., 2015; Gao, Alcauter, Smith, et al., 2015). However, by the end of the first year the orienting networks present a similar pattern of connectivity and they are anticorrelated to the default mode network (DMN) that it is recruited in mind-wandering states (Gao et al., 2011, 2013; Power et al., 2010). Executive networks (i.e., FPN and CON) have shown an even more protracted developmental trajectory, with evidence of further refinement up to adulthood (Dosenbach et al., 2010; Fair et al., 2009; Gao, Alcauter, Elton, et al., 2015).

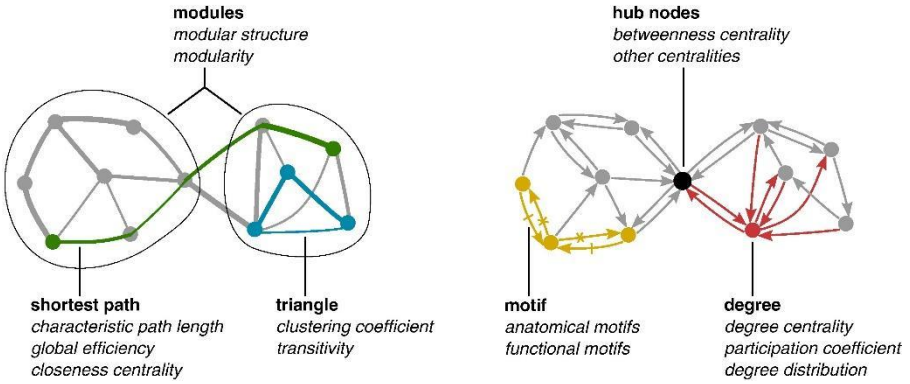

Fig. 1.3. Network topology measures. The measures of integration are represented in green, whereas those of integration are represented in blue. Red represents centrality measures, whereas yellow represents patterns of local connectivity. Extracted with permission from Rubinov & Sporns (2010).

The emergence of functional networks comes with the reconfiguration of topological network properties (Vértes & Bullmore, 2015; Zhao et al., 2019; see Fig, 1.4.). Despite of networks presenting a small-world distribution, hubs, and modules at birth (Asis-Cruz et al., 2015; Cao et al., 2016; Wen et al., 2019), functional networks are still immature. With age, brain hubs displace from primary to posterior areas, accompanied by gradual segregation of the modules (Cao et al., 2016; Yin et al., 2019). This specialization occurs by pruning irrelevant edges between modules and promoting within-module connectivity (Gao et al., 2011; Wen et al., 2019; Yin et al., 2019). At the same time, the emergence of long-range connections and their strengthening permits the connection of previously isolated brain regions (Vértes & Bullmore, 2015; Zhao et al., 2019). Consequently, the network capacity to integrate the information increases (Wen et al., 2019). These refinement processes seem to last at least until middle childhood (Fair et al., 2009; Fransson et al., 2011), although some authors found no differences between the first and second years (Gao et al., 2011). Driven by the drastic reconfiguration and strengthening of the edges, the global efficiency of information integration in the brain steadily increases until early childhood (Gao et al., 2011; Wu et al., 2013; but see Cao et al., 2014). Also, evidence has shown that hubs reach an adult-like distribution around the fifth year of life (Gao et al., 2011; Heuvel & Sporns, 2013).

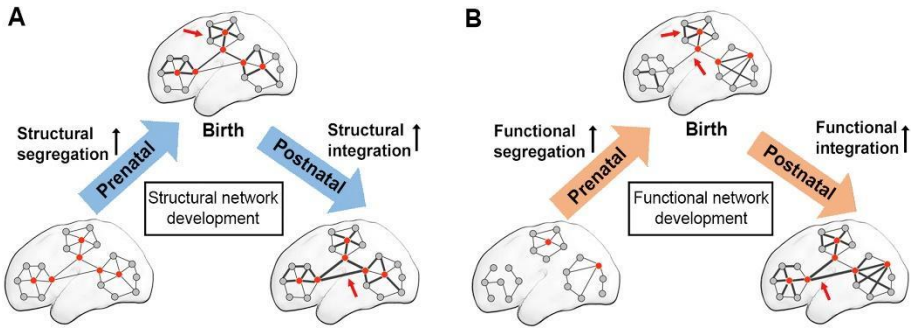

Fig. 1.4. Topological network development in infancy and early childhood. (A) Structural brain network development is well established before birth, and after birth, it mainly involves the strengthening of long-range connections. (B) Functional brain development is delayed compared to structural development. However, it followed a similar, albeit delayed, pattern. Extracted from Zhao et al. (2019) with permission.

One limitation of fMRI studies on connectivity analysis is its low temporal resolution. However, to date, only a few studies have employed other neuroimaging techniques to study functional network development in infancy and early childhood, yielding mixed results. For example, a study using MEG showed the development of somatosensory networks from random topology to small-world from infancy to childhood (Berchicci et al., 2015). In addition, two recent cross-sectional studies have reported topological variations in network properties with EEG recording. A high-density EEG study by Xie et al. (2019) found an increment in segregation in alpha and beta frequency bands from the sixth to the twelfth month of life, but a reduction in small-world topology. However, Hu et al. (2022) showed that small-world topology was already present at birth and the rest of parameters in their study were stable until the second year of life, suggesting the existence of a stationary period in the development of EEG network organization. Not supporting this stationarity of topological properties, changes in integration and segregation properties in EEG networks have been reported from childhood to adulthood. Specifically, results are consistent in showing age-related increases in segregation (Boersma et al., 2011; Miskovic et al., 2015; Smit et al., 2012), whereas both better integration or worse integration with age has been found (Bathelt et al., 2013; Boersma et al., 2011, 2013). This may be consequence of the steady increase in strength

of connections that also present a rapid maturation in the early years (Barry et al., 2004; Bell & Wolfe, 2007).

Given the involvement of functional networks (Cole et al., 2014; Marek & Dosenbach, 2018; Petersen & Posner, 2012) and connectivity (Fries, 2015; Palva & Palva, 2011; von Stein & Sarnthein, 2000) in cognition, some authors have addressed the relationship between executive process capacity, development, and connectivity parameters. Age-related changes in WM and EA in childhood are supported by the strengthening of fMRI/fNIRS connections within the regions of the FPN (Alcauter et al., 2015; Buss et al., 2014; Buss & Spencer, 2018; Fiske & Holmboe, 2019; Marek et al., 2015). In addition, from a network perspective, the progressive segregation of brain structural and functional networks underpins the emergence of executive control (Baum et al., 2017; Cui et al., 2020; Marek et al., 2015; Wang et al., 2021). Additionally, executive networks are the main contributors to individual differences in cognitive performance in children (Keller et al., 2022; Keller, Pines, et al., 2023) and executive networks have the largest weight to predict brain age employing machine learning algorithms (Dosenbach et al., 2010).

In terms of functional connectivity in specific frequency bands, high-frequency bands are thought to be involved in local communication, whereas low-frequency bands support long-range connectivity (Buzsáki, 2006; Marek & Dosenbach, 2018; von Stein & Sarnthein, 2000). Both alpha and theta connectivity seem to be modulated by attentional demands. For instance, internally directed attention appears to strengthen frontoparietal connections in the alpha band (Kam et al., 2019). Remarkably, theta and alpha band increase their connection strength when IC is required (vs. baseline state), but only the theta band can distinguish between reactive or moment-by-moment (vs. proactive; Braver, 2012) IC (Cooper et al., 2015). Alpha and theta connectivity are also involved in other attentional processes (Palva & Palva, 2011), memory (Muthukrishnan et al., 2020; Sauseng, Klimesch, Schabus, et al., 2005), and top-down modulation from anterior to posterior brain areas (Sadaghiani et al., 2012; Sadaghiani & Kleinschmidt, 2016). Importantly, the co-activation of executive network areas is linked to the strengthening of

connections from frontal to posterior areas in alpha band supporting its role of modulator of lower-order brain areas (Sadaghiani et al., 2012).

Infants show alpha and theta reconfigurations in evoked paradigms. From the eighth month, alpha connectivity between frontal and parietal areas increased while infants perform a WM + IC tasks (vs. baseline; Bell, 2001, 2002). This results has been recently replicated in other studies of the same group (Cuevas et al., 2012). On the other hand, theta band in infants has been linked to social conditions (Van Der Velde et al., 2021). Importantly, individual differences in alpha predict EA and WM capacities, with larger differences between evoked and baseline protocols as positive predictors (Bell & Fox, 1992). In addition, the development of alpha band connectivity forecasts EA and social competence from infancy to early childhood (Broomell et al., 2021; Whedon et al., 2016). This also occurs in other frequency bands, as children's performance in WM and intelligence is linked to the efficient integration of posterior and anterior areas in the beta band (Barnes et al., 2016; Wu et al., 2014).

Cross-sectional studies have also shed light on the relationship between functional connectome and EA. In general, in resting-state protocols with MRI, a more segregated yet efficiently integrated network has been linked to better performance in executive and intelligence tasks (Cole et al., 2012; Van Den Heuvel et al., 2009; but see Kruschwitz et al., 2018), which also occurs in EEG recording studies (Knyazev et al., 2017; Langer et al., 2012; Langeslag et al., 2013). In addition, the balance between segregation and integration in functional networks appears to be altered in neurodevelopmental disorders that compromise attention, such as ADHD (Henry & Cohen, 2019; Konrad & Eickhoff, 2010). For instance, recent studies have shown more segregated networks in adults and children diagnosed with ADHD (Ahmadi et al., 2021; Ghaderi et al., 2017 but see Ahmadlou et al., 2012), whereas others have found lower global efficiency in ADHD (Lin et al., 2014).

The results of previous experiments have revealed the significant changes in functional activity, both in oscillatory/aperiodic energy and the functional connectivity networks. The changes found in evoked and resting

state protocols underscores the rapid development of oscillatory and aperiodic brain function. This is shown in the increase of alpha energy, the displacement of the peak frequencies, and the similar functional roles of the frequency band in the evoked paradigms (Anderson & Perone, 2018; Cuevas & Bell, 2022). Additionally, brain functional networks drastically reconfigure their connectivity patterns. The orienting networks emerge around the sixth month of life (Gao et al., 2011) while the executive ones are delineated near the start of the second year of life (Gao et al., 2015; Gilmore et al., 2018). This maturation comes with better integration and larger segregation in the first three years of life, which seem to occur until adulthood in executive networks (Fair et al., 2009; Zhao et al., 2019).

The refinements of functional networks and oscillatory/aperiodic activity arguably underpins the development of attentional capacity that also undergo a profound maturation in the same period. Infants attentional control is initially driven by the environment, and gradually start to control volitionally their attentional focus (Hendry et al., 2019; Posner et al., 2014). Some months latter, they start to adjust their behavior, changing it when necessary (Conejero & Rueda, 2017; Hendry et al., 2016). The emergence of the networks responsible for those processes in adults broadly occurs in the same period. Orienting networks start to be delineated at the sixth month of life, and executive networks appearance is found in the end of the first year (Gao et al., 2011; Gao et al., 2015). The latter development of the executive network aligns with the more protracted development of CF and IC and supports the early role of orienting networks as a precursor controller system (Posner et al., 2014). Additionally, the gradual strengthening of frontoparietal connections supports the emergence of IC and WM in older children, and so does the progressive segregation of executive networks (Buss & Spencer 2018; Fiske & Holmboe, 2019; Marek et al., 2015).

Given the relevant role of oscillatory activity and functional connectivity in human cognition (Buzsáki, 2006; Fries, 2015) its development will probably be linked to EA maturation. With this respect, the gradual development of alpha and theta band, responsible for attentional and high-order cognitive processes, will be key in the maturation of attention. In this sense, presenting a more developed pattern of brain activity (i.e., larger

alpha, stronger connections) may result in better performance as it possible reflects the degree to which the brain is ready to exert a particular cognitive function. However, to testing this hypothesis is necessary to follow-up the children to explore the cognitive gains and brain function changes with age. To date, previous research has addressed this relationship mostly in cross-sectional studies or in older children. Longitudinal neuroimaging studies that evaluate both EEG measures and fine-grained tasks of attention in the first years are scarce (e.g., Braitwaite et al., 2020; Tan et al., 2023). Therefore, further studies combining both is necessary to deepen in the brain-behavior relationship in the first years of life.

Chapter 2: Aims and General Method

Chapter 2: Aims and Method

As this thesis is based on a longitudinal study, this chapter presents the goals and overall method of the study, which are common to the following experimental chapters. This chapter includes information about the aims of the thesis, experimental protocols, data preprocessing, and the analysis plan. Here, we provide a general guide for understanding what we aimed for and how we did it. Some of the details are repeated to ease the understanding in each chapter, and the hypotheses explained below are more general than those in the experimental chapters.

2.1. Aims

This thesis aimed to investigate the development of attention-based executive processes in infancy and early childhood, emphasizing the connection between brain function and behavior. The objectives of this dissertation were as follows:

1. Investigating changes in patterns and functional organization of brain electrophysiological activity during the first three years of life and its stability.
2. Examining the development and individual stability of executive attention (EA) during this early period.
3. Exploring the relationship between brain function and the early development of EA processes.

Several questions arise from these aims, which can be summarized into three main categories: developmental change, stability, and the brain-cognition relationship. That is, we aimed to understand whether measures of brain function and cognition vary in the first few years of life, whether individual differences and earlier performance significantly predict later time points, and how these variables relate to each other. Next, we provided a more specific focus on each topic.

2.1.1. Brain function development

EEG recordings in baseline protocols have been widely used in developmental neuroimaging over the past few decades, with previous studies utilizing the absolute or relative power in standard frequency bands

to investigate age-related changes. These studies have found significant developmental changes with age, including rapid maturation of the alpha band and changes in the low- and high-frequency bands. However, as discussed in the first chapter, these measurements conflate aperiodic and oscillatory activities that have different biological properties. This phenomena may have biased earlier reports on brain development, leading to reports of oscillatory changes that may not have occurred. To address this issue, it is important to employ a fine-grained distinction between oscillatory and aperiodic activity to determine which, if not both, undergoes changes and correlates with behavior. In the first experimental chapter (Chapter 3A), we aimed to explore brain function development while isolating oscillatory and aperiodic parameters and comparing them with age-related changes in relative power. Based on previous literature, we expected to find an increase in high frequencies (alpha, beta) and a reduction in low frequencies (theta) with age in relative power, as well as a flattening of aperiodic background activity. Generally, we predicted that relative power would conflate both oscillatory power and aperiodic components. Also, while alpha oscillatory activity was expected to increase with age, the developmental trajectory of the oscillatory power in other frequency bands was unclear.

In Chapter 3B, we analyze functional networks using EEG recordings to investigate brain connectivity development. Our aim was to explore the development of brain networks using graph theory measurements, as these measures provide a common framework for studying brain connectivity and exhibit significant reconfiguration with age. Most of the existent literature has been based on fMRI experiments and defined a clear age-related pattern, however few longitudinal studies have been conducted using EEG yielding mixed results. Thus, to ensure a comprehensive exploration of network development, we employed a multiverse perspective, computing connectivity using different synchronization measures to examine age-related changes. Our goal was to explore the specialization and integration of connectivity and its topology over time, and to assess whether previous results may be explained by the network construction process. We expected to find different trajectories for each measure, but the development of the network towards a more mature pattern in general. We hypothesized that brain networks would develop

towards a small-world connectivity pattern, promoting both segregation and efficient integration of information processing.

2.1.2. Flexibility and inhibitory control development

In Chapter 4, we explore the development of EA using two new child-friendly tasks: early childhood inhibitory touchscreen task (ECITT) and Bee-Attentive. The ECITT provides information about cognitive flexibility (CF) and inhibitory control (IC) but does not involve memory load as previous inhibition paradigms that have been used in infants and toddlers (e.g., A-not-B). Bee-Attentive combines a Go/NoGo paradigm with a visual-search task. Thus, it evaluates IC, sustained attention, and focused attention (see below). In these tasks, we expected a cost when children must withhold a prepotent answer (IC) to adapt trial by trial flexibly. In the Bee-Attentive task, we expected poorer performance in trials with a large (versus low) number of distractors. We also hypothesized that behavioral performance between tasks will be correlated, which would mean that cognitive performance is stable over time, and that current processes rely on previous simpler cognitive skills.

2.1.3. Bain function correlates of cognitive development

In chapters 5A and 5B, we explore whether the organization of functional activity correlates with individual differences in EA. The aim of this chapter is to understand whether a more mature pattern of brain function is positively correlated with children's cognitive performance. This should appear as a more segregated yet efficiently integrated network that is related to better executive attention, while in power we expect higher alpha power and flatter background to be a positive predictor.

2.2. The BEXAT and EDEXAT Projects

To achieve our goals, we conducted a longitudinal study from infancy to early childhood. The data included in this thesis are part of the data collected in two funded projects: the Babies Executive Attention Development Project (BEXAT) and the Early Development of Executive Attention Project (EDEXAT). The two projects followed a large cohort of

infants and they aimed to study the development of attention, brain function, and their relationship with the environment in five waves: 6, 9, 16, 36, and 48 months of life. In this thesis, we include an analysis up to the fourth session. By combining these four waves (Fig. 2.1), the project consisted of over 10 tasks, four EEG protocols, and questionnaires. However, we will only detail the paradigms included in this dissertation.

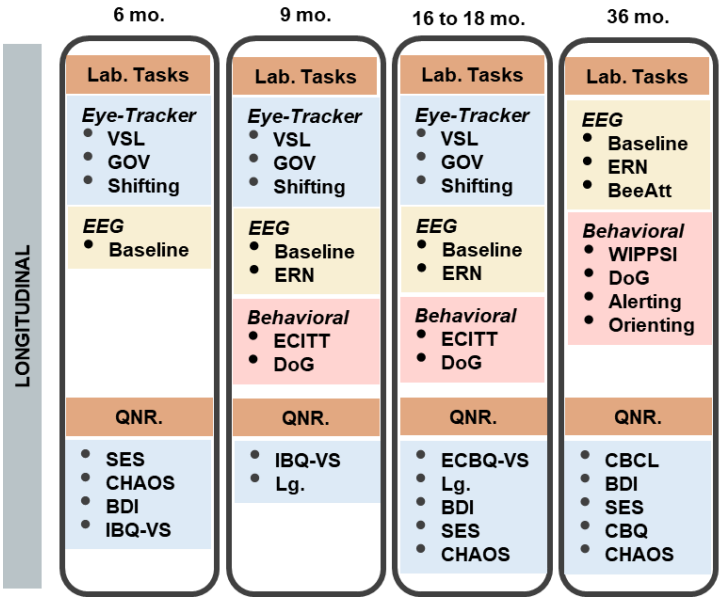

Fig. 2.1. Schematic summary of the BEXAT and EDEXAT projects. The figure displays each one of the behavioral and neuroimaging protocols (Lab. Tasks) and the questionnaires sent to the families (QNR.) in each session.

2.3. Demographical Information

Infants (initial $N = 160$) were recruited from nurseries, hospitals, and advertising in the metropolitan area of Granada (Spain). If families showed willingness to be included in the study, they were called when the infants were 6-mo. We followed these families at 9 (n =123), 16-18 (n = 93) and 36-37 (n = 94) months of life. Premature (gestational weeks < 37) and low weight (birth weight < 2.5 kg) infants were excluded from the analysis (n = 14). We also excluded infants at a risk of developing neurodevelopmental disorders (e.g., first degree relatives diagnosed with ADHD; n = 4). All families received

a voucher to be exchanged for a toy in a local store (sessions 1 to 3) or a payment of 25€ (session 4) in each session. The third session age range was due to the COVID-19 pandemic, which forced laboratories to interrupt research activity for several months and obliged us to widen the participant's age window for the third session.

Families provided information about their socio-demographic characteristics, economic status, and mental health (mother). Based on this information (n = 112 at 6 months, n = 75 at 16 months, and n = 72 at 36 months), we observed that the majority of children were only exposed to Spanish at home (84%). Bilingual families mostly talked in English to their children (n = 7), but there were also parents who spoke Portuguese (n = 1), Euskera (n = 1), Arab (n = 1), or German (n = 1). Mothers were the main caregiver, spending more than 6h per day with her children. The education level of the families was high, with nearly 60% having a post-compulsory degree (i.e., technical degree, bachelor's degree, or higher), and were above the poverty level according to the National Institute of Statistics (*INE*; 75%). A ~75% of the mothers did not have a clinical level of depression, although ~25% were above the threshold of mild depression or higher, as determined by the BDI-II questionnaire. See the Appendix of Chapter 2 for further information.

2.2. Apparatus, Questionnaires and Experimental Task

2.2.1. General structure of the sessions

All sessions included a set of behavioral and eye-tracking recordings. The first three sessions started with three eye-tracking protocols. The children then performed behavioral tasks followed by evoked EEG paradigms. The baseline EEG recording was always the last protocol. The children were seated over their caregiver's lap in the 6, 9 and 16 months of age sessions, while in the 36-mo. session the parents were seated inside the room. The first session lasted approximately 30 min, while the other sessions lasted between 1h and 1h 30min including resting between tasks and EEG preparation. The parents were instructed to not interfere with or interact with their children. We videotaped all tasks to qualitatively review the register prior to preprocessing for all behavioral and EEG protocols.

2.1.1.1. Behavioral Protocols

The early childhood inhibitory touchscreen task (ECITT)

We employed the ECITT to evaluate EA processes at 9 and 16 months of life. We used an Apple iPad tablet (screen: 9.7 In; resolution: 2048 × 1536 px) to present the stimuli. The task was programmed by Henrik Dvergsdal (Holmboe et al., 2021) and is available online (https://ecitt.app).

We followed the standard ECITT protocol described by Hendry et al. (2021). The session started with a *Familiarization Phase* to allow infants to interact with the tablet. In this phase, the experimenter encouraged the infants to touch a butterfly displayed on a tablet screen. If the child did not touch it, the experimenter modeled the action and provided positive feedback when the child imitated him or her. Afterwards, the infants completed a *Practice Block* in which a centrally positioned blue button with a "smiley face" (target button) appeared on the screen, and the experimenter prompted the infant to touch it. A short animation with music was presented as positive feedback after the infant tapped the button. This step was used to create an association between the target and the positive feedback. Once the infant demonstrated competence in touching the target button, the *Experimental Block* was initiated. During the experimental trials (Fig. 2.2), two blue buttons, one empty (blank button) and one with the "smile face" on it, were displayed on the sides (right or left) of the screen. The experimenter gently encouraged the infant to touch the target by saying 'Can you touch the smiley face?'. Correct touches were immediately followed by child-friendly feedback (short cartoon animation with music), whereas the stimuli remained unchanged following incorrect or off-button touch.

Each infant underwent a single block of 32 experimental trials. The target button appeared more frequently on one side of the screen (75% prepotent location) and less frequently on the opposite side (25% inhibitory location) of the screen. The prepotent location was counterbalanced between participants but was the same for each infant in the two longitudinal sessions (at 9 and 16 months of age). The experimental block began with at least three consecutive prepotent trials to establish an initial tendency. Trial selection

was pseudo-randomized, allowing a maximum of five prepotent trials in a row and a maximum of two consecutive inhibitory trials. Infant behavior was visually coded by the researchers to discard invalid trials (responding without looking, reaction time below 300ms, and/or parents signaling the correct answer). Infants were excluded if they did not reach 60% accuracy in prepotent trials, had fewer than two inhibitory trials, or did not complete at least 50% of the trials (Lui et al., 2021).

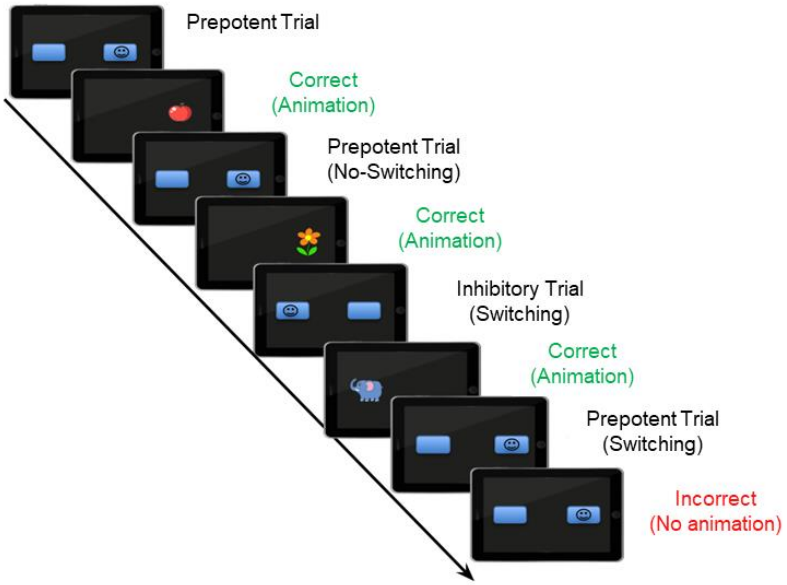

Fig. 2.2. Schematic representation of the ECITT task. The figure displays a sequence of trials in the experimental block, showing the three types of trial (PS, IS, PNS) and the feedback provided in hits (vs. errors).

Task performance on the ECITT was measured as the percentage of correct valid answers under three conditions: Prepotent Non-Switch (PNS), Prepotent Switch (PS), and Inhibitory Switch (IS). The PNS trials were those in which the target appeared at a prepotent location as in the previous trial. In the PS trials, the target appeared at a prepotent location but following a presentation in the inhibitory location. In the IS trials, the target appeared at the inhibitory location following the presentation at a prepotent location. Unlike previous studies using the ECITT, we decided to consider sequential changes in the target location to disentangle the IC from response-switching

costs, an effect related to CF and control (Koch et al., 2018). In addition, we computed two general indices of task performance: the Inhibitory Effect (PS Accuracy – IS Accuracy) and the Switching Effect (PNS Accuracy – PS Accuracy). The Inhibitory Effect measures the cost of accuracy owing to failure to inhibit touching the prepotent location, whereas the Switching Effect reflects the general costs of changing from one location to another. Note that the performance indices in our study vary from those used in previous studies on ECITT (e.g., Hendry et al., 2021). We provide the behavioral results using the original indices in the Appendix of Chapter 4.

Bee Attentive Task

At 36 months of age, we designed and programmed the Bee-Attentive task to evaluate executive and focused attention. The task was programmed in Eprime-2.0 and video recorded with the software of the Brain Vision Recording 2.0. The stimulus was presented on a 24-inch monitor (BenQ-XL24T) with a native resolution of 1920×1080 pixels. The answers were recorded using a Logitech k120 keyboard. The keyboard was covered to allow only the spacebar to be visible. The children performed the task while sitting in a chair, approximately 50 cm from the monitor screen.

The Bee-Attentive task combines the Go/NoGo rationale with a visual search task. This task has the objective of helping the Bee (Go stimulus) collect honey while avoiding helping the Wasp (NoGo stimulus) because it "stoles the honey from the Bee." Apart from the target stimulus, in each trial, the children must ignore irrelevant distractors (insects) that appear alongside. The distractor number varied depending on the trial load: low load (1–2 insects) and high load (5–6 insects). The size of the stimuli was 114 × 75 pixels.

All the children started with a *Discrimination Block* (Fig. 2.3A). In this block, experimenters showed the children a big picture of the Bee and the Wasp, and prompted them to express their differences (e.g., the Bee was more orange-like). Once the differences were noted, the researchers gave the children smaller pictures of Bee and Wasp. Children were asked to help the researcher put them where they belonged (i.e., smaller bees with a bigger

bee). There were 18 pictures in total (9 bees and 9 wasps), which had the same shape and position than the ones used in the experimental blocks.

Once the children understood the differences between the Bee and Wasp and correctly sorted the pictures, we started the *Instruction Block* (Fig. 2.3B). In this block, the experimenter told the children the goal of the game and instructed them to press the spacebar key when the Bee appeared but withheld answering if the target was a wasp. The instruction block consisted of eight trials (4 bees and 4 wasps). In the first four trials, both the Bee and Wasp appeared alone, and in the remaining four trials, the stimulus was presented along with the two insects. The sequence was always two bees followed by two wasps. In each instruction trial, the experimenter asked the infants what stimulus was on the screen and what they should do, encouraging them to press the bar in case the Bee was present. In the Wasp trials, we considered a correct answer if they told us that they should not press the key after seeing it. In the distractor trials, we instructed the children to avoid the insects because they were not relevant to the task. In these eight trials, the stimulus remained on the screen until children answered. Every time the children correctly responded to the Bee, positive feedback appeared (sound plus static image of the bee happy appeared for 1s), but if they pressed the key when the Wasp was present, a negative feedback sound plus an image of a sad bee was displayed. This block was repeated as many times as necessary until the children understood the dynamics of the task. Five children were excluded because they did not understand the instructions.

Once the children understood the task instructions, they proceeded with a *Practice Block*. Trials in this block had the same parameters as those in the *Experimental Blocks.* Thus, it was designed to make the infants used to the speed of the task. We encouraged the children to be as fast as possible but, at the same time, accurate enough to not help the Wasp. This block consisted of four trials, three bees, and one wasp that was always presented in that order. The stimulus was to last up to 6s or until the response, with a feedback sound of 1s, and an inter-stimulus interval randomly selected between .8 and 1.2 s (Fig. 2.3C). The distractors were randomly selected for either a Low Load (one to two insects) or a High Load (five to six insects). The practice block

was repeated the necessary times until the child showed a clear understanding of the instructions and was used to the task dynamics.

Finally, the *Experimental Blocks* took place. It consisted of 6 blocks of 20 trials (120 trials, 70% bees and 30% wasps; 50% low load and 50% high load). The blocks were self-balanced, thus displaying the general proportion of Go/NoGo and load conditions. Stimulus selection was random with three exceptions: 1) each block always started with three bees to create a tendency, 2) no more than four bees could appear sequentially, and 3) only two wasp trials could appear in a row. Between the blocks, the children received feedback based on their performance. It appeared as a "deposit" of honey that will fill with honey panels over the blocks. The panels were cumulative, and the current panels were added to the previously ones, making the ultimate objective of the "game" fulfilling the "honey deposit."

The performance on the task was measured by mean accuracy for each condition (e.g., Go Low load) to measure IC. Focalized attention was measured using the median RT and the standard deviation of the RT in the Go Low load (vs. Go High load) conditions. In addition, we computed performance after committing an error (vs. after a hit) in both RT (slowing after error; SAE) and accuracy as a measure of response adjustment (i.e. self-regulation). Finally, sustained attention was measured as the progression of performance over the experimental blocks. Children must have more than 50% accuracy, and 28 Go and 12 NoGo valid trials (*excluded* n = 3) to be included in the analysis. The researcher reviewed the video recordings of the sessions to determine the validity of the trials. Trials were marked as invalid when a child answered without looking at the screen, were faster than 200ms, and/or the parent helped him/her to determine the correct answer.

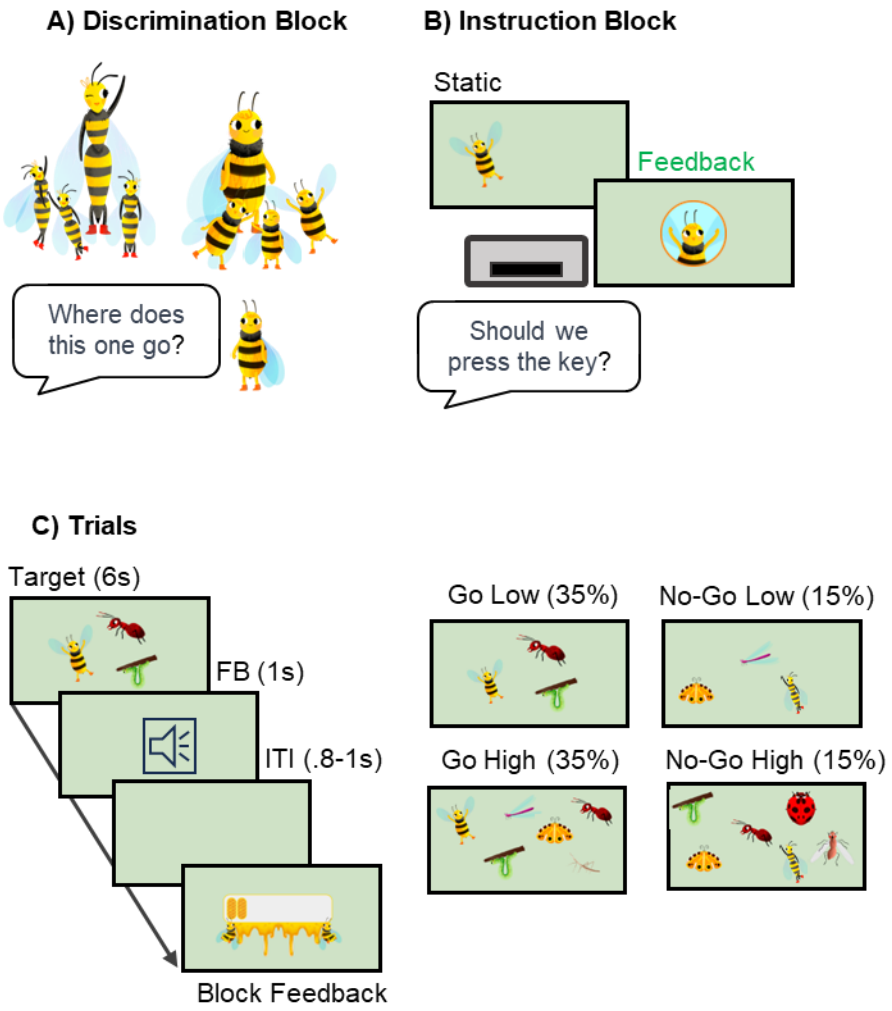

Fig. 2.3. Bee-Attentive task protocol. The figure shows the two initial blocks of the task (A, B) and a sequence of a typical experimental trial with the proportion of conditions by its side (C).

2.3. Electroencephalography

2.3.1. EEG recording

The resting state consisted of two blocks each one lasting 2 minutes. During the first block the experimenter used a device that blew soap bubbles, whereas at the second block a video was presented on the computer screen showing geometrical shapes and soft music. The presentation screen was the

same as that used in the Bee Attentive task. In all four sessions, we employed a high-density EGI geodesic net of 129 channels to record the brain signals. In the first three sessions, we recorded it using the software Net Station (Eugene, OR, USA), whereas in the fourth session, we changed the recording system to Brain Vision Ant Champ Plus (Brain Vision Recorder 2). We recorded the signal with a 1000 Hz frequency rate and filtered it online with high-pass (0.1 Hz) and low-pass (100 Hz) filters. The only difference between the acquisition set-up was in the online reference. As the brain vision system adapter did not support channel 129 of the EGI net (Cz – vertex reference), we referenced the signal to Cz in the first three sessions and to electrode 55, the most proximal in the middle line to Cz, in the fourth session. In the preprocessing step, the Cz electrode was reintroduced by spherically interpolating the surrounding electrodes.

2.3.2. EEG preprocessing

To process the EEG signal, we combined the MADE (Debnath et al., 2020) and APICE (Fló et al., 2022) pipelines in EEGlab (see the Appendix Fig. A2.4 for the scheme of the preprocessing steps). The signal was filtered (FIR; 0.2 – 48 Hz), and the boundary electrodes ($n = 20$) were excluded from further processing because they were excessively noisy (Fig. 2.4). Global bad channels (i.e., noisy in most of the register) were then detected using the EEGlab plug-in FASTER (Nolan et al., 2010) and removed from the dataset. Next, we created a copy of the dataset and computed an independent component analysis (ICA) after clearing the artifacts (high pass filtered to 1 Hz; segmented into 1s epochs; threshold = ±1000 μV; activity detected between 20 and 30 Hz). Bad components were detected using the children's version of the ADJUST plugin (Leach et al., 2020), which were copied into the original dataset and removed from the recording.

Over the continuous EEG data, we detected the "transient bad moments" with an adaptive threshold based on the power spectrum, amplitude, and variance of the signal. If these transient bad moments lasted less than 100ms, the pipeline targeted them using principal components analysis (PCA) and removed the components that explained up to .90 of the variances of that brief period. Then, the signal was divided into 5s (power) or 1s (connectivity) epochs (50% of overlapping), and we redefined the

"transient bad moments." The difference in the epoch length was due to the improved fit of longer epochs in power-spectrum decomposition (Rico-Picó et al., 2023; Schaworonkow & Voytek, 2021) and the larger reliability found in short epochs in the connectivity measures (Haartsen et al., 2020). If more than over the 30 percent of the signal within an epoch was marked as noisy, the epoch was removed. Otherwise, the channels of transient bad moments were interpolated within the epoch. Finally, the global bad channels initially excluded by FASTER were reintroduced using spherical interpolation, and the signal was re-referenced to the average. Over the remaining epochs, we applied a ±110μV voltage threshold, and in the case of 20% of the channels surpassed it, the epoch was discarded. Finally, experimenters visually inspected the segments and removed the bad segments if necessary. Children with less than 20s or 90s of clean valid data were excluded from power and connectivity analyses, respectively. In case where children had more than 10 global bad electrodes detected in the step two by FASTER plugin, participants were also excluded from the analysis (n = 0).

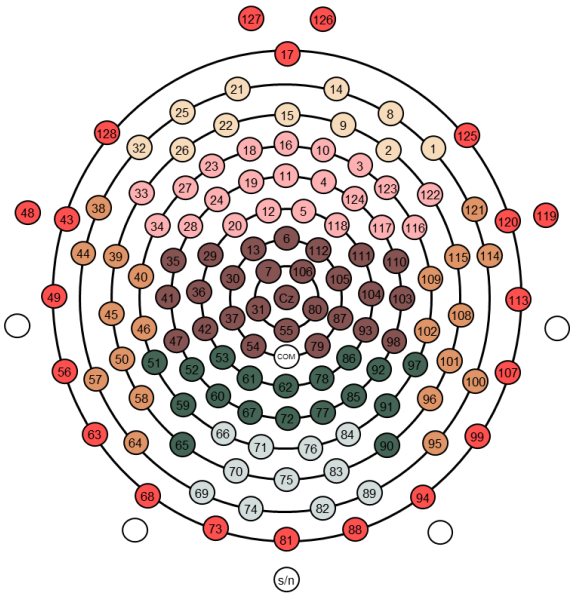

Fig. 2.4. Geodesic EGI layout employed in the EEG recordings. It shows the 129 electrodes filled by cluster: red (electrodes excluded), dark brown (central cluster), light brown (temporal), dark green (parietal), light green (occipital), pink (frontal), beige (frontal pole).

2.3.3. Power variables: aperiodic and oscillatory/relative power

We obtained the aperiodic and oscillatory parameters using the *Specparam* toolbox (Donoghue et al., 2020) through a MATLAB2021a wrapper (https://github.com/bfbarry/EEGLAB-specparam). This toolbox models the results of an FFT (1–20 Hz, 0.2 Hz steps) provided by the *pop_spectopo* function (Welch's method – 100% of signal) into aperiodic and oscillatory power. It considers the power at each frequency to be a combination of aperiodic and oscillatory activities. The aperiodic activity is defined as:

(1)

$$\mathrm{L}(f) = b - \log[f\mathrm{x}]$$

where L corresponds to the aperiodic power in each frequency (*f*), b is the offset value of the power, and χ is the aperiodic exponent. The oscillatory part consists of a series of Gaussian curves over the aperiodic components, modeled as:

(2)

$$Gn = a \times \exp(-\frac{(F-c)^2}{2w^2})$$

where a is the $\log_{10}$ amplitude of the peak, c is the center frequency (Hz), w is the standard deviation of the Gaussian (Hz), and F is the vector of frequencies. Therefore, the power spectrum consists of:

(3)

$$PSD = L + \sum_{n=0}^{N} Gn$$

where the power spectrum (PSD) is the sum of the aperiodic components and oscillatory Gaussian peaks.

The spectral fitting parameters were similar to those employed in previous infant studies (peak width limits: [2.5 Hz – 12 Hz]; maximum number of peaks: 5; aperiodic mode: fixed; peak threshold: 2; see Schaworonkow and Voytek, 2021). To ensure reliability of the results, we excluded channels with fit values below $R^2 = .95$. Infants must had at least 50% of electrodes surpassing that threshold per ROI to be included in the analysis.

We computed the oscillatory and relative powers in three frequency bands, theta, alpha, and beta. Alpha and theta frequency ranges were centered on the infants' individual alpha (IAF) and theta (ITF) peak frequencies over the parieto-occipital ROIs. We selected these ROIs and adapted the frequency ranges because the parieto-occipital area shows larger reconfiguration in infants when exposed to resting conditions, and the peak frequency steadily increases in the first years of life (Freschl et al., 2022; Marshall et al., 2002; Stroganova et al., 1999). After obtaining the IAF and ITF, we constructed a frequency range considering the full width at half maximum (FWHM) of the oscillatory Gaussian curve provided by the *Spectparam* toolbox for each infant (e.g., IAF ± FWHM alpha). The beta band range was considered to start at the upper limit of the alpha range plus 1 Hz to 20 Hz (i.e., IAF + FWHM alpha + 1 Hz – 20 Hz) because we did not find clear beta peaks in the power spectrum, in agreement with the literature (see Rayson et al., 2022). Frequency bands were indistinctly employed in the power and connectivity analysis.

To obtain oscillatory power, we subtracted the aperiodic background curve from the absolute power for each frequency band. The relative power was computed using the same frequency range as that of the oscillatory power. However, its computation consisted of dividing the absolute power of a frequency band by the power of all the power spectra (e.g., alpha absolute power / 1 to 20 Hz power). Each measurement was calculated per electrode and averaged over the cluster, excluding the electrodes with goodness of fit $R^2 < .95$. In the case of the IAF and ITF, we excluded electrodes that did not present a peak.

2.3.4. Network construction and graph variables

The connectivity measures were computed using the FieldTrip toolbox (Oostenveld et al., 2011). To estimate the spectral connectivity between pair of channels we used imaginary coherence (iCoh) and phase lag index derivates (weighted: wPLI, debiased weighted: dwPLI) because these measurements are resistant to instantaneous connectivity and therefore diminish the risk of volume conduction (Bastos & Schoffelen, 2016). The iCoh measure (Nolte et al., 2004) is the cross-correlation projected over the imaginary axis and evaluates the proportion of the signal of one electrode that can be explained by another, including both the signal amplitude and phase. The PLI and its derivatives (Vinck et al., 2011) capture the synchronization of the phase independent of the amplitude, and can be defined as:

$$\text{PLI} = |sign[\sin(\Delta\phi(tk))]|$$

where the *sign* is the signum function and the $\Delta\phi$ is the difference in the imaginary part of the signals' cross-spectrum between each electrode pair at the time point t for k timepoints per epoch. $||$ indicates that the values are considered absolute; thus, PLI values can range from 0 to 1. Then, the debiased weighted phase lag index (dwPLI) is calculated as follows:

(5)

$$\text{dwPLI} = \frac{(\sum \Delta\phi)^2 - \sum \Delta\phi^2}{(\sum |\Delta\phi|)^2 - \sum \Delta\phi^{2\cdot}}$$

The dwPLI considers the number of epochs to reduce bias by normalizing the values obtained from the weighted phase-lag index values.

Once the connectivity matrices were obtained, we used the brain connectivity toolbox in MATLAB (Rubinov & Sporns, 2010) to compute the graph parameters, with the exception of small-world propensity (SWP), which was calculated using the code provided by the authors (Muldoon et al., 2016). Raw adjacency matrix for each band was firstly filtered with a proportional threshold between .15 and .35 (.05 steps) and normalized or binarized (Fig. 2.5).

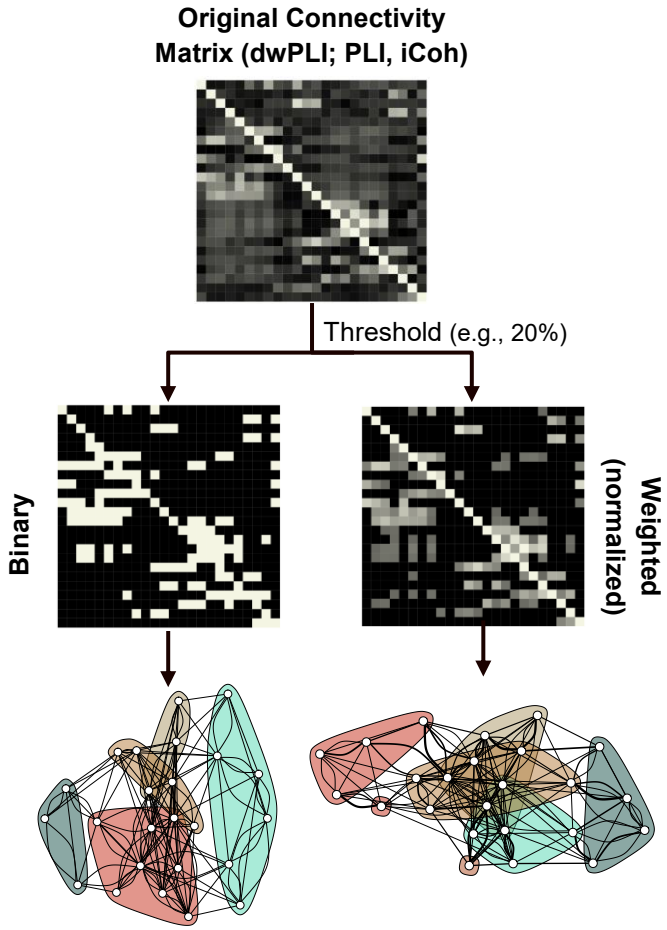

Fig. 2.5. Pipeline of the network constructions steps. Starting with the original connectivity matrix, the strongest percentage of connections is kept (proportional threshold) and their strength can be either retained (weighted) or transformed into a perfect connection (1; binary). Then the network is constructed, and its metrics computed.

Once filtered the networks, we computed the local and global efficiency of the networks and its general topology (SWP). SWP is computed by correcting the characteristic path length and clustering efficiency using random and lattice networks, which maximize long- and short-range connections, respectively. The SWP is computed as:

(6)

$$\Phi = 1 - \sqrt{\frac{\Delta_c^2 + \Delta_L^2}{2}}$$

where the SWP (Φ) results from 1 less the square root of the delta clustering (ΔC) and path length (ΔL). Delta clustering and path length can be defined as follows:

(7)

$$\Delta C = \frac{C_{latt}^{w} - C_{obs}^{w}}{C_{latt}^{w} - C_{rand}^{w}}$$

(8)

$$\Delta L = \frac{L_{obs}^{w} - L_{rand}^{w}}{L_{latt}^{w} - L_{rand}^{w}}$$

where *obs*, *latt*, and *rand* represent the observed, lattice, and random networks, respectively, and clustering corresponds to C^w and the characteristic path length with L^w.

We characterized the modularity of the networks by employing Louvain's algorithm (Blondel et al., 2008), because it optimizes the network structure while minimizing the connection between modules. Modularity was then explored using Newman's Q (2005) and the segregation of modules using the participation coefficient (Guimera & Amaral, 2005). Based on the results of the participation coefficient (P) and within-module z-degree, we classified the nodes into non-hubs (within-module z-degree < 2.5) and hubs (within-module z-degree > 2.5) following the guidelines of Guimera and Amaral (2005):

- *Non-Hubs*
    - Ultraperipheral (P < .30)
    - Peripheral (.30 < P < .62)
    - Non-Hub connector (.62 < P < .80)
    - Non-Hub kinless (P > .80)
- *Hubs*
    - Provincial hub (P < .30)
    - Connector hub (.30 < P < .75)
    - Kinless hub (P > .75).

2.4. Analysis Plan

All analyses were conducted using R software v4.2.1 (R Core Team) in RStudio (RStudio Team, 2020). Data manipulation was conducted using Tidyverse-related packages (Wickham et al., 2019), and data visualization was performed using ggplot2 (Wickham, 2016).

2.4.1. Longitudinal development of brain function and behavior

As attrition is common in developmental studies and missing data might affect the statistical power of the analysis and bias the results (Enders, 2013; Graham, 2009; Matta et al., 2018), we employed maximum likelihood estimation to address missing values. We included participants with at least half of the data points with valid data (e.g., two sessions with valid EEG data and two missing). Missing data was considered when 1) a technical problem occurred 2) a participant did not attend the session. Little's test determined that the data was missing completely at random (Little's test, $t(163) = 1.78$, $p = .205$). Additional analysis revealed that the socioeconomic status of the family did not vary between children who attended (vs. missed) the session at 9-mo. (EEG: $F < 1$; ECITT: $F(1,70) = 1.53$, $p = .22$), 16-mo. (EEG: $F < 1$; ECITT $F(1,70) < 1$), and 36-mo. (EEG: $F(1,52) < 1$).

We employed linear mixed models to explore the longitudinal changes that occurred in the behavioral and rs-EEG variables (*lme4 package:* Bates et al., 2014). The models were constructed using a bottom-up approach. First, we fitted the random effects (random intercept vs. random slope of time) and then added the fixed effects individually. We determined the fittest model based on the Akaike Information Criteria corrected (AICc), thus

correcting the fit by the number of independent variables. If the residuals were non-normally distributed (*performance package;* Lüdecke et al., 2021), we transformed the data based on the Tucker stair of the ladder transformation guide and re-ran the models in the first step. We employed the Satterthwaite approximation to compute the degrees of freedom and Nakagawa et al. (2017) R^2 formula for the effect size of conditional and marginal effects.

2.4.2. Stability analysis

The stability analysis consisted of the Spearman's rank correlation between each pair of sessions. In the case of rs-EEG, we explored both within-participants and spatial stability. Spatial stability consists of averaging the electrode values of all the participants, and then correlating it between sessions. Within-participant stability correlated the individual values of each participant of one session with the following one.

2.4.3. Relationship Analysis

When studying the relationship between cognition and brain function, we employed two different strategies for power and connectivity because of qualitative differences in the data.

2.4.3.1. Cognition and power variables

Given previous studies on brain power and cognition (e.g., Bell, 2002), we decided to employ the frontal cluster as the ROI for power and aperiodic components. In addition, we included the IAF and ITF over the parieto-occipital clusters averaged to address individual differences in the peak frequency. The *glmulti* package was used to study the relationship between ECITT and Bee-Attentive performance and functional brain power. This package conducts linear regressions by creating all possible combinations, given the matrix of independent variables, and finds the one that fits the best to predict the dependent variable. In the ECITT task, we examined concurrent (e.g., 9-mo EEG predicting 9-mo. ECITT) and longitudinal (9-mo EEG predicting 16-mo. ECITT) relationships between brain and behavior. In the case of Bee-Attentive, we only explored concurrent models. We transformed the raw values in cases where the residuals were non-normally distributed.

2.4.3.2. Cognition and functional connectome

As we aimed to introduce several ROIs in the analysis to explore how the graph property in each area was related to cognitive performance, we employed partial least squares (PLS) to reduce the dimensionality of the data. PLS methods are not different from other reduction analyses, such as PCA, but they maximize the covariance between two or more matrices of data, identifying the variables that contribute the most to those relationships (Wold, 1975). PLS methods create a series of components (i.e., latent variables), in which each variable is loaded with different weights. Therefore, it provides the opportunity to include several ROIs and frequency bands simultaneously, while avoiding collinearity problems. PLS analyses were conducted using the *MixOmics package* (Rohart et al., 2017) with an adaptation of the code provided by Johnson et al. (2021) in their study.

We conducted canonical PLS employing the *block.pls* function to predict a single variable for our behavioral tasks, thus limiting it to one component per matrix. We included the topological network properties in each session as separate matrices of data, and each held information about network properties divided by ROIs and frequency bands. Therefore, we employed 3-block and 4-block PLS (canonical, RGCCA, Horst's scheme) to study the relationship between ECITT and Bee-Attentive with functional networks, respectively. We evaluated both the direct (e.g., 6-mo. functional connectome – PS accuracy) and indirect paths (e.g., 6-mo. functional connectome is related to PS accuracy through a 9-mo functional connectome). We determined the significance of the direct paths based on the results of 5000 permutations, whereas the indirect paths and significant weights of the components were determined by 5000 bootstraps with replacement (Nitzl et al., 2016; Taylor & MacKinnon, 2012). If the beta coefficient of the direct paths was withing the 5% extreme values of the permuted distribution, it was considered significant. Indirect paths and reliable weights were decided using the 95% CI of the bootstrap results. If the bootstrap results did not cross the zero value (i.e., did not flip the sign), they were considered reliable.

Chapter 3A: Early Development of the EEG power: Oscillatory and Aperiodic Contributions

The content of this chapter has been partially published as Rico-Picó, J., Moyano, S., Conejero, Á., Hoyo, Á., Ballesteros-Duperón, M. Á., & Rueda, M. R. (2023). Early development of electrophysiological activity: contribution of periodic and aperiodic components of the EEG signal. *Psychophysiology*, e14360.

Both brain structure and function undergo profound changes in the first years of life, which are related to the emergence and development of cognitive processes (Gabard-Durnam & McLaughlin, 2020; Gilmore et al., 2018). Among the techniques that measure brain function, electroencephalography (EEG) has been widely used to characterize functional development in infants and toddlers because of its ease of use and adaptability (Saby & Marshall, 2012).

EEG signals provide information regarding neural oscillations, reflecting the synchronization and desynchronization of neuronal activation at different rhythms in both micro- and macro-neural circuits (Buzsáki, 2006; Buzsáki et al., 2012; Buzsáki & Draguhn, 2004; Cohen, 2017). In infants, EEG activity is usually recorded at rest (resting-state EEG; rs-EEG) because it offers information about the intrinsic activity of the brain without task constraints. As a result, rs-EEG has been widely implemented to explore brain function development, as it does not require following task instructions or paying attention to the stimuli. In infants, rs-EEG protocols usually involve an external source of stimulation (e.g., soap bubbles or stimuli presented on a screen) to help them to stay as calm as possible (Anderson & Perone, 2018; Bell & Cuevas, 2012; Saby & Marshall, 2012)

Resting-state EEG provides several measures ranging from signal energy to connectivity. However, the gold-standard measurement of infant rs-EEG consist of decomposing the signal to extract power in standard frequency bands: theta (3–6 Hz), alpha (6–9 Hz), beta (9–20 Hz), and gamma (+20 Hz; Saby & Marshall, 2012). The power of each frequency band can be obtained in absolute terms (i.e., the actual value obtained for a particular frequency) or relative terms when the energy of a particular frequency is divided by the power of the rest of the signal or frequency bands (e.g., theta–beta ratio; Anderson & Perone, 2018; Saby & Marshall, 2012).

When the development of rs-EEG is explored during the first years of life, the relative power is more sensitive than the absolute power because the latter can be affected by skull changes over the lifespan (Marshall et al., 2002). In fact, the transition from infancy to toddlerhood is a period of rapid reconfiguration of relative power in all frequency bands. Evidence suggests that the relative power in the theta band is higher in younger infants

(Orekhova et al., 2006). In addition, the alpha peak appears at around the fourth month of life. It appears as a sudden energy "bump" between 5 and 7 Hz, moves toward higher frequencies, and augments its relative power with age during the first years of life (Clarke et al., 2001; Gasser et al., 1988; MacNeill et al., 2018; Orekhova et al., 2006; Stroganova et al., 1999; Whedon et al., 2020). Furthermore, the alpha band relative power appears to show within-individual stability during infancy (Marshall et al., 2002). Finally, although research on higher-frequency bands in infants is still scarce, a study by Tierney et al. (2012) suggested a reduction in frontal beta and gamma between the fifth and twenty-fourth months of life.

Although previous research suggests that relative power is sensitive to developmental changes, it only considers the energy of standard frequency bands, which does not separate background activity (aperiodic) from oscillatory brain activity (Donoghue, Haller, et al., 2020; He, 2014; Ostlund et al., 2022; Voytek et al., 2015). In fact, EEG power is a composite of a 1/*f*-like curve that accounts for most of the signal (aperiodic background) with some "bumps" or peaks that appear over it (periodic or oscillatory activity). More specifically, the aperiodic background curve is defined using two parameters: *offset* (power at the lowest frequency of the aperiodic curve) and *slope* or *exponent* of the curve. In contrast, oscillatory brain activity refers to the frequency of the peaks and energy above the aperiodic curve and has different generators.

As a result of this conceptualization of EEG power, some authors argue that developmental variations in absolute and relative power can be attributed to changes in either the aperiodic or periodic components of the EEG (Donoghue et al., 2020; Ostlund et al., 2022). Consequently, different research groups have examined the maturation of aperiodic and oscillatory components (e.g., Cellier et al., 2021). Recent research has shown an aperiodic background curve in asleep newborns that flattens from birth to the seventh month of life (i.e., a reduction in the exponent; Fransson et al., 2013; Schaworonkow & Voytek, 2021). This pattern is constant as the aperiodic power curve becomes flatter from the age of three years onward (Hill et al., 2022; McSweeney et al., 2021; Voytek et al., 2015). Interestingly, the aperiodic parameters have been linked to cognitive processes and neurodevelopmental

disorders, which accounts for their biological importance (Demuru & Fraschini, 2020; Immink et al., 2021; Karalunas et al., 2021; Shuffrey et al., 2022). Studies on the oscillatory activity of rs-EEGs have focused on the alpha frequency band. The alpha peak frequency and number of alpha bursts increase in the first year of life (Schaworonkow & Voytek, 2021), and it generally increases its energy during childhood, suggesting a rapid reconfiguration of oscillatory brain activity (Cellier et al., 2021; Hill et al., 2022; McSweeney et al., 2021).

Cumulative research indicates that relative power is parallel to changes in the oscillatory and aperiodic components of the EEG. Consequently, both types of activity likely underlie age-related changes in relative power. Nevertheless, further research is needed to unveil the relationship between relative power and aperiodic and oscillatory components as well as the differential trajectories and stability of the signal in unexplored periods of the lifespan, such as the transition between infancy and toddlerhood. Therefore, we employed our longitudinal data based on rs-EEG in four different waves (at 6, 9, 16, 18, and 36 months of age) to explore aperiodic and oscillatory changes. We isolated the aperiodic components and oscillatory power in different standard bands (theta, alpha, and beta) and compared with the trajectory of relative power. In addition, we assessed the stability and contributions of oscillatory and aperiodic components to the relative power.

We expected to replicate the changes in relative power previously reported: a reduction in the relative power in the theta and beta bands but an increase in the relative power of the alpha band. We hypothesized similar trajectories of oscillatory power (versus relative power) and the flattening of the aperiodic background curve with age. Secondly, we predicted that measurements across waves would be correlated, indicating that rs-EEG measurements would be stable during the transition from infancy to early childhood. Thirdly, we expected that relative power would capture both aperiodic and oscillatory brain activities.

3A.2. Results

3A.2.1. Early development of rs-EEG power

We computed the aperiodic and oscillatory activities using the *Specparam* toolbox (Donoghue, Haller, et al., 2020). It models the absolute power as a background curve with Gaussian peaks over it (oscillatory). To explore developmental trajectories, we employed a linear mixed model, including Time, Time Squared and Cluster as well as Time × Cluster interaction as fixed effects. In this analysis, we included the frontal, central, parietal, and occipital clusters. We included a random intercept and slope in the time variable for each participant. All information regarding the participants is shown in Table 3A.1. In the main text of this chapter, we provide a graphical representation and description of the mean of all the electrodes included in the analysis and topological maps. See the Appendix of Chapter 3A for descriptive information on the individual clusters.

3A.2.1.1. Aperiodic parameters development

The exponent of the aperiodic background significantly diminished (marginal $r^2 = .41$, conditional $r^2 = .73$; Table 3A.2, and Fig. 3A.1 and Fig. 3A.2) from the sixth to the thirty-sixth months of life (time: $\beta = -0.25$, $t(687.50) = -14.30$, $p < .001$, 95% CI = [-0.28 – -0.22]), reducing the rate of change in the later months (time squared: $\beta = 0.03$, $t(177.63) = 6.11$, $p < .001$, 95% CI = [0.02 – 0.04]). Age-related reduction over the frontal cluster was lower than that over the central area ($\beta = 0.04$, $t(691.30) = 4.73$, $p < .001$, 95% CI = [0.02 – 0.06]), but the other clusters did not differ in the linear trajectory (all ts < 2). Pairwise comparison revealed a posterior-anterior pattern with larger exponent values in the occipital than in the rest of the clusters (all zs > 9.65, all ps < .001), equal values between the parietal and central clusters ($z < 1$), and lower values in the frontal cluster than in the other areas (all zs > -9.65, all ps < .001).

Table 3A.1

Demographic information of the children included in the EEG power longitudinal analysis.

Session	Sex	*n*	Demographics			EEG		
			Age (days)	*GW*	*BW*	*Trials*	R^2	*% Electrodes*
6-mo.	*F*	39	191.11 (6.52)	38.5 (2.12)	3261.25 (718.52)	14.82 (7.95)	0.99 (0.01)	0.02 (0.13)
	M	33	196 (7.86)	38.33 (1.49)	3062.56 (696.4)	14.55 (9.3)	0.99 (0.02)	0.03 (0.16)
9-mo.	*F*	23	284.57 (10.14)	38.86 (2.03)	3292.86 (762.94)	16.87 (10.26)	0.99 (0.01)	0.01 (0.12)
	M	23	289.12 (13.63)	38.14 (1.55)	2906.86 (643.51)	12.65 (7.16)	0.99 (0.02)	0.01 (0.11)
16-mo.	*F*	25	519.6 (22.98)	37.4 (1.86)	2838 (568.19)	14.44 (8.78)	0.99 (0.01)	0.02 (0.13)
	M	21	518.75 (19.56)	38.14 (1.55)	2836.14 (598.98)	16.14 (9.32)	0.99 (0.01)	0.02 (0.15)
36-mo.	*F*	25	1117.42 (13.47)	39.2 (1.83)	3578 (502.93)	21.16 (16.67)	0.99 (0.01)	0.01 (0.11)
	M	23	1129.48 (29.33)	38.83 (1.46)	3474.17 (367.85)	28.91 (19.4)	0.99 (0.01)	0.03 (0.16)

Note. F = Female, M = Male, GW = Gestation Weeks, BW = Birth Weight, % Electrodes = Percentage of electrodes excluded due to a goodness of fit $R^2 < .950$. The table displays the mean (standard deviation).

Table 3A.2

Descriptive statistics of the aperiodic parameters.

Parameter	Sex	6-mo.	9-mo.	16-mo.	36-mo.
Exponent	*F*	2 (0.25)	1.92 (0.22)	1.83 (0.21)	1.75 (0.19)
	M	2.03 (0.25)	1.93 (0.24)	1.88 (0.2)	1.78 (0.19)
Offset	*F*	1.87 (0.26)	1.92 (0.23)	1.88 (0.24)	1.82 (0.26)
	M	1.91 (0.24)	1.94 (0.24)	1.97 (0.22)	1.84 (0.25)

Note. F = Female, M = Male. The table displays the mean (standard deviation).

The offset aperiodic parameter (marginal r^2 = .54, conditional r^2 = .83) did not change over time (time t < 2), but the change rate had a negative significant quadratic effect (time squared: β = -0.03, t(703.10) = -5.27, p < .001, 95% CI = [-0.05 – -0.02]). Furthermore, the frontal and occipital clusters had larger linear changes than the central cluster (frontal: β = 0.09, t(707.05) = 9.67, p < .001, 95% CI = [0.07 – 0.10]; occipital: β = 0.04, t(707.05) = 4.31, p < .001, 95% CI = [0.02 – 0.06]), but the linear change between the parietal and central clusters did not differ (t < 2). The frontal area had a larger offset than the central cluster (z = 2.92, p = .02), but smaller than the parietal and occipital areas (all zs < -18.77, all ps < .001). The central cluster had a lower offset than the occipital and parietal areas (all zs < -21.69, all ps < .001), and the occipital area had a larger offset than the parietal area (z = 24.34, p < .001).

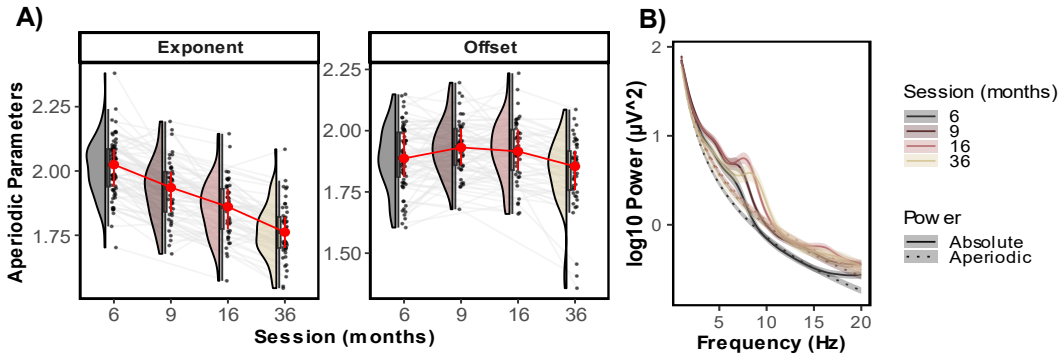

Fig. 3A.1. Slope and offset aperiodic component development. (A) Aperiodic exponent and offset development. Each dot corresponds to a participant, whereas the gray line represents the individual trajectory. (B) Absolute (solid line) and aperiodic (dashed line) power spectrum per session. The figure displays the mean and 2.5 the standard error (shaded area).

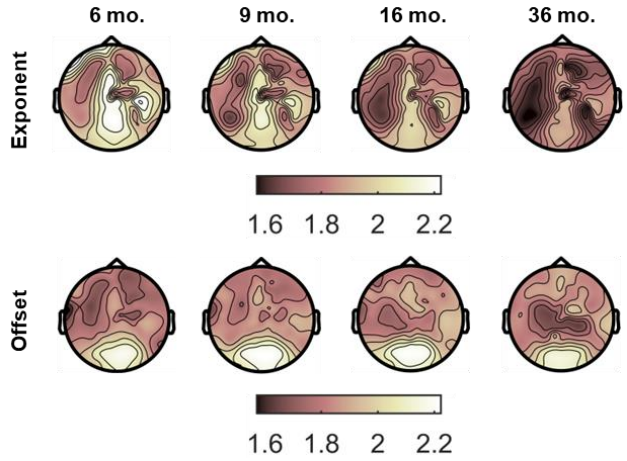

Fig. 3A.2. Topological development of the slope and offset aperiodic components.

3A.2.1.2. Oscillatory power development

Theta and Alpha Peaks

The channels with a clear theta peak (marginal r^2 = .09, conditional r^2 = .61; Table 3A.3) diminished from six months onward (time: β = -0.12, t(152.18) = -6.22, p < .001, 95% CI = [-0.16 – -0.08]), with a slower reduction over the frontal cluster (β = 0.06, t(152.18) = 3.02, p = .003, 95% CI = [0.02 – 0.10]). No other clusters differed in their linear trajectory (all ts < 2). Furthermore, there were no differences in the percentage of channels with a theta peak per cluster (all zs < 2.4, all ps > .08), except between the occipital cluster, which had a lower percentage than the frontal cluster (z = -3.88, p < .001).

Theta peak frequency (marginal r^2 = .19, conditional r^2 = .59; Fig. 3A.3) increased significantly in this period, pacing down the trajectory in later sessions (time: β = 0.63, t(518.20) = 9.81, p < .001, 95% CI = [0.50 – 0.75]; time squared: β = -0.17, t(591.63) = -7.22, p < .001, 95% CI = [-0.21 – -0.12]). The central and frontal clusters had the same increment rate (t < 2), but both the occipital (β = -0.15, t(627.98) = -4.53, p < .001, 95% CI = [-0.22 – -0.09]) and parietal (β = -0.09, t(622.13) = -2.84, p = .046, 95% CI = [-0.15 – -0.03]) clusters had slower increases in the peak frequency. The frontal cluster had a slower peak frequency than the rest of the areas (all zs < -3.26, all ps < .01). In addition,

the central cluster peak frequency was lower than that of the parietal and occipital areas (all *z*s < -4.29, all *p*s < .001), but there were no significant differences between the occipital and parietal clusters ($z < 2$, $p = 68$).

The percentage of channels that presented a peak within the alpha range (marginal $r^2 = .18$, conditional $r^2 = .57$) increased between 6 and 36 months of life (time: $\beta = 0.25$, $t(734.18) = 8.73$, $p < .001$, 95% CI = [0.19 – 0.30]), slowing down the increment in later months (time squared: $\beta = -0.08$, $t(741.58) = -8.52$, $p < .001$, 95% CI = [-0.10, -0.06]). The increment was faster in the frontal area ($\beta = 0.07$, $t(718.06) = 4.96$, $p < .001$, 95% CI = [0.04 – 0.10]) and slower over the occipital cluster ($\beta = -0.03$, $t(718.06) = -2.04$, $p = .042$, 95% CI = [-0.06 – -0.00]) than in the central cluster. There were no significant differences between clusters after correcting for multiple comparisons (all *z*s < 2).

Alpha peak frequency (marginal $r^2 = .49$, conditional $r^2 = .73$) significantly increased from 6.83 Hz to 8.4 Hz (time: $\beta = 1.47$, $t(716.20) = 17.74$, $p < .001$, 95% CI = [1.31 – 1.64]) reducing the change rate in the later months (time squared: ($\beta = -0.34$, $t(694.41) = -10.83$, $p < .001$, 95% CI = [-0.40 – -0.28]). We did not find any differences in alpha peak frequency between the clusters after correcting for pairwise comparisons (all *z*s < 2.07, all *p*s > .16). See Table 3A.3 and Fig. 3A.3.

Table 3A.3

Descriptive statistics of the power peaks per age.

	Sex	6-mo.		9-mo.		16-mo.		36-mo.	
		%.	*Freq.*	*%.*	*Freq.*	*%.*	*Freq.*	*%.*	*Freq.*
Alpha	*F*	0.87 (0.34)	6.84 (0.9)	0.95 (0.22)	7.21 (0.73)	0.99 (0.12)	7.83 (0.66)	0.96 (0.19)	8.5 (0.68)
	M	0.72 (0.45)	6.82 (1.04)	0.81 (0.4)	7.17 (0.91)	0.95 (0.22)	7.82 (0.73)	0.93 (0.26)	8.24 (0.69)
Theta	*F*	0.62 (0.49)	3.98 (0.62)	0.68 (0.47)	4.2 (0.54)	0.56 (0.5)	4.4 (0.45)	0.42 (0.49)	4.38 (0.48)
	M	0.7 (0.46)	3.97 (0.64)	0.76 (0.43)	4.18 (0.58)	0.72 (0.45)	4.26 (0.45)	0.49 (0.5)	4.33 (0.51)

Note. F = Female, M = Male. The table displays the mean (standard deviation) of the percentage of electrodes with clear oscillatory peaks and peak frequencies in the alpha and theta bands.

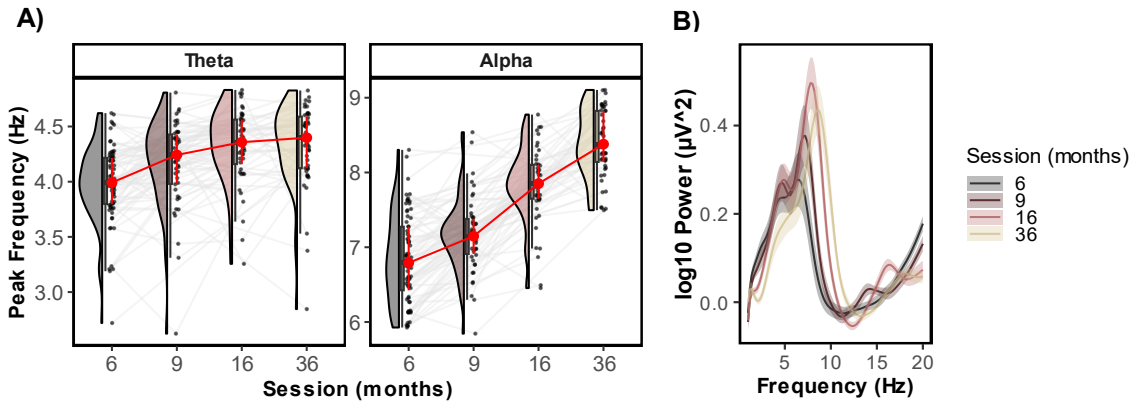

Fig. 3A.3. Peak frequency and oscillatory power development. (A) Peak frequency trajectories in theta and alpha bands. The gray lines represent the individual trajectories. (B) Oscillatory power development. The solid line represents the average per session, and the shaded area 2.5 times the standard error.

Theta Oscillatory Power

The oscillatory power in the theta band (marginal r^2 = .08, conditional r^2 = .68; Table 3A.4, Fig. 3A.4, Fig. 3A.5) neither linearly varied during this period nor had a significant quadratic effect (time: t < 1; time squared: β = -0.09, t(686.69) = -1.64, p = .101, 95% CI = [-0.19 – 0.02]). However, the occipital (β = -0.39, t(696.00) = -5.26, p < .001, 95% CI =[-0.54 – -0.25]) and parietal (β = -0.29, t(696.00) = -3.85, p < .001, 95% CI = [-0.43 – -0.14]) clusters showed a more negative linear trajectory than the central area, whereas the frontal cluster did not showed a different linear trajectory when compared to the central cluster (t < 2). Theta oscillatory power did not differ across areas after correcting for pairwise comparisons (all zs < 2.10, all ps > .15).

Alpha Oscillatory Power

Alpha oscillatory power increased significantly in this period (marginal r^2 = .23, conditional r^2 = .82) with a faster increment in the first months, followed by a paced change (time: β = 4.76, t(279.05) = 15.87, p < .001, 95% CI = [4.17 – 5.35]; time squared: β = -1.44, t(703.58) = -13.27, p < .001, 95% CI = [-1.65 – -1.23]). The frontal cluster had lower oscillatory power than the

other areas (all *z*s < -7.05, all *p*s < .001), with no other significant differences (all *z*s < 2.44, all *p*s > .07).

Beta Oscillatory Power

Beta oscillatory power (marginal r^2 = .21, conditional r^2 = .51) diminished in the study period, with a larger change in the first months (time: β = -0.72, t(792.10) = -4.05, p < .001, 95% CI = [-1.06 – -0.37]; time squared: β = 0.19, t(754.16) = 3.12, p = .002, 95% CI = [0.07 – 0.32]). The frontal cluster displayed a larger reduction (β = -0.37, t(694.45) = -3.98, p < .001, 95% CI = [-0.56 – -0.19]), but no other trajectories varied (all *t*s < 2). Furthermore, the frontal cluster had larger power than the other areas (all *z*s > 8.47, all *p*s < .001). In addition, the central and parietal clusters had larger powers than the occipital clusters (all *z*s < 2.94, all *p*s < .02), but they did not differ significantly (*z* < 2).

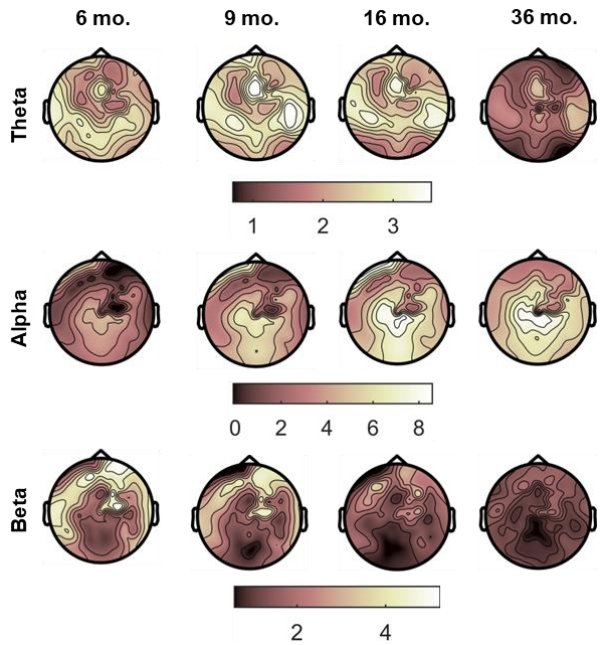

Fig. 3A.4. Topological development of oscillatory power.

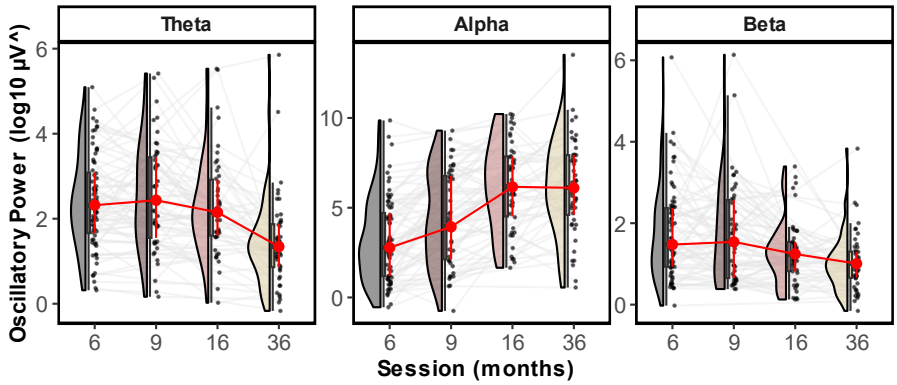

Fig. 3A.5. Oscillatory power development per frequency band. Each dot corresponds to a participant, and the gray lines represent individual trajectories.

3A.2.1.3. Relative power development

Theta Relative Power

The relative power in the theta band (marginal r^2 = .34, conditional r^2 = .77; Table) significantly decreased with age (time: β = -0.97, t(658.36) = -13.79, p < .001, 95% CI = [-1.11 – -0.83]) but paced the reduction rate in the later sessions (time squared: β = 0.21, t(677.26) = 7.74, p < .001, 95% CI = [0.16 – 0.26]). The central cluster presented a larger theta relative power than the rest of the areas (all zs > 3.44, all ps < .001), without any other significant pairwise comparison (all zs < 2.23, all ps < .11). See Fig. 3A.6 and 3A.7.

Alpha Relative Power

Alpha relative power (marginal r^2 = .28, conditional r^2 = .83) increased significantly (time: β = 5.14, t(211.08) = 18.58, p < .001, 95% CI = [4.59 – 5.68]) with a negative quadratic effect (time squared: β = -1.55, t(684.37) = -17.47, p < .001, 95% CI = [-1.72 – -1.37]). The linear trajectory did not interact significantly with the Cluster variable (all ts < 1). The frontal cluster had less relative power than other areas (all zs < -2.76, all ps < .01), but no other differences between clusters were found (all zs < 2.20, all ps > .12).

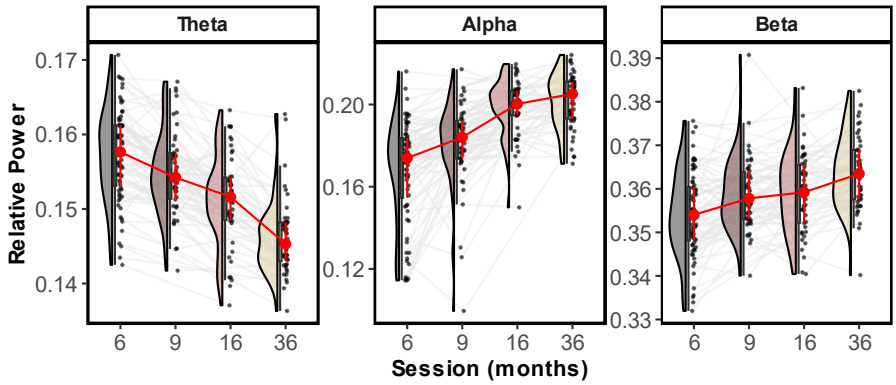

Fig. 3A.6. Relative power development per frequency band. The gray lines represent the individual trajectories, and the red line represents the average trajectory. Each dot corresponds to one participant.

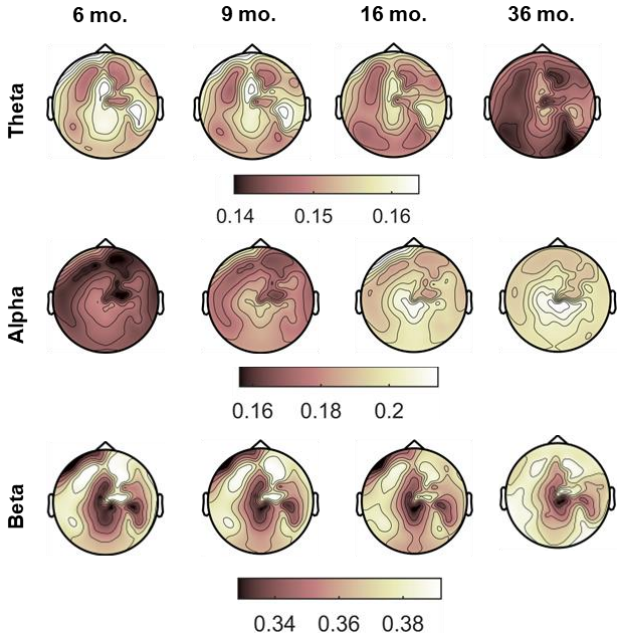

Fig. 3A.7. Topological development of relative power.

Table 3A.4

Descriptive statistics of oscillatory power per session and band.

z	Sex	Theta				Alpha				Beta			
		6-mo.	*9-mo.*	*16-mo.*	*36-mo.*	*6-mo.*	*9-mo.*	*16-mo.*	*36-mo.*	*6-mo.*	*9-mo.*	*16-mo.*	*36-mo.*
Oscillatory	*F*	2.28	2.35	2.33	1.4	3.68	5.01	6.89	6.43	1.7	1.4	1.18	1.14
		(1.56)	(1.57)	(1.51)	(1.48)	(2.85)	(2.79)	(2.92)	(2.92)	(2.47)	(2.05)	(1.67)	(1.51)
	M	2.54	2.73	2.31	1.52	2.63	3.88	5.41	5.93	1.78	2.03	1.42	0.92
		(1.36)	(1.59)	(1.45)	(1.21)	(2.65)	(3.43)	(3.31)	(3.56)	(2.47)	(2.82)	(1.93)	(1.38)
Relative	*F*	15.62	15.34	15.01	14.53	16.85	18.24	20.2	20.24	35.45	35.82	35.93	36.44
		(0.98)	(0.84)	(0.88)	(0.75)	(2.57)	(2.31)	(1.29)	(1.41)	(2.46)	(2.04)	(2.01)	(1.96)
	M	15.85	15.6	15.25	14.72	16.71	17.89	19.39	20.07	35.36	35.93	35.85	36.26
		(0.85)	(0.85)	(0.77)	(0.73)	(2.59)	(2.25)	(1.86)	(1.64)	(2.29)	(2.2)	(1.97)	(2.05)

Note. F = Female, M = Male. The table displays the mean (standard deviation) of the participants included in the linear mixed models.

Beta Relative Power

The relative power in the beta band (marginal r^2 = .34, conditional r^2 = .63) significantly increased (time: β = 0.59, t(771.52) = 3.73, p < .001, 95% CI = [0.28 – 0.90]) with slower change in later sessions (time squared: β = -0.14, t(727.20) = -2.46, p = .014, 95% CI = [-0.26, -0.03]). The occipital (β = 0.27, t(703.29) = 3.29, p = .001, 95% CI = [0.11 – 0.44]) and parietal (β = 0.26, t(703.29) = 3.12, p = .002, 95% CI = [0.10 – 0.43]) clusters had larger linear changes than the central cluster, but the frontal area did not vary (t < 1). The frontal cluster had a larger relative power than the rest of the areas (all zs > 7.88, all ps < .001), and the central cluster had an increased relative power in comparison to the parietal and occipital clusters (all zs > 11.51, all ps < .001). No differences were found between occipital and parietal clusters (z = 1.5, p = .44).

3A.2.2. Spatial and within-participant stability

To determine the stability of the electrophysiological measures, we first conducted Spearman rank correlations in pair waves (e.g., 6-to-9-mo. sessions) for the electrodes (i.e., spatial stability) in all variables (e.g., exponent, offset). If this analysis revealed spatial stability between sessions, we then conducted intra-individual variability over the average of the electrodes (i.e., subject values over time). Otherwise, we separately correlated the inter-individual variability for each cluster. See Table 3A.5 for descriptive statistics of the sample included in the stability analysis.

3A.2.2.1. Spatial stability

The spatial stability of the aperiodic parameters was high, independent of the session pair and the variable tested (slope: r_s > .91, all ps < .001; offset: r_s > .74, all ps < .001). Furthermore, spatial stability was significant (r_s > .54, all ps < .001; Table 3A.6 and Table 3A.7) for all power parameters (oscillatory and relative) and frequency bands (theta, alpha, and beta).

Table 3A.5

Demographic information of the participants included in the stability analysis.

Waves	Demographics				EEG		
	N (female)	*BW*	*GW*	*Age*	*Trials*	R^2	*% Electrodes*
6-mo. – 9-mo.	68 (32)	3.08 (0.65)	38.9 (1.97)	*6-mo.:* 195.86 (7.91) *9-mo.:* 285 (12.57)	*6-mo.:* 14.51 (8) *9-mo.:* 14.44 (8.93)	*6-mo.:* .99 (0) *9-mo.:* .99 (.01)	*6-mo.:* .03 (0.04) *9-mo.:* .03 (0.05)
9-mo. – 16-mo.	32 (16)	2.79 (0.67)	37.8 (1.7)	*9-mo.:* 284.55 (13) *16-mo.:* 517.18 (22.27)	*9-mo.:* 14.41 (8.41) *16-mo.:* 15.81 (10.39)	*9-mo.:* .99 (.01) *16-mo.:* .99 (0)	*9-mo.:* .04 (0.06) *16-mo.:* 0.01 (0.01)
16-mo. – 36-mo.	26 (14)	3.27 (0.31)	38.57 (1.81)	*16-mo.:* 525 (22.84) *36-mo.:* 1121.27 (23.17)	*16-mo.:* 17.65 (10.45) *36-mo.:* 27.31 (19.05)	*16-mo.:* .99 (.01) *36-mo.:* .99 (.01)	*16-mo.:* 0.01 (0.02) *36-mo.:* 0.01 (0.02)

Note. BW = Birth Weight (kg), GW = Gestation Weeks, Age (days). % Electrodes = Percentage of electrodes excluded due to a goodness of fit $R^2 < .950$. The table displays the mean (standard deviation).

Table 3A.6

Spatial stability in the relative and oscillatory power.

	Waves	Theta	Alpha	Beta
Oscillatory Power	*6-mo. – 9-mo.*	0.78*** [0.75 - 0.8]	0.97*** [0.97 - 0.98]	0.92*** [0.91 - 0.93]
	9-mo. – 16-mo.	0.84*** [0.82 - 0.85]	0.98*** [0.98 - 0.98]	0.87*** [0.86 - 0.89]
	16-mo. – 36-mo.	0.71*** [0.67 - 0.74]	0.88*** [0.86 - 0.89]	0.77*** [0.74 - 0.8]
Relative Power	*6-mo. – 9-mo.*	0.95*** [0.94 - 0.95]	0.98*** [0.98 - 0.98]	0.98*** [0.98 - 0.99]
	9-mo. – 16-mo.	0.92*** [0.91 - 0.93]	0.98*** [0.98 - 0.98]	0.96*** [0.95 - 0.96]
	16-mo. – 36-mo.	0.78*** [0.75 - 0.8]	0.86*** [0.85 - 0.88]	0.84*** [0.82 - 0.86]

Note. All correlations had N = 109, which was equal to the number of electrodes. The table displays the Spearman's rank correlation results [95% CI] obtained by correlating the average values of the electrodes between the sessions in each frequency band. Confidence intervals were computed using 1000 bootstrap replicates. *** $p < .001$.

Table 3A.7

Spatial stability of the aperiodic components.

Waves	Offset	Exponent
6-mo. - 9-mo.	0.98*** [0.97 - 0.98]	0.98*** [0.98 - 0.98]
9-mo. - 16-mo.	0.74*** [0.7 - 0.76]	0.91*** [0.9 - 0.92]
16-mo. - 36-mo.	0.84*** [0.82 - 0.86]	0.9*** [0.89 - 0.91]

Note. All correlations had N = 109, which was equal to the number of electrodes. The table displays the Spearman's rank correlation results [95% CI] obtained by correlating the average values of the electrodes between the sessions in each frequency band. Confidence intervals were computed using 1000 bootstrap replicates. *** $p < .001$.

3A.2.2.2. Within-participant stability

Given the high spatial stability, we correlated the individual values of each participant between sessions. Previous values in aperiodic components positively predicted the next session in all the pairs of sessions and condition (r_s > .35, all *p*s < .05). On average, relative power was positively related between all the pairs of sessions (r_s > .37, all *p*s < .05), except beta between 9 and 16 months of life (r_s = .12, *p* > .05) and alpha between 16 and 36 months of life (r_s = .24, *p* > .05). Oscillatory power was generally correlated between sessions in all combinations (r_s > .4, all *p*s < .05). See Tables 3A.7 and 3A.8.

3A.2.3. Aperiodic and oscillatory contributions to the relative power

We used a hierarchical linear mixed model to study the contributions of aperiodic and oscillatory powers to relative power, including Time and Time Squared, to control for age-related changes. The models were constructed using a bottom-up strategy, first testing the aperiodic contribution (offset and exponent), and then the oscillatory power. We selected the fittest model based on the AICc.

The theta band (marginal r^2 = .83, conditional r^2 = .89) was positively related to the exponent (β = 1.50, *t*(305.99) = 9.58, *p* < .001, 95% CI = [1.19 – 1.81]) and oscillatory power (β = 0.38, *t*(303.12) = 24.59, *p* < .001, 95% CI = [0.35 – 0.41]), but not with the offset (*t* < 1). Alpha relative power (marginal r^2 = .49, conditional r^2 = .60) was only significantly predicted by oscillatory power (β = 0.36, *t*(268.75) = 8.68, *p* < .001, 95% CI = [0.28 – 0.44]; aperiodic parameters: all *t*s < 2). Finally, relative power in the beta band (marginal r^2 = .59, conditional r^2 = .70) was positively related to beta oscillatory power (β = 0.52, *t*(305.83) = 13.53, *p* < .001, 95% CI = [.44, - .59]), but negatively related to both offset (β = -1.71, *t*(282.91) = -5.14, *p* < .001, 95% CI = [-2.36 – -1.06]) and exponent (β = -2.87, *t*(297.43) = -7.84, *p* < .001, 95% CI = [-3.59 – -2.15]) aperiodic components.

Table 3A.8

Within-participant stability in relative and oscillatory power.

	Waves	*n*	Theta	Alpha	Beta
Osc. Power	*6-mo. – 9-mo.*	79	0.59*** [0.53 -0.63]	0.58*** [0.53 - 0.63]	0.41*** [0.34 - 0.47]
	9-mo. – 16-mo.	39	0.33* [0.22 - 0.42]	0.6*** [0.52 - 0.67]	0.41* [0.31 - 0.5]
	16-mo. – 36-mo.	30	0.53** [0.43 - 0.62]	0.44* [0.33 - 0.54]	0.44* [0.33 - 0.54]
Rel. Power	*6-mo. – 9-mo.*	79	0.49*** [0.42 - 0.54]	0.33** [0.26 - 0.4]	0.47*** [0.4 - 0.52]
	9-mo. – 16-mo.	39	0.45** [0.36 - 0.53]	0.41** [0.31 - 0.5]	0.31 [0.21 - 0.41]
	16-mo. –36-mo.	30	0.43* [0.32 - 0.53]	0.23 [0.1 - 0.35]	0.37* [0.25 - 0.47]

Note. Osc. = Oscillatory, Rel. = Relative. The table displays Spearman's rank correlation results [95% CI]. Confidence intervals were computed using 1000 bootstrap replicates. * $p < .05$. ** $p < .01$. *** $p < .001$.

Table 3A.9

Within-participant stability in aperiodic components.

Waves	Offset	Exponent
6-mo. - 9-mo.	0.56*** [0.51 - 0.61]	0.57*** [0.52 - 0.62]
9-mo. - 16-mo.	0.42** [0.32 - 0.51]	0.36* [0.26 - 0.45]
16-mo. - 36-mo.	0.63*** [0.55 - 0.71]	0.36* [0.26 - 0.45]

Note. The table displays Spearman's rank correlation results [95% CI]. Confidence intervals were computed using 1000 bootstrap replicates. * $p < .05$. ** $p < .01$. *** $p < .001$.

3A.3. Discussion

The goal of this study was to understand the developmental trajectory of relative power, oscillatory, and aperiodic components and evaluate their stability in baseline rs-EEG in infants. In addition, we examined the contributions of the oscillatory power and aperiodic exponent and offset to relative power. Our results replicated earlier results (e.g., reduction in theta relative power) and expanded previous findings suggesting differential developmental curves when power was isolated from an aperiodic background. Additionally, the relative, oscillatory, and aperiodic components were stable across sessions, suggesting a large within-participant relationship with age. Finally, only alpha oscillatory activity was the main predictor of relative power, whereas the other bands incorporated aperiodic components.

3A.3.1. EEG power development

The offset did not change with age in our study, whereas the aperiodic exponent decreased with age in the four waves, slowing down the reduction change over time. This supports previous results in infants and children as well as the initial hypothesis, and signals a marked trajectory in the first years of life of the aperiodic exponent (Cellier et al., 2021; Donoghue, Haller, et al., 2020; Hill et al., 2022; McSweeney et al., 2021; Schaworonkow & Voytek, 2021; Voytek et al., 2015).

Our results showed that the aperiodic background curve flattens between 6 and 36 months of age (i.e., aperiodic curve power decays slower in older children). This suggests a change toward more excitatory activity in the excitatory/inhibitory balance (Gao et al., 2017; Voytek & Knight, 2015), which has been proven from adolescence to adulthood (Perica et al., 2022). Interestingly, the exponent and offset displayed an anterior-posterior pattern with larger intercepts in the posterior areas and a steeper aperiodic power curve. This may be related to protracted development in the frontal areas.

Contrary to our general prediction of similar development of relative power and oscillatory power, the development of relative power compared with periodic power displayed variations in theta and beta bands, and only was similar in the alpha band. First, the relative power in theta diminished

between 6 and 36 months of age, whereas theta oscillatory power did not exhibit age-related changes. Similarly, beta relative power increased with age, whereas oscillatory power diminished during the same period. Additionally, the channels with a clear alpha peak augmented in the studied period, whereas both the alpha and theta peaks increased the peak frequency. This is probably related to the maturation of the white matter, as previously suggested (Caffarra et al., 2022).

The developmental trajectories in relative power were similar to those in previous experiments with infants: a reduction in theta relative power and an increment in alpha relative power (Marshall et al., 2002; Orekhova et al., 2006; Stroganova et al., 1999). However, the beta results aligned with those of other studies that found an increase in absolute power (Wilkinson et al., 2023) but differed from to those of Tierney et al. (2012) that found a reduction of beta relative power. One difference is the nature of the relative power (vs. absolute), as well as the range employed (we removed from 21 Hz onward), which may explain the differences between our study and Tierney et al. (2012) findings.

When we isolated the oscillatory power over the power spectrum, only the alpha band showed the same results as in the earlier experiments with relative and absolute power (e.g., Marshall et al., 2002). This increment is consistent with age-related variations in the burst activity of the alpha band (Schaworonkow & Voytek, 2021). Additionally, the peak frequency in our study remained in the so called infant alpha range (Marshall et al., 2002; Orekhova et al., 2001; Stroganova et al., 1999) and given the trajectory found, alpha peak will likely achieve adult frequencies in childhood as found in previous experiments (Cellier et al., 2021; Freschl et al., 2022). One general aspect of relative and oscillatory power in our study was the quadratic shape of the developmental curves. Other studies have found larger changes in the first few months, followed by a reduction in the maturation rate. This has leaded to suggest the presence of two different developmental slopes (Bethlehem et al., 2022; Wilkinson et al., 2023).

3A.3.2. EEG power stability

The aperiodic measures were generally stable, with the distribution of values across electrodes and individual differences being constant throughout the sessions. Like the aperiodic components, rs-EEG relative and oscillatory power measurements were stable during the transition between infancy and early childhood. This stability was both spatial and within-participant, with only a few exceptions between the second and third (beta relative) and the third and fourth (alpha relative) sessions. This shows that earlier power distribution is a good predictor of the functional activity topology of the following sessions and that individual values are somehow predictive of future brain activity. Therefore, rs-EEG measures might be considered a fingerprint of individual brain activity (Demuru & Fraschini, 2020).

The stability results found aligns with previous research showing the stability of alpha relative power between 10 and 14 months and between 14 and 24 months of age, but not between 5 and 10 months of age (Marshall et al., 2002). These differences might be due to the increase in the age at the first session (from 5 to 6 months), which suggests that the EEG becomes more stable during this period. Another plausible explanation is the computation of the frequency range for each band. We focused on the alpha and theta peaks to capture inter-individual variability in our sample. For this reason, we computed the area around the peak based on the FWHM of each peak and children with a resolution of 0.2 Hz. This might have contributed to determining the stability between sessions, as each participant had its own frequency range in each band and this method also considered the Gaussian curve shape above the aperiodic background curve. In fact, the Gaussian width changes depending on the burst and rhythmic properties of the frequency (Ede et al., 2018). Thus, this range construction also accounts for the type of oscillation underlying the power spectrum to some extent.

The fact that the aperiodic power was more stable than the relative power supports the idea of the sensitivity of these measurements to individual variations and their distinctiveness in adults (Demuru and Fraschini, 2020). However, the lack of correlation between months 9-months-old and 16-months-old and 16-months-old to 36-months-old may be due to

the sample size of those analyses and the separation between sessions (e.g., $n_{9 \text{ to } 16 \text{ months}} = 32$).

3A.3.3. Contributions of aperiodic and oscillatory activity to relative power

The relative power was a mixture of oscillatory and aperiodic components in most frequency bands. Theta and beta relative powers were predicted by the exponent (theta) and both the exponent and offset in the case of beta band. Only alpha was explained by oscillatory power, without considering the contribution of other aperiodic components. Therefore, the relative power captured the oscillations above the aperiodic background activity; however, this was usually a mixture of aperiodic and periodic power.

Our results are consistent with those of an earlier study by Donoghue et al. (2020). They compared the correlation between aperiodic parameters and periodic power to several power ratios (e.g., theta/beta) with data from the MIPDB project and found that alpha ratios were more correlated with the direct power of alpha than aperiodic parameters; however, the opposite pattern appeared when the ratios did not include the alpha frequency band (e.g., theta/beta).

Our results also indicate that age-related changes in alpha power might bias the results of the rest of the frequency bands when computing relative power. In other words, the large increment in alpha energy seen in early development probably overshadows age-related changes in the periodic power of other frequency bands when the relative power is used.

3A.3.4. Limitations

The current study focused on the early development of rs-EEG power in different frequency bands, disentangling the aperiodic and oscillatory components from the theta to beta bands. Therefore, our range of frequencies was narrower than that in other studies with adults and children, as we were forced to remove +20 Hz owing to artifacts (see Rico-Picó et al., 2023 to explore these details). This is a constant problem in awake infant neuroimaging studies, as previous experiments has also found better fits after removing high-frequency bands (e.g., Schaworonkow & Voytek, 2021).

However, studies on asleep infants did not present these artifacts, revealing the difficulty of this study (Fransson et al., 2013).

Regarding the preprocessing, we wanted to compare the oscillatory power and aperiodic components of the signal to relative power in a classical approach. We anchored the frequency to the ITF and IAF over the corrected power spectrum by removing the aperiodic components, but we did not find a beta peak. Other studies have employed lagged-coherence measurements to reveal the beta peak, as it is less sensitive to muscular noise (Rayson et al., 2022). Additionally, even when we considered the brain power to be oscillatory and aperiodic, we assumed that the rs-EEG is a stationary signal. It is well known that the shapes of waves differ in each frequency band (Cole & Voytek, 2019). There is the possibility that our approach might be insufficient for capturing all the properties of the oscillatory power. In addition, oscillatory activity occurs in both sustained and phasic ways (Zich et al., 2020), and the amplitude of the burst may vary differently from the oscillatory power, even when the aperiodic background is removed. We explore these possibilities in the Appendix of Chapter 3A.

As infant protocols usually incorporate an active baseline, they cannot be considered to be purely at rest (Camacho et al., 2020). In fact, there are differences in oscillatory power development between open- and closed-eye development (Hill et al., 2022). Although this might be beneficial because an active baseline likely captures the general cognitive state when infants are awake, it hinders the comparison with adult rs-EEG studies. Complementing EEG recordings with other behavioral and peripheral registers could provide valuable insights to increase comparability between lifespan periods (Xie et al., 2018).

3A.4. Conclusion

Computing the relative power is one of the most common choices for studying rs-EEG signals in young samples. Patterns of the relative power of different frequency bands show rapid changes in the early years of life and are associated with the risk of cognitive development and neurodevelopmental disorders. Although it is usually assumed that the relative power purely represents oscillatory activity, the EEG signal conflates

aperiodic activity. Our results indicated that relative power development is partially driven by age-related changes in aperiodic activity, at least during the transition from infancy to early childhood. Therefore, the relative power probably captures both the aperiodic and oscillatory activities of the EEG power instead of the putative oscillations. This highlights the necessity of incorporating more fine-grained measurements of EEG power to unveil the mechanism underlying brain maturation and its relationship to cognitive processes.

Chapter 3B: Development of the EEG connectome

During the first three years of life, the human brain undergoes profound structural and functional changes (Collin & Heuvel, 2013; Gilmore et al., 2018). In the first postnatal month, brain volume and gray matter dramatically increase (Bethlehem et al., 2022; Knickmeyer, 2008) with unparallel changes in white matter (Miller, 2012; Ouyang et al., 2019, 2019). Changes in white matter paths result in the refinement of structural circuitry (Dubois, 2014; Stephens et al., 2020) followed by the emergence of functional brain networks (Gilmore et al., 2018; Vértes & Bullmore, 2015; Zhao, Xu, et al., 2019).

The study of functional network development has proliferated rapidly, owing to advances in neuroimaging techniques. In recent decades, the connectome concept of the human brain has also helped unveil the age-related reorganization of functional networks. This framework employs the graph theory to determine the topological properties of brain networks (Watts & Strogatz, 1998). It considers the brain as a group of nodes (e.g., gray matter, sensors) interconnected by edges (e.g., co-fluctuation of BOLD signal, coherence), which permits the use of common mathematical principles independently of the network scale.

The human brain possesses non-trivial topological characteristics that promote its efficiency (Bullmore & Sporns, 2012), including small-world architecture (Achard & Bullmore, 2007; Bassett & Bullmore, 2017; Vaessen et al., 2010), modular distribution (Alexander-Bloch et al., 2013; Salvador et al., 2005), and hub presence (He & Evans, 2010; van den Heuvel & Sporns, 2013; Tomasi & Volkow, 2011). Brain network connections are mostly short-range (vs. long-range), clustered within proximal areas to create specialized modules that are connected by long-range edges (Salvador et al., 2005). This maintains an optimal balance between wiring cost and flow integration (Bullmore & Sporns, 2012). Furthermore, most edges pass through a handful of nodes (hubs) that account for most of the connections and are interconnected between them. This permits the rapid and flexible reconfiguration of functional networks throughout the so-called rich-blub community (van den Heuvel & Sporns, 2011)

Functional networks emergence has been mainly explored using fMRI technique in the first years of life (Grayson & Fair, 2017; Vértes &

Bullmore, 2015). There is evidence that BOLD signal between brain areas co-fluctuate functionally in preterm infants at birth (Fransson et al., 2007; Smyser et al., 2010). However, the resultant networks are fragmented, except for the primary networks that are already delineated in neonates (Cao et al., 2017; Fransson et al., 2011). However, high-order networks gradually emerge in the first two years of life (Gao, Alcauter, Elton, et al., 2015; Gao, Alcauter, Smith, et al., 2015; Power et al., 2010), albeit with further refinements beyond early childhood (Dosenbach et al., 2010; Fair et al., 2009). At birth, the functional networks of neonates already follow a small-world topology (Asis-Cruz et al., 2015), are separated into modules (Wen et al., 2019), and possess hubs, whilst placed in more posterior areas in comparison to adults (Ball et al., 2014; Cao et al., 2016). In the following months, the brain modules became more segregated while reinforcing hub connections (Ball et al., 2014). This process results in an increase in clustering/local and global efficiency in the first few years (Zhao et al., 2019), which expands beyond childhood (Cao et al., 2014; Fair et al., 2008, 2009).

One limitation of fMRI is its low temporal resolution. Brain function occurs at different frequency speeds, creating micro- and macroscale functional circuits through coherence and phase synchrony (Buzsáki, 2006; Fries, 2015; Vinck et al., 2023). Furthermore, due to the invasiveness of fMRI (versus EEG/fNIRS), most studies have been conducted in slept/sedated infants. As a consequence, functional networks in fMRI resemble more to those of sleep (vs. awake) adults (Mitra et al., 2017). Therefore, alternative techniques such as EEG may complement previous fMRI studies.

To date, few studies have explored early connectome development using EEG (e.g., Xie et al., 2019). EEG networks in neonates display clustered connections over the anterior and posterior areas, and present a small-world-like topology (Omidvarnia et al., 2014; Tóth et al., 2017). Additionally, classic studies on the connectivity strength unveiled increases in the coherence between electrodes during development (Barry et al., 2004; Chu et al., 2015). However, the development of EEG connectome in the first few years of life remains unclear. Only two cross-sectional studies have explored this, with one finding a refinement in segregation and small-world (Xie et al., 2019) and other stable connectome parameters (Hu et al., 2022). Results beyond early

childhood are also mixed, reporting a larger segregation with age (Boersma et al., 2011; Kavčič et al., 2023) but either an improvement or decrease in integration cost depending on network construction choices (Miskovic et al., 2015; Smit et al., 2012, 2016).

Previous evidence suggests rapid changes in EEG networks with age, but current evidence is limited. In addition, studies have varied in electrode number and connectivity measures and were cross-sectional, which may have promoted previous inconsistencies. In this study, we addressed these limitations by performing a multiverse analysis of a longitudinal sample from infancy to early childhood. We then delineated the development of a functional network with the most consistent results obtained in the multiverse. We expected different trajectories according to the connectivity measures despite a general increase in connectivity strength. We further hypothesized the development of the functional networks towards a more segregated and modular yet efficiently integrated pattern of connectivity but only in some connectivity measures. Finally, we predicted that networks will be modular a present a small-world topology, and this topology will be promoted with the efficiency changes, but depending on the construction parameters of the network.

3B.2. Results

From the longitudinal sample, we included children who had at least two waves with valid data and two missing (valid $N = 85$) waves among the four waves included in the study (Table 3B.1; see also Appendix Fig. A3B.1 and Table A3B.1). The baseline EEG data were recorded using a high-density geodesic net. We then computed connectivity based on the phase lag (dwPLI and wPLI; Stam et al., 2007; Vinck et al., 2011) and imaginary coherence (iCoh; Nolte et al., 2004) measurements (Bastos & Schoffelen, 2016). We explored age-related changes in edge strength and network efficiency (global and local; Latora & Marchiori, 2001), small-world propensity (Muldoon et al., 2016), participation coefficient (Guimera & Amaral, 2005), and modularity (Newman, 2006) for a network density ranging from .15 to .35 with .05 increments. First we conducted a multiverse analysis (Fig. 3B.1) and then delineated the development of the network with the largest age-related changes.

Table 3B.1

Demographic information of the sample included in the analysis of the development of functional network.

Sex	*n*	BW	GW	Session Age (days)				Epoch Number			
				6-mo.	*9-mo.*	*16-mo.*	*36-mo.*	*6-mo.*	*9-mo.*	*16-mo.*	*36-mo.*
F	41	3.2 (0.37)	39.26 (1.38)	194.03 (9.29)	286.56 (10.43)	511.79 (19.94)	1121.1 (35.4)	271.24 (108.54)	269.81 (97.23)	247.68 (106.65)	309.05 (135.07)
M	44	3.38 (0.51)	39.56 (1.42)	193.1 (9.45)	283 (8.15)	512.61 (27.07)	1109.1 (20.7)	286 (124.02)	244.47 (93.66)	293.95 (151.99)	396.64 (81.28)

Note. F = Female, M = Male. The table displays the mean (SD) of birth weight (Kg; BW), gestational weeks (GW), age in the session, and epoch number.

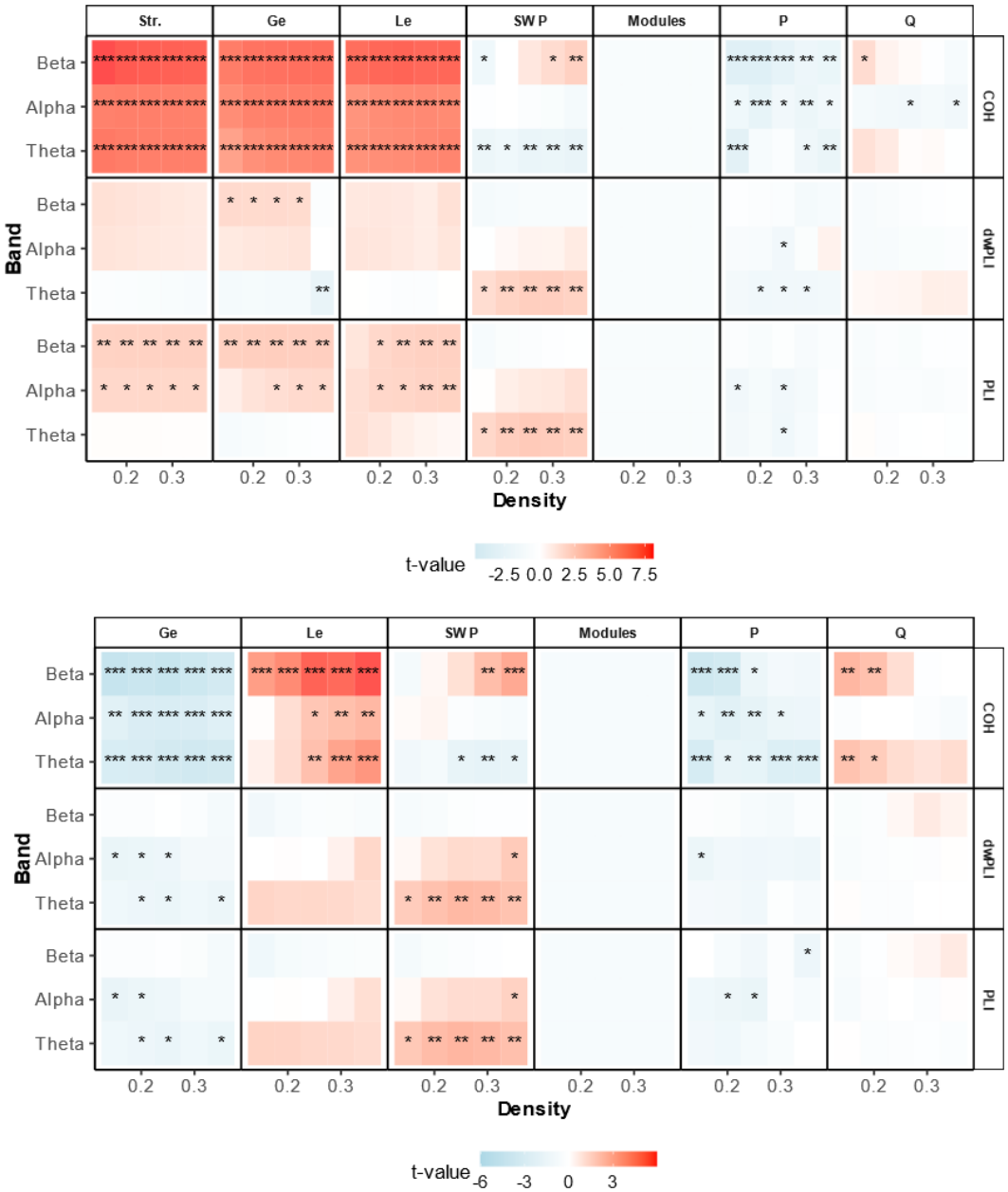

Fig. 3B.1. Multiverse analysis of network development. The figure displays the t-values of the time fixed effect in the linear mixed models divided by network parameters, band, and connectivity measures in the weighted (top) and binary (bottom) networks. Str. = strength, Ge = global efficiency, Le = local efficiency, SWP = small-world propensity, Modules = number of modules, P = Participation Coefficient, Q = Modularity. * $p < .05$, ** $p < .01$, *** $p < .001$.

3B.2.1. Development of electrophysiological brain network: a multiverse approach

Age-related network changes was explored using linear mixed models, including Time, and Time Squared as fixed effects, and subjects as random intercepts. We report the t-value statistic of the linear change as a proxy for time variations in Fig. 3B.1 (see Fig. A3B.2 in the Appendix of Chapter 3B). Connectivity strength increased in iCoh and PLI (alpha and beta) but remained constant in dwPLI. Both PLI and iCoh showed similar increases in global and local efficiencies. Small-world propensity increased in PLI/dwPLI (theta) and decreased in iCoh in the theta band. The participation coefficient of the nodes decreased in the iCoh measures, but not in the dwPLI/PLI measures. The number of modules and modularity did not change with age.

Binary networks showed similar patterns in participation coefficient and small-world propensity. However, local, and global efficiencies decreased in coherence-based binary networks and the PLI/dwPLI efficiency measures remained stable. Given the larger reconfiguration found in iCoh, we selected this connectivity measure (density = .25, weighted edges) to further analyze the development of electrophysiological networks.

3B.2.2. Network efficiency, centrality, and small-world topology development

The coherence-based network topology (Fig. 3B.2) presented two clusters over the posterior and frontal areas connected by long-range connections in alpha and theta, whereas beta band connectivity had a sparser connection pattern. The node degree and betweenness centrality (Fig. 3B.3) distribution was truncated to lower values, with a handful of nodes accounting for most connections in all frequency bands. The network descriptives can be found in Appendix Table A3B.2.

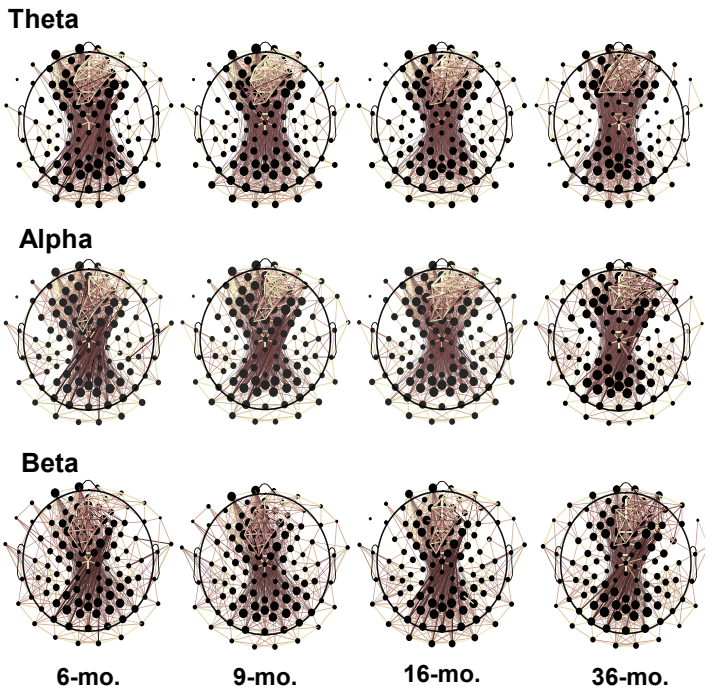

Fig. 3B.2. Network topology development. The figure displays pairwise connections of the top 25% of edges in the iCoh connectivity matrix averaged over the participants. Colors represent the strength of the connections, while the size of the nodes the degree. Lighter edges (vs. blacker or browner) represent stronger connections, and a larger node size indicates a higher node degree.

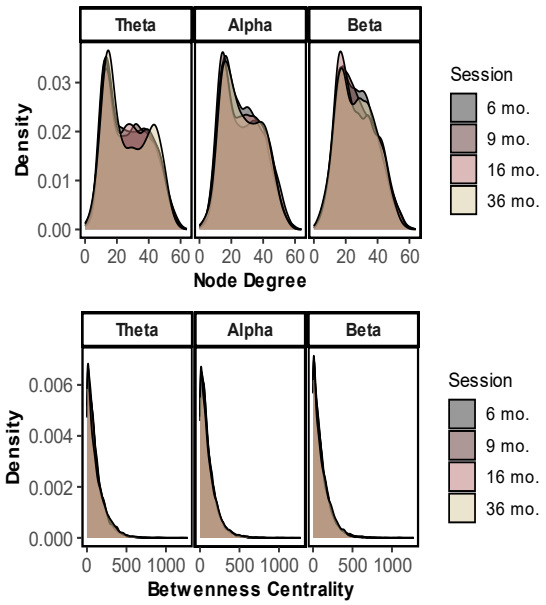

Fig. 3B.3. Node degree and betweenness centrality. The figure shows the proportion of nodes that had a given number of connections (node degree) or were crossed by a determined number of shortest path lengths (betweenness centrality).

Global Efficiency

The global efficiency (Fig. 3B.4 and Fig. 3B.5) increased with a negative quadratic effect in all the frequency bands: theta (marginal R^2 = .12, conditional R^2 = .34; time: β = 0.03, t(160.32) = 5.59, p < .001, 95% CI = [0.02 – 0.04]; time squared: β = -0.01, t(164.34) = -4.91, p < .001, 95% CI = [-0.01 – -0.01]), alpha (marginal R^2 = .17, conditional R^2 = .41; time: β = 0.04, t(159.38) = 6.35, p < .001, 95% CI = [0.03 – 0.05]; time squared: β = -0.01, t(163.05) = -5.17, p < .001, 95% CI = [-0.02 – -0.01]), and beta (marginal R^2 = .33, conditional R^2 = .54; time: β = 0.04, t(115.84) = 6.87, p < .001, 95% CI = [0.03 – 0.06]; time squared: β = -0.01, t(118.63) = -4.44, p < .001, 95% CI = [-0.02 – -0.01]).

Local Efficiency

The local efficiency (Fig. 3B.4 and Fig. 3B.5) linearly augmented with a negative quadratic effect independently of the frequency band studied: theta (marginal R^2 = .16, conditional R^2 = .81; time: β = 0.06, t(59.36) = 9.50, p < .001, 95% CI = [0.05 – 0.08]; time squared: β = -0.02, t(983.44) = -9.63, p < .001, 95% CI = [-0.02 – -0.02]), alpha (marginal R^2 = .15, conditional R^2 = .90 ; time: β = 0.08, t(60.76) = 10.06, p < .001, 95% CI = [0.07 – 0.10]; time squared: β = -0.02, t(1278.20) = -11.65, p < .001, 95% CI = [-0.03 – -0.02]), and beta (marginal R^2 = .24, conditional R^2 = .85; time: β = 0.09, t(64.60) = 13.30, p < .001, 95% CI = [0.08 – 0.11]; time squared: β = -0.02, t(1095.17) = -11.86, p < .001, 95% CI = [-0.03 – -0.02]). In the theta band, the temporal area had a larger linear increase than the rest of the clusters (β = 0.01, t(1031.70) = 2.68, p = .007, 95% CI = [0.0 – 0.01]), but no other differences were found (ts < 2). In the alpha band, the frontal and frontal-pole areas had smaller increments than the central cluster (β = [-0.01 – -0.02], all ts(1086.76) = -2.22, all ps < .027, 95% CI = [-0.02 – -0.00]), while the temporal cluster displayed the opposite pattern (β = 0.01, t(1086.76) = 2.08, p = .038, 95% CI = [0.00 – 0.01]). No other interactions were significant (all ts < 2). In the beta band, we did not find any significant interactions between cluster and time (all ts < 2).

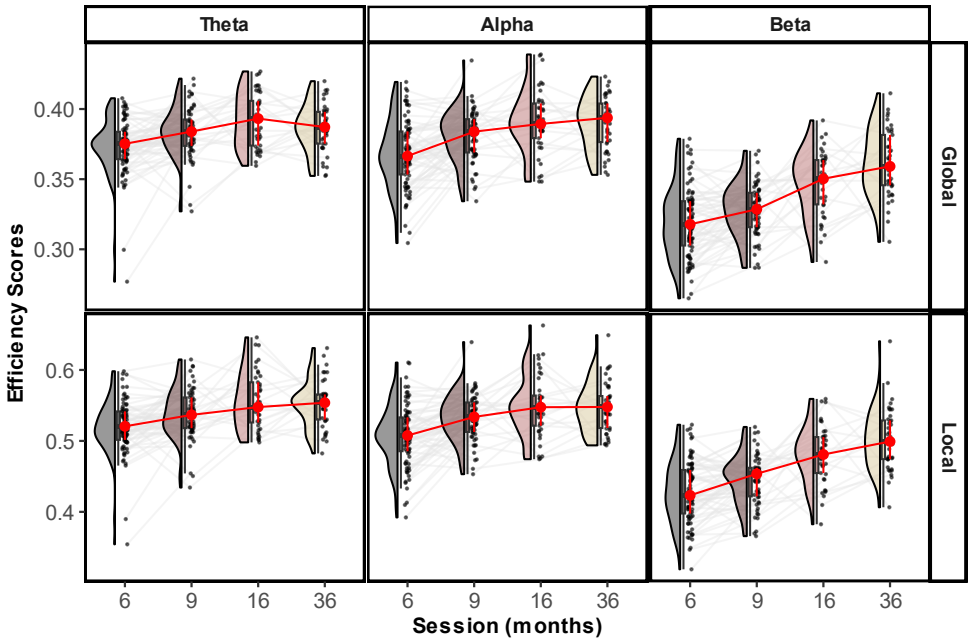

Fig. 3B.4. Network global and local efficiency development. The figure shows the global (top) and local (bottom) efficiency maturation in each frequency band. Each participant corresponds to a dot and the gray lines represent individual trajectories.

Local efficiency varied across clusters in the theta band. The temporal cluster did not vary in local efficiency when compared to the frontal area (z = 1.70, p = .53) and the parietal area did not differ from the central area (z = -2.23, p = .229). In addition, the central and parietal areas had smaller local efficiency than the other clusters (all zs < -7.64, all ps < .001), while the temporal and frontal clusters had smaller values than the occipital and frontal-pole areas (all zs < -7.47, all ps < .001). Finally, the frontal pole had a larger local efficiency than the occipital cluster (z = 2.96, p = .04).

Alpha band local efficiency distribution analysis revealed no differences between the frontal, temporal, and occipital areas (all zs < 2, all ps > .42). Those clusters in alpha had larger values than the central and parietal areas (all zs > 9.46, all ps < .001), but smaller values than the frontal-pole cluster (all zs < -9.48, all ps < .001). The frontal-pole cluster had larger values than the central and parietal areas (zs > 20.91, all ps < 001), whereas the central

cluster had lower local efficiency scores than the parietal cluster (z = -6.70, p < .001).

In the beta band, the occipital, frontal pole, and temporal regions did not differ (all zs < 2.40, all ps > .14), but the frontal pole had larger values than the temporal cluster (z = 4.26, p < .001). These three clusters had a larger local efficiency than the rest or areas (all zs > 4.25, all ps < .001), whereas the frontal cluster had a larger local efficiency than the central and parietal clusters (all zs > 3, all ps < .03). The central cluster had augmented local efficiency compared with the parietal cluster (z = 3.10, p = .02).

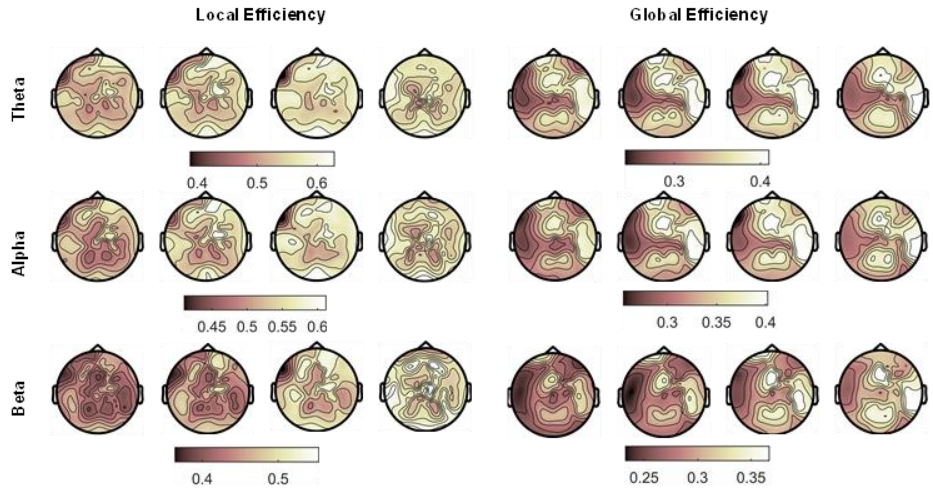

Fig. 3B.5. Development of network efficiency topology. This figure shows the global and local efficiency parameters averaged over the participants across the electrodes. Note that, as the global efficiency formula does not provide a value per electrode, we consider global efficiency as 1/(Avg. Path length of the node). This formula is equivalent to global efficiency when removed the summatory of all the electrodes.

Network Centrality

The values of the maximum betweenness centrality (Fig. 3B.6 and Fig. 3B.7) did not change over time, independent of the frequency band: theta (marginal R^2 = .01, conditional R^2 = .14; t < 2), alpha (marginal R^2 = .01, conditional R^2 = .03; t < 2), and beta (R^2 < .01, conditional R^2 = .21; t < 1) frequency bands.

Regarding the theta band, the parietal cluster had the largest betweenness centrality (all zs > 4.17, all ps < .001), whereas the central cluster did not vary when compared to the frontal and frontal-pole areas (all zs < 2.62, all ps > .09). Additionally, the frontal cluster presented higher betweenness centrality compared to the frontal-pole (z = 3.57, p < .001). These three clusters were more centralized than the occipital and temporal areas (all zs > 7.75, all ps < .001) and the temporal areas had larger values than the occipital cluster (z = 4.09, p = .001).

In the alpha band, the parietal and central (z < 2), occipital and temporal (z < 2), and frontal and frontal-pole (z < 1) regions had equivalent betweenness centrality. The parietal and central clusters had the largest centrality (all zs > 5.45, all ps < .001), followed by the frontal and frontal-pole (all zs > 4.52, all ps < .001).

Beta band distribution analysis revealed equal betweenness centrality values in the central and parietal clusters (z = 2.04, p = .32), which also presented higher centrality than the other areas (all zs > 3.57, all ps < .001). The frontal and frontal-pole (z <1) and the temporal and occipital pole (z < 2) had equivalent values, with higher betweenness over the frontal clusters (all zs > 4.52, all ps < .001).

Small-World Propensity

The small-world topology (Fig. 3B.6) did not vary in theta (marginal R^2 = .02, conditional R^2 = .50; time: t < 2) or alpha (no fixed effects) bands. In the beta band, SWP decreased over time with a positive quadratic effect (marginal R^2 = .03, conditional R^2 = .41; time: β = -0.02, t(137.57) = -2.92, p = .004, 95% CI = [-0.04 – -0.01; time squared: β = 0.01, t(143.23) = 2.83, p = .004, 95% CI = [0.00 – 0.02]).

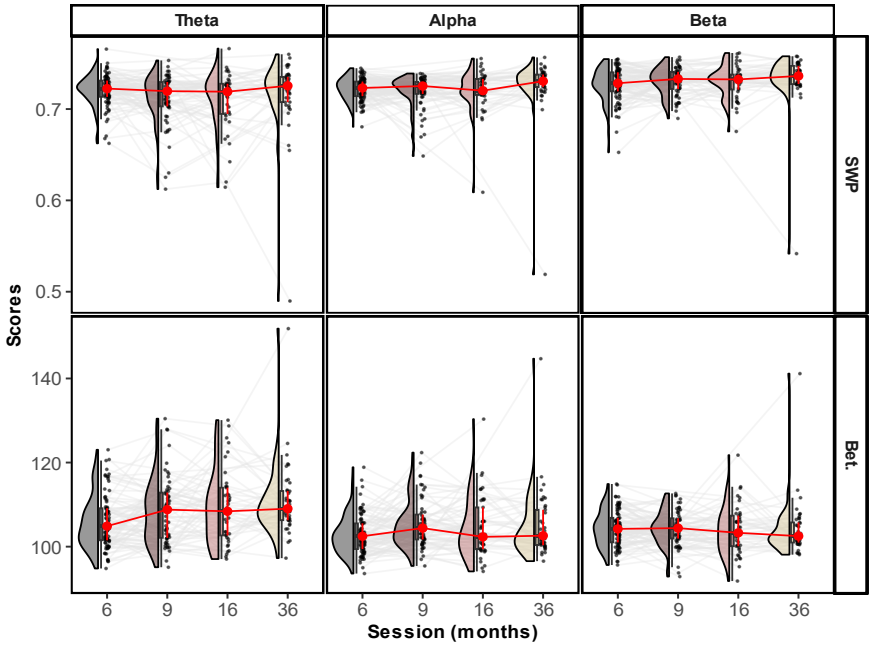

Fig. 3B.6. Small-world topology and centrality development. The figure shows the individual values of small world propensity (SWP) index and the betweenness centrality (Bet.) and their trajectory. The gray lines represent individual trajectories, and the red line represents the average trajectory.

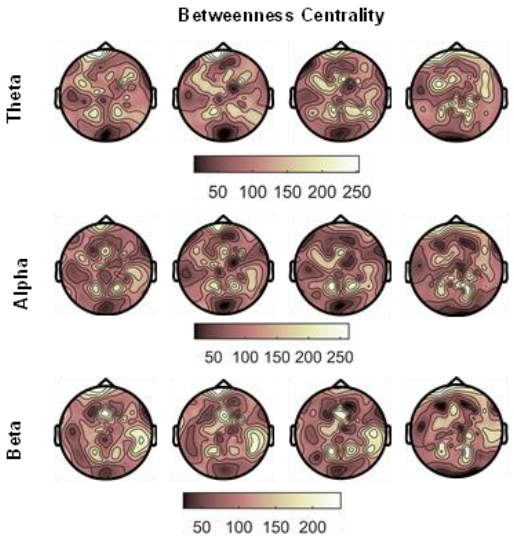

Fig. 3B.7. Development of betweenness centrality topology. The figure displays the mean values of betweenness centrality per electrode across participants per session, age, and frequency band.

3B.2.3. Modularity development

In addition to modularity and propensity score, we computed within-module z-score connections to determine the role of the nodes in the network. We classified the nodes based on the guidelines of Guimera and Amaral (2005). Only a handful of nodes could be considered hubs (within-module z-score >> 2.5) across all participants, sessions, and bands (theta: three hubs, alpha: three hubs, beta: 0 hubs). Therefore, we focused only on non-hub nodes during development (Fig. 3B.8). The participation coefficient and modularity development are displayed in Fig. 3B.9, and the topological development of the participation coefficient is shown in Fig. 3B.10.

Theta

Regarding the theta node type proportion (marginal R^2 = .35, conditional R^2 = .43), most of the electrodes were peripheral (all zs < 7.74, all ps < .001), followed by non-hub connectors (all zs > 3.93, all ps < .001) and ultra-peripheral ones (z = 3.13, p = .01).

Theta participation coefficient decreased with a positive quadratic effect (marginal R^2 = .47, conditional R^2 = .51; time: β = -0.05, t(1346.53) = -4.63, p < .001, 95% CI = [-0.07 – -0.03]; time squared: β = 0.01, t(1347.47) = 2.20, p = .044, 95% CI = [0.00 – 0.02]). The frontal, frontal-pole, and occipital areas showed smaller reductions with age when compared to the central cluster (β = [0.02 – 0.03], ts(1263.58) > 2.45, all ps < .014, 95% CI = [0.00 – 0.04]), but no other interaction was significant (all ts < 2). Participation coefficient scores did not differ among occipital, frontal, and central clusters (all zs < 2). These three areas had larger values than the frontal-pole and temporal clusters (all zs > 12.80, all ps < .001), but lower values than the parietal ones (all zs < -4.91, all ps < .001). The parietal cluster had higher values than the temporal and frontal-pole clusters (all zs > 6.13, all ps < .001) and the temporal cluster had lower values than the frontal-pole (z = -8.21, p < 001).

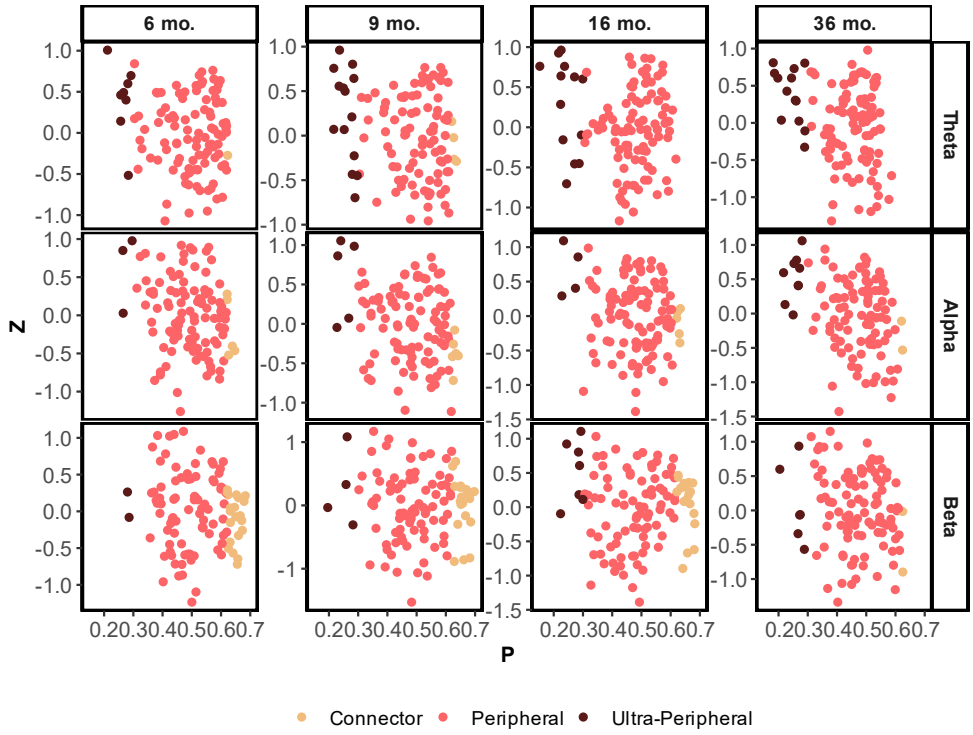

Fig. 3B.8. Node roles per session and frequency band. The figure displays the z-score degree (Z) and participation coefficient (P) averaged across the participants for each electrode. The color represents the role of the nodes: beige (connector), pink (peripheral), or brown (ultra-peripheral). Note that none of the electrodes could be considered a hub (Z << 2.5) when averaged.

Alpha

Alpha nodes (marginal R^2 = .34, conditional R^2 = .44) were predominantly peripheral (all *z*s > 3.51, all *p*s < .001), followed by connector non-hub nodes (all *z*s > 10.30, all *p*s < .001), and ultra-peripheral and kinless nodes were equally present (*z* < 2).

The alpha participation coefficient (marginal R^2 = .43, conditional R^2 = .48) linearly decreased during this period (time: β = -0.04, t(1346.97) = -3.37, p < .001, 95% CI = [-0.06 – -0.02]; time squared: t < 2). The frontal and frontal-pole areas had smaller reduction rates (β = [0.02 – 0.03], t(1264.29) > 2.25, ps < .025, 95% CI = [0.00 – 0.04]) than the central area, with no other significant interaction (t < 2). The parietal cluster had the largest participation coefficient

value (all *z*s > 3.97, all *p*s < .001), and the occipital and frontal areas had equal participation coefficient (*z* < 1), and displayed larger values than the frontal-pole, central, and temporal clusters (all *z*s > 4.82, all *p*s < .001). The temporal cluster had the lowest participation coefficient score (all *z*s < 13.31, all *p*s < .001), and the central cluster had a higher value than the frontal pole (*z* = 5.82, *p* < .001).

Beta

In the beta band (marginal R^2 = .30, conditional R^2 = .42), kinless electrodes were the scarcest (all *z*s < 11.19, all *p*s < .001), whereas most nodes were peripheral (all *z*s > 17.02, all *p*s < .001), followed by non-hub connectors (all *z*s > 19.49, all *p*s < .001).

The participation coefficient of the electrodes decreased with a positive quadratic effect (marginalR^2 = .47, conditional R^2 = .51; time: β = -0.05, *t*(1346.53) = -4.63, *p* < .001, 95% CI = [-0.07 – -0.03]; time squared: β = 0.01, *t*(1347.47) = 2.02, *p* = .043, 95% CI = [0.00 – 0.02]). The frontal, frontal-pole, and occipital clusters decreased more slowly than the central cluster (β = [0.02 – 0.03], *t*(1263.58) > 2.45, *p*s < .014, 95% CI = [0.00 – 0.03]), but no other interactions were significant (all *t*s < 2). The frontal, central, and occipital clusters had equivalent participation coefficients (all *z*s < 1), and the three had larger values than the temporal and frontal-pole areas (all *z*s > 12.80, all *p*s < .001), but smaller than the parietal zone (all *z*s < 4.91, all *p*s < .001). The parietal area participation coefficient was higher when compared to the temporal and frontal-pole (all *z*s > 18.93, all *p*s < .001), with larger values in the frontal-pole than in the parietal area (*z* = 8.21, *p* < .001).

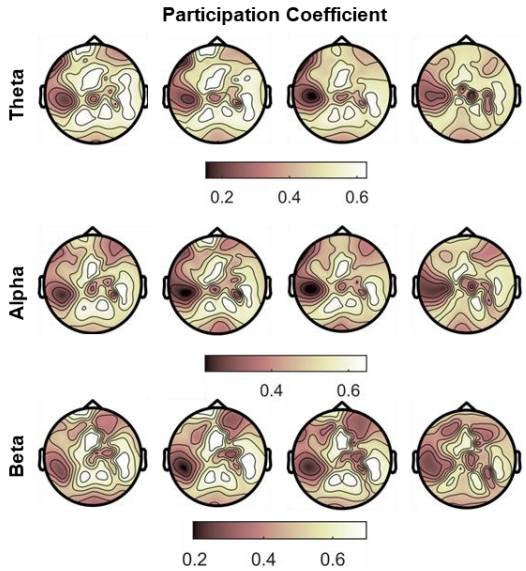

Fig. 3B.9. Topological development of participation coefficient. The figure displays the mean values of the participation coefficient per electrode across participants per session, age, and frequency band.

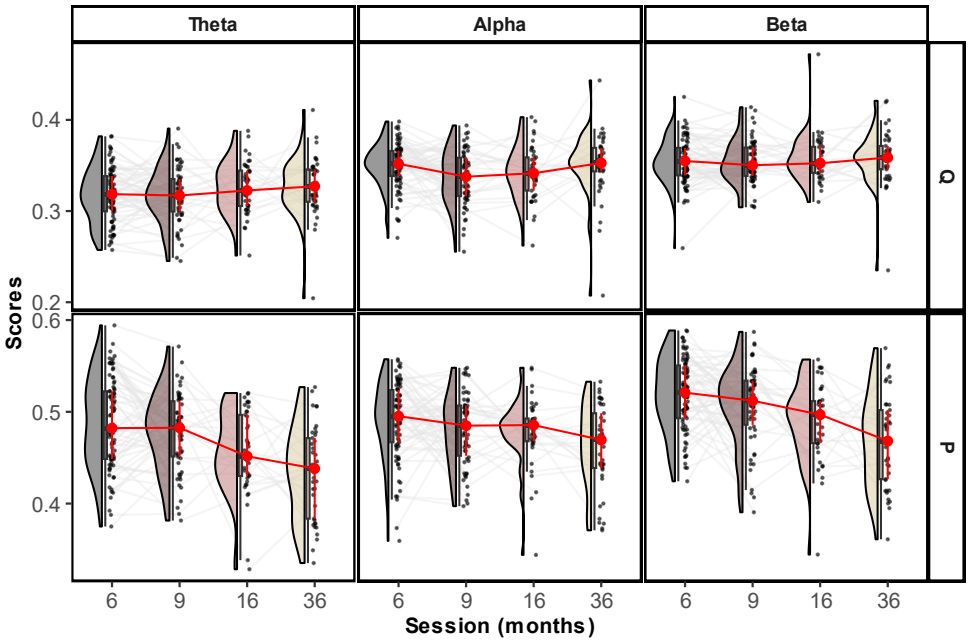

Fig. 3B.10. Network modularity and participation segregation coefficient development. The figure displays Newman's Q value of modularity and participation coefficient. Each dot corresponds to a participant, and the gray lines represent individual trajectories.

3B.2.4. Brain Networks Topologic Stability

To study topological stability (Table 3B.2), we averaged the values across the participants to obtain a single value for each electrode, session, and band. Then, we correlated them between session pairs (e.g., 6-mo. to 9-mo.). Individual stability is presented in the Appendix of Chapter 3B. Because we needed the value of each node, we could not perform the analysis using the SWP value. In addition, we substituted the global efficiency with the inverse of the shortest path length for each electrode.

Spatial stability was high and independent of network measurement and frequency band (r_s = [.45 – .99], all *p*s < .001). In addition, within-participant spatial stability was high, with more than half of the children presenting a similar distribution between sessions, except in betweenness centrality. See Table 3B.3. and Appendix Tables A3B.5, A3B.6, and Fig. A3B.3.

Table 3B.2

Descriptive information of the sample included in the stability analysis.

Waves	**Demographics**				**EEG**
	N (female)	*BW (kg)*	*GW*	*Age (days)*	*Epoch Number*
6-mo. – 9-mo.	63 (28)	3.14 (0.68)	38.86 (1.88)	*6-mo.:* 196.18 (7.87) *9-mo.:* 284.4 (12.5)	*6-mo.:* 293.51 (120.37) *9-mo.:* 253.7 (95.77)
9-mo. – 16-mo.	29 (14)	2.97 (0.63)	38.22 (1.86)	*9-mo.:* 285.78 (14.2) *16-mo.:* 520.3 (21.2)	*9-mo.:* 238.72 (86.54) *16-mo.:* 255.97 (140.18)
16-mo. – 36-mo.	24 (11)	3.34 (0.35)	39.14 (1.46)	*16-mo.:* 527.38 (19.41) *36-mo.:* 1123.84 (20.77)	*16-mo.:* 268.38 (145.9) *36-mo.:* 371.29 (97.26)

Note. BW = Birth Weight, GW = Gestation Weeks. The table displays the mean (standard deviation).

Table 3B.3

Spatial stability of functional network properties.

	Waves	Theta	Alpha	Beta
L	*6-mo. - 9-mo.*	0.99*** [0.99 - 0.99]	0.97*** [0.97 - 0.97]	0.98*** [0.98 - 0.98]
	9-mo. - 16-mo.	0.99*** [0.98 - 0.99]	0.99*** [0.99 - 0.99]	0.98*** [0.97 - 0.98]
	16-mo. - 36-mo.	0.92*** [0.91 - 0.93]	0.88*** [0.86 - 0.89]	0.84*** [0.82 - 0.86]
Str.	*6-mo. - 9-mo.*	0.99*** [0.99 - 0.99]	0.97*** [0.97 - 0.97]	0.97*** [0.96 - 0.97]
	9-mo. - 16-mo.	0.98*** [0.98 - 0.99]	0.99*** [0.99 - 0.99]	0.98*** [0.98 - 0.98]
	16-mo. - 36-mo.	0.91*** [0.89 - 0.92]	0.86*** [0.84 - 0.87]	0.81*** [0.78 - 0.83]
Leff	*6-mo. - 9-mo.*	0.97*** [0.97 - 0.97]	0.95*** [0.94 - 0.95]	0.96*** [0.95 - 0.96]
	9-mo. - 16-mo.	0.94*** [0.93 - 0.94]	0.93*** [0.92 - 0.94]	0.91*** [0.9 - 0.92]
	16-mo. - 36-mo.	0.54*** [0.49 - 0.59]	0.56*** [0.51 - 0.6]	0.51*** [0.46 - 0.56]
Bet.	*6-mo. - 9-mo.*	0.92*** [0.91 - 0.93]	0.88*** [0.86 - 0.89]	0.85*** [0.83 - 0.87]
	9-mo. - 16-mo.	0.88*** [0.86 - 0.89]	0.88*** [0.87 - 0.9]	0.86*** [0.84 - 0.87]
	16-mo. - 36-mo.	0.48*** [0.43 - 0.53]	0.48*** [0.43 - 0.53]	0.45*** [0.4 - 0.51]
P	*6-mo. - 9-mo.*	0.97*** [0.97 - 0.98]	0.93*** [0.92 - 0.94]	0.93*** [0.92 - 0.94]
	9-mo. - 16-mo.	0.93*** [0.92 - 0.94]	0.93*** [0.93 - 0.94]	0.95*** [0.94 - 0.96]
	16-mo. - 36-mo.	0.73*** [0.69 - 0.76]	0.69*** [0.66 - 0.72]	0.79*** [0.76 - 0.81]

Note. The table displays the Spearman's rank correlation results [95% CI] obtained by correlating the average values of the electrodes between the sessions for each network parameter, pair of sessions, and frequency bands. Bet = Betweenness centrality. Leff = Local Efficiency, P = Participation Coefficient. L = Path length, Str. = Strength. All correlations had N = 109, which was equal to the number of electrodes. Confidence intervals were computed using 1000 bootstrap replicates. *** $p < .001$.

3B.3. Discussion

In this study, we aimed to explore the developmental maturation of electrophysiological connectome. First, we conducted a multiverse analysis with three connectivity measurements (dwPLI, PLI, and iCoh), different network densities, and edge types (binary vs. weighted). We then analyzed the development of the weighted iCoh network, which showed the most consistent results. In general, our results indicate a profound reconfiguration of brain network properties, improving both integration and segregation without affecting the general topology of the net.

3B.3.1. Multiverse Analysis

The developmental trajectory of the connectome varied depending on the connectivity measurement and the edge type. Networks constructed with weighted edges derived from iCoh connectivity presented larger age-related variation and consistent patterns of results. Furthermore, the results between the binary (vs. weight) networks differed significantly in global integration, although both had similar results in terms of network segregation properties. These differences may be attributed to the underlying principles of the connectivity measures. While iCoh captures amplitude and phase properties, PLI/dwPLI relies only on phase synchronization (Bastos & Schoffelen, 2016). Therefore, networks constructed using different measures probably capture similar but nonoverlapping processes. Importantly, the differences between phase-based and coherence-based networks occurred also when the networks were binarized. Therefore, it is unlikely that the variations in edge strength found accounts alone for the differences between iCoh and PLI/dwPLI in our study.

The pattern of results in the multiverse conducted mostly coincided with that of previous studies when divided by connectivity measures. Phase connectivity networks increase their segregation with age (Hu et al., 2022; Smit et al., 2016; Xie, Mallin, et al., 2019) with either no change (Hu et al., 2022; Xie et al., 2019) or an increase in integration capability (Kavčič et al., 2023; Smit et al., 2012). Coherence networks in childhood decrease their integration costs with age in the alpha band (Miskovic et al., 2015). Additionally, the strengthening of PLI and coherence has been previously reported, revealing an increase in the capacity to connect electrodes (Barry

et al., 2004; Bell & Wolfe, 2007b; Righi et al., 2014; Smit et al., 2012; Thatcher et al., 2008).

One difference from previous studies is the SWP improvement in PLI and the decrease in the iCoh theta band network. This finding contrasts with previous results in infancy, which found either stable or decreasing SWI properties (Xie et al. 2019; Hu et al. 2022). These changes might be driven by the sample (longitudinal vs. cross-sectional) and the computed parameters. We employed SWP (vs. small-world index; SWI), which contrasts the original network with lattice and random surrogate networks, whereas previous studies normalized only with random networks. In addition, the lack of change in integration may be derived by considering the normalized parameters in other studies instead of efficiency parameters (Xie et al., 2019; Hu et al., 2022).

Surprisingly, age-trend changes in the binary network had the same segregation pattern, but the opposite was true for the integration efficiency. Previous studies that explored the connectivity backbone with the minimum spanning tree approach have shown similar results, with decentralization and larger integration costs from middle childhood onwards (Boersma et al., 2011, 2013; Smit et al., 2012; Smit et al., 2016). It is possible that the binary network in EEG recording misleads the real integration capacity because it ignores the strengthening of the long-range connections that occur during this period (e.g., Thatcher et al., 2008). Indeed, some authors have highlighted the relevance of edges in networks to fully understand their topology (Betzel et al., 2023; Faskowitz et al., 2022).

3B.3.2. Brain Network Development

The weighted coherence-based network showed a general improvement in the efficiency and further segregation of modules with age. These variations were mainly quadratic, coinciding with other functional properties of EEG (Rico-Picó et al., 2023; Wilkinson et al., 2023) and the drastic maturation between birth and age three of brain structure (Bethlehem et al., 2022).

The connectome presented two clusters in the occipital-parietal and frontal areas. This aligns with the findings of previous EEG studies in infants

(Omidvarnia et al., 2014; Shrey et al., 2018; Tóth et al., 2017) that have revealed a clear configuration of connections from birth. These two clusters had large intracluster connections, with weaker connections between distal areas. In addition, the nodes presented a truncated distribution of node degree/betweenness centrality, with only a few nodes (but not hubs) accounting for most of the shortest path lengths. This truncated distribution of node centrality is also present in fMRI (Salvador et al., 2005) and accounts for the presence of a small-world topology (Bassett & Bullmore, 2017), as indicated in our study by SWP values > .6. However, segregation/integration capability changed with age. Infants' functional networks became capable of integrating information independent of the frequency band. In addition, local efficiency increased, being lower in the middle lines and largely changing in the peripheral zones (e.g., temporal clusters).

Infants' networks were modular on average (Q > .3). Despite not varying in modularity scores with age, network modules also underwent reconfiguration toward a more segregated pattern. The nodes pertaining to more centered areas segregated more than the peripheral ones, with evidence of larger intermodule connectivity in the parieto-central areas. Therefore, the between-module connections generally weaken, which is consistent with the changes in local efficiency. Surprisingly, the spatial distribution settled from the first session, revealing the results of spatial stability correlations.

Our results for increasing efficiency were consistent with previous fMRI results (Gao et al., 2011; Zhao, Xu, et al., 2019) and partially coincided with previous literature with EEG, as stated above. In fMRI, infant' brain is already modular (Wen et al., 2019) and presents hubs (Ball et al., 2014; van den Heuvel et al., 2018) with primary networks delineated at birth (Fransson et al., 2011). In addition, network nodes become more integrated with age, owing to the appearance of long-range connections that integrate distal areas, but at the same time they become more segregated promoting the specialization of functional connectome (Yin et al., 2019).

Contrary to the fMRI literature, our networks did not present any hubs, the modules were less defined, and the spatial distribution was stable over time. In fMRI, hubs tend to synchronize together and move forward in anterior and more distributed areas with age, promoting a rich-club structure

(Oldham & Fornito, 2019; Wen et al., 2019). It is possible that EEG, even when employing a high-density net, has an insufficient spatial resolution to capture the presence of hubs. In addition, we had a larger density of networks (vs. fMRI), as usual in EEG studies, which might have resulted in the delineation of sparser modules. In fact, a recent study by Xie et al. (2019) showed a similar topographic reconfiguration (vs. fMRI) when the source space was reconstructed, which suggests the limitations of functional networks over the sensor space.

The reconfiguration of the functional networks may have been driven by white matter maturation (Chu et al., 2015). The first year of life is characterized by an increase in the density of synapses, followed by selective pruning and myelination (Ouyang et al., 2019). White matter sensory tracts in neonates are mostly delineated (Dubois, 2014), and during this period, structural connections are strengthened via myelination with a posterior anterior pattern (Dean et al., 2014). Importantly, structural circuitry influences functional activity in fMRI (Deco et al., 2013; Honey et al., 2009; Hwang et al., 2013). In addition, EEG connectivity strength is related to white matter maturation, which varies according to myelination and pruning periods (Bosch-Bayard et al., 2022; Smit et al., 2012). Given the parallel changes in the white matter compared with functional activity, the maturation of short- and long-range connections probably supports the integration of brain function (Chu et al., 2015; Gilmore et al., 2018).

Another possible explanation for the gradual segregation of functional networks is related to alertness level development. Recent studies have shown higher segregation in awake (versus asleep) infants (Smith et al., 2021). Therefore, the regulation of circadian rhythms and the gradual increase in tonic alert states in infants (Dias & Figueiredo, 2020; Paavonen et al., 2020) might contribute to the progressive specialization of brain networks.

3B.3.3. Limitations and future directions

The present study employed an identical baseline for all sessions. Compared with adult protocols, the resting-state protocol involves the presence of both sounds and images. Therefore, it is possible that the

networks varied, as the children's states were not purely mind-wandering. In fact, an infant's network configuration varies across sustained (versus inattentive) states (Xie et al., 2019). Therefore, future studies will benefit from the concurrent recording of attention-related variables such as heart rate. In addition, our analysis was based on EEG sensors. Other studies that reconstructed the signal (Chirumamilla et al., 2023; Xie et al., 2019) found differences between the sensor (vs. source) networks. Therefore, reconstructing the signal, preferably with the same infant MRI template, would contribute to further exploration of the EEG network development. In addition, multi-imaging studies will be helpful for aligning structural, BOLD, and electrophysiology-based networks because previous studies have found different connectivity profiles in each neuroimaging technique (e.g., Omidvarnia et al., 2014).

3B.4. Conclusion

Functional networks undergo profound reconfiguration in the first years of life towards a more segregated but efficiently integrated topology. To date, most of the results have explored network development in asleep infants using fMRI, and only a handful of studies have addressed it using EEG providing mixed findings. In this study, we showed that part of the inconsistency in previous research may be driven by connectivity and network construction. In addition, we delineated the maturation of functional networks based on the coherence between electrodes, as it showed the most reliable results. This network presented a stable small-world topology and modularity, but it increased the segregation and integration capacity of the networks with age. This underscores the development towards a more segregated yet efficient functional network from infancy to early childhood.

Chapter 4: Executive Attention Development and Stability from Infancy to Early Childhood

Part of the content of this chapter has been submitted as Rico-Picó, J., García de Soria Bazan, M.C., Conejero, A., Moyano, S., Hoyo, A., and Ballesteros-Duperón, M.A., Holmboe, K. and Rueda, M.R, Oscillatory But Not Aperiodic Frontal Brain Activity Predicts the Development of Executive Control from Infancy to Toddlerhood. Available at SSRN: https://ssrn.com/abstract=4614554 or http://dx.doi.org/10.2139/ssrn.4614554

Efficient attentional mechanisms are necessary for goal-oriented and self-regulated behavior (Rueda et al. 2021). According to Petersen and Posner's model (2012), attention has three core functions (alerting, orienting, and executive) that support volitional and flexible behavior. Alerting involves maintaining an optimal level of activation, while orienting is the ability to move attentional focus to the surrounding and inner elements according to goals and stimuli salience. Executive attention (EA) refers to the ability to adapt behavior to context requirements and readjust in shorter time scales when needed. This includes flexibility (CF), inhibitory control (IC), and monitoring. These processes are essential for cognitive and socio-emotional adjustment as difficulties with these functions have been associated with poorer outcomes (Allan et al., 2014; Moffitt et al., 2011).

The development of endogenous orienting and EA is protracted compared to other simpler processes, but it rapidly develops during the first three years of life (Colombo, 2001; Hendry et al., 2016, 2019). In the first three months of life, infants cannot voluntarily displace their attentional focus (Atkinson et al., 1992; Johnson et al., 1991). By the third month, infants start to endogenously shift their gaze to explore their surroundings based on their interests (Canfield & Haith, 1991; Hendry et al., 2019; Moyano et al., 2023; Shafto et al., 2012). This is shown by their ability to disengage, anticipate, and use contextual knowledge to guide their attentional focus (Amso & Scerif, 2015; Markant & Amso, 2016; Tummeltshammer & Amso, 2018). Orienting capacity improves with age in parallel with other executive mechanisms, which will ease the selection of relevant information for our goals (Gerhardstein & Rovee-Collier, 2002; Moyano et al., 2022, 2023; Woods et al., 2013).

The development of endogenous orienting is thought to precede the emergence of EA processes (Conejero & Rueda, 2017; Hendry et al., 2016) and seem to underpinning voluntary control until the executive networks reach a mature state (Posner et al., 2014). However, there is evidence of EA networks recruitment before the twelfth month of life in tasks involving working memory (WM), incongruency effects, and conflict (Bell, 2002; Berger et al., 2006; Berger & Posner, 2023; Ellis et al., 2021; Köster et al., 2019; Stahl & Feigenson, 2015). In addition, infant-friendly IC paradigms, such as the A-

not-B task, speak of the rapid development of executive processes between infancy and toddlerhood (Clearfield et al., 2006; Diamond, 1985; Holmboe et al., 2018; Johansson et al., 2014), although it may be partially a consequence of age-related changes in WM capacity (Holmboe, 2021). However, recently researchers have addressed this limitation, showing similar developmental patterns when the task does not involve WM, underscoring the rapid development of CF and IC independently of memory processes (Fiske et al., 2022; Hendry et al., 2021; Holmboe et al., 2021).

Beyond toddlerhood, EA processes undergo quantitative and qualitative changes due to the maturation of FPN and CON (Posner et al., 2014). Additionally, children can understand more complex verbal instructions. This makes them suitable for adult-like paradigms that involve CF and IC as the reverse categorization task (Gerardi-Caulton, 2000; Hongwanishkul et al., 2005; Kochanska et al., 2000; Zelazo et al., 2003), albeit with simplified versions in some cases (Carlson, 2005; Garon et al., 2014; Rueda et al., 2004). IC and CF continue to develop until adolescence and early adulthood, reducing the cost of flexibly adapting behavior and inhibiting a prepotent response (Carver et al., 2001; Casey et al., 1997; Johnstone et al., 2005; Mehnert et al., 2013; Rothbart et al., 2003). Simultaneously, orienting capacity continues to improve as they become more capable of exploring complex scenarios (Woods et al., 2013).

Although early childhood EA tasks accurately assess IC and CF, they do not consider the interaction between two or more attentional processes (e.g., orienting and executive). Additionally, evaluating the three attentional processes and their interactions (e.g., child version of the attentional network task, ANT; Rueda, 2004) seem to be not suitable in children younger than 3 and a half years of age (Casagrande et al., 2022). Therefore, these tasks do not account for other attentional processes that are key to self-regulating behavior, such as selecting relevant elements. Also, EA is usually evaluated by measuring the accuracy in incongruent or inhibitory situations. This is disadvantageous for impulsive-like children but fail to capture other profiles of children that may make an error because they are easily distracted (i.e., attentional focus differences). To overcome these shortcomings, we have developed a Bee-Attentive task. This task combines a Go/NoGo rationale

with a visual-search paradigm. Consequently, it permits the comparison of performance in prepotent and inhibitory trials, and simultaneously manipulates the load requirements of the trial (i.e., a low number of distractors vs. a high number of distractors). To properly answer this task, children must ignore irrelevant distractors (focused attention) top-down guiding their gaze to search for the target. In addition, they had to withhold their answers when a NoGo trial appears. Therefore, the task aims to capture both impulsive and distracted children by evaluating the cost of inhibiting the answer and finding the target.

EA processes are hypothesized to emerge from simpler cognitive processes, making it feasible to predict current cognitive abilities in complex processes from simpler ones in previous sessions (Conejero & Rueda, 2017; Hendry et al., 2016). Indeed, some studies have reported consistent individual differences between infancy and early childhood. For instance, a recent study by Conejero et al. (2023) found that early attentional processes predict neural markers of IC in early childhood, while other studies have shown stable individual differences linking early orientation to posterior EA capacity (Gagne & Saudino, 2016; Hughes & Ensor, 2005; Johansson et al., 2016; Rothbart et al., 2003; Veer et al., 2017). However, other authors have not found positive associations between EA tasks (Hendry et al., 2021; Miller & Marcovitch, 2015), which might reflect the continuity and discontinuity of cognitive abilities in childhood.

Altogether, evidence suggests the rapid maturation of EA in the first few years of life, but there is a lack of consensus regarding the stability of executive processes, and more research is needed on novel tasks that isolate attentional mechanisms and explore their interactions. Therefore, the objectives of this study were threefold: 1) to evaluate the development of CF and IC over a wider range than previous studies using the ECITT (9 – 16 vs. 10 – 16 months of age), 2) to behaviorally test the newly developed Bee-Attentive task (36 months of age), and 3) to explore the stability of attentional processes between toddlerhood and early childhood in these tasks. We predicted a general improvement in infant performance in the ECITT task during the transition from infancy to toddlerhood. Regarding Bee-Attentive task, we expected worse accuracy in the NoGo trials (versus Go trials) and

slower RT when the number of distractors increased. We hypothesized an interaction between the load (low vs. high) and the type of trial (Go vs. NoGo), with a larger rate of commission errors in the low-load condition but higher omission errors in high-load trials. Finally, we predicted the stability between the two sessions in the ECITT and between the ECITT task and Bee-Attentive performance.

4.2. Results

4.2.1. Longitudinal development of inhibitory control and stability in the ECITT task

To examine the development of the ECITT task, linear mixed models were conducted. These included Trial Type, Time, and Trial Type × Time as fixed effects. Radom effects were tested for both random intercept, and random intercept plus random slope. However, only the random intercept model converged. Thus, all models presented with ECITT included random intercepts per child. We included in the analysis (Table 4.1) those children who had both sessions with valid data, or at least one session with valid data and the other one missing (9-mo: n = 57, female n = 26, M valid trials = 18.74; SD valid trials = 3.61; 16-mo: n = 51, female n = 25, M valid trials = 28.59; SD valid trials = 4.3). Performance was determined by accuracy in the PNS (*prepotent non-switch,* prepotent trials preceded by a prepotent trial), PS (*prepotent switch,* prepotent trial preceded by an inhibitory trial) and IS (*inhibitory switch,* inhibitory trial after a prepotent trial). We also computed two indices: Inhibitory Effect (PS accuracy – IS accuracy) and Shifting Effect (PS – PNS accuracy).

Table 4.1

Demographic information of the sample included in the longitudinal analysis of the ECITT task.

Sex	GW (weeks)	BW (kg)	Session Age (days)	
			9-mo.	*16-mo.*
Female	39.36 (1.25)	3.26 (0.4)	284.65 (9.41)	514.79 (22.89)
Male	39.67 (1.29)	3.35 (0.44)	285.22 (7.66)	522.75 (25.82)

Note. GW = gestation weeks; BW = birth weight. This table presents the data of the 74 infants included in the linear mixed models (9-mo. n = 57; 16-mo. n = 51). The table shows the mean (standard deviation).

The general accuracy of the ECITT in the direct indices (i.e., PS, PNS, and IS; marginal R^2 = .32, conditional R^2 = .41; Fig. 4.1 and Table 4.2) increased between 9 and 16 months (β = 0.16, t(331.11) = 3.09, p = .003, 95% CI = [0.06 – 0.27]). In addition, after multiple comparisons, children had greater accuracy in the PNS trials than in the IS and PS trials (all zs > 5.82, all ps < .001), while they were more accurate in the PS trials than in the IS trials (z = 7.21, p < .001). The Type of Trial × Age interaction was not statistically significant (t < 2). Regarding the indexes computed, neither the Switching Effect (marginal R^2 < .01, conditional R^2 = .14; t < 1) nor the Inhibitory Effect (marginal R^2 < .01, conditional R^2 = .01; t = 1) changed between sessions (See Fig. A4.1 of the Appendix of Chapter 4).

Table 4.2

Mean (standard deviation) performance in the ECITT task at 9 and 16 months of age.

Session	Sex	Accuracy			Inhibitory Effect	Switching Effect
		IS	*PNS*	*PS*		
9-mo.	*Female*	0.35 (0.28)	0.8 (0.1)	0.63 (0.25)	0.27 (0.34)	0.18 (0.21)
	Male	0.51 (0.26)	0.85 (0.1)	0.72 (0.19)	0.2 (0.33)	0.13 (0.12)
16-mo.	*Female*	0.51 (0.32)	0.93 (0.1)	0.68 (0.22)	0.18 (0.34)	0.25 (0.23)
	Male	0.6 (0.35)	0.89 (0.19)	0.77 (0.23)	0.17 (0.42)	0.12 (0.31)

Note. This table presents the data of the 74 infants included in the linear mixed models (9-mo. n = 57; 16-mo. n = 51).

It is possible that some of these trajectories are significant, whereas others fail to reach significance. To explore this assumption, we analyzed the development of each trial type. Accuracy increased in the PNS (marginal R^2 = .09, conditional R^2 = .35; β = 0.11, t(123) = 3.50, p < .001, 95% CI = [0.05 – 0.17]) and IS (marginal R^2 = .05, conditional R^2 = .37; β = 0.18, t(63.52) = 2.77, p = .007, 95% CI = [0.05 – 0.30]), but not in the PS trials (marginal R^2 = .02, conditional R^2 = .11; t < 2).

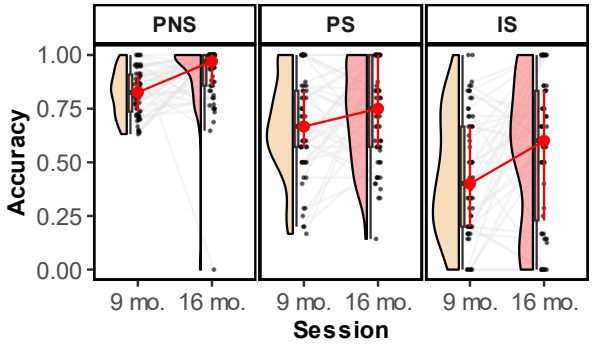

Fig. 4.1. ECITT performance development. The figure shows the accuracy for each type of trials at 9-mo. and 16-mo. Each dot represents a participant, and the gray lines represent the individual trajectories.

To determine the stability of the ECITT task and account for the missing values, we conducted a linear model including the 9-mo. performance as a predictor of the 16-mo. performance. This was conducted for each variable with a random intercept per participant to compute the stability of the measurements. Only IS accuracy was related between the two sessions (adj $R^2 = .16$; $\beta = 0.40$, $F(1,73) = 2.74$, $p < .01$, 95% CI = [0.13 0.80]), with no other significant relationship (all Fs < 1; Table 4.3).

Table 4.3

Linear regression models predicting the ECITT performance at 16-mo. based on 9-mo. results.

	Overall Model			**Regression Parameters**			
	df	r^2	*F*	*B (SE)*	*95% CI*	β	*z*
PNS	1, 72	0.03	<1	-0.28 (0.25)	[-0.78 0.21]	-0.18	-1.12
PS	1, 72	0.01	<1	0.09 (0.16)	[-0.21 0.41]	0.10	0.62
IS	**1, 72**	**0.16**	**7.72****	**0.47 (0.17)**	**[0.13 0.80]**	**0.40**	**2.74****
SE	1, 72	0.02	<1	0.09 (0.16)	[-0.21 0.41]	0.10	0.62
IE	1, 72	<0.01	<1	0.06 (0.19)	[-0.32 0.43]	0.10	0.29

Note. The regression model included FIML to account for missing data ($N = 74$). The beta and CI estimates were computed using 5000 bootstraps. PNS = Prepotent Non-Switch accuracy; PS = Prepotent Switch accuracy; IS = Inhibitory Switch accuracy; SE = Switching Effect index; IE = Inhibitory Effect index. ** $p < .01$.

4.2.2. Bee attentive task: behavioral results

Bee-Attentive performance was analyzed using linear mixed models with random intercepts per participant with the Type of Trial (Go vs. NoGo) and load condition (low vs. high). In the case of RT, we explored the

children's median RT and SD RT with load condition as a fixed effect to evaluate the cost of searching for a target and distractibility, respectively. See Table 4.4. for demographic information of the participants included in the analysis.

Table 4.4

Demographic information of the sample included in the Bee-Attentive task analysis.

Sex	*n*	Go		NoGo		BW	GW	Age (days)
		High	*Low*	*High*	*Low*			
Female	31	37.87 (6.27)	37.84 (6.78)	16.23 (2.84)	16.1 (2.8)	3.48 (0.54)	39.59 (1.45)	1115.68 (16.11)
Male	38	37.26 (7.8)	37.18 (7.99)	15.79 (3.62)	15.55 (3.36)	3.37 (0.41)	39.48 (1.33)	1120.61 (31.12)

Note. BW = Birth Weight (kg); GW = gestational weeks. The table shows the mean values (standard deviation).

The model that best fitted the accuracy included only the Type of Trial as a fixed effect (marginal R^2 = .23, conditional R^2 = .48). This model revealed that children performed worse in the NoGo trials than in the Go trials (β = -0.24, $t(207)$ = -10.86, p < .001, 95% CI = [-0.28 – to-0.19]). In addition, high-load trials were slower than low-load trials (marginal R^2 = .06, conditional R^2 = .84; β = -276.84, $t(69)$ = -7.11, p < .001, 95% CI = [-354.05 – -198.84]), and the variability in RT was smaller under low-load (vs. high-load) conditions (marginal R^2 = .02, conditional R^2 = .70; β = -71.20, $t(69)$ = -2.47, p = .016, 95% CI = [-128.64 – -13.75]) (Fig.4.2, Table 4.5).

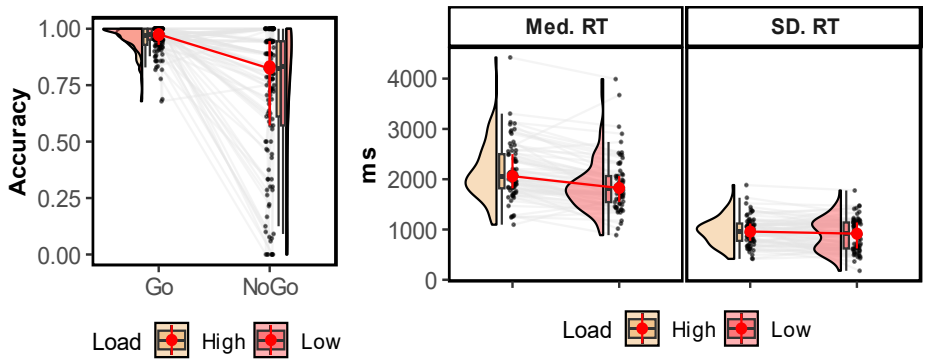

Fig. 4.2. Bee-Attentive task performance. The figure displays the mean accuracy divided by the distractor load and the median RT and SD. RT in Go hits (right). It displays the individual values (dots) and trajectories (gray lines).

Table 4.5

Descriptive statistics of performance in the Bee-Attentive task.

Sex	Go				NoGo (Acc.)	
	High		*Low*		*High*	*Low*
	Acc	RT	Acc	RT		
Female	0.94 (0.23)	2165 (1044.58)	0.96 (0.21)	1838 (995.86)	0.77 (0.42)	0.8 (0.4)
Male	0.96 (0.19)	2000.5 (1045.16)	0.97 (0.16)	1738 (1009.03)	0.72 (0.45)	0.73 (0.44)

Note. The table displays the mean (standard deviation) of the accuracy and RT variables.

We further examined the effects of committing an error (vs. hit) on RT and accuracy (see Fig. 4.3. and Appendix Table A4.3). We used a linear mixed model introducing Sequence Type (After Error vs. After Hit), Type of Trial (Go vs. NoGo), and Load condition (low vs. high) in the accuracy analysis. In the RT derivatives, we only included the Sequence Type and Load condition. Children were slower after committing an error (marginal R^2 = .04, conditional R^2 = .35; β = -317.25, t(199.73) = -7.11, p < .001, 95% CI = [-354.05 – -198.84]), but this did not affect RT variability (marginal R^2 < .01, conditional R^2 = .27; t < 1). No interactions were included in the RT model. Regarding accuracy (marginal R^2 = .14, conditional R^2 = .31), we found better performance after an error in Go trials (β = .12, t(432.45) = 3.85, p < .001, 95% CI = [0.06 – 0.18]), but NoGo trials had detrimental performance (β = -.33, t(434.45) = -9.91, p < .001, 95% CI = [-0.40 – -0.27]). This analysis did not interact with load conditions (t < 1).

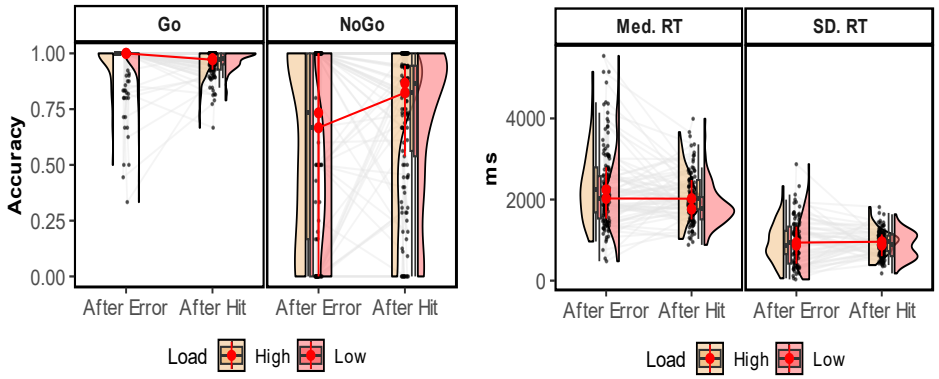

Fig. 4.3. Performance after committing an error in the Bee-Attentive task. The figure displays the accuracy divided by trial type (Go vs. No-Go) and load (high vs. load), and the median RT and SD RT in Go trials in the trials preceded by an accurate answer (hit) or error. Each dot corresponds to an individual value, whereas the gray lines represent the individual trajectory.

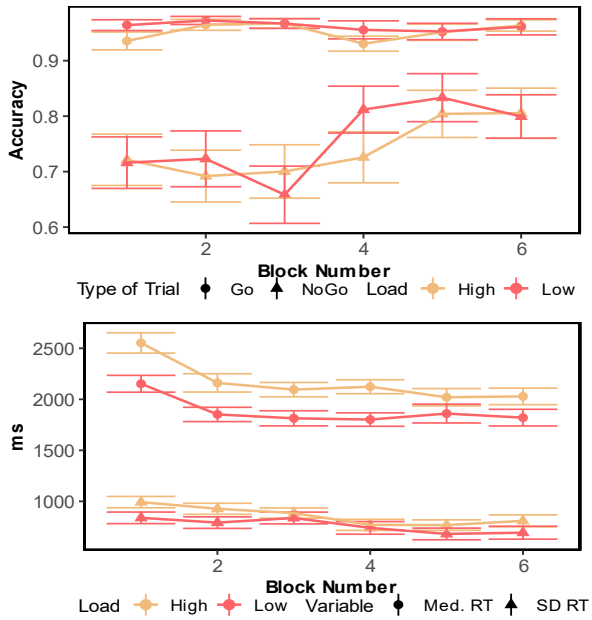

Fig. 4.4. Performance per block in the Bee-Attentive task. The figure displays the accuracy divided by load (high vs. load) and trial type (Go vs. NoGo), and the median RT and SD RT in Go trials across the blocks. It shows the mean value of the participants and the error bars corresponding to the standard error.

4.2.3. Relationship between the Bee-Attentive and ECITT tasks

To evaluate the stability between the ECITT task and Bee-Attentive, we conducted Spearman's rank correlation between the ECITT variables and

the Bee-Attentive ones. We correlated the accuracy in PS, PNS, and IS with the accuracy, RT, SAE, and RT cost (RT high-load – RT low-load) in the Bee-Attentive task. To be included in the analysis, children had to have valid data for both tasks (Table 4.6). See Appendix Table 4.6, for further details on the performance of the sample in both tasks. These analyses revealed that ECITT accuracy at 16-mo. (absolute r_s = [-.39 – .09], all *p*s > .05) was not related to Bee-Attentive variables after correcting for multiple comparisons (see Table 4.7).

Table 4.6

Demographic descriptives of the participants behavioral stability analysis between the ECITT and Bee-Attentive tasks.

Sex	*n*	BW	GW	Session Age (days)	
				16-mo.	*36-mo.*
Female	18	3440 (538.1)	39.76 (1.44)	514.78 (22.03)	1116.92 (18.24)
Male	25	3269.23 (335.9)	39.48 (1.33)	514.24 (19.64)	1119.18 (35.53)

Note. BW = Birth Weight (Kg), GW = Gestation Weeks

Table 4.7

Spearman's Rank Correlation between the ECITT performance at 16-mo. and the Bee-Attentive at 36-mo.

Bee-Attentive		ECITT		
		IS	**PNS**	**PS**
ACC	*Go*	0.04 [-0.07 - 0.14]	0 [-0.1 - 0.11]	0.01 [-0.09 - 0.12]
	No Go	-0.06 [-0.17 - 0.05]	-0.12 [-0.22 - -0.01]	-0.07 [-0.18 - 0.04]
RT	*Median RT*	-0.01 [-0.12 - 0.09]	-0.01 [-0.12 - 0.09]	-0.1 [-0.2 - 0.01]
	SD RT	0.09 [-0.02 - 0.19]	-0.07 [-0.18 - 0.04]	-0.04 [-0.15 - 0.06]
	RT Cost	-0.14 [-0.24 - -0.03]	0.02 [-0.09 - 0.12]	-0.04 [-0.15 - 0.06]
	SAE	-0.14 [-0.25 - -0.04]	-0.39 [-0.48 - -0.3]	0 [-0.11 - 0.11

Note. Confidence Intervals were computed using 5000 bootstraps. It displays the coefficient and 95% CI.

4.3. Discussion

The main goal of this chapter was to study the development of IC and CF from infancy to toddlerhood and examine the performance of three-year-old children on the newly developed Bee-Attentive task. We also aimed to test the stability of the IC and CF measurements, withing task (i.e., between 9 and 16 months of age in the ECITT), and between two IC child-friendly paradigms (16 months of age and 36 months of age). We evaluated infants' IC and CF by means of their performance of the ECITT protocol, which had been previously demonstrated to be appropriate for infants as young as 10 months of age (Fiske et al., 2022; Holmboe et al., 2021; Hendry et al., 2021). We also developed the Bee-Attentive paradigm, which combines the rationale of Go/NoGo and visual-search tasks.

Our results indicate that there is a significant development of IC in the transition from infancy to toddlerhood despite the persistent difficulty in changing attention from one target location to another on a trial-by-trial basis. Moreover, we found that the Bee-Attentive task was suitable for three-year-old children. They performed over the chance level in the Go and NoGo conditions, showing the expected main effects, such as the RT increment in the high (vs. low) load condition. Finally, we found stability within the ECITT task in the most complex trials (IS), but ECITT performance was not linked to Bee-Attentive task.

4.3.1. Executive control development from infancy to toddlerhood

Unlike prior studies that used the ECITT (Fiske et al., 2022; Hendry et al., 2021; Lui et al., 2021), we separately analyzed prepotent trials based on whether they were preceded by a change in the target location (PS vs. PNS trials). At both 9 and 16 months of age, participants experienced greater difficulty touching the target button on the prepotent location when it was previously displayed at the non-prepotent location compared with repeating the prepotent location. This switching cost implies that, to respond successfully, infants must adjust their attention to the target's location on a trial-by-trial basis. Previous studies has shown that infants who were better able to switch between prepotent and inhibitory trials (in both directions) also made fewer errors in the A-not-B task (Hendry et al., 2021). This result

underscores the relevance of trial-by-trial adjustments and the involvement of both inhibition and flexibility mechanisms in the performance of A-not-B and ECITT tasks.

Beyond the response-switching cost, we found that responses to IS trials were the most challenging for infants of both ages. IS trials require withholding a strong response prepotency (IS trials were preceded by PNS trials ~83% of the time) in addition to effective switching of attention to the opposite location. Therefore, the ECITT provides a measure of both CF and IC, which can be dissociated in terms of behavioral accuracy.

Age-related changes in task performance revealed different developmental trajectories for inhibition and switching flexibility. Developmental changes were observed in PNS trials, suggesting that building a prepotent tendency improves with age. We also observed an improvement in the accuracy of the IS trials with age, despite the lack of change in the performance of the PS trials. This pattern of results suggests that the observed change in IS with age can be attributed exclusively to the enhancement of inhibitory control skills, while the response-adjustment cost for changing the spatial location of the target remains of a similar magnitude. Indeed, we observed similar age-related changes (better inhibition and accuracy in non-switch trials at 16 months) when we computed the indices in the ECITT task, as reported in previous studies (see Appendix of Chapter 4). This pattern reveals an additional dissociation between flexibility of CF and IC. However, this differs from previous experiments studying development from 10 to 16 months of life (Hendry et al., 2021), which might be attributed to the wider age range explored in this study. In addition, we did not find any significant correlation between age in days and toddlers' performance at 16 months session (Appendix Table A4.2).

4.3.1. Bee-Attentive Performance

Regarding the Bee-Attentive task, we found the expected main effects of IC and visual search. Children were more accurate at Go (vs. NoGo) and performed with a larger variability in RT and slower when a high number (vs. low number) of distractors appeared. This accounted for the difficulty of withholding a prepotent answer and the searching costs in the task. In

addition, they self-regulated their behavior after an error, indicating their ability to adjust their answers.

Previous studies have reported accuracy cost when children must suppress an answer in several paradigms such as Go/NoGo (Casey et al., 1997). Their capacity to inhibit answers in inhibitory trials reaches a plateau in late childhood in Go/NoGo tasks, although this capacity continue to mature in more challenging paradigms (Carver et al., 2001; Johnstone et al., 2005; Mehnert et al., 2013). In addition, children can perform visual search tasks starting in infancy (Amso & Johnson, 2006; Gerhardstein & Rovee-Collier, 2002; Tummeltshammer & Amso, 2018), which is consistent with their capacity to distinguish between the target and distractors, even when they are semantically related in our task. As expected, the number of distractors affects children's performance, which will improve in the following years (Amso & Scerif, 2015; Woods et al., 2013).

The slower RT found after the commission and error replicates the classical effect found in other tasks (Dudschig & Jentzsch, 2009; Jentzsch & Dudschig, 2009). Surprisingly, this affected their performance differently in the Go (vs. NoGo) trials. Children were more accurate after an error in the Go trials, but the accuracy of the NoGo trials diminished. This may be due to the feedback employed. We displayed a "buzz" sound was when children failed an answer. This might have served as a phasic alerting tone that redirected their attentional focus to the screen and augmented their arousal. Consequently, it is possible that anticipated answers occurred when the children detected something like a target, which reduced the accuracy of the NoGo trials but promoting it in the Go trials.

Contrary to our hypothesis, we did not observe any significant interaction between the load condition and accuracy. In addition, children performed better in the latter blocks than in the first. This was shown as an increase in the NoGo trial accuracy during the task, with lower RT and variability in the RT, especially in low-load conditions. In addition, compared to other tasks in which children had larger problems withholding their answers, our sample performed well in the NoGo trials (Carlson, 2005).

Several factors may have contributed to these results. First, it is possible that the time between trials (~2s) negatively affected building prepotency. Other tasks have shown that the strength of prepotency is essential to understanding the performance of inhibitory trials in childhood, as three-year-olds are unable to stop answering in very prepotent trial or when they have already initiated a motor response (Bedard et al., 2002; Zelazo, 2015). Thus, more dynamic trials would lead to higher inhibition costs. Additionally, the time window for answering was large compared to children's performance. As shown in Fig. 4.2, the slowest median RT was approximately 4s, and children needed about 3s on average to answer correctly in the high-load condition. This may have reduced the difficulty of inhibitory and prepotent trials because they had sufficient time to search for a target and provide a response. Increasing the number of distractors, reducing the time window, and making distractors more similar could help achieve interaction effects. In addition, adjusting the time window to individual differences in RT may help identify larger inhibitory and visual search costs across tasks and prevent the maintenance of performance over the blocks. Regarding the block effects it is possible that the increment across blocks could be due to increased practice in distinguishing between Bee and Wasp. This can be solved by adapting the time window or changing the target stimulus after two or three blocks, although the last solution would hinder the compression of the task because it affects to the storytelling and introduces new elements.

4.3.3. Executive attention stability

In this study, we found within- but not between-task performance stability. In line with the results of Hendry et al. (2021), we found that previous performance in IS trials was positively linked with accuracy in the same trials at 16 months of age. This was significant, even after controlling for PS and PNS accuracy, although both significantly contributed to the prediction of IS performance (Appendix Table A4.1). These results suggest that the building blocks of EA (IC and CF) emerge in infancy and are likely to be based on brain mechanisms that, although likely to be subject to both environmental and constitutional variables, show a certain degree of developmental stability in this early maturational period when the same task is employed (Bornstein, 2014; Conejero et al., 2023; Hendry et al., 2016).

The stability from the ECITT to the Bee-Attentive task was not significant despite having a similar rationale, which contrasts part of the literature. For example, better performance at 30 months in a visual search task has been linked to hot IC at 36 months (Veer et al., 2017), and IC at 9 months was a positive predictor of children's performance in IC at 24 months of age with different paradigms (Holmboe et al., 2018). However, early results also failed to find within- and between-task stability. For example, the A-not-B task did not predict ECITT performance several months later (Hendry et al., 2021), and A-not-B performance was not related between 14 and 18 months of age (Miller & Marcovitch, 2015; see Petersen et al., 2016). In addition, in stability studies, only a few variables usually correlate between earlier and current performance between infancy and toddlerhood. For instance, in a recent study conducted in our laboratory, only three tasks were significantly related to longitudinal sessions (Conejero et al., 2023), which has also been found in other laboratories (Broomell et al., 2021).

This instability may be related to the time at which the measures were taken. Some studies have found greater stability beyond the second year of life (Hughes & Ensor, 2005; Kloo & Sodian, 2017; Kochanska et al., 2000) and between simpler paradigms (Posner et al., 2014) but not between the first and third years of life (Gagne & Saudino, 2016; but see Joyce et al., 2018). This reveals the heterogeneity of the stability in the development of executive processes (Bornstein, 2014). One possible explanation for this difference is the changes in the functional networks that underpin these functions (Hendry et al., 2016; Posner et al., 2014). The protracted development of executive networks may have created a qualitative change in how the tasks were conducted, thus provoking a discontinuity in the measurements.

4.3.4. Limitations and future studies

The current study was limited by its modest sample size, particularly in the stability analysis (n = 43 between ECITT and Bee-Attentive). In addition, we only explored the stability between the ECITT and the Bee-Attentive despite having several research protocols concurrent with both tasks (e.g., Gap-Overlap task, Spatial Incongruency task). Employing other tasks or reducing the time between sessions might help find stability over time (Conejero & Rueda, 2017; Hendry et al., 2016). In fact, some authors

argue that indirect paths between predictors can be more sensitive when temporal moments are distal (Shrout & Bolger, 2002), which may be assessed by employing more complex multilevel analyses, such as lagged cross-panel lags or structural modeling.

Although one of the main advantages of the ECITT is that it allows the administration of a greater number of trials than other infant-appropriate IC tasks (e.g., the A-not-B task), the ECITT version still presents a limited number of trials. In addition, the probability of the occurrence of a non-switch inhibitory trial was low (~13%). New variations in ECITT, increasing the number of trials, and including switch and non-switch inhibitory trials in an equivalent proportion will help to further dissociate the contribution of CF and IC processes in the performance of this task. Additionally, the first version of the Bee-Attentive method had some design limitations. Because of the session volume in the fourth session, in which they were also 16-mo. sessions, we could not pilot the task before its implementation. Consequently, the time window and the number of distractors were not properly adjusted to three-year old performance, although we found the expected main effects. However, future studies could benefit from reducing the time window or adjusting it individually to create larger inhibitory costs, as discussed previously.

4.4. Conclusion

In our study, we presented evidence of the early emergence of EA processes at the end of the first year of life. Our results indicate that between infancy and toddlerhood, IC skills improve when using a newly developed task (ECITT) that permits a more fine-grained measurement of EA (i.e., IC and CF) than previously used measures (A-not-B task and parent-reported questionnaires). This is in line with recent research and supports the feasibility of ECITT with an independent longitudinal sample. In addition, we developed a new task that aimed to evaluate IC and focused attention by combining a Go/NoGo task with a visual search paradigm. Despite it was the first version, this task was doable for three-year-old children and created a cost to inhibit the answer and search for the targets. This task may serve with some modifications to evaluate two of the attention functions, providing

valuable attentional indices earlier than other more complex tasks, such as the child-ANT.

Chapter 5A: Oscillatory and Aperiodic contribution to Executive Attention Development

Part of the content of this chapter has been submitted as Rico-Picó, J., García de Soria Bazan, M.C., Conejero, A., Moyano, S., Hoyo, A., and Ballesteros-Duperón, M.A., Holmboe, K. and Rueda, M.R, Oscillatory But Not Aperiodic Frontal Brain Activity Predicts the Development of Executive Control from Infancy to Toddlerhood. Available at SSRN: https://ssrn.com/abstract=4614554 or http://dx.doi.org/10.2139/ssrn.46145

The capacity to flexibly adjust behavior in a goal-oriented manner relies on executive attention (EA) processes (Rueda et al., 2021). EA involves the ability to inhibit (IC; Inhibitory Control) and flexibly modify behavior (CF), which has proven its impact on daily life (Allan et al., 2014; Conejero & Rueda, 2017; Moffitt et al., 2011; Tang et al., 2020).

Studies in the last decade have indicated that the foundation of EA originates from simpler building blocks in the first months of life (Diamond, 2013; Fiske & Holmboe, 2019; Hendry et al., 2016). First-year infants rapidly improve their performance in IC + working memory (WM) tasks such as the A-not-B (Clearfield et al., 2006; Diamond, 1985, 1990; Johansson et al., 2014) and other tasks that isolate IC and CF components like the ECITT (Holmboe et al., 2021). Children's performance in EA continues to improve rapidly beyond the second birthday, as shown by their ability to resolve more demanding paradigms, such as Go/NoGo (Casey et al., 1997), Dimensional Desk Sorting Card (Zelazo, 2023; Zelazo et al., 2003), and Attentional-Network Test (Casagrande et al., 2022; Rueda et al., 2004), but with a large margin to improve, as shown by their inability to conduct the stop-signal task (Carver et al., 2001).

The development of EA is thought to be supported by the maturation of frontal brain structure and function (Bell & Cuevas, 2012; Cuevas & Bell, 2022; Diamond, 2013; Fiske and Holmboe, 2019; Gilmore, 2018). To study the maturation of frontal brain activity, most experiments have employed EEG recordings at rest (rs-EEG) because of their adaptability and ease of use in infants (Saby & Marshall, 2012). The gold standard measure of rs-EEG in developmental samples is the absolute or relative power of canonical bands, such as theta (3–6 Hz) and alpha (6–9 Hz).

Longitudinal studies have shown a profound reconfiguration of these measurements in the first years of life (e.g., an increase in alpha power), highlighting the potential of EEG to capture brain maturation (Anderson & Perone, 2018; Marshall et al., 2002; Orekhova et al., 2006; Stroganova et al., 1999). More importantly, individual differences in power have been associated with EA development during infancy (Bell & Cuevas, 2016). For example, greater frontal alpha power at rest and larger differences between

rest and task-evoked alpha power are related to better EA (Bell, 2001; Bell and Deater-Deckard, 2007; Bell and Fox, 1997, 1992; Hofstee et al., 2022; Wolfe and Bell, 2004). In addition, infants' theta modulation at rest or its values in evoked paradigms suggest that it is related to high-order cognition (Begus et al. 2015, Braithwaite et al. 2020; Conejero et al. 2016).

A limitation of using absolute/relative power is that it conflates narrow and broadband activity (Donoghue et al., 2020; Ostlund et al., 2022). When the EEG signal is analyzed in terms of the power of different frequency bands, most of the energy follows a power-law decay curve (aperiodic), whereas only the peaks of energy above this curve represent oscillatory activity (He, 2014; Voytek et al., 2015). In fact, aperiodic activity is the most important predictor of several band ratios (e.g., theta/beta), except for the alpha band (Donoghue, Dominguez, et al., 2020; Rico-Picó et al., 2023). In addition, the aperiodic curve flattens throughout the lifespan (Cellier et al., 2021; Fransson et al., 2013; Hill et al., 2022; McSweeney et al., 2021; Rico-Picó et al., 2023; Voytek et al., 2015), and only the alpha band exhibits the same trajectory of oscillatory (versus relative) power (Rico-Picó et al., 2023; Schaworonkow and Voytek, 2021). Thus, previous results may have been misled by co-occurring aperiodic maturation, particularly in the theta band, which is influenced by the aperiodic exponent (Donoghue et al., 2020). Furthermore, recent studies have linked disorders that compromise EA to the aperiodic components of EEG signals (Karalunas et al. 2021; Shuffrey et al. 2022).

Cumulative research has confirmed the involvement of the frontal areas and network topological characteristics in the development of cognition. However, more research is needed, especially by means of isolating the oscillatory (vs. aperiodic) components of brain function. This study aimed to explore the contributions of oscillatory (frontal power and parietal frequency) and aperiodic components to EA. We expected a flatter aperiodic exponent and a larger alpha power to be significantly related to EA proficiency. However, as theta power ratios are highly related to aperiodic activity, we anticipated that the association between that band and EA might disappear when controlling for aperiodic background activity.

5A.2. Results

We used the ECITT (9-mo., and 16-mo.) and Bee-Attentive (36-mo.) tasks to evaluate EA. We selected the PNS, IS, and PS variables in the ECITT to evaluate the infants' and toddlers' performance. In the Bee-Attentive task, we included the accuracy in Go and NoGo trials, and the median RT, SD RT, and RT costs to measure IC and focalized attention.

We extracted the oscillatory power in the alpha and theta bands and aperiodic exponent over the frontal cluster and computed the peak frequency of alpha (IAF; individual alpha frequency) and theta (ITF; individual theta frequency) because of the age-related steady increase. Peak frequency was extracted from the parieto-occipital area, as these clusters display larger reconfiguration in resting states in infants, and the emergence of an alpha peak appears over them (Stroganova et al., 1999). See Fig. 5A.1. for a schematic representation of the power modulation between oscillatory (versus aperiodic) activities in the sample included in the ECITT analysis.

We conducted a multiple regression analysis including the oscillatory/aperiodic brain variables as predictors of children's behavior. Instead of creating a model with all variables, we selected the fittest model using the R package *glmulti.* This package selects the fittest mode to determine the contribution of independent variables that result in the lowest values of AICc, thus correcting for the number of variables. In the case of ECITT, we evaluated concurrent and longitudinal associations, while regarding to Bee-Attentive, we studied only the concurrent relationship.

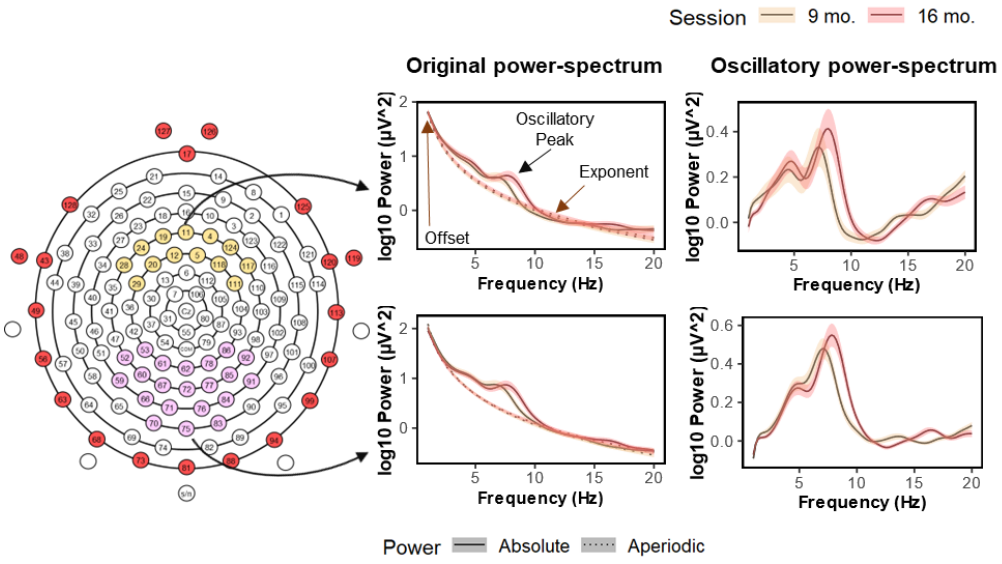

Fig. 5A.1. EEG layout and power decomposition. The figure represents the layout of the EGI net, and the colors represent the boundary-excluded electrodes (red), occipital-parietal cluster to detect and extract the frequency peaks (pink), and frontal cluster included in which we computed the oscillatory power and exponent (yellow). It also displays the absolute power and aperiodic activity per age, signaling the relevant parameters and the oscillatory power spectrum. The lines in the graph represent the mean, and the shaded area correspond to 2.5 standard error. This figure was constructed using the participants included in the ECITT analysis as a general representation of the power spectrum decomposition procedure.

5A.2.1. Aperiodic and oscillatory power correlates of the ECITT task

The descriptive information about the participants are presented in Table 5A.1. Infants with less than 20s of clean data in the EEG recording (concurrent analysis: 9-mo $n = 6$, 16-mo. $n = 1$; cross-session analysis: $n = 2$) or missing EEG data (concurrent analysis: 9-mo $n = 17$, 16-mo. $n = 27$; cross-session analysis, $n = 28$) were excluded from the analysis. Females had more epochs before preprocessing at 9-mo. than males (all ts > 16, all ps < .001), while males had longer recordings at 16-mo. ($t = 25$, $p < .001$).

Table 5A.1

Demographic information of the participants included the regression models between rs-EEG power and behavioral performance in the ECITT task.

		***n* (female)**	**GW**	**BW**	**Session Age**	**Valid Trials**	***rs-EEG***	
							Clean Epochs	R^2
Concurrent	*9-mo.*	37 (15)	39.49 (1.38)	3.30 (0.43)	284.67 (10.16)	18.84 (3.27)	15.40 (9.26)	.98 (.01)
	16-mo.	37 (21)	39.33 (1.3)	3.24 (0.38)	513.40 (20.51)	29.63 (2.53)	15.35 (9.51)	.99 (.01)
Longitudinal	-	35 (18)	39.58 (1.33)	3.31 (0.39)	*9-mo.*: 283.66 (10.68) *16-mo.*: 515.25 (21.78)	*16-mo.*: 28.07 (4.92)	*9-mo.*: 12.69 (6.98)	*9-mo.*: .98 (.01)

Note. This table presents the data of infants who had valid data for both the rs-EEG and ECITT tasks. Data are presented as mean (standard deviation). GW = gestational weeks; BW = birth weight (kg). The valid trials corresponded to the ECITT task. R^2 represents the fit of power spectrum decomposition.

However, the number of cleaned epochs did not differ between the analysis groups (all $t < 1.05$) or sex ($t = 1.10$). We found differences in the goodness of fit of the power decomposition, although only ~5% of the electrodes did not have the required fit (excluded $n = 0$; electrodes excluded $M_{9\text{-mo.}} = 4.2\%$, $M_{16\text{-mo.}} = 2.1\%$; Supp. Table 1; Supp. Fig. 2). Among the ROIs included in the analysis, the parieto-occipital clusters had a better fit than the frontal area (all ts > 7.04, all ps < .001), but there were no differences between the occipital and parietal areas ($t < 1$). The goodness of fit was lower at 9-mo. than at 16-mo. recording sessions (all ts > 4.17, all ps < 001), and females had larger fit values than males, independent of session (all ts > 5, all ps < 001). Therefore, given the differences in the goodness of fit between the ROIs and sex, we controlled for these variables in the regression analysis. See Appendix Tables A5A1–A5A3 and Appendix Fig. A5A.1 to A5A.3 to further detail the sample and performance in the ECITT task and power parameters.

The concurrent EEG activity at 9 months was a significant predictor of ECITT performance on PS (adj. $R^2 = .21$, $F(4,31) = 3.286$, $p = .023$) and PNS (adj. $R^2 = .22$, $F(2, 32) = 4.19$, $p = .013$) trials (Fig. 5A.2A) but was not associated with IS accuracy ($F < 2$). PS accuracy was positively predicted by ITF ($\beta = 0.41$, $t(31) = 2.27$, $p = .011$), and the model included alpha power, but it was not significant ($t < 2$). PNS accuracy was related to ITF ($\beta = 0.41$, $t(32) = 2.71$, $p = .030$). With respect to concurrent regressions at 16-mo., neither the PNS nor the IS accuracy fittest model included any independent variable. In addition, the PS at 16 months was not related to concurrent EEG activity (all Fs < 2).

In the longitudinal analysis, the PS accuracy at 16-mo. was significantly predicted by EEG at 9 months session (adj. $R^2 = .50$, $F(4, 30) = 9.75$, $p < .001$; Fig. 5A.2B) by alpha ($\beta = 0.55$, $t(30) = 4.49$, $p < .001$) and theta oscillatory power ($\beta = 0.42$, $t(30) = 3.43$, $p = .002$). However, IS and PNS at 26-mo. (all Fs < 2) were not significantly predicted by EEG activity at 9-mo. See Table 5A.2 for further details on the models and Fig. 5A.2.

Table 5A.2

Linear regression models predicting concurrent performance in the ECITT task and aperiodic and oscillatory power.

Sessions			Overall Model				Regression Parameters		
			Predictor	*df*	r^2	*F*	*B (SE)*	*95% CI*	*β*	*t*
Concurrent	***9-mo.***	*PNS*	Intc.	3, 32	0.22	4.19*	0.48 (0.18)	[0.11 – 0.85]	-	2.67*
			ITF	-	-	-	0.11 (0.04)	[0.03 – 0.19]	0.41	2.71*
		PS	Intc.	4, 31	0.21	3.28*	0.02 (0.40)	[-0.81 – 0.84]	-	<1
			ITF	-	-	-	0.23 (0.10)	[0.02 – 0.43]	0.41	2.27*
			AO	-	-	-	-0.02 (0.02)	[-0.06 – 0.01]	-0.25	-1.41
		IS	Intc.	4, 31	0.06	1.58	-0.93 (0.83)	[-2.66 – 0.81]	-	-1.09
			ITF	-	-	-	0.12 (0.10)	[-0.09 – 0.34]	0.21	1.19
			AE	-	-	-	0.53 (0.30)	[-0.09 – 1.14]	0.33	1.74
	16-mo.	*PNS*	Intc.	2, 34	0.00	< 1	-0.11 (8.33)	[-17.04 – 16.83]	-	< 1
		PS	Intc.	3, 33	0.00	1.01	7.25 (19.48)	[-32.40 – 46.88]	-	<1
			IAF	-	-	-	-0.15 (0.09)	[-0.34 – 0.03]	-1.67	-1.67
		IS	Intc.	2, 34	0.00	1.06	1.59 (25A.20)	[-49.61 – 52.80]	-	<1
Longitudinal		*PNS*	Intc.	2, 34	0.02	<1	0.90 (0.06)	[0.77 – 1.02]	-	14.77***
		PS	Intc.	4, 30	0.50	9.725***	0.47 (0.12)	[0.23 – 0.71]	-	4.06***
			TO	-	-	-	0.06 (0.02)	[0.02 – 0.10]	0.42	3.43**
			AO	-	-	-	0.05 (0.01)	[0.03 – 0.07]	0.55	4.49***
		IS	Intc.	3, 31	0.02	1.26	1.25 (0.57)	[0.40 – 2.72]	-	2.75*
			ITF	-	-	-	-0.24 (0.13)	[0.53 – 0.03]	-0.32	-1.84

Note. CI estimates were computed using 5000 bootstraps. Intc. = Intercept, AO = Alpha Oscillatory Power, TO = Theta Oscillatory Power, ITF = Individual Theta Frequency, IAF = Individual Alpha Frequency, PNS = Prepotent Non-Switch accuracy; PS = Prepotent Switch accuracy; IS = Inhibitory Switch accuracy. All analyses were controlled for sex and goodness of fit of the aperiodic/oscillatory modelling of brain activity *** $p < .001$, ** $p < .01$, *$p < .05$, # $p < .1$.

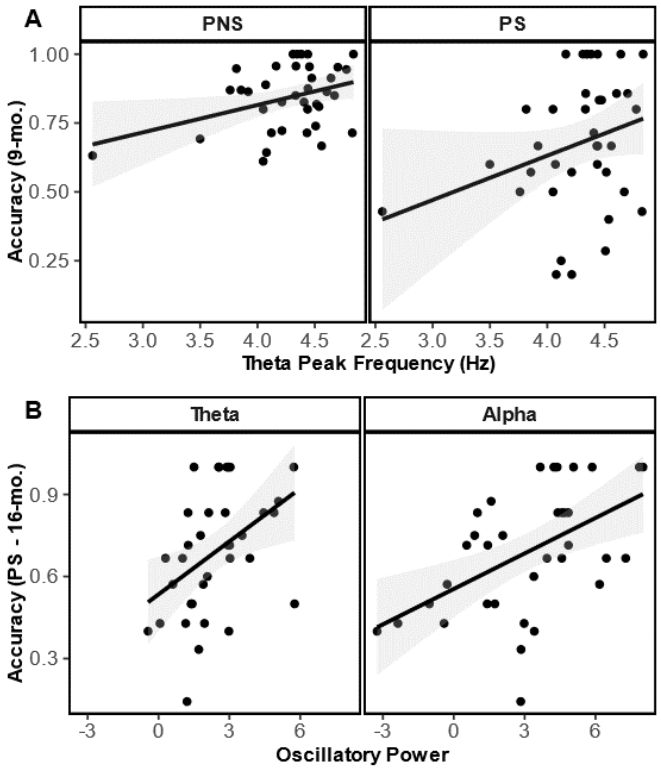

Fig. 5A.2. Regression plots of significant EEG power variables related to ECITT performance. The figure displays the significant regressions concurrently at 9-mo. (A) and EEG at 9-mo. to behavior at 16-mo. (B). PNS = Prepotent Non-Switch, PS = Prepotent Switch.

5A.2.2. Aperiodic and oscillatory power correlates of the Bee-Attentive task

Of the 69 participants with valid data in the Bee-Attentive task, 14 (female $n = 7$) participants did not finish the EEG recording after completing the task, and 10 children did not have enough valid data in the EEG (female $n = 4$). The average R^2 of the power models was .99 ($SD < .01$) after excluding the electrodes that fitted below .95 in the power spectrum decomposition (<1% excluded). Males and females did not differ in total register time, fit of the models, and retained data (all ts < 1). See Table 5A.3 for further details of the demographic information of the sample and the Appendix of Chapter 5A provides further information regarding the fit of the EEG models and power and Bee-Attentive descriptives of the sample included in the analysis.

Table 5A.3

Demographic information of the participants included in the regression models between rs-EEG power and Bee-Attentive performance.

n **(female)**	**Session Age (months)**	**Valid Trials**	***Block Number***	***rs-EEG***		
				Total Epochs	*Clean Epochs*	R^2
44 (26)	37.27 (0.81)	101.47 (25.50)	5.41 (1.00)	94.02 (10.02)	24.68 (16.82)	.99 (.01)

Note. This table presents the data of infants who had valid data for both rs-EEG and Bee-Attentive. Valid trials and blocks correspond to the Bee-Attentive task. R^2 represents the fit of the power spectrum decomposition. Data are presented as the mean (standard deviation).

The results of the regression models are depicted in Table 5A.4. Individual differences in reaction time derivates (median RT, SD RT, RT Cost) of the Bee-Attentive task were not concurrently predicted by EEG power parameters (all Fs < 2). The accuracy of the Go trials was marginally predicted by electrophysiological activity (adj. R^2 = .12, F (3,36) = 2.74, p = .057). In that model, alpha peak frequency had a positive relationship (β = 0.44, t(36) = 2.73, p = .003) and theta peak frequency was also selected in the model, but without a significant association (t < 2). Similarly, NoGo trials (adj. R^2 = .07, F (2,37) = 2.56, p = .081) accuracy model showed a trend in relation to EEG activity, but all predictors were non-significant (IAF: t < 2).

Table 5A.4

Linear regression models predicting concurrent performance of the Bee Attentive task at 36-mo. session.

Variable	Predictor	Overall Model			Regression Parameters			
		df	r^2	*F*	*B (SE)*	*95% CI*	*β*	*t*
Go Acc.	*Intc.*	3, 36	0.12	2.74#	0.62 (0.13)	[0.35 – 0.89]	-0.14	4.69***
	IAF	-	-	-	0.04 (0.01)	[0.01 – 0.06]	0.43	2.73**
	ITF	-	-	-	0.01 (0.02)	[-0.04 – 0.05]	0.04	< 1
NoGo Acc.	*Intc.*	2, 37	0.07	2.56#	0.64 (0.17)	[0.30 – 0.98]	-0.22	3.80***
	IAF	-	-	-	0.04 (0.02)	[-0.00 – 0.07]	0.22	1.81
Go RT	*Intc.*	2, 37	0.00	< 1	3450.20 (1219.49)	[979.28 – 5921.12]	0.06	2.83**
	IAF	-	-	-	-329.85 (269.03)	[-874.97 – 215.26]	-0.20	1.23
SD RT	*Intc.*	3, 36	0.02	< 2	2054.71 (791.09)	[450.31 – 3659.11]	0.10	2.6*
	IAF	-	-	-	-156.70 (79.50)	[-317.93 – 4.54]	-0.32	-1.97
	ITF	-	-	-	41.10 (119.02)	[-200.29 – 282.50]	0.06	< 1
RT Cost	*Intc.*	3, 36	0.01	1	-1108.25 (970.19)	[-3075.88 – 859.38]	0.11	-1.14
	IAF	-	-	-	147.33 (97.50)	[-50.41 – 345.06]	0.25	1.51
	ITF	-	-	-	35.05 (145.97)	[-260.99 – 331.09]	0.04	< 1

Note. CI estimates were computed using 5000 bootstraps. ITF = Individual Theta Frequency, IAF = Individual Alpha Frequency, Intc. = Intercept. All the analysis were controlled by sex and goodness of fit of the aperiodic/oscillatory modelling of brain activity *** $p < .001$, ** $p < .01$, *$p < .05$, # $p < .1$.

5A.3. Discussion

In this study, we aimed to investigate the association between EA and oscillatory and aperiodic activity. We measured EA processes using two newly developed child-friendly tasks: ECITT and Bee-Attentive. Both are suited to evaluate the dissociable components of EA, such as CF, IC, and sustained attention, at different ages. We measured EA with the ECITT at 9-mo and 16-mo of age, while we employed the Bee-Attentive at 36-mo. Our results indicate that there was a significant association between oscillatory activity, but not aperiodic activity, between rs-EEG and the ECITT task. However, we did not find no association was found with the Bee-Attentive paradigm.

Although other studies have shown a relationship between frontal activity and aspects of infants' behavior, our study is the first to dissociate oscillatory and aperiodic components and measure performance on the ECITT and Bee-Attentive tasks. Our results revealed specific concurrent and longitudinal associations between task performance, frontal oscillatory power, and ITF in the ECITT task. However, we did not find a significant relationship between the aperiodic exponent component and ECITT, or any component with Bee-Attentive. This finding highlights the relevance of oscillatory brain activity in predicting behavioral skills, in agreement with prior findings that considered high-order cognitive processes (Broomell et al., 2016; Broomell et al., 2021), and also suggests the need for more research to fully understand the lack of correlation between some tasks and brain functioning.

5A.3.1. Alpha and theta oscillatory activity

Regarding the associations found, the oscillatory power of the theta band at 9-mo. was a positive predictor of the PS trials at 16-mo., and ITF was a concurrent predictor in the PNS and PS trials at 9-mo. This is consistent with results from previous studies that found theta to be a predictor of cognitive capability in infancy and childhood/adulthood (Braithwaite et al., 2020; Perone et al., 2018), and the involvement of ITF in cognitive control (Senoussi et al., 2022). Regarding to oscillatory power, the studies of Jones et al.(2020) and Braithwaite et al. (2020) found better non-verbal cognitive abilities in infants who increased theta power in a resting state protocol

several months before. In contrast, Tan et al., (2023) and Perone et al. (2018, 2019) found a negative relationship between theta power and intelligence in adulthood, and self-regulation and executive function in infancy and early childhood, respectively. Thus, previous findings are mixed, depending on the approach used to compute power. Studies that found a negative relationship used relative power ratios, whereas others used power variation.

Given that theta relative power and other derivatives (e.g., theta/beta ratio) are influenced by the aperiodic exponent (Donoghue, Dominguez, et al., 2020; Rico-Picó et al., 2023), a negative relationship between theta and cognitive capacities may occur due to age-related flattening of the background curve (e.g., Schaworok and Voytek, 2020; Cellier et al., 2021). Indeed, a steeper background curve (i.e., a larger exponent) has been associated with attention deficit, hyperactivity risk, and poorer executive functions in an autism risk sample of infants (Begum-Ali et al., 2022; Carter Leno et al., 2022; Karalunas et al., 2021). However, in the current study, theta oscillatory power was isolated from aperiodic background activity, which may be more similar to the evoked and modulation paradigms. There is evidence of higher frontal theta in conflict paradigms and infants (Berger et al., 2006; Conejero et al., 2016) and resource allocation of cognition in dynamic stimuli (Jones et al., 2020) with matures augmenting its energy (Clarke et al., 2001). Thus, the pattern found may be more related to evoked theta and be a marker of attentional control, as occurs in adults (Cavanagh & Frank, 2014; Köster et al., 2021; Köster & Gruber, 2022).

Regarding alpha oscillatory power, we found a positive longitudinal relationship with PS accuracy. This is consistent with the results of previous studies that found an association between frontal alpha power and performance in the A-not-B task (Broomell et al., 2021) and EA experimental procedures (Hofstee et al., 2022). Alpha is considered key to high-order cognition during development (Cuevas & Bell, 2022), and has been consistently related to top-down processes involved in visuospatial attention, cognitive control, and brain communication (Alamia et al., 2023; Clayton et al., 2018; Fries, 2015; Klimesch et al., 2007). Furthermore, although the overall model was not significant, the accuracy in the Bee-Attentive task had IAF as a predictor. In fact, the alpha peak frequency over the parietal areas has been related to information sampling (Freschl et al., 2022), and previous

studies employing the alpha peak have found it to be associated with non-verbal cognitive domains in infants (Carter-Leno et al., 2021).

Given the early developmental trajectories of alpha and theta oscillatory activity, which highlights the steady increase in IAF and ITF, and the augment of alpha oscillatory power (Freschl et al., 2022; Rico-Picó et al., 2023; Schaworonkow and Voytek, 2021), our regression models indicated a more mature pattern of brain oscillatory activity at 9-mo. in alpha and theta rhythms were linked to better EA functioning in the ECITT task.

Overall, our results with the ECITT task indicate the involvement of oscillatory activity in the development of cognition, whose maturation may be necessary for the emergence of EA in the second year of life. In addition, alpha and theta bands were co-predictors of infant performance in PS trials. Several cognitive mechanisms are involved in any condition of the ECITT task. In PNS, the capacity to create a preponderant answer is required, while in PS and IS trials, children must suppress the tendency to keep responding on the same side, in addition to disengaging their attentional focus from the previous location and reorienting to the new one. Therefore, alpha and theta band may jointly contribute to their performance albeit being related to different process, such as it has been seen with reactive (vs. proactive; see Braver, 2012) control (Clements et al., 2021; Cooper et al., 2015). This support the contributive role of alpha and theta bands (see Clayton et al., 2015; Cuevas & Bell, 2022; Klimesch, 1999; Saby & Marshall, 2012).

5A.3.2. Aperiodic activity

In our study, we did not find any significant contribution from the aperiodic exponent to ECITT or Bee-Attentive performance. This is consistent with a recent study that found no significant differences in children who scored low (vs. high) on the Behavioral Inhibition Questionnaire and had the same exponent values as their peers (Ostlund et al., 2022). However, previous studies have reported the contribution of aperiodic activity to cognition in offline and online paradigms in both developmental and adult samples (e.g., Donoghue et al., 2020; Karalunas et al., 2022). For instance, a recent study by Carter Leno et al. (2022) found that the interaction between aperiodic exponent and EA was a significant predictor of autistic traits. Therefore, despite the lack of a relationship between aperiodic activity and behavior in

our study, aperiodic activity has shown constant links with cognition, and more studies are needed to fully understand its relationship with infant behavior.

5A.3.3. Different associations between ECITT and Bee-Attentive

Our results revealed longitudinal and concurrent associations at 9-mo. but no at 16-mo. between brain oscillatory activity and task performance during an ECITT task. There is good evidence that baseline EEG can be a predictor of later behavior (Brito et al., 2016; Jones et al., 2020; Whedon et al., 2020). However, some studies have found concurrent, but not longitudinal, relationships between rs-EEG and cognitive capabilities (Carter Leno et al., 2021). Also, the lack of association with Bee-Attentive may be due to several factors, ranging from the sensitivity of the task to the selection of brain areas and properties of the rs-EEG included in the analysis. A recent study by Gordillo et al. (2023) supports the difficulty in correlating rs-EEG and behavior. In their study, they measured several EEG properties (e.g., power and connectivity) and related them to an individual's performance on several tasks. Their results showed that only some correlations between brain and behavior were significant and that those differed between the age groups (young vs. old adults). This has also been shown in infant EEG, finding either no correlation or correlation between the same task and protocols in two different groups (e.g., Cuevas & Bell, 2012; Bell & Cuevas, 2010). One factor that may improve the results is the consideration of the time points of the measurements when examining the factors that impact the change and stability of the measures. Introducing trajectories or individual slopes, albeit not always feasible, provides valuable information about how the state of maturation at a particular time point predicts developmental changes in cognitive skills, and might reconcile the literature.

5A.3.3. Limitations and Future Directions

The current study was limited by the relatively small sample size. This was in part due to the COVID-19 pandemic, which forced laboratories to interrupt their activities for a period of several months. This negatively impacted the attrition rate of families. Despite the modest sample size, our findings are in line with previous literature linking oscillatory activity in baseline protocols and behavior during infancy and childhood.

Regarding electrophysiological measurements, we computed the oscillatory power based on the assumption that the signal was stationary. As discussed in Chapter 3A, narrowband activity (oscillatory) can also appear in transient bursts that may not generate a peak (Ede et al. 2018; Quinn et al. 2019; Rayson et al. 2022; Zitch et al. 2020). Therefore, extracting the properties of these transient activities may benefit the study of the associations between brain activity and behavior, either via microstates in networks and power (Brown & Gartstein, 2023), with peripheral measurements to gain insight into cognitive states (e.g., Xie et al., 2018; 2019), or with evoked paradigms compared to baseline (e.g., Cuevas & Bell, 2012; Fiske et al., 2022).

5A.4. Conclusion

The first years of life are characterized by dramatic changes in both behavior and brain function. Evidence suggests that simpler building cognitive blocks give rise to EA, which is parallel to structural and functional brain development. In this study, we aimed to characterize the relationship between EA processes and brain activity in relation to oscillatory and aperiodic brain activity. We found that oscillatory power and peak frequency were concurrent and longitudinal predictors of infant performance, respectively. This contributes to the understanding of the relationship between intrinsic brain function and cognitive outcomes such as intelligence (Braithwaite et al., 2022), academic performance (Whedon et al., 2020), social adjustment (Fleming et al., 2020), and personality and temperament traits (Tang et al., 2020). Thus, investigating both early neural and behavioral indicators may help identify potential predictors of children's general adjustment and learning abilities.

Chapter 5B: Functional Connectome and Executive Attention

Cognitive processes emerge from the coordinated activity of brain regions regardless of their level of complexity. Brain regions are interconnected through structural circuits that facilitate functional co-activation of adjacent and distant regions, enabling the human brain to support flexible cognitive processing (Honey et al., 2009). High-order cognitive processes have been linked to interconnected sets of brain areas that are discernible at rest and during task-related paradigms (e.g., CON and FPN; Dosenbach et al., 2008; Petersen & Posner, 2012; Yeo et al., 2011). These networks undergo rapid development in the first few years of life (Gilmore et al., 2018; Vértes & Bullmore, 2015), which is thought to supports the emergence of executive attention (EA) processes (Diamond, 2013; Fiske & Holmboe, 2019; Posner et al., 2014).

Research in the last two decades has combined functional connectivity with the graph theory framework to study age-related functional network reconfiguration (Watts & Strogatz, 1998). This framework considers the brain as a set of nodes (e.g., electrodes) united by a set of functional or structural edges (e.g., coherence). When applied to the human brain, it presents an optimal balance between the wiring cost and efficient integration of brain areas (Bullmore & Sporns, 2012) sustained by the creation of specialized modules that are united by long-range connections (Alexander-Bloch et al., 2013; Salvador et al., 2005). This results in a small-world architecture, as brain networks are neither clustered nor present a random distribution of edges (Achard & Bullmore, 2007; Bassett & Bullmore, 2017; Vaessen et al., 2010).

Similar to structural networks (Collin & Heuvel, 2013; Ouyang et al., 2019) or isolated brain function (Anderson et al., 2022), functional networks go through a drastic reconfiguration in the first years of life (Gilmore et al., 2018; Grayson & Fair, 2017; Vértes & Bullmore, 2015; Zhao, Mishra, et al., 2019). Sensorimotor and primary networks are mostly delineated at birth (Fransson et al., 2007, 2011; Smyser et al., 2010), whereas orientation and executive networks show a more protracted pattern (Dosenbach et al., 2010; Fair et al., 2009; Gao, Alcauter, Elton, et al., 2015; Gao, Alcauter, Smith, et al., 2015; Gao et al., 2011). The development of EA networks is accompanied by an increase in local specialization while also improving network integration

in both fMRI (Cao et al., 2016; Yin et al., 2019) and EEG recordings (Boersma et al., 2011, 2013; Kavčič et al., 2023; but see Xie et al., 2019). In addition, infant networks are already modular and have small-world topology at an early age, although this will continue to develop into adulthood in some high-order networks (Asis-Cruz et al., 2015; Fair et al., 2009; Hu et al., 2022; Wen et al., 2019). Therefore, networks tend to dissociate from others and increase their specialization in the first few years of life, while the emergence of long-range connections promotes network integration (Zhao, Xu, et al., 2019).

Functional connectivity and the balance between segregation and integration have been linked to the development of EA processes in childhood and adulthood (Baum et al., 2017; Keller et al., 2022; Keller, Pines, et al., 2023). The gradual segregation of the frontoparietal network mediates the maturation of EA in childhood (Wang et al., 2021), and the brain network properties underlies adult and child performance in high-order cognitive tasks that involve working memory (WM), EA, and intelligence (Hilger et al., 2017; Marek et al., 2015; Pamplona et al., 2015; Reineberg & Banich, 2016; Van Den Heuvel et al., 2009; but see Kruschwitz et al., 2018). In EEG, larger segregation and lower integration costs are predictive of fluid reasoning (Langer et al. 2012). Also, children and adults diagnosed with ADHD show alterations in the balance between segregation and integration (Henry & Cohen, 2019), although some inconsistencies have been found, depending on neuroimaging techniques and frequency bands (Ahmadlou et al., 2012; Furlong et al., 2021; Lin et al., 2014). This speaks for the relevance of functional connectome in cognitive individual differences.

Despite not using a connectome approach, functional and structural connections are predictors of cognitive capacity in the first years of life. Using EEG, a larger synchronization of alpha over the frontal area in infancy has been associated with EA processes (Cuevas et al., 2012), and its maturation predicts EA from infancy to early childhood (Broomell et al., 2021; Whedon et al., 2016). In evoked paradigms, age-related changes in fMRI/fNIRS synchronization between frontoparietal areas, mostly comprising the FPN areas, are related to the emergence of WM and EA (Alcauter et al., 2015; Buss et al., 2014; Buss & Spencer, 2018; Marek et al., 2015). Therefore, frontoparietal integration in the first years of life is key for the emergence of

EA processes (Fiske & Holmboe, 2019), which coincides with the relevant role of these structures in high-order cognition (Cole et al., 2012; Jung & Haier, 2007; Keller et al., 2022; Marek & Dosenbach, 2018)

Cumulative research has confirmed the involvement of frontoparietal network areas and topological network characteristics in executive process development. To date, only a handful of studies have addressed this question in toddlerhood and early childhood, mostly using fMRI/fNIRS, which captures the slow dynamics of brain function. However, higher frequency activity in the alpha and theta bands is related to long-range integration (e.g., von Stein & Sarnthein, 2000), rapidly evolving in the transition from infancy to early childhood (Chapter 3B), and is associated with individual differences in EA processes (Bell, 2001, 2002). Therefore, this study aimed to explore this research gap by investigating the contribution of the segregation and integration of the brain network in the alpha and theta bands to children's cognitive capacity at 16 and 36 months of age. We anticipated that larger segregation and a more efficiently integrated network would be positively related to children's performance.

5B.2. Results

To evaluate the relationship between functional network topology and EA, we computed clustering and path length measurements as proxies of segregation and integration characteristics, respectively. We aimed to introduce three brain areas into the models: frontal-pole, frontal, and parietal clusters, given the relevance of frontoparietal areas in human cognition (e.g., Dosenbach et al., 2008; Petersen & Posner, 2012). In addition, given the multiverse results of Chapter 3B, iCoh was selected as the connectivity measurement to construct the networks. The network density included in this analysis was .25 and the weights of the edges were maintained. Behavioral performance was assessed with the ECITT (PS, PNS, and IS trials) and Bee-Attentive task (Go and NoGo accuracy, and Go RT, Go RT SD, and Go RT cost).

We conducted a partial least squares (PLS) analysis to examine the relationship between network properties and EA. We introduced 4 matrices of data in the case of ECITT and 5 regarding Bee-Attentive (e.g., graph properties at 6-mo., 9-mo., and 16-mo., predicting ECITT performance). We constructed models to predict a single variable from our behavioral tasks (e.g., PS), limiting it to one component variable per matrix. Therefore, to study the relationship between ECITT and Bee-Attentive and brain function, we employed 4-block and 5-block PLS and evaluated both direct and indirect paths. In the ECITT task, we had three direct paths: functional connectivity latent variable (FC_{var}) at 6-mo. (d), 9-mo. (c), and 16-mo. (c′), predicting behavior, and three indirect paths. In the Bee-Attentive, we had four direct paths (d, c, c′, c′′, c′′′) between FC_{var}, and four indirect paths (d, c′, c′′, c′′′) following the same rationale. See Fig. 5B.1 for a schematic representation of the direct and indirect paths. Significance/reliability of direct and indirect paths was measured with 5000 permutations and bootstrapping, respectively.

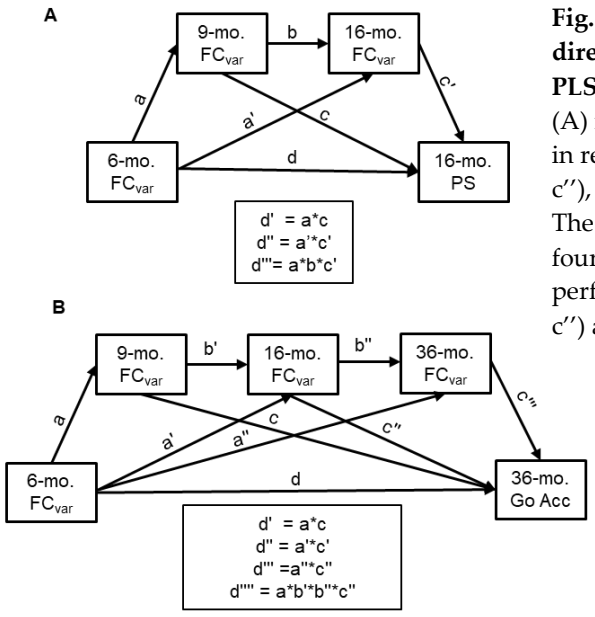

Fig. 5B.1. Schematic diagram of direct and indirect paths in the PLS analysis. The ECITT task (A) included three directs paths in relation with behavior (d, c, c′′), plus three indirect paths. The Bee-Attentive task included four direct paths between performance and FC_{var} (d, c, c′, c′′) and four indirect paths.

Children must have valid data on the behavioral variables to be included in the analysis. In addition, they had to have at least two valid data points and two missing data points in the EEG recording. As PLS does not handle missing values and needs to be imputed beforehand, we imputed them by employing the mean trajectory of each parameter per electrode and frequency band (trajMean imputation) due to the longitudinal characteristics of our dataset (Jahangiri et al., 2023).

5B.2.1. Functional network topology and ECITT performance

The information relating to the sample included in the analysis is displayed in Tables 5B.1 and Table 5B.2. See in the appendix of Chapter 5B the Tables A5B.1 and A5B.2 for details about the performance of the ECITT and functional properties of the sample included in the analysis.

Table 5B.1

Demographic information of the sample included in the relationship analysis between ECITT and functional network properties.

Sex	***n***	**BW (kg)**	**GW**	**Session age (days)**		
				6-mo.	*9-mo.*	*16-mo.*
Female	26	3.3 (0.44)	39.68 (1.41)	192.71 (9.09)	284.18 (8.43)	515.83 (26.89)
Male	29	3.26 (0.35)	39.44 (1.08)	193.36 (8.9)	285.19 (11.13)	512.25 (18.56)

Note. BW = Birth Weight, GW = Gestation Weeks. The table shows the mean values (standard deviation).

Table 5B.2

Mean number of trials (SD) in each session of the EEG and ECITT at 16-mo.

Sex	***n***	**EEG**			**ECITT**			
		6-mo.	9-mo.	16-mo.	PS	PNS	IS	Total
Female	26	271.24 (108.54)	269.81 (97.23)	247.68 (106.65)	5.92 (1.16)	14.44 (3.24)	7.63 (1.28)	29.25 (7.9)
Male	29	286 (124.02)	244.47 (93.66)	293.95 (151.99)	5.62 (1.63)	14.24 (3.75)	7.31 (1.65)	29.66 (5.43)

PS accuracy (Fig. 5B.2A) was not directly predicted by FC_{var} at 6-mo. (β = 0.39, $p_{original}$ = .879, $p_{permuted}$ = .922) or 9-mo. (β = 0.39, $p_{original}$ = .010, $p_{permuted}$ = .183) but was significantly related to FC_{var} at 16-mo. (β = 0.24, $p_{original}$ = .075, $p_{permuted}$ = .008). Direct paths linking FC_{var} between sessions were at least marginally related after the permutation procedure (FC_{var} from 6-mo. to 9-mo.: β = 0.38, $p_{original}$ = .003, $p_{permuted}$ = .088; FC_{var} from 6-mo. to 16mo.: β = 0.47, *partial* < .001, *permuted* = .008; FC_{var} from 9-mo. to 16-mo.: β = 0.41, $p_{original}$ = .001, $p_{permuted}$ = .037). The permutation test revealed significant mediation paths between FC_{var} at 6-mo. and PS through the FC_{var} in the other sessions (d'': β = 0.10, $p_{permuted}$ = .020, 95% CI = [-0.00 – 0.24]; d'': β = 0.04, $p_{permuted}$ = .007, 95% CI = [-0.00 – 0.12]) but those paths were not reliable according to the bootstrapping results. The reliable loadings in FC_{var} were almost identical in each session, with positive weights in the clustering and negative weights in the path length. The stronger weights appeared over the frontal and frontal-pole and, in general, alpha had larger weights than theta.

PNS accuracy at 16-mo. was only related to FC_{var} at 16-mo. (β = 0.18, $p_{original}$ = .182, $p_{permuted}$ = .009), but it was not directly predicted by FC_{var} in other sessions (all $ps_{original}$ > 345; all $ps_{permuted}$ > .297). FC_{var} was significantly associated between 6-mo. to 16-mo. (β = 0.47, $p_{original}$ < .001, $p_{permuted}$ = .009) and 9-mo. to 16-mo. (β = 0.43, $p_{original}$ < .001, $p_{permuted}$ = .023) sessions, but this association was only marginal between the first and second waves (β = 0.39, $p_{original}$ = .003, $p_{permuted}$ = .096). None of the indirect paths between FC_{var} and PNS performance were reliable (see Fig. 5B.2B). The independent variables that reliably loaded onto FC_{var} included clustering and path length over the frontal and parietal areas, with positive and negative weights, respectively.

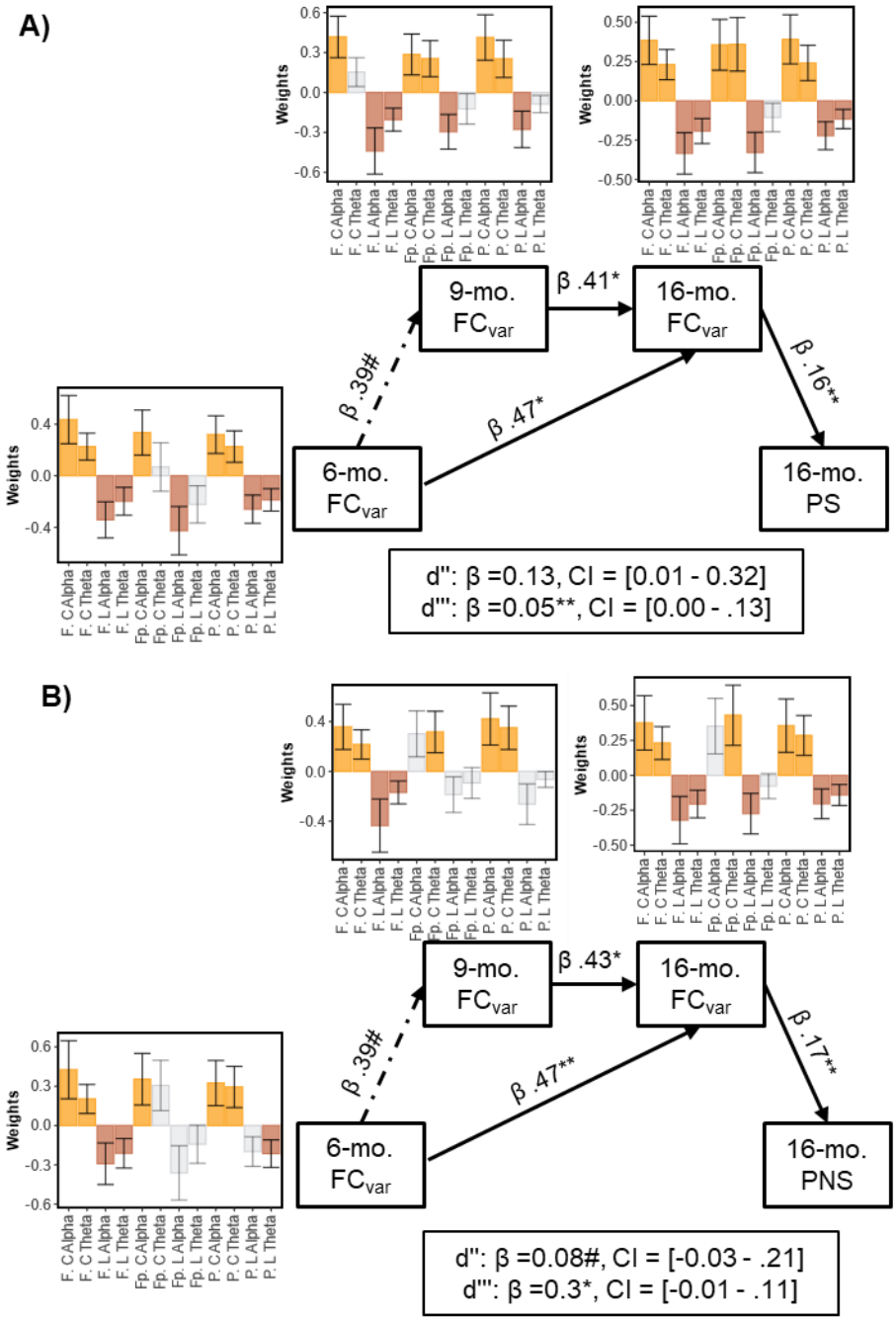

Fig. 5B.2. PLS analysis for predicting PS/PNS performance based on functional network properties. The figure displays the significant path after permutation testing and the indirect paths between PS (A), PNS (B), and FC_{var}. The colored weights represent reliable factor loadings (yellow = clustering, orange = path length), whereas gray represents unreliable factor loadings. F = Frontal, Fp. = frontal pole, P = Parietal, L = Path Length, C = Clustering Coefficient. $^{**}p < .01$, $^{*}p < .05$, # $p < .10$.

The pattern of the results with IS was similar to that of PS and PNS. We found stability between sessions in FC_{var}, or at least a trend after permutation procedure (FC_{var} from 6-mo. to 9-mo.: β = 0.39, $p_{original}$ = .004, $p_{permuted}$ = .086; FC_{var} from 6-mo. to 16-mo.: β = 0.46, $p_{original}$ < .001, $p_{permuted}$ = .013; FC_{var} from 9-mo. to 16-mo.: β = 0.42, $p_{original}$ = .028, $p_{permuted}$ = .039), and an association between FC_{var} at 16-mo. and IS accuracy (β = 0.17, $p_{original}$ = .075, $p_{permuted}$ = .008), while the other direct paths were not significant or marginal (6-mo. FC_{var} to IS: β = 0.02, $p_{original}$ = .879, $p_{permuted}$ = .922; 9-mo. FC_{var} to IS: β = 0.29, $p_{original}$ = .010, $p_{permuted}$ = .073). Indirect paths through FC_{var} were significant and reliable (d'': β = 0.13, $p_{permuted}$ = .02, 95% CI = [0.01 – 0.24]; d'': β = 0.05, $p_{permuted}$ = .03, 95% CI = [0.02 – 0.11]). Reliable loadings were scarce and mainly over frontal areas (see Fig. 5B.4).

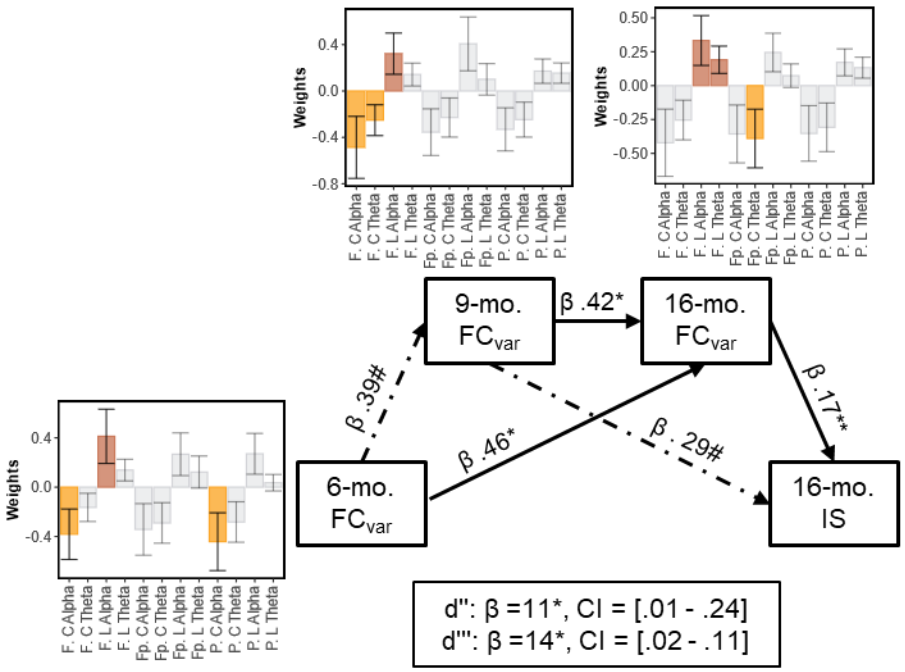

Fig. 5B.3. PLS analysis for predicting IS performance based on functional network properties. The figure displays the significant path after permutation testing and indirect paths between IS and FC_{var}. The colored weights represent reliable factor loadings (yellow = clustering, orange = path length), whereas gray represents unreliable factor loadings. F = Frontal, Fp. = frontal pole, P = Parietal, L = Path Length, C = Clustering Coefficient. ** p < .01, * p < .05, # p < .10.

5B.2.2. Functional network topology and Bee-Attentive performance

All information regarding the demographic descriptives of the sample of the analysis between Bee-Attentive and functional networks can be found in Tables 5B.3 and 5B.4. The performance and network parameters can be seen in Appendix Tables A5B.3 and A5B.4. Among all the variables studied (Go and NoGo accuracy, and median RT, SD RT, and RT cost), none had significant associations, either direct or indirect, with FC_{var}. Only the RT cost was marginally related to FC_{var} at 9-mo. (β = 0.39, $p_{original}$ = .004, $p_{permuted}$ = .086) and 16-mo. sessions (β = 0.39, $p_{original}$ = .004, $p_{permuted}$ = .072). The figures of these analyses can be found in the Appendix of this chapter.

Table 5B.3

Mean number of trials (SD) in each session of the EEG and Bee-Attentive at 36 months.

Sex	*n*	EEG				Bee Attentive			
		6-mo.	*9-mo.*	*16-mo.*	*36-mo.*	*Go*		*No Go*	
						Low	High	Low	High
F	25	286.05 (108.35)	313.08 (88.15)	250.5 (91.46)	320.87 (123.36)	37.8 (9.79)	37.45 (10.85)	15.75 (5)	15.55 (4.07)
M	22	250.45 (102.24)	234.25 (69.3)	314.46 (156.16)	397.44 (76.6)	35.95 (7.24)	36.2 (7.74)	15.55 (3.55)	15.4 (3.12)

Note. F = Female, M = Male.

Table 5B.4

Demographic information of the sample included in the relationship analysis between Bee-Attentive and functional network properties.

Sex	*n*	BW (kg)	GW	Session Age (days)			
				6-mo.	*9-mo.*	*16-mo.*	*36-mo.*
Female	25	3415.45 (528.14)	39.5 (1.44)	192.8 (8.49)	282.96 (6.46)	514.68 (26.55)	1112.81 (19.03)
Male	22	3372.5 (341.98)	39.56 (1.38)	194.86 (8.82)	288.26 (13.46)	519.4 (22.78)	1124 (33.57)

Note. BW = Birth Weight, GW = Gestation Weeks.

5B.3 Discussion

The main goal of the current study was to investigate the associations between EA and the brain functional connectome in a developmental sample from infancy to early childhood. To this end, we evaluated EA using two tasks suited to evaluate the dissociable components of EA: ECITT and Bee-Attentive. Children performed the Bee-Attentive task when they were 36-mo., while toddlers performed the ECITT at 16 months of age. We then associated individual differences in EA with brain function measured with the segregation and integration network characteristics over the frontal, parietal, and frontal-pole electrodes in the alpha and theta bands. Overall, our results showed that there was a significant association between the functional connectome and children's performance in the ECITT task, but no significant relationship was found in the Bee-Attentive task.

5B.3.1. Functional connectivity and cognitive capacity

Both PS and PNS trial accuracy were predicted by a component factor that included mostly frontal and parietal areas, with larger loads in the alpha band than in the theta band. The direction of the loads was negative for path length and positive for clustering coefficient. As shown in Chapter 3B, this corresponds to a more mature pattern of functional networks as the clustering coefficient and global efficiency (i.e., inverse of the path length) increased with age. Other studies have shown this developmental pattern in the first years of life, although mainly in fMRI studies (Vértes & Bullmore, 2015; Zhao, Xu, et al., 2019), and the results coincide with the efficient brain theory, in which the optimal balance between a highly specialized yet efficiently integrated network benefits cognitive performance (Barbey, 2018; Bullmore & Sporns, 2012; van den Heuvel et al., 2009). However, in the IS trials, we found the opposite pattern, with the clustering coefficient and path length over the frontal areas being negative and positive predictors, respectively, of children's performance. This suggests that an optimal balance between segregation and integration may depend on task requirements, as we further discuss below.

Previous studies have supported the involvement of functional connectivity in early cognition (Bell & Fox, 1992; Broomell et al., 2021; Cuevas et al., 2012; Whedon et al., 2016). For example, 9-mo. infants with stronger

frontal-temporal connections in alpha exhibit better IC control (Bell & Fox, 1992) and larger age-related changes in frontal coherence in alpha are positive predictors of CF and IC capacity (Broomell et al., 2021; Whedon et al., 2016). Additionally, better integration between frontoparietal areas in the beta band is a positive predictor of WM capacity and intelligence (Barnes et al., 2016), and these connections are strengthened after cognitive training (Astle et al., 2015).

The structural and functional properties of brain networks are also associated with individual differences and the protracted emergence of EA (Langer et al., 2012). The gradual specialization of structural modules over the frontoparietal network mediates the emergence of high-order cognitive processes in childhood (Baum et al., 2017), and age-related changes in executive rs-fMRI networks promote the development of cognitive control (Cui et al., 2020; Marek et al., 2015; Wang et al., 2021). This has also been shown in fNIRS studies, as the gradual strengthening of connections between the frontal and parietal areas sustains IC development in early childhood (Buss et al., 2014; Buss & Spencer, 2018).

Previous, cross-sectional studies in childhood and adulthood have shown that more segregated and efficiently connected networks improve performance in attention and intelligence independent of neuroimaging techniques, such as fMRI (Cole et al., 2012; Finn et al., 2015; Stevens et al., 2012; Van Den Heuvel et al., 2009; but see Kruschwitz et al., 2018), and EEG (Knyazev et al., 2017; Langer et al., 2012; Langeslag et al., 2013; Zakharov et al., 2020). Remarkably, functional connectivity imbalance is a characteristic of ADHD, albeit with some mixed results depending on the task, neuroimaging modality, and frequency band (Henry & Cohen, 2019). For instance, in their study Furlong et al. (2021) found larger global efficiency in ADHD, while others found augmented local efficiency but reduced global efficiency (Lin et al., 2014), or variations on network segregation (Ahmadi et al., 2021; Ahmadlou et al., 2012; Ghaderi et al., 2017). Therefore, our results align with the association between functional connectome topology and individual cognitive differences.

The involvement of both the frontal and parietal electrodes in PS/PNS, but to a lesser extent in IS, coincides with the relevance of the

frontoparietal areas in flexible adjustment and high-order cognitive processes (Keller et al., 2022; Marek & Dosenbach, 2018; Petersen & Posner, 2012). Indeed, several authors have highlighted their relevance in previous theories, such as the parieto-frontal intelligence theory (P-FIT; Jung & Haier, 2007), the multiple demand system (Duncan, 2010), and the network theory of intelligence (Barbey, 2018). In all these, coincident with the efficient network proposal, the integration of the frontal and parietal areas is crucial to explain complex behavior. Indeed, previous studies have highlighted the relevance of their integration in self-regulation (Karama et al., 2011; Knyazev et al., 2017; Langeslag et al., 2013). Consequently, the maturation of frontoparietal connections is arguably one of the most relevant factors explaining the emergence of executive processes (Stevens et al., 2012; Uddin et al., 2011).

One distinction between our study and previous research in EEG is that we did not evaluate the direct connections between the frontal and parietal areas but employed a network approach with .25 of the connections. Therefore, the integration cost in each cluster represents the capacity to integrate with all other electrodes, independent of the existence or absence of direct paths. This might have helped to find a relationship with behavior, as other studies have found a global reconfiguration while performing demanding cognitive tasks (Cooper et al., 2015).

5.3.2. Alpha and theta bands connectivity and cognition

Both alpha and theta were co-predictors of toddlers' performance, which may suggest a lack of specificity in the results. However, the alpha and theta bands have previously been shown to underpin high-order cognitive processes (Clayton et al., 2015; Klimesch, 2012). Demanding tasks trigger the strengthening and reconfiguration of theta and alpha band connections between frontoparietal areas when active control (vs. baseline) is required (Cooper et al., 2015). Furthermore, alpha and theta connectivity has been associated with sustained internally driven attention (Clayton et al., 2015; Kam et al., 2019; Palva & Palva, 2011), memory (Muthukrishnan et al., 2020; Sauseng et al., 2010), online adaptation (Oehrn et al., 2014), and top-down modulation of posterior areas (Fries, 2015; Sadaghiani et al., 2012). This reconfiguration of functional connectivity occurs even in infancy, as Cuevas

and Bell's groups have repeatedly shown in the alpha band (e.g., Cuevas et al., 2012), suggesting that online reconfiguration occurs from an early age.

Simultaneous EEG/MEG – MRI experiments have revealed that functional connectivity in the alpha band is related to the underlying BOLD signal. In fact, the co-activation of executive network areas is related to the strengthening of alpha connections (Sadaghiani et al., 2012), which is consistent with the top-down influence of the alpha band on posterior areas (Alamia et al., 2023). Therefore, the involvement of both the alpha and theta bands in our study is consistent with their functional roles in evoked paradigms and their function as long-range integrator mechanisms (Marek & Dosenbach, 2018; von Stein & Sarnthein, 2000). In addition, given the complexity of the ECITT, it is possible that both are co-predictors because they support complementary, albeit different, cognitive processes.

5.3.3. Optimal network configuration for different cognitive processes

One puzzling result in our study is the different direction of the load in the PS/PNS compared with the IS. Having larger segregation and better integration costs was positive for the prepotent side, but not for the inhibitory side performance. These results may be a consequence of distinct optimal network configurations in relation to behavior. As stated above, according to rs-fMRI development, a more mature brain is more segregated and efficient should predict better cognitive performance (Bullmore & Sporns, 2012). However, the opposite pattern emerges when adults conduct tasks that involve the coordination of different networks (Cohen & D'Esposito, 2016; Finc et al., 2020). That is, despite the large proportion of connections shared between rs- and task-related networks (Cole et al., 2014; Hansen et al., 2015; Krienen et al., 2014), segregation and integration may be specific to each mental state. Consequently, the optimal values of the connectome topology will rely on task demands. A recent study by Wang et al. (2021) supports this perspective, as they found different contributions of segregation and network efficiency to different aspects of the task (RT vs. general cognition).

Given the impact of cognitive states in network topology, the differences between PS/PNS and IS may be a consequence of our baseline. We made soap bubbles (Block 1) and presented a dynamic video (Block 2) to keep the children soothed. This is different from the classical adult protocol for

eyes open or closed. Our baseline implied salient stimuli designed to capture children's attention. Thus, it implies exogenous attention or even guided orientation due to how salient and positive they are for children. Previous studies have shown that EEG relies heavily on the environment, and that the alpha and theta bands are sensitive to cognitive demands (Bell, 2001, 2002; Stroganova et al., 1999) and are reconfigured during periods of attention (vs. inattention), even within the same protocol (Xie et al., 2018; Xie, et al., 2019). In fact, in case of employing the same protocol as adults, the cognitive resources for children may differ, as being quiet might require greater control in young developmental samples (Camacho et al., 2020). Therefore, it is possible that we related the configuration of the networks while orienting children's attentional focus, which may have caused some discrepancies between the PS/PNS and IS.

5B.3.4 Limitations and future directions

This study presents the same limitations identified in Chapter 5A, such as modest sample size, task design, and varying cognitive states at baseline. Our analysis focused on frontal-parietal clusters, as suggested by previous studies linking cognitive performance and brain function, and we evaluated clustering and path-length averaging across the electrodes. That is, we chose to include the average path length per electrode as a proxy for the general cost of integrating the electrode with all other channels. It is possible that individual electrodes within the clusters contribute differently to the relationship with EA, or that individual pairs of connections are more relevant than others. Thus, thresholding the network and computing the distance between electrodes could be an approach to further explore brain function and integration properties with behavior. In addition, we included only clustering and path lengths as indicators of segregation and integration properties, respectively. These measures do not consider the modularity of networks. Therefore, adding information about the Q value, participation coefficient, or within-module z-degree could provide insightful result

5B.4. Conclusion

The EA processes mature rapidly during the first years of life. These functions rely on functional networks that mostly involve frontoparietal brain areas (Petersen & Posner, 2012) that also undergo a profound reconfiguration in the first years of life (Gao, Alcauter, Elton, et al., 2015; Vértes & Bullmore, 2015). In addition, oscillatory communication between brain areas is essential for cognitive processes (Buzsáki 2006; Fries 2015). In this study, we explored the relationship between brain oscillatory networks and EA using the ECITT and Bee-Attentive tasks in a developing sample. We found that different topological characteristics were related to individual variations in ECITT performance, but not in Bee-Attentive. PS and PNS accuracy were related to a more efficiently integrated and segregated network in the alpha and theta bands, whereas IS displayed the opposite pattern. In both cases, alpha and theta bands were co-predictors of cognitive performance. Thus, our results suggest that early topology is related to behavior, contributing to the understanding of the involvement of brain networks in childhood behavior.

Chapter 6: General Discussion

In this doctoral dissertation, we studied age-related changes in brain functional activity, executive attention (EA development, and their relationships in a longitudinal study from the sixth to the thirty-sixth month of life. We recorded functional brain activity using EEG in a baseline protocol and extracted oscillatory/aperiodic and connectivity measurements. Behavior was measured using two new child-friendly tasks (Bee-Attentive and ECITT) that aimed to evaluate cognitive flexibility (CF), inhibitory control (IC), and focused attention. Overall, the results of this thesis support the drastic maturation that takes place in the first three years of life, both behaviorally and in EEG recordings, and their interplay during this period.

6.1. Brain Maturation Comes with Oscillatory, Aperiodic, and Communication Changes

Electrophysiological brain maturation was measured based on the power and functional connectome. In Chapter 3A, we isolated oscillatory power from aperiodic background electrophysiological activity, while in Chapter 3B, we employed graph theory from a multiverse perspective to delineate network organizational changes from infancy to early childhood.

Previous research on rs-EEG power development primarily explored either absolute and/or relative power and, in some instances, the frequency peaks of the alpha and theta bands. In the case of the alpha band, the characteristic peak in the power spectrum begins to manifest around the fourth month of life, characterized by transient activity at lower frequencies compared to adults (Smith, 1938). During the initial months of life, the alpha peak shifts towards higher frequencies while gradually amplifying its power (Freschl et al., 2022; Marshall et al., 2002). Conversely, studies examining the theta and beta bands have revealed increases in power when absolute power is considered (Dustman et al. 1999; Jing et al. In 2010, Wilkinson et al. 2023), but when relative power or power ratios are taken into account, a decrease in low-frequency (i.e., theta) power is observed (Marshall et al., 2002; Perone et al., 2018).

Recently, the power spectrum used in longitudinal studies was redefined to distinguish oscillatory activity from aperiodic activity (He, 2014;

Voytek & Knight, 2015). This distinction is crucial for understanding the biological mechanisms underlying oscillatory activity as they differ from those of the aperiodic background (Gao et al., 2017; He et al., 2010; Trujillo et al., 2019). While the aperiodic background is consequence of the balance between inhibitory and excitatory currents (Gao et al., 2017; Perica et al., 2022), each frequency band has its own brain mechanisms (Buzsáki, 2006; Wang, 2010). Importantly, this inhibitory/excitatory balance also varies with age, which is shown in the flattening of the aperiodic curve (Brandes-Aitken et al., 2023; Cellier et al., 2021; Schaworonkow & Voytek, 2021). Also, the contribution of aperiodic activity is one of the most influential factors in power ratios (Donoghue et al., 2020), underscoring its significance in the study of EEG power.

In Chapter 3A, we found changes in aperiodic and oscillatory brain activity, revealing distinct developmental patterns when oscillatory activity is isolated from aperiodic power (vs. relative power). The alpha band exhibited a similar trajectory in relative and oscillatory power, while theta relative power diminished with age (in contrast to no change in oscillatory power) and beta band power increased (as opposed to a reduction in oscillatory power). Additionally, the proportion of the alpha peak increase while augmenting its peak frequency (approximately 1.5 Hz). Additionally, at 6 months, infants exhibited two frequency peaks (present in approximately 50% of children) in the alpha and theta bands. The prevalence of theta peaks decreased with age, suggesting the gradual emergence of alpha as dominant rhythm. Concerning aperiodic activity, we found a consistent flattening of the background curve in the first years of life, and aperiodic components were significant predictor of theta- and beta-band relative power beyond the influence of oscillatory activity.

Aperiodic background flattening has been observed from birth to the sixth month of life and extends beyond three years of age to adulthood (Cellier et al., 2021; Hill et al., 2022; Schaworonkow & Voytek, 2021). This flattening process is linked to the maturation of glutamatergic currents and implies a general shift towards more excitatory activity in the excitatory/inhibitory balance (Perica et al., 2022). Thus, Chapter 3A highlights the significance of segregating aperiodic and oscillatory activity and unveils

the possible confounding of previous studies by 1) the conflation of aperiodic and oscillatory activity in relative power, and 2) the overshadowing of the development of other bands by the emergence of the alpha rhythm. That is, as power flattens with age, increases in high-frequency power may be due to gradual flattening in the aperiodic background curve. Consequently, the relative power also may decrease at lower frequencies. Additionally, while the alpha band exhibits a steady increase in energy, part of the results in the relative ratios may be driven by the lack of a peak over the power spectrum. Finally, changes in alpha power aligned with previous research findings, particularly from infancy to early childhood (Marshall et al. 2002) and other studies exploring alpha oscillatory power also shown a profound reconfiguration (Cellier et al., 2021; McSweeney et al., 2021; Schaworonkow & Voytek, 2021).

The patterns uncovered in Chapter 3A do not mean that oscillatory activity in the theta and beta bands remains stable with age. Several evoked paradigms have revealed age-related changes in time frequency analysis. As infants grow old, theta power increases during conflict tasks (Adam et al., 2020; Chevalier et al., 2021; Van Noordt et al., 2022) and so does beta power during motor paradigms (Rayson et al., 2023). Consequently, one limitation of the power spectrum approach is the loss of temporal information. We addressed this concern in Appendix 3A. In this concise analysis, we evaluated the signal rhythmicity and self-predictability of the oscillations over time (Fransen et al., 2015). Moreover, we employed the p-method to assess the presence and properties of the bursts. Our findings indicate that the alpha band is self-predictable over approximately five cycles, which implies that it is sustained, whereas the theta and beta bands primarily rely on transient bursts. Intriguingly, the alpha activity gradually transitioned to a sustained activity across sessions at least in parieto-central areas. Furthermore, the burst amplitude increased in all three bands, which signalled the limitations of the stationary power spectrum in evaluating other bands.

Discrepancies between the static power spectrum and burst methodologies suggest that non-stationary processing may prove crucial in the investigation of rhythms beyond the alpha band. Indeed, the

developmental trajectory we observed aligns with previous findings from the evoked paradigms. As previously mentioned, both the theta and beta bands show increased power with age. This increase is believed to reflect the maturation of cognitive mechanisms and follows an inverted "u" shaped pattern (e.g., Lo, 2018). Initially, evoked activity is absent, followed by a substantial increase combined with over recruitment of brain areas, to finally achieve a more specific and efficient brain activity. This pattern is observed with various event-related potentials, including P3 and N2 (Hämmerer et al., 2010; Pires et al., 2014) that exhibit a gradual trajectory parallel to the emergence of executive control. This phenomenon also extends to time-frequency analysis in infancy, as infants' potentials are typically larger, more prolonged, and appear at later latencies than those of older children and adults (e.g., Adam et al., 2020; Conejero et al., 2016).

In Chapter 3B, we explored the functional connectome within the alpha, theta, and beta bands. Previous studies have primarily relied on direct connections as a reference measure (Barry et al., 2004; Thatcher et al., 2008). This approach considers the existence of direct synchronization between every pair of electrodes, which deviates from the most plausible communication pattern incorporating short- and long-range connections along with intermediary edges (Bullmore & Sporns 2012). Thus, direct connections do not adequately capture the topology of functional networks or provide insights into the efficiency of the functional connectivity. Over the past few decades, researchers have employed graph theory in combination with functional neuroimaging to address these limitations (Watts & Strogatz, 1998). This theory enables a more comprehensive characterization of brain networks based on common mathematical principles, irrespective of the scale of the network.

At birth, somatosensory networks are predominantly delineated, whereas attentional and executive networks remain immature. Orienting and executive networks progressively emerge, becoming more defined around the sixth and twelfth month of life, respectively (Gilmore et al., 2018). The maturation of functional networks seems to be driven by two fundamental principles: integration and segregation (Gilmore et al. 2018; Yin et al. 2019; Zhao et al. 2019). During development, networks tend to strength

connections within proximal, highly interconnected areas (Fransson et al., 2007, 2011; Yin et al., 2019), while strengthening crucial long-range connections between these nodes and pruning the irrelevant ones (Gao, Alcauter, Elton, et al., 2015; Gao, Alcauter, Smith, et al., 2015; Gao et al., 2011). Despite the temporal limitations of fMRI, it has been the preferred method for exploring brain network development. However, brain communication occurs at different frequency rhythms, each with distinct communicative roles (Fries, 2015; Marek & Dosenbach, 2018; von Stein & Sarnthein, 2000). Hence, to complement the fMRI literature, we explored the development of the functional connectome using the graph theory approach as previous studies employing functional connectome in the first three years of life are scarce and yielded mixed results (e.g., Hu et al., 2022; Xie et al., 2019).

In chapter 3B, we initially conducted a multiverse analysis to examine the differences between the network construction preprocessing steps. This analysis revealed profound reconfigurations in the coherence-based and phase-based methods, particularly when they were not debiased. Notably, weighted networks exhibited an opposite trajectory in global efficiency compared with binary networks, while displaying a similar pattern in age-related segregation. This suggests that while segregation remains a consistent phenomenon in network development, the integration cost may be high for the brain if the strength of the connections is not considered. As the brain promotes the strengthening of top connections, the creation of new long-range connections may be less costly, even if initially perceived as non-optimal.

Subsequently, in Chapter 3B, we conducted a more detailed analysis of coherence networks, as they exhibited the largest reconfiguration with age. These coherence networks revealed two distinct clusters places over the frontal and parietal/occipital regions. These clusters accounted for the majority of connections and were clearly segregated from the remaining clusters but interconnected throughout intermediate long-range connections. Furthermore, we observed that infant networks were modular and presented a small-world topology; however, these parameters were stable in the transition from infancy to early childhood. In addition, throughout the

sessions, the functional network became more segregated, promoting specialization and an increase in local and global efficiency.

The findings in Chapter 3B aligned with the presence of parietal and frontal clusters and the early emergence of a small-world topology (Hu et al., 2022; Omidvarnia et al., 2014; Shrey et al., 2018). Nevertheless, prior research has reported mixed results regarding maturation trajectories, with some studies showing stability in topology parameters, whereas others indicated a reduction of small world topology with age (Hu et al., 2022; Xie et al., 2019). Furthermore, the development of the integration cost of the network has shown different trajectories among studies (Miskovic et al., 2015), whilst the progressive gradual segregation of the functional connectome in EEG has been constantly reported (Boersma et al., 2011, 2013; Kavčič et al., 2023). Our multiverse approach contributed to determine that some of these inconsistencies may be attributed to variations in processing steps and highlights the importance of reporting multiple measurements within the study, establishing different trajectories for each frequency band.

The patterns observed in coherence-based networks resemble the strengthening of direct connectivity observed in other studies (Barry et al., 2004). Additionally, an increase in functional integration and segregation has been reported in fMRI studies (Vértes & Bullmore, 2015; Zhao et al., 2019). However, our findings deviate in two ways from fMRI studies: 1) we did not identify hubs and 2) our networks remained spatially stable. These discrepancies contrast with fMRI studies in neonates showing that hubs are already present at this age and the posterior-anterior transition of hubs occurs in the first months (Asis-Cruz et al., 2015; Wen et al., 2019). It is possible that the EEG space constraints may have reduced the sensitivity to developmental changes in topology. However, our results are similar to the reconfiguration principles proposed in fMRI studies and, consequently, suggest that the functional connectome matures towards a more efficient configuration.

Chapters 3A and 3B of this thesis demonstrated the drastic reconfiguration in brain function that occurs within the initial three years of life. This period is characterized by a dramatic rate of maturation, which may

be unparalleled by any other period in the human lifespan. From birth to the end of the third year, a series of developmental milestones occur (Bethlehem et al., 2022). Concurrently, white matter proliferates, promoting the refinement of structural circuitry through the formation of novel connections and the reinforcement of existing connections via myelination of neural tracts (Dubois, 2014; Ouyang et al., 2019). These structural changes are followed by shifts in the functional characteristics of the brain. Consonant with these changes, our investigation revealed a transition in dominant brain oscillation, which evolves toward a rhythmic pattern and increases its peak frequency and power. Additionally, functional brain networks became more specialized, and the efficiency of network integration was enhanced. Notice that the observed trajectories exhibited a quadratic trend in most cases, consistent with the notion of steeper developmental changes occurring in the first months of life. To further increase our understanding, future studies should consider combining neuroimaging techniques, incorporating even younger participants, and recording peripheral activity measures to capture the infant's and toddlers' cognitive state. All these implementations will offer a more comprehensive perspective of early neurodevelopment.

6.2. Age-related Gains in EA

In Chapter 4, we explored the development of EA processes, employing two child-friendly tasks, the ECITT and Bee-Attentive tasks. Our findings collectively highlight the maturation of IC and CF and that it is plausible to assess two attentional processes in children as young as three years old.

The ECITT (Holmboe et al., 2021), conceived by one of our collaborators, was designed to assess IC and CF without relying on memory processes or verbal instructions. Instead, it is based on a contingency learning. In this task, two blue rectangles are presented in a tablet screen, and one contains a "smiley face." On most occasions, it appears on one side of the screen (75%) while in occasional trials is placed in the opposite place (25%). This design promotes building a prepotent answer, which needs to be suppressed when the target appears in the infrequency location (IS trials; IC). It also evaluates the cost to flexibly switch when the target returns to the prepotent place (PS trials, CF). Our findings revealed that IS were the most

challenging trials, followed by PS, and those in which the smiley face appeared several times on the prepotent side on a row were the easiest (PNS). This task was doable at 9-mo. sessions, as infants' performance was superior to the chance level. This is one month earlier than previous studies and suggest that it can be implemented in younger samples. Additionally, 16-mo. toddlers demonstrated better performance IS and PNS than in the second session, but no changes in PS accuracy. This suggests the rapid development of IC albeit the stabile capacity of CF processes in this task between sessions. Notably, individual performance in IS trials at 9 months was a significant predictor of IS performance several months later, revealing the stability of this cognitive process within task.

To evaluate the EA in 3 years old children, we developed the Bee-Attentive task. It was designed to concurrently evaluate executive and focused attention by combining the rationale of a Go/NoGo paradigm with a visual-search protocol. Children were asked to help the Bee (80% of trials; Go) to collect honey by pressing a button when it appeared, while avoiding press the button when the Wasp was present (20% of trials; NoGo). Simultaneously, other bugs appeared on the screen in two possible conditions: low load (1–2 insects) and high load (5–6 insects).

Our results denoted that child performed above the chance in Go and NoGo trials, and the task presented the general inhibitory cost when the Wasp appeared as the accuracy on NoGo was lower. Intriguingly, this pattern did not vary with the load conditions, as accuracy levels held similar values in low and high load scenarios. However, RT and its variability suffer when the high load condition occurred. In this task, children also were able to self-regulate following an error provided by their slower RT and higher accuracy. Thus, the differences found between the PNS/IS and Go/NoGo trials signal the online adaptation of children's behavior. In addition, our study revealed that three-year-old children self-regulate their behavior following an error, resulting in improved performance in Go trials, albeit at the cost of slower reaction times. However, NoGo trials showed a reduction in performance, possibly linked to the augment in arousal level because of the feedback sound.

In regard to PS/IS and NoGo trials, our findings indicated that infants could inhibit their responses, despite exhibiting a higher error rate compared to easier trials. However, we did not observe any significant differences in PS between the second and third sessions, whereas children exhibited improvements in IS trials. The early capacity to inhibit and flexibly change found in the ECITT aligns with other infant tasks measuring IC, such as A-not-B and Fraze-Frame (e.g., Holmboe et al., 2018). Furthermore, the development of IC is consonant with previous literature on A-not-B, as infants and toddlers progressively become more capable of change the prepotent answer (Bell & Adams, 1999; Clearfield et al., 2006; Diamond, 1985). However, our results differ from those reported by Hendry et al. (2021), who did not observe age-related changes between 10 and 16 months of age in the ECITT task. One possibility to explain this discrepancy is considering when the ECITT session took place. Infants in our study were younger in the first, and older in the second session, which increased the gap between longitudinal waves. In fact, the development of IC occurred using both IS and the original index of IC proposed by Hendry et al. (2021). Therefore, the temporal separation likely accounted for the differences between studies.

The lack of change found in PS trials between sessions suggests that CF capacity is stable and may reach a plateau at an early age. Notwithstanding this idea, researchers have shown that difficulties in changing both within- and between-tasks further develop later on (Zelazo et al., 1996, 2003). For instance, children's capacity to flexibly shift rules in the DCCS task is not achieved until the second year in simplified versions of the task to reduce conflict (Garon et al., 2014). Therefore, CF continues to improve with age, which probably signal that either the age of the sessions was not separated enough of that the ECITT can not capture developmental changes in CF.

Finally, we showed that combine and extract several attentional markers from one task at age three years old. Previous attentional protocols, such as the child version of the ANT, are not suitable until nearly the fourth age because of the complex instructions (Casagrande et al., 2022; Rueda et al., 2004). We achieved this by giving a history line behind children' actions,

while adding several blocks of practice. However, nearly a 10% of the children did not comprehend the instructions. This represents the difficulty for some children probably due a language barrier. In addition, despite of the general cost of inhibiting and orienting in high load conditions, that probably will get reduced in the following months (Gerhardstein & Rovee-Collier, 2002; Woods et al., 2013), it is possible that the parameters chosen were suboptimal because the lack of interactions and the median RT found. Infants performed equally well in both low and high load conditions, and only needed approximately half of the maximum time of the target in the most difficult conditions. Further versions need to adjust such parameters to make searching and IC more challenging.

In summary, our current findings provide insights into the development in IC processes and children's capacity to engage in more complex task. These results align with other paradigms, such as A-not-B, which highlight similar developmental changes. Future investigations should consider exploring IC and CF in intermediate and older children using the ECITT task to further delineate its developmental trajectory. Additionally, our newly designed Bee-Attentive task showed consistent markers of IC and self-regulation, similar to those found in other IC and search paradigms.

6.3. Developing Oscillations for a Rhythmically Sampled World

In the final experimental chapters of this dissertation, we studied the relationship between oscillatory/aperiodic activity and functional connectome with infant behavior. While previous research has explored the relationship between brain oscillations and cognitive development in children and adults, this study contributes to the literature by focusing on the early years of life (0-3 years) and emphasizing the developmental aspects of oscillatory activity and functional networks. These chapters offer novel insights into the specific relationship between EEG aperiodic/oscillatory activity and connectomes with attentional processes.

In Chapter 5A, we explored the relationship between ECITT and Bee-Attentive with the aperiodic exponent and oscillatory activity (peak

frequency and power) of the theta and alpha bands. Our findings revealed significant concurrent relationships between PS and theta peak frequency, and oscillatory power at 9-mo. predicted the performance of PS trials at 16-mo. Intriguingly, we did not find significant relationships in the Bee-Attentive task. Hence, the relationship found may be task dependent in our study.

In Chapter 5B we delved into the association between the segregation and integration properties of functional networks placed over the parieto-frontal areas and ECITT performance. Remarkably, we observed that a more segregated and globally efficient network was as a positive predictor of PS/PNS trials, whilst the opposite pattern occurred in IS trials. Moreover, both alpha and theta oscillations were co-predictors of children's performance, highlighting its role in cognitive control. However, associations between the Bee-Attentive task and brain function were not significant.

Previous research has shown at a positive association between higher alpha activity or greater differences between baseline and task-related protocols and children's EA capacity (Bell, 2002; Cuevas & Bell, 2022; Whedon et al., 2020). Likewise, in studies that explored theta modulation in baseline larger reconfiguration of theta band was related to intelligence and EA from infancy to toddlerhood (Begus et al., 2015; Braithwaite et al., 2020; Jones et al., 2020). Moreover, despite not showing any significant results in our study, alpha peak frequency has been considered a marker of developmental changes in relation to cognition (Grandy et al., 2013; Leno et al., 2021), and both theta and alpha peaks are sensitive to environmental variations and task demands (Mierau et al., 2017; Senoussi et al., 2022).

Surprisingly, our results did not reveal any significant association with the aperiodic exponent of the power spectrum. Some authors have hypothesized that, given that exponent reflects the balance between GABAergic and glutamatergic currents, it would be relevant to typical and atypical development (Ostlund et al., 2022). In fact, aperiodic exponent has been linked to conditions such as ADHD, ASD, and human cognition, both in baseline and task-evoked protocols (Immink et al., 2021; Shuffrey et al., 2022). Consequently, it is unlikely that the aperiodic background does not

significantly contribute to infant cognition, and it is plausible that we may have missed this association or that it is specific to other cognitive processes.

Brain network configuration and connectivity have a crucial role in the development of high-order cognitive functions and individual differences (Keller et al., 2022; Marek et al., 2015; Posner et al., 2014). For example, the maturation of cognitive control is linked to the gradual specialization of executive networks (Baum et al., 2017). As children grow older the connections between frontal and parietal areas increase their strength while they perform WM and IC tasks (Buss et al., 2014; Buss & Spencer, 2018). In addition, the early development of frontoparietal and cinguloopercular network areas aligns broadly with the rapid progression of EA (Fiske & Holmboe, 2019; Keller et al., 2023; Posner et al., 2014) and differences in functional network properties among adults and children has been associated with fluid intelligence and executive processes (Cole et al., 2012; Hilger et al., 2017; Schultz & Cole, 2016; Van Den Heuvel et al., 2009; but see Kruschwitz et al., 2018). This underscores the significance of network topology. In fact, even when all the networks are considered together, the executive ones are the principal contributors to children's cognitive performance (Cui et al., 2020; Keller et al., 2023). This corroborates the relevant role of frontoparietal connections in high-level cognitive control and intelligence (Barbey, 2018; Duncan, 2010; Jung & Haier, 2007). Consequently, our study provides further support for its relevance, as it reveals a direct relationship between network segregation and integration and the individual differences observed in EA.

One striking finding in our results was the opposite contributions of functional connectivity in PS/PNS and IS. Thus, it is possible that the optimal balance between segregation and integration differs for each cognitive component. Additionally, the baseline employed may be qualitatively different from adults resting-state protocols (Camacho et al., 2020). In fact, even small changes in the stimulus alter electrophysiological brain activity (Anderson et al., 2022; St. John et al., 2016; Stroganova et al., 1999). Given that we make soap bubbles and presented a dynamic video, our baseline paradigm probably captures children's attention exogenously; thus, affecting the sign of the relationship. In addition, recent studies has also reported

different optimal balance depending on the cognitive processes in adults (Cohen & D'Esposito, 2016) and modifications of network topology according to infant's attentive state (Xie et al., 2019).

Alpha and theta were co-predictors in most of our analysis. There is extensive evidence associating alpha and theta bands to high-order cognition. Evoked theta activity is related to memory, long-range integration, monitoring, and conflict resolution (Cavanagh and Frank, 2014; Herweg et al., 2020; Klimesch, 1999; Sauseng et al., 2010), while alpha is a multifaceted rhythm (Clayton et al., 2018; Wang, 2010) involved in attention and perception processes (Freschl et al., 2022; Klimesch, 2012; Mierau et al., 2017) via modulation of the activity in several areas (Alamia & VanRullen, 2019; Jensen & Mazaheri, 2010; Sadaghiani et al., 2012; Sadaghiani & Kleinschmidt, 2016). Given their relevant roles in cognition, both alpha and theta may be co-predictor of cognitive functions although probably with different roles. For example, connectivity in the alpha band during cognitive control is less specific than the connectivity in theta band (Cooper et al., 2015), and reactive control triggers alpha activity, while proactive control is linked to theta band (Clements et al., 2021).

Supporting the involvement of both alpha and theta bands in infants' and toddlers' cognition, previous studies have highlighted their modulation in evoked paradigms. Frontal alpha in infancy is recruited in WM + IC tasks (task; Bell & Fox, 2018; Cuevas et al., 2012; Swingler et al., 2011), but simultaneously its power is reduced in sustained attention periods (Bell & Wolfe, 2007b; Xie et al., 2018). In addition, posterior alpha at baseline has similar qualitative roles in comparison to adults (Stroganova et al., 1999), albeit it is triggered in anticipatory attention (Orekhova et al., 2001; Stroganova et al., 1998). Theta band also augments under similar circumstances than adults. Anticipating a stimulus increases theta power (Stroganova et al., 1998), it is affected by cognitive resources allocation and attentional state (Braithwaite et al., 2020; Xie et al., 2018; Xie et al., 2019) with some of these processes starting in the third month (Brandes-Aitken et al., 2023). Additionally, evoked theta over frontal areas is enhanced when infants explore and object, which predicts posterior object recognition (Begus et al.,

2015; Wass et al., 2018), and also is triggered when infants witnesses an error (Berger et al., 2006; Conejero & Rueda, 2018; Köster et al., 2019, 2021).

The early recruitment of alpha and theta band constate its critical role in cognition from birth. Alpha and theta rhythms, in conjunction with other non-explored rhythms in this thesis (e.g., delta, beta, gamma), tailor infants' and toddlers' cognition, biasing how they perceive the world and interact with it. Thus, its development is crucial as we live in a highly rhythmic world and a large part of the stimulus surrounding us follows a cyclic structure, ranging from the day-night cycle to walking. Oscillatory synchronization and desynchronization enable us to attend, process, and respond to sensory stimuli and capture information as we built the world based on our capacities but also we modulate brain function to adapt to the world (Charalambous & Djebbara, 2023).

This interaction between brain, body, and environmental rhythms is studied with resonance and entrainment, although in very young participants it involves mostly rhythmic auditive/visual stimulation (Calderone et al., 2014; Köster et al., 2023). Resonance consist of the oscillatory activity coupling with an external rhythm but disappearing when it is absent, whereas entrainment implies the alignment of oscillatory activity to the regular patterns and also predict them (Lakatos et al., 2008; Obleser & Kayser, 2019; Raja, 2021). This is constrained by the preferent oscillatory rhythms of our brain, whose activity may be slightly adjusted to cognitive demands but without altering its operating range (Fries, 2005, 2015; Helfrich et al., 2018, 2019; Obleser & Kayser, 2019).

The relevance of oscillatory activity entrainment has been constated with the adaptation of peak frequency to task demands (Mierau et al., 2017; Senoussi et al., 2022). In complex protocols, alpha and theta peak increase its frequency, adapt to the frequency of the task, and even may alter perception depending on the relationship between the stimulus appearance and the phase of the oscillatory activity (Lakatos et al., 2008, 2019; Mierau et al., 2017). This coupling serves to capture the regularities and predict, anticipate, and optimize our behavior (De Graaf et al., 2013; Spaak et al., 2014). This makes alpha a visual candidate for visual integration (Freschl et al., 2022 for a

developmental perspective), while theta entrainment has been related to error detection and memory consolidation (Clouter et al., 2017; Hanslmayr et al., 2019; Köster et al., 2019).

In infancy, visual stimulation protocols has revealed changes in perception, such as visual acuity and contrast sensitivity (Norcia et al., 1978; Norcia & Tyler, 1984), and attentional paradigms in which flickering stimulation proximal to alpha band triggers its power (Robertson et al., 2012). This entrainment also occurs with more complex protocols. For example, visual entrainment of theta band while watching unexpected outcomes, results in a burst of theta activity (Köster et al., 2019). Additionally, during language and music infant's oscillatory activity adapt to the rhythm (Cirelli et al., 2016; Nguyen et al., 2023), which indeed is a marker of language acquisition (Nguyen et al., 2023).

Altogether our results and previous literature suggest that brain oscillations and cognition are steadily linked since infancy. The maturation of oscillatory activity probably reflects adaptability and plasticity of the brain during this period. The shift in peak frequencies, aperiodic/oscillatory changes, and network configuration provides to children the necessary tools to adapt their behavior to their environment as those changes will ultimately shape how children perceive and interact in the early years (Bánki et al., 2022; Köster et al., 2023; Wass et al., 2022).

6.4. Developmental In(stability): Key Factors in Open Systems

Throughout this thesis, we aimed to explore the relationship between the measurements, either within EEG or cognitive process or between them. Sometimes, EEG was highly correlated, albeit decreasing as the temporal intervals between sessions extended. This also occurred with behavioral measures, with IC being related within task, but not between tasks. Brain function was also related to some of the cognitive variables, especially in the ECITT task. This pattern underscores the complexity of the stability in the first three years of life. Previous research has yielded similar insights into the associations between oscillatory activity and brain cognition (Clearfield et al., 2006; Conejero et al., 2023; Gagne & Saudino, 2016; Marshall et al., 2002;

Miller & Marcovitch, 2015; Veer et al., 2017) as these investigations found both significant associations, but also lack of relationship. Even in evoked protocols, the association between brain and cognition is not always present (Cuevas et al., 2012; Gordillo et al., 2023; Rico-Picó et al., 2021; Whedon et al., 2020). Several plausible reasons may account for this pattern: 1) in infancy measures are noisier than adults, and the relationship may be truncated; 2) both quantitative and qualitative changes occur in this period (Posner et al., 2014); and 3) there are other variables that may affect individual differences (Bornstein, 2014).

When we study the stability and the interrelationship between variables, we assume that children's position within a hierarchy including their peers remains unchanged over time. That is, we might expect that a child who outperformed their peers several months ago continue to demonstrate better performance in the current session. This assumption lies on the premise that all the children follow identical developmental trajectories, or event that those with greater cognitive capacity will undergo larger changes. Nevertheless, children do not grow in a vacuum; their growth rate and development are shaped by a constant interaction between environmental and biological factors that influence both cognition and brain function. Thus, when we explore the concept of stability within a developing system, we must consider the complex interplay between the inherent characteristics (nature) and the external influence (nurture) that jointly alter the development. That is, cognitive and brain function development is not deterministic, but probabilistic, because we are partially dependent on the environment and our biological constraints (Bornstein, 2014; Johnson, 2011; Johnson & Haan, 2015).

A large percentage of cognitive capacity and brain function and structure is related to heritable factors, although the percentage explained varies depending on the age, cognitive process, and brain area (Briley & Tucker-Drob, 2013; Eyler et al., 2012; Haworth et al., 2010). For example, neurodevelopmental disorders, such as ADHD and ASD are highly heritable (Larsson et al., 2014; Wang et al., 2017) and the proportion of variability explained solely by genetics increases with age (Briley & Tucker-Drob, 2013; Haworth et al., 2010). In addition, brain structure is more influenced than

functional activity, specially in the hub connections (Arnatkeviciute, Fulcher, Bellgrove, et al., 2021; Arnatkeviciute, Fulcher, Oldham, et al., 2021; Ge et al., 2017; Thompson et al., 2013). Additionally, brain function heritability appears independently of the recording technique (Colclough et al., 2017; Fornito et al., 2011; van Den Heuvel et al., 2013).

While genetic factors undoubtedly contribute to the variability in cognitive processes and brain function, a deterministic view of human development would imply a static development without being influenced by children's environment. To date, there is evidence that, even when genetic components account for substantial portion of individual variability, there are multitude of factors that influence brain and cognition. This influence is particularly relevant during sensitive period, mostly in the first years of life, when the cognitive process and brain function and structure are dramatically maturing (Gabard-Durnam & McLaughlin, 2020; Thompson & Steinbeis, 2020). Thus, shared environmental factors or the perpetuation of parenting styles in those periods may explain part of the shared variance (Engelhardt et al., 2019; Petrill et al., 2004). These external factors can either nourish or hinder the maturation the development of cognitive and brain function by modifying their trajectory.

Among the factor that negatively impact children's development, socioeconomic status, stress, and maternal health has shown a profound relationship. Being raised in poverty (Brito et al., 2016; Otero, 1997; Otero et al., 2003; Tooley et al., 2020; Xie, Jensen, et al., 2019), having high stress levels (Barrero-Castillero et al., 2019; Evans & Schamberg, 2009; Lammertink et al., 2022; Pierce et al., 2020; Troller-Renfree et al., 2020), or that their mother had mental health problems (Coyl et al., 2002; Power et al., 2021) alters both brain function and cognition. In fact, some researchers claim that the impact of socioeconomic status on cognitive development involves alterations in brain structure and function (Farah, 2017; Johnson et al., 2016; Noble et al., 2012). Importantly, when these conditions are altered, the maturational trajectory moves toward a standard value within the developmental period (Marshall & Fox, 2004; Troller-Renfree et al., 2022). For example, teaching relaxation techniques to mothers has shown a positive impact on the newborns' brain (van Den Heuvel et al., 2015, 2018), and providing monetary

help to families below the poverty line affects infants' electrophysiological activity (Troller-Renfree et al., 2022).

On the opposite side, children's development can be nourished with day-a-day activities. Being regularly exposed to a second language (Kovacs & Mehler, 2009) or live within a cognitively stimulant environment (Wass et al., 2011; Wass, 2015; Forssman et al., 2018) favours children's cognitive capacity. This also occurs at the brain level, in which children who perform cognitive training usually present a more mature pattern of activity after the it is finished (Astle et al., 2015; Rueda et al., 2012; Pozuelos et al., 2019), although some of the training variance may be due to genetic factors (Musso et al., 2022; Zhao et al., 2020), and the effect size might be smaller and specific than initially thought (Diamond & Ling, 2016). Thus, brain and cognitive development occur through a constant interaction between natura and nurture. Maturation is not a passive process; instead, biology permits plasticity and adaptation to environmental factors throughout experience, which probably affects the stability of the measurements (Johnson, 2011; Johnson & Haan, 2015).

It is possible that part of the stability found occurs not because of differences in cognitive processes itself but because of the experience provided by an earlier acquisition of a cognitive domain, especially in the first years when its maturation occurs as a cascade of processes (Conejero & Rueda, 2017; Hendry et al., 2016). This initial scaffolding may help to maintain a certain distance from peers, but due to genetic and environmental factors this stability would probably decrease over time when those capacities are more stable.

Other factor that we must consider when discussing stability in very young samples is qualitative and quantitative changes that take place during early childhood (Siegler 2007). While children grow older, their become able to resolve more complex problems not only because changes in their capacity but due to variations in how they perform the tasks (Best & Miller, 2010; Johnson & Haan, 2015; Munakata et al., 2012). This happens especially in the first years of life when brain networks undergo profound reconfiguration. The asynchronous development of brain networks, with the protracted

development of executive networks (Fair et al., 2009; Gilmore et al., 2018; Vértes & Bullmore, 2015), probably contributes to the instability found in the first years of life (Posner et al., 2014). Additionally, given that infants/toddlers have goals, albeit simpler than doing taxes, they need to regulate their behavior. Thus, it is unlikely that they do not have resources to achieve it. If we think about it, suppressing our thoughts while watching a movie is not as different from how infants distract themselves by observing a colourful rattle when they are angry.

This involvement of different brain areas is shown in evoked neuroimaging protocols. In critical periods of the development of a function (e.g., WM), children's brains are usually overrecruited compared to adults, which is considered a signal of a non-efficient process (Buss et al., 2014; Buss & Spencer, 2018; Fiske et al., 2023). For instance, this has been shown in the transition from reactive to proactive control that occurs during childhood (Hämmerer et al., 2010) in which preparatory and inhibitory evoked potentials mature accordingly to the implemented strategy. Importantly, these qualitative changes are intertwined with the development of other cognitive processes, such as WM, and the latter partially relies on basic attentional mechanisms, such as distractor suppression (Gonthier et al., 2019; Plebanek & Sloutsky, 2019; Troller-Renfree et al., 2020). This interaction is also shown in our longitudinal study, as we have found inverted u shaped trajectories with some of the behavioral tasks. The infants in our study increases the number of perseverations to then decrease it (Moyano in prep.), which also occur in other tasks such as the A-not-B (Clearfield et al., 2006) and the differences in disengagement capacity (Nakagawa & Sukigara, 2013, 2019). Thus, beyond the networks involved, also the interaction with other process will contribute the instability in these periods. However, all these quantitative and qualitative variation will lead ultimately to flexibly adapt to the world.

6.5. Conclusion

Cumulative research has shed light on the early development of cognitive processes and their underpinning biological mechanisms. The first three years of life have plenty of changes, both in behavior and in brain

function. In this period, infant brains grow to reach nearly adult size, and their connections become more selective and stronger than they were previously affecting to functional activity. With every moth, the infants' electrophysiological activity becomes more adult-like. The alpha oscillations start to gradually emerge, the aperiodic background flattens, and the network topology becomes more efficient, yet specialized. Parallel to this, the self-regulation capacity increases. Infant behavior moves from environmentally driven to be directed by internal goals. Their ability to stop inefficient or incorrect and preponderant answers improve, and they can perform more complex tasks. This change from infancy to toddlerhood is intertwined with the development of brain function. However, these associations do not always appear, and there is sometimes a lack of correlation between the brain and behavior, and even between one's own behaviors. Thus, this period is characterized by a dramatic change that includes both stability and instability within a person. Arguably, qualitative, and environmental factor can explain partially these results because humans are, in the end, open systems and, as Borstein once wrote (2014) "the plastic natura of psychological functions ensures both stability and instability across the life course (…) many developmental processes are (…) continuous and discontinuous (…) Infants' status does not fix a child as to be stable does mean to be immutable."

General Summary

English

The capacity to act in a self-regulated manner and adjust to the surrounding environment requires attentional processes (Rueda et al., 2021). Posner's model (Petersen & Posner, 2012; Posner & Petersen, 1990) identifies three attentional mechanisms (alerting, orienting, and executive/control), which are dependent on five distinct brain networks: the alerting, dorsal attention network (DAN), ventral attention network (VAN), frontoparietal network (FPN), and cinguloopercular network (CON). The alerting network maintains the optimal level of activation, guided by CON and FPN, whereas the orienting mechanisms direct our focus towards elements that are salient or relevant to our goals. FPN and CON regulate our behavior, adapting it to our goals when necessary. Consequently, FPN and CON play critical roles in endogenous and adaptive behavior, involving processes such as monitoring, flexibility (CF), and inhibition (IC).

The three attention mechanisms interact in a coordinated manner to achieve our objectives. If the alert level is not optimal, we may overlook important information (i.e. low levels of alertness) or make impulsive mistakes (i.e. high levels of alertness). It is also essential to ignore irrelevant information to select informative elements for our goals. Finally, we must determine the best course of action, execute it, and evaluate its consequences, making the necessary adjustments when our goals are not achieved. These processes, which are fully developed in adults, are not present in infants because of the immaturity of their attentional networks (Gilmore et al., 2018). This restricts how they interact with the world during the first few years of life. Initially, infants' attention is driven by external stimuli; however, in the first semester of life, they will start to control their attention endogenously (Conejero & Rueda, 2017; Hendry et al., 2016, 2019).

Executive processes show the most protracted development when compared to orienting and alerting. Although in the first years of life volitional control seem to rely on orienting networks because of the immaturity of executive networks (Gao, Alcauter, Elton, et al., 2015; Posner et al., 2014), the later are recruited for specific tasks that involve a high degree of attentional control and require frontal brain regions (Ellis et al., 2021; Fiske

& Holmboe, 2019). This early recruitment is evident through changes in functional frontal brain activity when infants experience incongruent elements (Ellis et al., 2021), observe an error or unexpected event (Berger et al., 2006; Conejero et al., 2016; Stahl & Feigenson, 2015), and engage in complex tasks that require the inhibition of irrelevant information and of behavior (Bell, 2001, 2002).

The early development of executive attention (EA) is constated by the infants' capacity to flexibly adapt their behavior and inhibiting when needed. Starting at sixth months of life, infants start to exhibit flexibility and inhibition of their behavior and gaze. Infants at this age can withhold a prepotent answer when it does not lead to the desired outcomes (Diamond, 1985; Kovacs & Mehler, 2009). This cost of inhibiting and modifying a response decreases with age (Clearfield et al., 2006; Cuevas & Bell, 2010), although their development may be linked to other processes, such as memory (Holmboe et al., 2018). Certain paradigms, such as the Early Childhood Inhibitory Touchscreen Task (ECITT), have managed to limit the influence of memory on cognitive flexibility (CF) and inhibitory control (IC) protocols for infants, as they follow a contingency-based learning rationale. This task can be performed starting at 10 months of age and previous studies have suggested an increase in IC capacity between the first and second year of life (Fiske et al. 2022; Hendry et al. 2021; Holmboe et al. 2021; Liu et al. 2020). This supports the development of IC independently of memory although only four studies has employed these tasks.

Beyond infancy and toddlerhood, the ability to sustain attention for an extended period (sustained attention) and to inhibit distractions (focused attention) increases (Brandes-Aitken et al., 2019; Woods et al., 2013). In addition, children become capable of performing tasks with larger CF and IC requirements that involve verbal instructions. This entails conducting protocols similar to those of adults, such as the Go/NoGo tasks, stop-signal tasks (Carver et al., 2001), or the child version of the Attention Network Test (ANT; Casagrande et al., 2022; Rueda et al., 2004). Children's capacity to perform those tasks denotes their ability to resolve CF and IC, a capacity that will increase beyond the preschool period (Johnstone et al., 2005; Pozuelos et al., 2014; Rueda et al., 2004; Zelazo et al., 2003). However, most of the

paradigms only assess one cognitive procedure, and it is not until nearly fourth year of life that the interaction of attentional processes can be evaluated (Casagrande et al., 2022; Rueda et al., 2004).

The development of EA relies on the maturation of brain structure and function (Astle et al., 2023; Fiske & Holmboe, 2019; Johnson, 2011). During the period between birth and the third birthday, the brain structure undergoes rapid and significant development (Bethlehem et al., 2022), which ultimately affects functional activity (Gilmore et al., 2018). To date, the development of focalized activity in infants and toddlers has been measured mostly with EEG in baseline states due to its easiness and adaptability (Saby & Marshall, 2012). EEG has typically been employed to measure the power of standard frequency bands (e.g., alpha, theta, and beta), that show a profound reconfiguration of energy in the first years of life (Anderson & Perone, 2018). The dominant frequency (alpha) gradually emerges, its energy increases, and its peak shifts towards higher frequencies (Freschl et al. 2022; Marshall et al. 2002). Similarly, other frequency bands also undergo rapid reconfiguration, although the results have been mixed (Perone et al., 2018; Wilkinson et al., 2023).

The maturation of the alpha and theta bands, which are associated with attentional and cognitive control processes (Cavanagh & Frank, 2014; Klimesch, 2012), has been linked to individual differences in executive attention and intelligence during childhood (Bell & Fox, 1992; Braithwaite et al., 2020; Cuevas et al., 2012; Cuevas & Bell, 2022; Jones et al., 2020), highlighting their relevance in development. However, the resting-state energy was considered both in absolute and relative terms in those studies. Recent studies indicate that power conflates oscillatory and aperiodic activity with different biological bases (Donoghue et al., 2020; He, 2014; Voytek & Knight, 2015). This may have affected previous studies, as both aperiodic and oscillatory energy mature independently (Cellier et al., 2021; McSweeney et al., 2021; Schaworonkow & Voytek, 2021), and aperiodic activity has also been associated with individual differences in cognition (Arnett et al., 2021; Donoghue et al., 2020).

In addition to changes in localized brain activity, functional networks undergo profound reconfiguration during this period. This is of particular significance because cognition arises from the interconnection between different brain regions (Corbetta & Shulman, 2002; Dosenbach et al., 2008) and connections in the alpha and theta frequency bands are crucial for attentional processes and long-range integration (Clayton et al., 2015; Fries, 2015; Marek & Dosenbach, 2018; von Stein & Sarnthein, 2000). Indeed, connectivity in alpha and theta frequencies appears to increase with age (Barry et al., 2004; Thatcher et al., 2008), and has been associated with individual differences in executive attention and working memory (Broomell et al., 2021; Whedon et al., 2016).

A limitation of direct connectivity measures is that they do not consider functional activity as an interconnected network, because they only capture synchronization between two areas/electrodes. Therefore, they do not allow for the examination of differences in topology and assume that all connections occur without intermediary steps. However, there is evidence that functional networks possess non-trivial topological characteristics relevant to information transmission and cognition, which are reflected when considering areas/electrodes as members of a functional network (Bullmore & Sporns, 2012; Sporns, 2013).

With age, functional networks refine, becoming more specialized and segregated, and the cost to integrate all the areas is reduced throughout the emergence and strengthening of long-range connections (Asis-Cruz et al., 2015; Fransson et al., 2011; Gao et al., 2011; Zhao et al., 2019). The development of brain networks is hierarchical and follows the same pattern as attentional processes. Sensory networks mature first, followed by alerting networks, then orienting networks, and finally executive ones (Gao, Alcauter, Elton, et al., 2015; Gao, Alcauter, Smith, et al., 2015). However, the developmental pattern in EEG functional networks is not well studied, as only two experiments have addressed it, yielding mixed results (Hu et al., 2022; Xie et al., 2019).

Similar to localized brain activity, cognitive development has been associated with the topology of functional and structural networks (Baum et

al., 2017; Keller et al., 2022; Marek et al., 2015). Generally, having more segregated and efficient networks is related to the maturation of EA, and the strengthening connections between the frontal and parietal areas contributes to age-related improvement in IC and working memory during childhood (Buss et al., 2014; Buss & Spencer, 2018; Marek et al., 2015). Individual differences in the topology of functional networks have been linked to intelligence and executive attention processes, especially in frontoparietal areas (Cole et al., 2012; Langer et al., 2012; van Den Heuvel et al., 2009). Furthermore, brain networks are susceptible to variations in attentional states and IC (Cooper et al., 2015; Xie et al., 2019) and neurodevelopmental disorders that compromise attentional processes, such as ADHD, show alterations in the brain topology (Henry & Cohen, 2019; Shephard et al., 2019).

Altogether, the first three years of life are characterized by rapid development in executive attention and brain activity, both at the oscillatory/aperiodic and functional network levels. However, more research is needed to further characterize the development of EA and its relationship with brain function employing finer-grained measures. Therefore, the objective of this thesis was to explore the early development of executive attention, resting brain activity, and their interrelation within a period of six months to thirty-six months of age in a longitudinal cohort. To this aim, we formulate three main research goals with their respective research questions:

1. *Development*
    a. What is the development of a functional connectome for EEG?
    b. How do the oscillatory and aperiodic powers vary with age?
    c. Does EA improve during this period?
2. *Individual differences across the lifespan*
    a. Is functional brain activity stable over time?
    b. Is brain topology constant during this period?
    c. Does early performance on the same task predict later performance?
    d. Is EA stable when the task varies?

3. *Brain-Behavior Relationship*
    a. Is oscillatory and aperiodic EEG activity linked to EA?
    b. Is the organization of functional networks associated with individual differences in EA?

To address these research questions, we conducted a longitudinal study. It followed the same population of children from six months to 36 months of age in four waves: 6, 9, 16, 36 months of age. In this study, resting-state brain activity was recorded using high-density EE. We extracted oscillatory activity in three frequency bands (theta, alpha, and beta) and aperiodic activity. Additionally, we computed functional connectivity and explored functional networks combining it with graph theory on various synchronization measures. We evaluated network integration, segregation, modularity, and topology. EA was assessed using the ECITT task at 9 and 16 months of age, and we developed the Bee-Attentive task for the session at 36 months. The ECITT task allows for the evaluation of CF and IC, whereas the Bee-Attentive task provides measures of sustained attention, focused attention, and IC by combining a visual search protocol with an inhibition task. Finally, we investigated whether functional brain activity predicts performance on the ECITT and Bee-Attentive tasks and examined the stability of each measure and their interrelationship.

Our results indicated that both oscillatory power and aperiodic components varied with age. In our study, the peak frequencies of the alpha and theta bands shifted towards higher frequencies, and the oscillatory energy in the alpha band augmented. Similarly, the aperiodic background curve became flatter, indicating changes in the balance between inhibitory and excitatory brain activities. When we compared the development of oscillatory activity with traditional measures (relative power), only alpha exhibited a similar trajectory. In addition, theta and beta were related to aperiodic components. This suggests that changes occur in both oscillatory and aperiodic activities and separating them is necessary to understand their contribution to cognitive processes.

At the functional network level, our multiverse analyses determined different developmental trajectories depending on the connectivity measures used to construct the network. Coherence-based networks exhibited the most dramatic and consistent age-related changes. These networks displayed two main clusters (frontal and parietal) containing the nodes with most of the connections. Furthermore, the networks displayed a small-world topology and were modular from the first session onwards, but these properties did not change across sessions. However, the modules became more segregated over time, and local and global efficiency increased. These changes in the capacity to integrate and segregate information were accompanied by an increase in connection strength and, in conjunction with the rest of the results, indicated the maturation of functional networks toward a more efficient and specialized topology.

Between 9 and 16 months of age, performance on the ECITT task improved in inhibitory trials (IS) and prepotent trials. However, PS did not change with age. This indicated a general improvement in task performance, with a significant increase in IC capacity between infancy and toddlerhood. At 3 years of age children performed over chance on the Bee-Attentive task. They showed costs in inhibiting responses when an infrequent stimulus appeared (IC) and their reaction time and response variability increased when there were more distractors. Additionally, they were able to self-regulate their responses as the accuracy and reaction time varied and increased, respectively, after committing an error. Children's performance improved over the course of the task as they reduced their reaction time and errors in inhibitory trials throughout the blocks of trials. These results indicate that this task is suitable for measuring diverse aspects of EA with 36-months-old children. However, parameter variations may be considered to elicit larger conflict in this task.

In terms of stability in the EEG recording, we found that individual differences in oscillatory and aperiodic activity were constant between sessions (i.e., individual values in previous waves predicted the current one), except for relative power between 9 and 16 months (beta band), and between 16 months and 36 months (alpha band). Functional networks parameters were not correlated between session, with a handful of exception, such as the

alpha band for efficiency measures between 6 and 9 months of age. However, in terms of both power and functional network properties, its topological distribution was highly related between the sessions. This may indicate an early distribution of the oscillatory activity independently of within-participants stability. Behavioral performance between sessions was only related in the IS trials of the ECITT task, even when controlling for other task measures. We did not find significant correlations between any variables of the ECITT and the Bee-Attentive task at 36 months.

Finally, oscillatory activity but not aperiodic parameters were related to individual differences in the ECITT task. The peak frequency of the theta band predicted children's performance in the PNS and PS trials at 9 months. Similarly, oscillatory activity in the alpha and theta bands at nine months predicted PS at 16 months. In both cases, a more mature oscillatory pattern (higher frequency and oscillatory energy) was associated with better task performance. Functional networks were also related to performance on the ECITT task. A more efficient and segregated network was positively related to PS/PNS, whereas an inverse pattern was observed for IS. However, there was no relationship with the Bee-Attentive task for any EEG measure. Therefore, our results indicate that brain activity can predict behavior although this relationship may depend on the task.

Altogether, this thesis demonstrates that both brain activity and EA rapidly develop between six and thirty-six months of age. Children's functional networks became more globally and locally efficient, while the oscillatory power in the dominant rhythm rapidly mature parallel to the flattening of the aperiodic background, which constates the rapid maturation that takes place in this period. Also, they become more proficient in IC tasks in this period. Finally, we found individual differences in EEG power measures and within-task performance was maintained over the sessions, with some relationships between brain function and EA. However, this did not occur always, which suggest that this period is highly dynamic and combines both stability and instability.

Español

La capacidad de actuar de forma autorregulada requiere de procesos atencionales (Rueda et al., 2021). El modelo atencional de Posner y Petersen (Petersen & Posner, 2012; Posner & Petersen, 1990) identifica tres mecanismos (alerta, orientación, y ejecutivo) que recaen en cinco redes cerebrales: red de alerta, red dorsal de orientación (*dorsal attention netwok,* DAN), red ventral de orientación (*ventral attention network,* VAN), red ejecutiva frontoparietal (*frontoparietal network* FPN), y red ejecutiva cíngulo-opercular (*cingulo-opercular network*¸ CON). La red de alerta procura un estado de activación óptimo, guiada por CON y FPN, mientras que las redes de orientación guían nuestro foco atencional en función de nuestras metas y la saliencia de los estímulos del entorno. Las redes FPN y CON dirigen nuestro comportamiento, adaptándolo en función de las metas y ajustándolo cuando no se están logrando. Por tanto, FPN y CON son esenciales para el comportamiento voluntario y flexible de la conducta e involucran procesos de monitorización del contexto, flexibilidad (*cognitive flexibility*; CF) e inhibición (*inhibitory control*; IC).

Para poder conseguir nuestras metas, la acción coordinada entre los tres mecanismos atencionales es esencial. Sin un nivel adecuado de alerta puede que obviemos elementos relevantes (i.e., bajos niveles de alerta) o cometamos errores de impulsividad (i.e., altos niveles de alerta). Además, dada la complejidad de un entorno lleno de estímulos, necesitamos ignorar la información irrelevante para nuestras metas. Finalmente, debemos determinar el mejor plan de acción para nuestro objetivo según el contexto, realizarlo, y cambiarlo en caso de ser necesario. Estos procesos, que ya están establecidos en la edad adulta, no están presentes de igual forma en edades tempranas dada la inmadurez de las redes atencionales (Posner et al., 2014). Esto limita cómo interactúan los/as niños/as con su entorno en los primeros años de vida. Al principio, su atención se guía por los elementos externos, pero en los primeros seis meses de vida empezarán a controlar su atención de forma endógena (Conejero & Rueda, 2017; Hendry et al., 2016, 2019).

La atención ejecutiva presenta una trayectoria de desarrollo más gradual cuando se compara con la capacidad de orientación y de alerta.

Aunque en edades tempranas el control voluntario de la atención parece recaer en las redes de orientación dada la inmadurez de FPN y CON (Gao, Alcauter, Elton, et al., 2015; Posner et al., 2014), éstas son reclutadas para tareas puntuales que involucran un alto grado de control de la atención y que requieren de zonas cerebrales frontales (Ellis et al., 2021; Fiske & Holmboe, 2019). Esto se muestra en los cambios de actividad cerebral frontal cuando los bebés presencian elementos incongruentes (Ellis et al., 2021), observan un error (Berger et al., 2006; Conejero et al., 2016; Stahl & Feigenson, 2015), y realizan tareas complejas que requieren inhibir la información irrelevante (Bell, 2001, 2002).

El desarrollo de la atención ejecutiva se constata por la capacidad temprana que presentan los bebés de inhibir y cambiar flexiblemente su respuesta. A partir del sexto mes de vida, los/as bebés cambian su patrón de respuesta e inhiben su conducta y la mirada cuando no obtienen las consecuencias deseadas. Por ejemplo, son capaces de detener una respuesta prepotente cuando no los lleva a su objetivo (Diamond, 1985; Kovacs & Mehler, 2009). Los costes de inhibir y modificar la respuesta disminuyen con la edad (Clearfield et al., 2006; Cuevas & Bell, 2010), aunque su desarrollo puede estar ligado a otros procesos como la memoria (Holmboe et al., 2018). Paradigmas más recientes como la tarea de inhibición para pantalla táctil para la niñez temprana (*Early Childhood Inhibitory Touchscreen Task;* ECITT) han conseguido limitar la influencia de la memoria en protocolos de CF e IC para bebés pues se basan en el establecimiento de contingencias. La ECITT se puede realizar a partir de los 10 meses de edad, y estudios previos sugieren el desarrollo gradual del IC entre el primer y segundo año de vida (Fiske et al., 2022; Hendry et al., 2021; Holmboe et al., 2021; Liu et al., 2020), lo que sugiere un desarrollo marcado de IC y CF más allá de procesos de memoria, aunque únicamente cuatro estudios han explorado su desarrollo.

A partir del segundo año de vida, la capacidad sostener la atención por un período prolongado (atención sostenida) e inhibir los distractores (atención focalizada) incrementa (Brandes-Aitken et al., 2019; Woods et al., 2013). A su vez, los niños son capaces de realizar tareas con un coste de CF e IC mayor y que, además, requieren instrucciones verbales. Esto conlleva realizar protocolos similares a los adultos como las tareas Go/NoGo, stop-

signal (Carver et al., 2001), o la versión para niños de la prueba de las redes atencionales (*attention network test*, ANT; Casagrande et al., 2022; Rueda et al., 2004). El realizar estas tareas indican que las capacidades de CF e IC maduran más allá de la infancia, viéndose una mejoría hasta después de la etapa prescolar (Johnstone et al., 2005; Pozuelos et al., 2014; Rueda et al., 2004; Zelazo et al., 2003). Sin embargo, la mayoría de los paradigmas evalúa individualmente los procesos cognitivos, obviando su interacción, y paradigmas que evalúan varios procesos no se pueden emplear hasta cerca de los 4 años (Casagrande et al., 2022; Rueda et al., 2004).

El desarrollo en la atención ejecutiva se sustenta en la maduración de la estructura cerebral y funcional (Astle et al., 2023; Fiske & Holmboe, 2019; Johnson, 2011). En el período entre el nacimiento y el tercer año de vida, la estructura cerebral atraviesa un desarrollo drástico (Bethlehem et al., 2022), que en última estancia afecta a la actividad funcional (Gilmore et al., 2018). Para evaluar los cambios en la actividad funcional, el EEG ha sido uno de los protocolos más empleados dada su adaptabilidad (Saby & Marshall, 2012). El EEG usualmente se ha empleado para medir la energía en bandas de frecuencia estandarizadas (p.ej., alpha, theta, beta), que muestran una gran reconfiguración en los primeros tres años de vida (Anderson & Perone, 2018). El ritmo dominante en EEG (alpha) emerge gradualmente, su energía se incrementa y su pico se desplaza hacia frecuencias más elevadas con la edad (Freschl et al., 2022; Marshall et al., 2002). Del mismo modo, otras bandas también sufren una rápida reconfiguración, aunque con resultados mixtos hasta la fecha (Perone et al., 2018; Wilkinson et al., 2023).

La maduración de las bandas alpha y theta, relacionadas con procesos atencionales y de control cognitivo (Cavanagh & Frank, 2014; Klimesch, 2012), se ha relacionado con diferencias individuales en atención ejecutiva e inteligencia durante la niñez (Bell & Fox, 1992; Braithwaite et al., 2020; Cuevas et al., 2012; Cuevas & Bell, 2022; Jones et al., 2020), lo que revela su relevancia en el desarrollo. Sin embargo, la energía en reposo se ha estudiado de forma absoluta o relativa en estudios previos. Sin embargo, investigaciones recientes indican que la energía del EEG es el resultado de actividad oscilatoria y aperiódica, que cuentan con bases biológicas diferenciadas (Donoghue et al., 2020; He, 2014; Voytek & Knight, 2015). Esto

puede haber afectado a estudios previos puesto que tanto la energía aperiódica como oscilatoria maduran de forma independiente (Cellier et al., 2021; McSweeney et al., 2021; Schaworonkow & Voytek, 2021) y la actividad aperiódica también se ha relacionado con diferencias individuales en la cognición (Arnett et al., 2021; Donoghue et al., 2020).

Además de cambios en actividad cerebral localizada, las redes funcionales también se reconfiguran en este periodo. Esto es de especial relevancia ya que la cognición surge de la interconexión entre diferentes áreas cerebrales (Corbetta & Shulman, 2002; Dosenbach et al., 2008) y las conexiones en alpha y theta son cruciales para los procesos atencionales (Clayton et al., 2015; Fries, 2015; Marek & Dosenbach, 2018; von Stein & Sarnthein, 2000). La conectividad funcional en alpha y theta parece incrementar con la edad (Barry et al., 2004; Thatcher et al., 2008), lo que se ha relacionado con diferencias individuales en atención ejecutiva y memoria de trabajo (Broomell et al., 2021; Whedon et al., 2016).

Una limitación de las medidas de conectividad directa es que no considera la actividad funcional como una red interconectada pues sólo evalúan la sincronización entre dos áreas/electrodos. Por tanto, no permite examinar diferencias en topología, y asume que todas las conexiones ocurren sin intermediarios. Sin embargo, existe evidencia de que las redes funcionales poseen características topológicas relevantes para la transmisión de la información y cognición que se refleja al considerar las áreas/electrodos como miembros de una red funcional (Bullmore & Sporns, 2012; Sporns, 2013).

Con la edad, las redes funcionales se refinan, volviéndose más especializadas y disminuyendo el coste de integrar la red por la aparición y fortalecimiento de conexiones de largo alcance (Asis-Cruz et al., 2015; Fransson et al., 2011; Gao et al., 2011; Zhao et al., 2019). El desarrollo de las redes cerebrales es, además, jerárquico y sigue el mismo patrón que los procesos atencionales. Primero maduran las redes sensoriales, luego las redes de alerta, seguidamente las redes de orientación, y finalmente las redes ejecutivas (Gao, Alcauter, Elton, et al., 2015; Gao, Alcauter, Smith, et al., 2015). Sin embargo, el patrón de desarrollo en las redes funcionales en EEG

no está definido, pues sólo dos estudios lo han abordado y han arrojado resultados mixtos (Hu et al., 2022; Xie, Mallin, et al., 2019).

Al igual que ocurre con la actividad cerebral localizada, el desarrollo de la cognición se ha relacionado con la topología de las redes funcionales y estructurales (Baum et al., 2017; Keller et al., 2022; Marek et al., 2015). Por lo general, presentar redes más segregadas entre sí y eficientes se relaciona con la maduración de la atención ejecutiva, y el fortalecimiento de las conexiones entre áreas frontales y parietales da pie a la mejoría en IC y memoria de trabajo (Buss et al., 2014; Buss & Spencer, 2018; Marek et al., 2015). Diferencias individuales en la topología de las redes funcionales se han asociado con variaciones en inteligencia y procesos de atención ejecutiva, en especial en áreas de FPN (Cole et al., 2012; Langer et al., 2012; Van Den Heuvel et al., 2009). Asimismo, las redes cerebrales son susceptibles a variaciones del estado atencional y diferentes tipos de IC (Cooper et al., 2015; Xie et al., 2019) y trastornos del desarrollo que comprometen los procesos atencionales como el trastorno de déficit de atención e hiperactividad (TDAH) muestran alteraciones en la topología cerebral (Abbas et al., 2021; Henry & Cohen, 2019; Shephard et al., 2019).

En conjunto, la literatura previa indica un rápido desarrollo de la atención ejecutiva y actividad cerebral, tanto a nivel oscilatorio como de redes funcionales. Sin embargo, la investigación en relación con el desarrollo de la atención ejecutiva y su relación con la actividad cerebral con medidas más precisas es todavía necesaria especialmente en los primeros años de vida. Por ello, el objetivo de la presente tesis ha sido explorar el desarrollo temprano de la atención ejecutiva, la actividad cerebral en reposo, y su interrelación en un período entre los seis meses y los treinta y seis meses de vida. De esta forma, nos planteamos tres ejes principales de investigación con sus respectivas preguntas:

1) *Desarrollo*
    a. ¿Cuál es el desarrollo del conectoma funcional en EEG?
    b. ¿Cómo varía la energía oscilatoria y aperiódica con la edad?
    c. ¿Mejora la atención ejecutiva en este período?

2) *Diferencias individuales a lo largo del desarrollo*
    a. ¿Predice la actividad funcional temprana la de momentos posteriores?
    b. ¿Existe una distribución topológica de la actividad cerebral que se mantiene a lo largo de la niñez temprana?
    c. ¿Se relaciona la ejecución temprana en la misma tarea la posterior ejecución?
    d. ¿Las diferencias individuales en atención ejecutiva se mantienen aún cuando la tarea varía?
3) *Interrelación cerebro-comportamiento*
    a. ¿Está la energía cerebral relacionada con la atención ejecutiva?
    b. ¿Explica la conectividad funcional parte de las diferencias individuales en atención ejecutiva?

Para responder a las preguntas de investigación, se llevó a cabo un estudio longitudinal. Éste siguió a la misma población de niños/as desde los 6 meses hasta los 36 meses de vida en cuatro sesiones: 6, 9, 16, y 36 meses de edad. En ese estudio se evaluó la actividad cerebral en estado de reposo con un EEG de alta densidad. Computamos la energía oscilatoria en tres bandas de frecuencia (theta, alpha, y beta) y se extrajeron los componentes aperiódicos. Asimismo, calculamos la conectividad funcional y evaluamos su desarrollo empleando la teoría de grafos en diferentes medidas de sincronización, evaluando la integración, segregación, modularidad, y topología de las redes. La atención ejecutiva se examinó con la tarea ECITT a los 9 y 16 meses de edad, y desarrollamos la tarea Bee-Attentive a los 36 meses. La tarea ECITT permite evaluar CF e IC, mientras que la Bee-Attentive ofrece medidas de atención sostenida, atención focalizada, e IC al combinar un protocolo de búsqueda visual con una tarea de inhibición. Finalmente, comprobamos si la actividad cerebral funcional podía predecir la ejecución en la ECITT y la Bee-Attentive, y la estabilidad que poseía cada una de las medidas.

Nuestros resultados indicaron que la energía oscilatoria y aperiódica varían con la edad. En nuestro estudio, la frecuencia de los picos de alpha y theta incrementó, y la energía oscilatoria de la banda alpha aumentó. Del

mismo modo, la curva aperiódica se volvió más plana, mostrando así cambios en la balanza entre la actividad cerebral inhibitoria y excitatoria. Cuando comparamos el desarrollo de la actividad oscilatoria con medidas tradicionales (energía relativa), únicamente alpha presentó la misma trayectoria. Además, theta y beta estuvieron relacionadas con los componentes aperiódicos. Esto sugiere que se producen tanto cambios en la actividad oscilatoria como aperiódica, y que separarlos es necesario para entender la contribución a los procesos cognitivos.

A nivel de redes funcionales, el análisis de multiverso determinó que existía diferencias en cuanto a la medida de conectividad utilizada para construir la red. Las redes construidas con medidas de sincronización basadas en la coherencia mostraron los mayores cambios y sus resultados fueron más consistentes. Esas redes poseían dos clústeres (frontal y parietal) que contenían los nodos con mayor número de las conexiones. Asimismo, las redes poseían la topología de mundo pequeño desde la primera sesión y eran modulares, aunque estas propiedades no variaron a lo largo de las sesiones. Sin embargo, los módulos se volvieron más segregados con el tiempo, y la eficacia local y global aumentó. Estos cambios en la capacidad de integrar y segregar la información fueron acompañados de un aumento en la fuerza de las conexiones y, en conjunto con el resto de los resultados, indicaron la maduración de las redes funcionales hacia una topología más eficiente y especializada.

La ejecución entre los 9 y los 16 meses en la tarea ECITT aumentó en los ensayos inhibitorios (IS) y en los prepotentes. Sin embargo, los ensayos prepotentes con cambio (PS) no variaron con la edad. Esto indica un aumento en general para realizar la tarea, y del IC. A los 36 meses, los/as niños/as realizaron la tarea Bee-Attentive con una ejecución por encima del azar. Estos/as también mostraron costes de inhibir la respuesta cuando aparecía un estímulo infrecuente (IC) y su tiempo de reacción y variabilidad en la respuesta aumentó cuando existía mayor número de distractores. Asimismo, fueron capaces de autorregular sus respuestas, pues la tasa de acierto variaba y se volvieron más lentos tras cometer un error. Su ejecución a lo largo de los bloques de la tarea mejoró, disminuyendo su tiempo para responder y el número de errores en la condición inhibitoria. Estos resultados indicaron que

esta tarea es capaz de generar conflicto y es factible con niños/as de 36 meses de edad. Sin embargo, algunos parámetros podrían ajustarse para incrementar el conflicto de la tarea.

A nivel de estabilidad de las diferencies individuales dentro de las medidas de EEG, encontramos que la energía relativa, oscilatoria y la actividad aperiódica estaba relacionada entre sesiones, salvo la energía relativa entre los 9 y 16 meses (beta) y entre los 16 meses y 36 meses (alpha). El conectoma funcional en momentos tempranos no predecía las características de las redes funcionales en las siguientes sesiones, salvo algunas excepciones como en la banda alpha en medidas de eficiencia entre los 6 y 9 meses de edad. Sin embargo, tanto a nivel de energía y propiedades de las redes funcionales, encontramos una distribución topológica constante a lo largo de las sesiones. Por ejemplo, en conectividad las zonas frontales siempre presentaron un clúster de conexiones. Esto puede indicar que las medidas de energía son más estables y menos dependientes del momento temporal, pero en ambos casos que existe una distribución específica de la actividad funcional. La ejecución entre sesiones sólo estuvo significativamente relacionada en los ensayos IS de la tarea ECITT. Sin embargo, la ECITT a los 16 meses no predecía las diferencias individuales de la Bee-Attentive a los 36 meses.

La actividad oscilatoria, pero no aperiódica, se asoció las diferencias individuales en la tarea ECITT en nuestro estudio. La frecuencia del pico de la banda de theta predijo de forma concurrente el desempeño de los niños/as ensayos prepotentes y de PS a los 9 meses. Asimismo, la actividad oscilatoria en alpha y theta a los 9 meses predijo significativamente PS a los 16 meses. En ambos casos, un patrón oscilatorio más maduro (mayor frecuencia y energía oscilatoria) se relacionaba con mejor ejecución en la tarea. Las redes funcionales también estuvieron relacionadas con la ejecución en la tarea ECITT. Presentar una red más eficiente y segregada se relacionaba positivamente con PS/PNS, pero el patrón inverso lo hizo con IS. Sin embargo, no hubo relación con la tarea Bee-Attentive ninguna medida del EEG. Por tanto, nuestros resultados indicaron que la actividad cerebral es capaz de predecir el comportamiento, pero la relación puede variar según la tarea.

General Summary

En conjunto, esta tesis muestra que tanto la actividad cerebral como la atención ejecutiva se desarrollan rápidamente entre los seis y treinta y seis meses de vida. El conectoma funcional en EEG se volvió más eficiente tanto local como globalmente, mientras que la energía oscilatoria del ritmo dominante (alpha) se desarrolló rápidamente y el componente aperiódico de la energía cerebral se volvió menos pronunciado en frecuencias más altas. A su vez, los/as niños/as se volvieron mejores en tareas que requieren IC. Finalmente, encontramos que las diferencias individuales se mantenían en el caso de la energía en el EEG y dentro de la misma tarea (ECITT) en los ensayos inhibitorios, además de relaciones significativas entre la actividad cerebral y la atención ejecutiva. No obstante, esto no ocurrió prediciendo la Bee-Attentive ni en las medidas de conectoma funcional, lo que sugiere que este período es dinámico y combina estabilidad e inestabilidad.

References

References

Achard, S., & Bullmore, E. (2007). Efficiency and cost of economical brain functional networks. *PLoS Computational Biology*, *3*(2), 17.

Adam, N., Blaye, A., Gulbinaite, R., Delorme, A., & Farrer, C. (2020). The role of midfrontal theta oscillations across the development of cognitive control in preschoolers and school-age children. *Developmental Science*, *23*(5), 12936.

Ahmadi, M., Kazemi, K., Kuc, K., Cybulska-Klosowicz, A., Helfroush, M. S., & Aarabi, A. (2021). Disrupted Functional Rich-Club Organization of the Brain Networks in Children with Attention-Deficit/Hyperactivity Disorder, a Resting-State EEG Study. *Brain Sciences*, *11*(7), 938. https://doi.org/10.3390/brainsci11070938

Ahmadlou, M., Adeli, H., & Adeli, A. (2012). Graph Theoretical Analysis of Organization of Functional Brain Networks in ADHD. *Clinical EEG and Neuroscience*, *43*(1), 5-13. https://doi.org/10.1177/1550059411428555

Alamia, A., Terral, L., D'ambra, M. R., & VanRullen, R. (2023). Distinct roles of forward and backward alpha-band waves in spatial visual attention. *eLife*, *12*, e85035. https://doi.org/10.7554/eLife.85035

Alamia, A., & VanRullen, R. (2019). Alpha oscillations and traveling waves: Signatures of predictive coding? *PLOS Biology*, *17*(10), e3000487. https://doi.org/10.1371/journal.pbio.3000487

Alcauter, S., Lin, W., Smith, J. K., Goldman, B. D., Reznick, J. S., Gilmore, J. H., & Gao, W. (2015). Frequency of spontaneous BOLD signal shifts during infancy and correlates with cognitive performance. *Developmental Cognitive Neuroscience*, *12*. https://doi.org/10.1016/j.dcn.2014.10.004

Alexander-Bloch, A., Raznahan, A., Bullmore, E., & Giedd, J. (2013). The convergence of maturational change and structural covariance in human cortical networks. *Journal of Neuroscience*, *33*(7), 2889-2899. https://doi.org/10.1523/JNEUROSCI.3554-12.2013

Allan, N. P., Hume, L. E., Allan, D. M., Farrington, A. L., & Lonigan, C. J. (2014). Relations between inhibitory control and the development of academic skills in preschool and kindergarten: A meta-analysis. *Developmental Psychology*, *50*(10), 2368.

References

Amso, D., & Johnson, S. P. (2006). Learning by selection: Visual search and object perception in young infants. *Developmental Psychology*, *42*(6), 1236-1245. https://doi.org/10.1037/0012-1649.42.6.1236

Amso, D., & Scerif, G. (2015). The attentive brain: Insights from developmental cognitive neuroscience. *Nature Reviews Neuroscience*, *16*(10), 606-619. https://doi.org/10.1038/nrn4025

Anderson, A. J., & Perone, S. (2018). Developmental change in the resting state electroencephalogram: Insights into cognition and the brain. *Brain and Cognition*, *126*, 40-52. https://doi.org/10.1016/j.bandc.2018.08.001

Anderson, A. J., Perone, S., & Gartstein, M. A. (2022). Context matters: Cortical rhythms in infants across baseline and play. *Infant Behavior and Development*, *66*, 101665. https://doi.org/10.1016/j.infbeh.2021.101665

Arnatkeviciute, A., Fulcher, B. D., Bellgrove, M. A., & Fornito, A. (2021). Where the genome meets the connectome: Understanding how genes shape human brain connectivity. *NeuroImage*, *244*, 118570. https://doi.org/10.1016/j.neuroimage.2021.118570

Arnatkeviciute, A., Fulcher, B. D., Oldham, S., Tiego, J., Paquola, C., Gerring, Z., Aquino, K., Hawi, Z., Johnson, B., Ball, G., Klein, M., Deco, G., Franke, B., Bellgrove, M. A., & Fornito, A. (2021). Genetic influences on hub connectivity of the human connectome. *Nature Communications*, *12*(1), 4237. https://doi.org/10.1038/s41467-021-24306-2

Arnett, A. B., Fearey, M., Peisch, V., & Levin, A. R. (2021). Reduced Dynamic Aperiodic Spectral Slope Marks Atypical Neural Information Processing in Children With Attention Deficit Hyperactivity Disorder. *SSRN Electronic Journal*. https://doi.org/10.2139/ssrn.3960707

Asis-Cruz, J. D., Bouyssi-Kobar, M., Evangelou, I., Vezina, G., & Limperopoulos, C. (2015). Functional properties of resting state networks in healthy full-term newborns. *Scientific Reports*, *5*. https://doi.org/10.1038/srep17755

Astle, D. E., Barnes, J. J., Baker, K., Colclough, G. L., & Woolrich, M. W. (2015). Cognitive Training Enhances Intrinsic Brain Connectivity in

Childhood. *The Journal of Neuroscience*, *35*(16), 6277-6283. https://doi.org/10.1523/JNEUROSCI.4517-14.2015

Aston-Jones, G., Rajkowski, J., Kubiak, P., & Alexinsky, T. (1994). Locus coeruleus neurons in monkey are selectively activated by attended cues in a vigilance task. *The Journal of Neuroscience*, *14*(7), 4467-4480. https://doi.org/10.1523/JNEUROSCI.14-07-04467.1994

Atkinson, J., Hood, B., Wattam-Bell, J., & Braddick, O. (1992). Changes in infants' ability to switch visual attention in the first three months of life. En *Perception* (Vol. 21, pp. 643-653).

Badre, D., & Nee, D. E. (2018). Frontal Cortex and the Hierarchical Control of Behavior. *Trends in Cognitive Sciences*, *22*(2), 170-188. https://doi.org/10.1016/j.tics.2017.11.005

Ball, G., Aljabar, P., Zebari, S., Tusor, N., Arichi, T., Merchant, N., Robinson, E. C., Ogundipe, E., Rueckert, D., Edwards, A. D., & Counsell, S. J. (2014). Rich-club organization of the newborn human brain. *Proceedings of the National Academy of Sciences*, *111*(20), 7456-7461. https://doi.org/10.1073/pnas.1324118111

Bánki, A., Brzozowska, A., Hoehl, S., & Köster, M. (2022). Neural Entrainment vs. Stimulus-Tracking: A Conceptual Challenge for Rhythmic Perceptual Stimulation in Developmental Neuroscience. *Frontiers in Psychology*, *13*, 878984. https://doi.org/10.3389/fpsyg.2022.878984

Barbey, A. K. (2018). Network Neuroscience Theory of Human Intelligence. *Trends in Cognitive Sciences*, *22*(1), 8-20. https://doi.org/10.1016/j.tics.2017.10.001

Barnes, J. J., Woolrich, M. W., Baker, K., Colclough, G. L., & Astle, D. E. (2016). Electrophysiological measures of resting state functional connectivity and their relationship with working memory capacity in childhood. *Developmental Science*, *19*(1), 19-31. https://doi.org/10.1111/desc.12297

Barrero-Castillero, A., Morton, S. U., Nelson, C. A., & Smith, V. C. (2019). Psychosocial stress and adversity: Effects from the perinatal period to adulthood. *NeoReviews*, *20*(12), e686-e696. https://doi.org/10.1542/neo.20-12-e686

Barry, R. J., Clarke, A. R., McCarthy, R., Selikowitz, M., Johnstone, S. J., & Rushby, J. A. (2004). Age and gender effects in EEG coherence: I.

Developmental trends in normal children. *Clinical Neurophysiology*, *115*(10), 2252-2258. https://doi.org/10.1016/j.clinph.2004.05.004

Barwick, F., Arnett, P., & Slobounov, S. (2012). EEG correlates of fatigue during administration of a neuropsychological test battery. *Clinical Neurophysiology*, *123*(2), 278-284. https://doi.org/10.1016/j.clinph.2011.06.027

Bassett, D. S., & Bullmore, E. (2006). Small-World Brain Networks. *The Neuroscientist*, *12*(6), 512-523. https://doi.org/10.1177/1073858406293182

Bassett, D. S., & Bullmore, E. T. (2017). Small-World Brain Networks Revisited. *The Neuroscientist*, *23*(5), 499-516. https://doi.org/10.1177/1073858416667720

Bastos, A. M., Lundqvist, M., Waite, A. S., Kopell, N., & Miller, E. K. (2020). Layer and rhythm specificity for predictive routing. *Proceedings of the National Academy of Sciences*, *117*(49), 31459-31469. https://doi.org/10.1073/pnas.2014868117

Bastos, A. M., & Schoffelen, J. M. (2016). A tutorial review of functional connectivity analysis methods and their interpretational pitfalls. *Frontiers in Systems Neuroscience*, *9*, 175.

Bates, D., Mächler, M., Bolker, B., & Walker, S. (2014). *Fitting Linear Mixed-Effects Models using lme4* (arXiv:1406.5823). arXiv. http://arxiv.org/abs/1406.5823

Bathelt, J., O'Reilly, H., Clayden, J. D., Cross, J. H., & Haan, M. D. (2013). Functional brain network organisation of children between 2 and 5years derived from reconstructed activity of cortical sources of high-density EEG recordings. *NeuroImage*, *82*, 595-604. https://doi.org/10.1016/j.neuroimage.2013.06.003

Baum, G. L., Ciric, R., Roalf, D. R., Betzel, R. F., Moore, T. M., Shinohara, R. T., Kahn, A. E., Vandekar, S. N., Rupert, P. E., Quarmley, M., Cook, P. A., Elliott, M. A., Ruparel, K., Gur, R. E., Gur, R. C., Bassett, D. S., & Satterthwaite, T. D. (2017). Modular Segregation of Structural Brain Networks Supports the Development of Executive Function in Youth. *Current Biology*, *27*(11). https://doi.org/10.1016/j.cub.2017.04.051

Bedard, A.-C., Nichols, S., Barbosa, J. A., Schachar, R., Logan, G. D., & Tannock, R. (2002). The Development of Selective Inhibitory Control

Across the Life Span. *Developmental Neuropsychology*, *21*(1), 93-111. https://doi.org/10.1207/S15326942DN2101_5

Begum-Ali, J., Goodwin, A., Mason, L., Pasco, G., Charman, T., Johnson, M. H., & Jones, E. J. H. (2022). Altered theta–beta ratio in infancy associates with family history of ADHD and later ADHD-relevant temperamental traits. *Journal of Child Psychology and Psychiatry*, *63*, 1057-1067. https://doi.org/10.1111/jcpp.13563

Begus, K., Southgate, V., & Gliga, T. (2015). Neural mechanisms of infant learning: Differences in frontal theta activity during object exploration modulate subsequent object recognition. *Biology Letters*, *11*(5), 20150041.

Bell, M. A. (2001). Brain electrical activity associated with cognitive processing during a looking version of the A-not-B task. *Infancy*, *2*(3), 311-330.

Bell, M. A. (2002). Power changes in infant EEG frequency bands during a spatial working memory task. *Psychophysiology*, *39*(4), 450-458. https://doi.org/10.1017/S0048577201393174

Bell, M. A., & Adams, S. E. (1999). Comparable performance on looking and reaching versions of the A-Not-B task at 8 months of age. *Infant Behavior and Development*, *22*(2), 221-235. https://doi.org/10.1016/S0163-6383(99)00010-7

Bell, M. A., & Cuevas, K. (2012). Using EEG to Study Cognitive Development: Issues and Practices. *Journal of Cognition and Development*, *13*(3), 281-294. https://doi.org/10.1080/15248372.2012.691143

Bell, M. A., & Cuevas, K. (2016). *Psychobiology of executive function in early development*.

Bell, M. A., & Deater-Deckard, K. (2007). Biological Systems and the Development of Self-Regulation: Integrating Behavior, Genetics, and Psychophysiology. *Journal of Developmental & Behavioral Pediatrics*, *28*(5), 409-420. https://doi.org/10.1097/DBP.0b013e3181131fc7

Bell, M. A., & Fox, N. A. (1992). The relations between frontal brain electrical activity and cognitive development during infancy. *Child Development*, *63*(5), 1142-1163.

Bell, M. A., & Fox, N. A. (1997). Individual differences in object permanence performance at 8 months: Locomotor experience and brain electrical

activity. *Developmental Psychobiology: The Journal of the International Society for Developmental Psychobiology*, *31*(4), 287-297.

Bell, M. A., & Fox, N. A. (2018). The Relations between Frontal Brain Electrical Activity and Cognitive Development during Infancy. *Child Development*, *63*(5), 1142-1163.

Bell, M. A., & Wolfe, C. D. (2007a). Changes in brain functioning from infancy to early childhood: Evidence from EEG power and coherence during working memory tasks. *Developmental Neuropsychology*, *31*(1), 21-38.

Bell, M. A., & Wolfe, C. D. (2007b). The Use of the Electroencephalogram in Research on Cognitive Development. En L. A. Schmidt & S. J. Segalowitz (Eds.), *Developmental Psychophysiology* (1.ª ed., pp. 150-170). Cambridge University Press. https://doi.org/10.1017/CBO9780511499791.008

Benasich, A. A., Gou, Z., Choudhury, N., & Harris, K. D. (2008). Early cognitive and language skills are linked to resting frontal gamma power across the first 3 years. *Behavioural Brain Research*, *195*(2), 215-222. https://doi.org/10.1016/j.bbr.2008.08.049

Berchicci, M., Tamburro, G., & Comani, S. (2015). The intrahemispheric functional properties of the developing sensorimotor cortex are influenced by maturation. *Frontiers in Human Neuroscience*, *9*. https://doi.org/10.3389/fnhum.2015.00039

Berger, A., & Posner, M. I. (2023). Beyond Infant's Looking: The Neural Basis for Infant Prediction Errors. *Perspectives on Psychological Science*, *18*(3), 664-674. https://doi.org/10.1177/17456916221112918

Berger, A., Tzur, G., & Posner, M. I. (2006). Infant brains detect arithmetic errors. *Proceedings of the National Academy of Sciences of the United States of America*, *103*(33), 12649-12653. https://doi.org/10.1073/pnas.0605350103

Best, J. R., & Miller, P. H. (2010). A Developmental Perspective on Executive Function. *Child Development*, *81*(6), 1641-1660. https://doi.org/10.1111/j.1467-8624.2010.01499.x

Bethlehem, R. A. I., Seidlitz, J., White, S. R., Vogel, J. W., Anderson, K. M., Adamson, C., Adler, S., Alexopoulos, G. S., Anagnostou, E., Areces-Gonzalez, A., Astle, D. E., Auyeung, B., Ayub, M., Bae, J., Ball, G., Baron-Cohen, S., Beare, R., Bedford, S. A., Benegal, V., … Alexander-

Bloch, A. F. (2022). Brain charts for the human lifespan. *Nature*, *604*(7906), 525-533. https://doi.org/10.1038/s41586-022-04554-y

Betzel, R. F., Faskowitz, J., & Sporns, O. (2023). *Living on the edge: Network neuroscience beyond nodes. Trends in cognitive sciences*.

Blakey, E., Visser, I., & Carroll, D. J. (2016). Different Executive Functions Support Different Kinds of Cognitive Flexibility: Evidence From 2-, 3-, and 4-Year-Olds. *Child Development*, *87*(2), 513-526. https://doi.org/10.1111/cdev.12468

Blondel, V. D., Guillaume, J. L., Lambiotte, R., & Lefebvre, E. (2008). Fast unfolding of communities in large networks. *Journal of Statistical Mechanics: Theory and Experiment*, *2008*(10), 10008.

Boersma, M., Smit, D. J. a, Boomsma, D. I., Geus, E. J. c de, Waal, H. A. delemarre-Van de, & Stam, C. J. (2013). Growing Trees in Child Brains: Graph Theoretical Analysis of Electroencephalography-Derived Minimum Spanning Tree in 5- and 7-Year-Old Children Reflects Brain Maturation. *Brain Connectivity*, *3*(1), 50-60. https://doi.org/10.1089/brain.2012.0106

Boersma, M., Smit, D. J. A., Bie, H. M. A. D., Baal, G. C. M. V., Boomsma, D. I., Geus, E. J. C. D., Waal, H. A. D.-V. D., & Stam, C. J. (2011). Network analysis of resting state EEG in the developing young brain: Structure comes with maturation. *Human Brain Mapping*, *32*(3), 413-425. https://doi.org/10.1002/hbm.21030

Bornstein, M. H. (2014). Human Infancy...and the Rest of the Lifespan. *Annual Review of Psychology*, *65*(1), 121-158. https://doi.org/10.1146/annurev-psych-120710-100359

Bosch-Bayard, J., Biscay, R. J., Fernandez, T., Otero, G. A., Ricardo-Garcell, J., Aubert-Vazquez, E., & Harmony, T. (2022). EEG effective connectivity during the first year of life mirrors brain synaptogenesis, myelination, and early right hemisphere predominance. *NeuroImage*, *252*, 119035.

Botvinick, M. M., Braver, T. S., Barch, D. M., Carter, C. S., & Cohen, J. D. (2001). Conflict monitoring and cognitive control. *Psychological Review*, *108*(3), 624-652. https://doi.org/10.1037/0033-295X.108.3.624

Braithwaite, E. K., Jones, E. J., Johnson, M. H., & Holmboe, K. (2020). Dynamic modulation of frontal theta power predicts cognitive ability in infancy. *Developmental Cognitive Neuroscience*, *45*, 100818.

References

Brandes-Aitken, A., Metser, M., Braren, S. H., Vogel, S. C., & Brito, N. H. (2023). Neurophysiology of sustained attention in early infancy: Investigating longitudinal relations with recognition memory outcomes. *Infant Behavior and Development*, *70*, 101807. https://doi.org/10.1016/j.infbeh.2022.101807

Braver, T. S. (2012). The variable nature of cognitive control: A dual mechanisms framework. *Trends in Cognitive Sciences*, *16*(2), 106-113. https://doi.org/10.1016/j.tics.2011.12.010

Briley, D. A., & Tucker-Drob, E. M. (2013). Explaining the Increasing Heritability of Cognitive Ability Across Development: A Meta-Analysis of Longitudinal Twin and Adoption Studies. *Psychological Science*, *24*(9), 1704-1713. https://doi.org/10.1177/0956797613478618

Brito, N. H., Fifer, W. P., Myers, M. M., Elliott, A. J., & Noble, K. G. (2016). Associations among family socioeconomic status, EEG power at birth. *And Cognitive Skills during Infancy. Developmental Cognitive, neuroscience, 19*, 144-151.

Broomell, A. P. R., Savla, J., Calkins, S. D., & Bell, M. A. (2021). Infant electroencephalogram coherence and early childhood inhibitory control: Foundations for social cognition in late childhood. *Developmental Psychology*, *57*(9), 1439-1451. https://doi.org/10.1037/dev0001241

Brown, K. L., & Gartstein, M. A. (2023). Microstate analysis in infancy. *Infant Behavior and Development*, *70*, 101785. https://doi.org/10.1016/j.infbeh.2022.101785

Bulf, H., Johnson, S. P., & Valenza, E. (2011). Visual statistical learning in the newborn infant. *Cognition*, *121*(1), 127-132. https://doi.org/10.1016/j.cognition.2011.06.010

Bullmore, E., & Sporns, O. (2012). The economy of brain network organization. *Nature Reviews Neuroscience*, *13*(5), 336-349. https://doi.org/10.1038/nrn3214

Buss, A. T., Fox, N., Boas, D. A., & Spencer, J. P. (2014). Probing the early development of visual working memory capacity with functional near-infrared spectroscopy. *NeuroImage*, *85*, 314-325. https://doi.org/10.1016/j.neuroimage.2013.05.034

Buss, A. T., & Spencer, J. P. (2018). Changes in frontal and posterior cortical activity underlie the early emergence of executive function.

Developmental Science, *21*(4), e12602. https://doi.org/10.1111/desc.12602

Buzsáki, G. (2006). Rhythms of the Brain. En *Rhythms of the Brain*. https://doi.org/10.1093/acprof:oso/9780195301069.001.0001

Buzsáki, G., Anastassiou, C. A., & Koch, C. (2012). The origin of extracellular fields and currents—EEG, ECoG, LFP and spikes. *Nat. Rev. Neurosci*, *13*, 407-420.

Buzsáki, G., & Draguhn, A. (2004). Neuronal Oscillations in Cortical Networks. *Science*, *304*(5679), 1926-1929. https://doi.org/10.1126/science.1099745

Caffarra, S., Kanopka, K., Kruper, J., Richie-Halford, A., Roy, E., Rokem, A., & Yeatman, J. D. (2022). *Development of the alpha rhythm is linked to visual white matter pathways and visual detection performance* [Preprint]. Neuroscience. https://doi.org/10.1101/2022.09.03.506461

Cai, D., Deng, M., Yu, J., Nan, W., & Leung, A. W. (2021). The relationship of resting-state EEG oscillations to executive functions in middle childhood. *International Journal of Psychophysiology*, *164*, 64-70.

Calderone, D. J., Lakatos, P., Butler, P. D., & Castellanos, F. X. (2014). Entrainment of neural oscillations as a modifiable substrate of attention. *Trends in Cognitive Sciences*, *18*(6), 300-309. https://doi.org/10.1016/j.tics.2014.02.005

Camacho, M. C., Quiñones-Camacho, L. E., & Perlman, S. B. (2020). Does the child brain rest?: An examination and interpretation of resting cognition in developmental cognitive neuroscience. *NeuroImage*, *212*, 116688. https://doi.org/10.1016/j.neuroimage.2020.116688

Canfield, R. L., & Haith, M. M. (1991). Young infants' visual expectations for symmetric and asymmetric stimulus sequences. *Developmental Psychology*, *27*(2), 198-208. https://doi.org/10.1037//0012-1649.27.2.198

Cantiani, C., Piazza, C., Mornati, G., Molteni, M., & Riva, V. (2019). Oscillatory gamma activity mediates the pathway from socioeconomic status to language acquisition in infancy. *Infant Behavior and Development*, *57*. https://doi.org/10.1016/j.infbeh.2019.101384

Cao, M., He, Y., Dai, Z., Liao, X., Jeon, T., Ouyang, M., Chalak, L., Bi, Y., Rollins, N., Dong, Q., & Huang, H. (2017). Early Development of Functional Network Segregation Revealed by Connectomic Analysis

of the Preterm Human Brain. *Cerebral cortex (New York, N.Y. : 1991)*, *27*(3). https://doi.org/10.1093/cercor/bhw038

Cao, M., Huang, H., Peng, Y., Dong, Q., & He, Y. (2016). Toward Developmental Connectomics of the Human Brain. *Frontiers in Neuroanatomy*, *10*. https://doi.org/10.3389/fnana.2016.00025

Cao, M., Wang, J. H., Dai, Z. J., Cao, X. Y., Jiang, L. L., Fan, F. M., Song, X. W., Xia, M. R., Shu, N., Dong, Q., Milham, M. P., Castellanos, F. X., Zuo, X. N., & He, Y. (2014). Topological organization of the human brain functional connectome across the lifespan. *Developmental Cognitive Neuroscience*, *7*, 76-93. https://doi.org/10.1016/j.dcn.2013.11.004

Carlson, S. M. (2005). Developmentally Sensitive Measures of Executive Function in Preschool Children. *Developmental Neuropsychology*, *28*(2), 595-616.

Carter Leno, V., Begum-Ali, J., Goodwin, A., Mason, L., Pasco, G., Pickles, A., Garg, S., Green, J., Charman, T., Johnson, M. H., Jones, E. J. H., the EDEN, Vassallo, G., Burkitt-Wright, E., Eelloo, J., Gareth Evans, D., West, S., Hupton, E., Lewis, L., … Taylor, C. (2022). Infant excitation/inhibition balance interacts with executive attention to predict autistic traits in childhood. *Molecular Autism*, *13*(1), 46. https://doi.org/10.1186/s13229-022-00526-1

Carver, A. C., Livesey, D. J., & Charles, M. (2001). Age Related Changes in Inhibitory Control as Measured by Stop Signal Task Performance. *International Journal of Neuroscience*, *107*(1-2), 43-61. https://doi.org/10.3109/00207450109149756

Casagrande, M., Marotta, A., Martella, D., Volpari, E., Agostini, F., Favieri, F., Forte, G., Rea, M., Ferri, R., Giordano, V., Doricchi, F., & Giovannoli, J. (2022). Assessing the three attentional networks in children from three to six years: A child-friendly version of the Attentional Network Test for Interaction. *Behavior Research Methods*, *51*, 1403-1415. https://doi.org/10.3758/s13428-021-01668-5

Casey, B. J., Trainor, R. J., Orendi, J. L., Schubert, A. B., Nystrom, L. E., Giedd, J. N., Castellanos, F. X., Haxby, J. V., Noll, D. C., Cohen, J. D., Forman, S. D., Dahl, R. E., & Rapoport, J. L. (1997). A Developmental Functional MRI Study of Prefrontal Activation during Performance of a Go-No-Go Task. *Journal of Cognitive Neuroscience*, *9*(6), 835-847. https://doi.org/10.1162/jocn.1997.9.6.835

References

Cavanagh, J. F., & Frank, M. J. (2014). Frontal theta as a mechanism for cognitive control. *Trends in Cognitive Sciences*, *18*(8), 414-421. https://doi.org/10.1016/j.tics.2014.04.012

Cellier, D., Riddle, J., Petersen, I., & Hwang, K. (2021). The development of theta and alpha neural oscillations from ages 3 to 24 years. *Developmental Cognitive Neuroscience*, *50*, 100969. https://doi.org/10.1016/j.dcn.2021.100969

Charalambous, E., & Djebbara, Z. (2023). On natural attunement: Shared rhythms between the brain and the environment. *Neuroscience & Biobehavioral Reviews*, *155*, 105438. https://doi.org/10.1016/j.neubiorev.2023.105438

Chatham, C. H., Frank, M. J., & Munakata, Y. (2009). Pupillometric and behavioral markers of a developmental shift in the temporal dynamics of cognitive control. *Proceedings of the National Academy of Sciences of the United States of America*, *106*(14), 5529-5533. https://doi.org/10.1073/pnas.0810002106

Chevalier, N., Hadley, L. V., & Balthrop, K. (2021). Midfrontal theta oscillations and conflict monitoring in children and adults. *Developmental Psychobiology*, *63*(8), e22216. https://doi.org/10.1002/dev.22216

Chirumamilla, V. C., Hitchings, L., Mulkey, S. B., Anwar, T., Baker, R., Larry Maxwell, G., De Asis-Cruz, J., Kapse, K., Limperopoulos, C., Du Plessis, A., & Govindan, R. B. (2023). Functional brain network properties of healthy full-term newborns quantified by scalp and source-reconstructed EEG. *Clinical Neurophysiology*, *147*, 72-80. https://doi.org/10.1016/j.clinph.2023.01.005

Chu, C. J., Tanaka, N., Diaz, J., Edlow, B. L., Wu, O., Hämäläinen, M., Stufflebeam, S., Cash, S. S., & Kramer, M. A. (2015). EEG functional connectivity is partially predicted by underlying white matter connectivity. *NeuroImage*, *108*, 23-33. https://doi.org/10.1016/j.neuroimage.2014.12.033

Cirelli, L. K., Spinelli, C., Nozaradan, S., & Trainor, L. J. (2016). Measuring Neural Entrainment to Beat and Meter in Infants: Effects of Music Background. *Frontiers in Neuroscience*, *10*. https://doi.org/10.3389/fnins.2016.00229

References

Clark, C. A. C., Cook, K., Wang, R., Rueschman, M., Radcliffe, J., Redline, S., & Taylor, H. G. (2023). Psychometric properties of a combined go/no-go and continuous performance task across childhood. *Psychological Assessment*, *35*(4), 353-365. https://doi.org/10.1037/pas0001202

Clarke, A. R., Barry, R. J., McCarthy, R., & Selikowitz, M. (2001). Age and sex effects in the EEG: Development of the normal child. *Clinical Neurophysiology*, *112*(5), 806-814. https://doi.org/10.1016/S1388-2457(01)00488-6

Clayton, M. S., Yeung, N., & Cohen Kadosh, R. (2015). The roles of cortical oscillations in sustained attention. *Trends in Cognitive Sciences*, *19*(4), 188-195. https://doi.org/10.1016/j.tics.2015.02.004

Clayton, M. S., Yeung, N., & Cohen Kadosh, R. (2018). The many characters of visual alpha oscillations. *European Journal of Neuroscience*, *48*(7), 2498-2508. https://doi.org/10.1111/ejn.13747

Clearfield, M. W., Diedrich, F. J., Smith, L. B., & Thelen, E. (2006). Young infants reach correctly in A-not-B tasks: On the development of stability and perseveration. *Infant Behavior and Development*, *29*(3), 435-444. https://doi.org/10.1016/j.infbeh.2006.03.001

Clements, G. M., Bowie, D. C., Gyurkovics, M., Low, K. A., Fabiani, M., & Gratton, G. (2021). Spontaneous Alpha and Theta Oscillations Are Related to Complementary Aspects of Cognitive Control in Younger and Older Adults. *Frontiers in Human Neuroscience*, *15*, 621620. https://doi.org/10.3389/fnhum.2021.621620

Clohessy, A. B., Posner, M. I., & Rothbart, M. K. (2001). Development of the functional visual field. *Acta Psychologica*, *106*(1-2), 51-68. https://doi.org/10.1016/S0001-6918(00)00026-3

Clouter, A., Shapiro, K. L., & Hanslmayr, S. (2017). Theta Phase Synchronization Is the Glue that Binds Human Associative Memory. *Current Biology*, *27*(20), 3143-3148.e6. https://doi.org/10.1016/j.cub.2017.09.001

Cohen, J. R., & D'Esposito, M. (2016). The segregation and integration of distinct brain networks and their relationship to cognition. *Journal of Neuroscience*, *36*(48). https://doi.org/10.1523/JNEUROSCI.2965-15.2016

References

Cohen, M. X. (2016). Midfrontal theta tracks action monitoring over multiple interactive time scales. *NeuroImage*, *141*, 262-272. https://doi.org/10.1016/j.neuroimage.2016.07.054

Cohen, M. X. (2017). Where Does EEG Come From and What Does It Mean? *Trends in Neurosciences*, *40*(4), 208-218. https://doi.org/10.1016/j.tins.2017.02.004

Cohen, M. X., & Donner, T. H. (2013). Midfrontal conflict-related theta-band power reflects neural oscillations that predict behavior. *Journal of Neurophysiology*, *110*(12), 2752-2763. https://doi.org/10.1152/jn.00479.2013

Colclough, G. L., Smith, S. M., Nichols, T. E., Winkler, A. M., Sotiropoulos, S. N., Glasser, M. F., Van Essen, D. C., & Woolrich, M. W. (2017). The heritability of multi-modal connectivity in human brain activity. *eLife*, *6*, e20178. https://doi.org/10.7554/eLife.20178

Cole, M. W., Bassett, D. S., Power, J. D., Braver, T. S., & Petersen, S. E. (2014). Intrinsic and Task-Evoked Network Architectures of the Human Brain. *Neuron*, *83*(1), 238-251. https://doi.org/10.1016/j.neuron.2014.05.014

Cole, M. W., Yarkoni, T., Repovs, G., Anticevic, A., & Braver, T. S. (2012). Global Connectivity of Prefrontal Cortex Predicts Cognitive Control and Intelligence. *Journal of Neuroscience*, *32*(26), 8988-8999. https://doi.org/10.1523/JNEUROSCI.0536-12.2012

Cole, S. R., & Voytek, B. (2017). Brain Oscillations and the Importance of Waveform Shape. *Trends in Cognitive Sciences*, *21*(2), 137-149. https://doi.org/10.1016/j.tics.2016.12.008

Cole, S., & Voytek, B. (2019). Cycle-by-cycle analysis of neural oscillations. *Journal of Neurophysiology*, *122*(2), 849-861. https://doi.org/10.1152/jn.00273.2019

Collin, G., & Heuvel, M. P. V. D. (2013). The ontogeny of the human connectome: Development and dynamic changes of brain connectivity across the life span. *Neuroscientist*, *19*(6), 616-628. https://doi.org/10.1177/1073858413503712

Colombo, J. (2001). The Development of Visual Attention in Infancy. *Annual Review of Psychology*, *52*(1), 337-367. https://doi.org/10.1146/annurev.psych.52.1.337

References

Colombo, J., & Degen Horowitz, F. (1987). Behavioral State as a Lead Variable in Neonatal Research. *Source: Merrill-Palmer Quarterly*, *33*(4), 423-437.

Conejero, Á., Guerra, S., Abundis-Gutiérrez, A., & Rueda, M. R. (2016). Frontal theta activation associated with error detection in toddlers: Influence of familial socioeconomic status. *Developmental science*. https://doi.org/10.1111/desc.12494

Conejero, Á., Rico-Picó, J., Moyano, S., Hoyo, Á., & Rueda, M. R. (2023). Predicting behavioral and brain markers of inhibitory control at preschool age from early measures of executive attention. *Frontiers in Psychology*, *14*, 983361. https://doi.org/10.3389/fpsyg.2023.983361

Conejero, A., & Rueda, M. R. (2017). Early development of executive attention. *Journal of Child & Adolescent Behavior*, *5*(2).

Conejero, Á., & Rueda, M. R. (2018). Infant temperament and family socio-economic status in relation to the emergence of attention regulation. *Scientific Reports*, *8*(1). https://doi.org/10.1038/s41598-018-28831-x

Cooper, P. S., Wong, A. S. W., Fulham, W. R., Thienel, R., Mansfield, E., Michie, P. T., & Karayanidis, F. (2015). Theta frontoparietal connectivity associated with proactive and reactive cognitive control processes. *NeuroImage*, *108*, 354-363. https://doi.org/10.1016/j.neuroimage.2014.12.028

Corbetta, M., Patel, G., & Shulman, G. L. (2008). The Reorienting System of the Human Brain: From Environment to Theory of Mind. *Neuron*, *58*(3), 306-324. https://doi.org/10.1016/j.neuron.2008.04.017

Corbetta, M., & Shulman, G. L. (2002). Control of goal-directed and stimulus-driven attention in the brain. *Nature Reviews Neuroscience*, *3*(3), 201-215. https://doi.org/10.1038/nrn755

Coull, J. T., Nobre, A. C., & Frith, C. D. (2001). Noradrenergic alpha2 agonist clonidine modulates behavioral and neuroanatomical correlates of human attentional orienting and alerting. *Cerebral Cortex*, *11*(1), 73-84. https://doi.org/10.1093/cercor/11.1.73.

Courage, M. L., & Cowan, N. (2022). *The development of memory in infancy and childhood*. Psychology Press.

Coyl, D. D., Roggman, L. A., & Newland, L. A. (2002). Stress, maternal depression, and negative mother-infant interactions in relation to infant attachment. *Infant Mental Health Journal*, *23*(2), 145-163. https://doi.org/10.1002/imhj.10009

References

Csibra, G., Tucker, L. A., & Johnson, M. H. (2001). Differential Frontal Cortex Activation before Anticipatory and Reactive Saccades in Infants. *Infancy*, *2*(2), 159-174. https://doi.org/10.1207/s15327078in0202_3

Cuevas, K., & Bell, M. A. (2010). Developmental progression of looking and reaching performance on the a-not-b task. *Developmental Psychology*, *46*(5), 1363-1371. https://doi.org/10.1037/a0020185

Cuevas, K., & Bell, M. A. (2022). EEG frequency development across infancy and childhood. *The Oxford Handbook of EEG Frequency*, *293*.

Cuevas, K., Swingler, M. M., Bell, M. A., Marcovitch, S., & Calkins, S. D. (2012). Measures of frontal functioning and the emergence of inhibitory control processes at 10 months of age. *Developmental Cognitive Neuroscience*, *2*(2), 235-243. https://doi.org/10.1016/j.dcn.2012.01.002

Cui, Z., Li, H., Xia, C. H., Larsen, B., Adebimpe, A., Baum, G. L., Cieslak, M., Gur, R. E., Gur, R. C., Moore, T. M., Oathes, D. J., Alexander-Bloch, A. F., Raznahan, A., Roalf, D. R., Shinohara, R. T., Wolf, D. H., Davatzikos, C., Bassett, D. S., Fair, D. A., … Satterthwaite, T. D. (2020). Individual Variation in Functional Topography of Association Networks in Youth. *Neuron*, *106*(2), 340-353.e8. https://doi.org/10.1016/j.neuron.2020.01.029

D'Angelo, M. C., Milliken, B., Jiménez, L., & Lupiáñez, J. (2013). Implementing flexibility in automaticity: Evidence from context-specific implicit sequence learning. *Consciousness and Cognition*, *22*(1), 64-81. https://doi.org/10.1016/j.concog.2012.11.002

Davies, P. L., Segalowitz, S. J., & Gavin, W. J. (2004). Development of Response-Monitoring ERPs in 7- to 25-Year-Olds. *Developmental Neuropsychology*, *25*(3), 355-376. https://doi.org/10.1207/s15326942dn2503_6

De Graaf, T. A., Gross, J., Paterson, G., Rusch, T., Sack, A. T., & Thut, G. (2013). Alpha-Band Rhythms in Visual Task Performance: Phase-Locking by Rhythmic Sensory Stimulation. *PLoS ONE*, *8*(3), e60035. https://doi.org/10.1371/journal.pone.0060035

Dean, D. C., III, O'Muircheartaigh, J., Dirks, H., Waskiewicz, N., Lehman, K., Walker, L., & Deoni, S. C. (2014). Modeling healthy male white matter and myelin development: 3 through 60 months of age. *Neuroimage*, *84*, 742-752.

References

Debnath, R., Buzzell, G. A., Morales, S., Bowers, M. E., Leach, S. C., & Fox, N. A. (2020). The Maryland analysis of developmental EEG (MADE) pipeline. *Psychophysiology*, *57*(6). https://doi.org/10.1111/psyp.13580

Deco, G., Ponce-Alvarez, A., Mantini, D., Romani, G. L., Hagmann, P., & Corbetta, M. (2013). Resting-state functional connectivity emerges from structurally and dynamically shaped slow linear fluctuations. *Journal of Neuroscience*, *33*(27), 11239-11252.

Dehaene-Lambertz, G., & Spelke, E. S. (2015). The Infancy of the Human Brain. *Neuron*, *88*(1), 93-109. https://doi.org/10.1016/j.neuron.2015.09.026

Demuru, M., & Fraschini, M. (2020). EEG fingerprinting: Subject-specific signature based on the aperiodic component of power spectrum. *Computers in Biology and Medicine*, *120*, 103748. https://doi.org/10.1016/j.compbiomed.2020.103748

Den Heuvel, M. P., & Sporns, O. (2011). Rich-club organization of the human connectome. *Journal of Neuroscience*, *31*(44), 15775-15786.

Diamond, A. (1985). Development of the Ability to Use Recall to Guide Action, as Indicated by Infants' Performance on AB. *Child Development*, *56*(4), 868-883.

Diamond, A. (1990). Developmental time course in human infants and infant monkeys, and the neural bases of, inhibitory control in reaching a. *Annals of the New York Academy of Sciences*, *608*(1), 637-676.

Diamond, A. (2013). Executive functions. *Annual Review of Psychology*, *64*, 135.

Diamond, A., & Doar, B. (1989). The performance of human infants on a measure of frontal cortex function, the delayed response task. *Developmental Psychobiology*, *22*(3), 271-294. https://doi.org/10.1002/dev.420220307

Diamond, A., & Ling, D. S. (2016). Conclusions about interventions, programs, and approaches for improving executive functions that appear justified and those that, despite much hype, do not. *Developmental Cognitive Neuroscience*, *18*, 34-48. https://doi.org/10.1016/j.dcn.2015.11.005

Dias, C. C., & Figueiredo, B. (2020). Sleep-wake behaviour during the first 12 months of life and associated factors: A systematic review. *Early Child Development and Care*, *190*(15), 2333-2365. https://doi.org/10.1080/03004430.2019.1582034

References

Donoghue, T., Dominguez, J., & Voytek, B. (2020). Electrophysiological Frequency Band Ratio Measures Conflate Periodic and Aperiodic Neural Activity. *Eneuro*, *7*(6), ENEURO.0192-20.2020. https://doi.org/10.1523/ENEURO.0192-20.2020

Donoghue, T., Haller, M., Peterson, E. J., Varma, P., Sebastian, P., Gao, R., Noto, T., Lara, A. H., Wallis, J. D., Knight, R. T., Shestyuk, A., & Voytek, B. (2020). Parameterizing neural power spectra into periodic and aperiodic components. *Nature Neuroscience*, *23*(12), 1655-1665. https://doi.org/10.1038/s41593-020-00744-x

Doria, V., Beckmann, C. F., Arichi, T., Merchant, N., Groppo, M., Turkheimer, F. E., Counsell, S. J., Murgasova, M., Aljabar, P., Nunes, R. G., Larkman, D. J., Rees, G., & Edwards, A. D. (2010). Emergence of resting state networks in the preterm human brain. *Proceedings of the National Academy of Sciences of the United States of America*, *107*(46), 20015-20020. https://doi.org/10.1073/pnas.1007921107

Dosenbach, N. U. F., Fair, D. A., Cohen, A. L., Schlaggar, B. L., & Petersen, S. E. (2008). A dual-networks architecture of top-down control. *Trends in Cognitive Sciences*, *12*(3), 99-105. https://doi.org/10.1016/j.tics.2008.01.001

Dosenbach, N. U. F., Nardos, B., Cohen, A. L., Fair, D. A., Power, J. D., Church, J. A., Nelson, S. M., Wig, G. S., Vogel, A. C., Lessov-Schlaggar, C. N., Barnes, K. A., Dubis, J. W., Feczko, E., Coalson, R. S., Pruett, J. R., Barch, D. M., Petersen, S. E., & Schlaggar, B. L. (2010). Prediction of Individual Brain Maturity Using fMRI. *Science*, *329*(5997), 1358-1361. https://doi.org/10.1126/science.1194144

Dubois, J. (2014). The early development of brain white matter: A review of imaging studies in fetuses, newborns and infants. *Neuroscience*, *276*, 48-71.

Dudschig, C., & Jentzsch, I. (2009). Speeding before and slowing after errors: Is it all just strategy? *Brain Research*, *1296*, 56-62. https://doi.org/10.1016/j.brainres.2009.08.009

Duncan, J. (2010). The multiple-demand (MD) system of the primate brain: Mental programs for intelligent behaviour. *Trends in Cognitive Sciences*, *14*(4), 172-179. https://doi.org/10.1016/j.tics.2010.01.004

Dustman, R. E., Shearer, D. E., & Emmerson, R. Y. (1999). Life-span changes in EEG spectral amplitude, amplitude variability and mean

frequency. *Clinical Neurophysiology*, *110*(8), 1399-1409. https://doi.org/10.1016/S1388-2457(99)00102-9

Ede, F., Quinn, A. J., Woolrich, M. W., & Nobre, A. C. (2018). Neural oscillations: Sustained rhythms or transient burst-events? *Trends in neurosciences*, *41*(7), 415-417. https://doi.org/10.1016/j.tins.2018.04.004

Ellis, C. T., Skalaban, L. J., Yates, T. S., & Turk-Browne, N. B. (2021). Attention recruits frontal cortex in human infants. *Proceedings of the National Academy of Sciences of the United States of America*, *118*(12). https://doi.org/10.1073/pnas.2021474118

Enders, C. K. (2013). Dealing With Missing Data in Developmental Research. *Child Development Perspectives*, *7*(1), 27-31. https://doi.org/10.1111/cdep.12008

Engelhardt, L. E., Church, J. A., Paige Harden, K., & Tucker-Drob, E. M. (2019). Accounting for the shared environment in cognitive abilities and academic achievement with measured socioecological contexts. *Developmental Science*, *22*(1), e12699. https://doi.org/10.1111/desc.12699

Engle, R. W., & Kane, M. J. (2003). Executive Attention, Working Memory Capacity, and a Two-Factor Theory of Cognitive Control. En *Psychology of Learning and Motivation* (Vol. 44, pp. 145-199). Elsevier. https://doi.org/10.1016/S0079-7421(03)44005-X

Eschmann, K. C. J., Bader, R., & Mecklinger, A. (2018). Topographical differences of frontal-midline theta activity reflect functional differences in cognitive control abilities. *Brain and Cognition*, *123*, 57-64. https://doi.org/10.1016/j.bandc.2018.02.002

Espy, K. A., Kaufmann, P. M., McDiarmid, M. D., & Glisky, M. L. (1999). Executive Functioning in Preschool Children: Performance on A-Not-B and Other Delayed Response Format Tasks. *Brain and Cognition*, *41*(2), 178-199. https://doi.org/10.1006/brcg.1999.1117

Evans, G. W., & Schamberg, M. A. (2009). Childhood poverty, chronic stress, and adult working memory. *Proceedings of the National Academy of Sciences of the United States of America*, *106*(16), 6545-6549. https://doi.org/10.1073/pnas.0811910106

Eyler, L. T., Chen, C.-H., Panizzon, M. S., Fennema-Notestine, C., Neale, M. C., Jak, A., Jernigan, T. L., Fischl, B., Franz, C. E., Lyons, M. J., Grant, M., Prom-Wormley, E., Seidman, L. J., Tsuang, M. T., Fiecas, M. J. A.,

Dale, A. M., & Kremen, W. S. (2012). A Comparison of Heritability Maps of Cortical Surface Area and Thickness and the Influence of Adjustment for Whole Brain Measures: A Magnetic Resonance Imaging Twin Study. *Twin Research and Human Genetics*, *15*(3), 304-314. https://doi.org/10.1017/thg.2012.3

Fair, D. A., Cohen, A. L., Dosenbach, N. U. F., Church, J. A., Miezin, F. M., Barch, D. M., Raichle, M. E., Petersen, S. E., & Schlaggar, B. L. (2008). The maturing architecture of the brain's default network. *Proceedings of the National Academy of Sciences*, *105*(10), 4028-4032. https://doi.org/10.1073/pnas.0800376105

Fair, D. A., Cohen, A. L., Power, J. D., Dosenbach, N. U. F., Church, J. A., Miezin, F. M., Schlaggar, B. L., & Petersen, S. E. (2009). Functional Brain Networks Develop from a "Local to Distributed" Organization. *PLoS Computational Biology*, *5*(5), e1000381. https://doi.org/10.1371/journal.pcbi.1000381

Fan, J., McCandliss, B. D., Sommer, T., Raz, A., & Posner, M. I. (2002). Testing the efficiency and independence of attentional networks. *Journal of Cognitive Neuroscience*, *14*(3), 340-347.

Farah, M. J. (2017). The Neuroscience of Socioeconomic Status: Correlates, Causes, and Consequences. *Neuron*, *96*(1), 56-71. https://doi.org/10.1016/j.neuron.2017.08.034

Faskowitz, J., Betzel, R. F., & Sporns, O. (2022). Edges in brain networks: Contributions to models of structure and function. *Network Neuroscience*, *6*(1), 1-28.

Fiebelkorn, I. C., & Kastner, S. (2019). A Rhythmic Theory of Attention. *Trends in Cognitive Sciences*, *23*(2), 87-101. https://doi.org/10.1016/j.tics.2018.11.009

Figueiredo, B., Dias, C. C., Pinto, T. M., & Field, T. (2016). Infant sleep-wake behaviors at two weeks, three and six months. *Infant Behavior and Development*, *44*, 169-178. https://doi.org/10.1016/j.infbeh.2016.06.011

Finc, K., Bonna, K., He, X., Lydon-Staley, D. M., Kühn, S., Duch, W., & Bassett, D. S. (2020). Dynamic reconfiguration of functional brain networks during working memory training. *Nature Communications*, *11*(1), 2435. https://doi.org/10.1038/s41467-020-15631-z

Finn, E. S., Shen, X., Scheinost, D., Rosenberg, M. D., Huang, J., Chun, M. M., Papademetris, X., & Constable, R. T. (2015). Functional connectome

fingerprinting: Identifying individuals using patterns of brain connectivity. *Nature Neuroscience*, *18*(11), 1664-1671. https://doi.org/10.1038/nn.4135

Fiske, A., Collins-Jones, L. H., De Klerk, C., Lui, K. Y. K., Hendry, A., Greenhalgh, I., Hall, A., Dvergsdal, H., Scerif, G., & Holmboe, K. (2023). *The Neural Correlates of Response Inhibition across the Transition from Infancy to Toddlerhood: An fNIRS study* [Preprint]. PsyArXiv. https://doi.org/10.31234/osf.io/w7mkq

Fiske, A., & Holmboe, K. (2019). Neural substrates of early executive function development. *Developmental Review*, *52*, 42-62. https://doi.org/10.1016/j.dr.2019.100866

Fiske, A., Klerk, C., Lui, K. Y. K., Collins-Jones, L., Hendry, A., Greenhalgh, I., Hall, A., Scerif, G., Dvergsdal, H., & Holmboe, K. (2022). The neural correlates of inhibitory control in 10-month-old infants: A functional near-infrared spectroscopy study. *NeuroImage*, *257*, 119241. https://doi.org/10.1016/j.neuroimage.2022.119241

Fleming, C. B., Stevens, A. L., Vivero, M., Patwardhan, I., Nelson, T. D., Nelson, J. M., & Mason, W. A. (2020). Executive control in early childhood as an antecedent of adolescent problem behaviors: A longitudinal study with performance-based measures of early childhood cognitive processes. *Journal of Youth and Adolescence*, *49*(12), 2429-2440.

Fló, A., Gennari, G., Benjamin, L., & Dehaene-Lambertz, G. (2022). Automated Pipeline for Infants Continuous EEG (APICE): A flexible pipeline for developmental cognitive studies. *Developmental Cognitive Neuroscience*, *54*, 101077. https://doi.org/10.1016/j.dcn.2022.101077

Fockert, J. D., Rees, G., Frith, C., & Lavie, N. (2004). Neural Correlates of Attentional Capture in Visual Search. *Journal of Cognitive Neuroscience*, *16*(5), 751-759. https://doi.org/10.1162/089892904970762

Fornito, A., Zalesky, A., Bassett, D. S., Meunier, D., Ellison-Wright, I., Yücel, M., Wood, S. J., Shaw, K., O'Connor, J., Nertney, D., Mowry, B. J., Pantelis, C., & Bullmore, E. T. (2011). Genetic Influences on Cost-Efficient Organization of Human Cortical Functional Networks. *The Journal of Neuroscience*, *31*(9), 3261-3270. https://doi.org/10.1523/JNEUROSCI.4858-10.2011

References

Fox, M. D., Corbetta, M., Snyder, A. Z., Vincent, J. L., & Raichle, M. E. (2006). Spontaneous neuronal activity distinguishes human dorsal and ventral attention systems. *Proceedings of the National Academy of Sciences*, *103*(26), 10046-10051. https://doi.org/10.1073/pnas.0604187103

Fransson, P., Åden, U., Blennow, M., & Lagercrantz, H. (2011). The functional architecture of the infant brain as revealed by resting-state fMRI. *Cerebral Cortex*, *21*(1), 145-154. https://doi.org/10.1093/cercor/bhq071

Fransson, P., Metsäranta, M., Blennow, M., Åden, U., Lagercrantz, H., & Vanhatalo, S. (2013). Early Development of Spatial Patterns of Power-Law Frequency Scaling in fMRI Resting-State and EEG Data in the Newborn Brain. *Cerebral Cortex*, *23*(3), 638-646. https://doi.org/10.1093/cercor/bhs047

Fransson, P., Skiöld, B., Horsch, S., Nordell, A., Blennow, M., Lagercrantz, H., & Åden, U. (2007). Resting-state networks in the infant brain. *Proceedings of the National Academy of Sciences*, *104*(39), 15531-15536. https://doi.org/10.1073/pnas.0704380104

Freschl, J., Azizi, L. A., Balboa, L., Kaldy, Z., & Blaser, E. (2022). The development of peak alpha frequency from infancy to adolescence and its role in visual temporal processing: A meta-analysis. *Developmental Cognitive Neuroscience*, *57*, 101146. https://doi.org/10.1016/j.dcn.2022.101146

Friedman, N. P., & Miyake, A. (2017). Unity and diversity of executive functions: Individual differences as a window on cognitive structure. *Cortex*, *86*, 186-204.

Fries, P. (2005). A mechanism for cognitive dynamics: Neuronal communication through neuronal coherence. *Trends in Cognitive Sciences*, *9*(10), 474-480. https://doi.org/10.1016/j.tics.2005.08.011

Fries, P. (2015). Rhythms for Cognition: Communication through Coherence. *Neuron*, *88*(1), 220-235. https://doi.org/10.1016/j.neuron.2015.09.034

Fu, Z., Sajad, A., Errington, S. P., Schall, J. D., & Rutishauser, U. (2023). Neurophysiological mechanisms of error monitoring in human and non-human primates. *Nature Reviews Neuroscience*, *24*(3), 153-172. https://doi.org/10.1038/s41583-022-00670-w

Furlong, S., Cohen, J. R., Hopfinger, J., Snyder, J., Robertson, M. M., & Sheridan, M. A. (2021). Resting-state EEG connectivity in young

children with ADHD. *Journal of Clinical Child & Adolescent Psychology*, *50*(6), 746-762.

Gabard-Durnam, L., & McLaughlin, K. A. (2020). Sensitive periods in human development: Charting a course for the future. *Current Opinion in Behavioral Sciences*, *36*, 120-128. https://doi.org/10.1016/j.cobeha.2020.09.003

Gagne, J. R., & Saudino, K. J. (2016). The development of inhibitory control in early childhood: A twin study from 2–3 years. *Developmental Psychology*, *52*(3), 391-399. https://doi.org/10.1037/dev0000090

Gao, R., Peterson, E. J., & Voytek, B. (2017). Inferring synaptic excitation/inhibition balance from field potentials. *NeuroImage*, *158*, 70-78. https://doi.org/10.1016/j.neuroimage.2017.06.078

Gao, W., Alcauter, S., Elton, A., Hernandez-Castillo, C. R., Smith, J. K., Ramirez, J., & Lin, W. (2015). Functional network development during the first year: Relative sequence and socioeconomic correlations. *Cerebral Cortex*, *25*(9), 2919-2928. https://doi.org/10.1093/cercor/bhu088

Gao, W., Alcauter, S., Smith, J. K., Gilmore, J. H., & Lin, W. (2015). Development of human brain cortical network architecture during infancy. *Brain Structure and Function*, *220*(2), 1173-1186. https://doi.org/10.1007/s00429-014-0710-3

Gao, W., Gilmore, J. H., Giovanello, K. S., Smith, J. K., Shen, D., Zhu, H., & Lin, W. (2011). Temporal and spatial evolution of brain network topology during the first two years of life. *PLoS ONE*, *6*(9). https://doi.org/10.1371/journal.pone.0025278

Gao, W., Gilmore, J. H., Shen, D., Smith, J. K., Zhu, H., & Lin, W. (2013). The synchronization within and interaction between the default and dorsal attention networks in early infancy. *Cerebral Cortex*, *23*(3), 594-603. https://doi.org/10.1093/cercor/bhs043

Garon, N., Smith, I. M., & Bryson, S. E. (2014). A novel executive function battery for preschoolers: Sensitivity to age differences. *Child Neuropsychology*, *20*(6), 713-736. https://doi.org/10.1080/09297049.2013.857650

Gasser, T., Verleger, R., Bächer, P., & Sroka, L. (1988). Development of the EEG of school-age children and adolescents. I. Analysis of band

power. *Electroencephalography and Clinical Neurophysiology*, *69*(2), 91-99. https://doi.org/10.1016/0013-4694(88)90204-0

Ge, T., Holmes, A. J., Buckner, R. L., Smoller, J. W., & Sabuncu, M. R. (2017). Heritability analysis with repeat measurements and its application to resting-state functional connectivity. *Proceedings of the National Academy of Sciences*, *114*(21), 5521-5526. https://doi.org/10.1073/pnas.1700765114

Gerardi-Caulton, G. (2000). Sensitivity to spatial conflict and the development of self-regulation in children 24-36 months of age. *Developmental Science*, *3*(4), 397-404. https://doi.org/10.1111/1467-7687.00134

Gerhardstein, P., & Rovee-Collier, C. (2002). The Development of Visual Search in Infants and Very Young Children. *Journal of Experimental Child Psychology*, *81*(2), 194-215. https://doi.org/10.1006/jecp.2001.2649

Ghaderi, A. H., Cognitive Neuroscience Laboratory, Department of Psychology, University of Tabriz, Tabriz, Iran., Nazari, M. A., Cognitive Neuroscience Laboratory, Department of Psychology, University of Tabriz, Tabriz, Iran., Shahrokhi, H., Research Center of Psychiatry and Behavioral Sciences, Tabriz University of Medical Sciences, Tabriz, Iran., Darooneh, A. H., & Department of Physics, Faculty of Sciences, University of Zanjan, Zanjan, Iran. (2017). Functional Brain Connectivity Differences Between Different ADHD Presentations: Impaired Functional Segregation in ADHD-Combined Presentation but not in ADHD-Inattentive Presentation. *Basic and Clinical Neuroscience Journal*, *8*(4), 267-278. https://doi.org/10.18869/nirp.bcn.8.4.267

Gilmore, J. H., Knickmeyer, R. C., & Gao, W. (2018). Imaging structural and functional brain development in early childhood. *Nature Reviews Neuroscience*, *19*(3), 123-137. https://doi.org/10.1038/nrn.2018.1

Gonthier, C., Zira, M., Colé, P., & Blaye, A. (2019). Evidencing the developmental shift from reactive to proactive control in early childhood and its relationship to working memory. *Journal of Experimental Child Psychology*, *177*, 1-16. https://doi.org/10.1016/j.jecp.2018.07.001

References

Gordillo, D., Ramos Da Cruz, J., Moreno, D., Garobbio, S., & Herzog, M. H. (2023). Do we really measure what we think we are measuring? *iScience*, *26*(2), 106017. https://doi.org/10.1016/j.isci.2023.106017

Graham, J. W. (2009). Missing Data Analysis: Making It Work in the Real World. *Annual Review of Psychology*, *60*(1), 549-576. https://doi.org/10.1146/annurev.psych.58.110405.085530

Grandy, T. H., Werkle-Bergner, M., Chicherio, C., Lövdén, M., Schmiedek, F., & Lindenberger, U. (2013). Individual alpha peak frequency is related to latent factors of general cognitive abilities. *Neuroimage*, *79*, 10-18.

Grayson, D. S., & Fair, D. A. (2017). Development of large-scale functional networks from birth to adulthood: A guide to the neuroimaging literature. *NeuroImage*. https://doi.org/10.1016/j.neuroimage.2017.01.079

Groeschel, S., Vollmer, B., King, M. D., & Connelly, A. (2010). Developmental changes in cerebral grey and white matter volume from infancy to adulthood. *International Journal of Developmental Neuroscience*, *28*(6), 481-489. https://doi.org/10.1016/j.ijdevneu.2010.06.004

Guimera, R., & Amaral, L. A. N. (2005). Cartography of complex networks: Modules and universal roles. *Journal of Statistical Mechanics: Theory and Experiment*, *2005*(02), 02001.

Haartsen, R., Velde, B. van der, Jones, E. J. H., Johnson, M. H., & Kemner, C. (2020). Using multiple short epochs optimises the stability of infant EEG connectivity parameters. *Scientific Reports*, *10*(1). https://doi.org/10.1038/s41598-020-68981-5

Hämmerer, D., Li, S.-C., Müller, V., & Lindenberger, U. (2010). An electrophysiological study of response conflict processing across the lifespan: Assessing the roles of conflict monitoring, cue utilization, response anticipation, and response suppression. *Neuropsychologia*, *48*(11), 3305-3316. https://doi.org/10.1016/j.neuropsychologia.2010.07.014

Hansen, E. C. A., Battaglia, D., Spiegler, A., Deco, G., & Jirsa, V. K. (2015). Functional connectivity dynamics: Modeling the switching behavior of the resting state. *NeuroImage*, *105*, 525-535. https://doi.org/10.1016/j.neuroimage.2014.11.001

References

Hanslmayr, S., Axmacher, N., & Inman, C. S. (2019). Modulating Human Memory via Entrainment of Brain Oscillations. *Trends in Neurosciences*, *42*(7), 485-499. https://doi.org/10.1016/j.tins.2019.04.004

Haworth, C. M. A., Wright, M. J., Luciano, M., Martin, N. G., De Geus, E. J. C., Van Beijsterveldt, C. E. M., Bartels, M., Posthuma, D., Boomsma, D. I., Davis, O. S. P., Kovas, Y., Corley, R. P., DeFries, J. C., Hewitt, J. K., Olson, R. K., Rhea, S.-A., Wadsworth, S. J., Iacono, W. G., McGue, M., … Plomin, R. (2010). The heritability of general cognitive ability increases linearly from childhood to young adulthood. *Molecular Psychiatry*, *15*(11), 1112-1120. https://doi.org/10.1038/mp.2009.55

He, B. J. (2014). Scale-free brain activity: Past, present, and future. *Trends in Cognitive Sciences*, *18*(9), 480-487. https://doi.org/10.1016/j.tics.2014.04.003

He, Y., & Evans, A. (2010). Graph theoretical modeling of brain connectivity. *Current Opinion in Neurology*, *23*(4), 341-350.

Helfrich, R. F., Breska, A., & Knight, R. T. (2019). Neural entrainment and network resonance in support of top-down guided attention. *Current Opinion in Psychology*, *29*, 82-89. https://doi.org/10.1016/j.copsyc.2018.12.016

Helfrich, R. F., Fiebelkorn, I. C., Szczepanski, S. M., Lin, J. J., Parvizi, J., Knight, R. T., & Kastner, S. (2018). Neural Mechanisms of Sustained Attention Are Rhythmic. *Neuron*, *99*(4), 854-865.e5. https://doi.org/10.1016/j.neuron.2018.07.032

Hendry, A., Greenhalgh, I., Bailey, R., Fiske, A., Dvergsdal, H., & Holmboe, K. (2021). Development of directed global inhibition, competitive inhibition and behavioural inhibition during the transition between infancy and toddlerhood. *Developmental Science*. https://doi.org/10.1111/desc.13193

Hendry, A., Johnson, M. H., & Holmboe, K. (2019). Early Development of Visual Attention: Change, Stability, and Longitudinal Associations. *Annual Review of Developmental Psychology*, *1*(1), 251-275. https://doi.org/10.1146/annurev-devpsych-121318-085114

Hendry, A., Jones, E. J. H., & Charman, T. (2016). Executive function in the first three years of life: Precursors, predictors and patterns. *Developmental Review*, *42*, 1-33. https://doi.org/10.1016/j.dr.2016.06.005

References

Henry, T. R., & Cohen, J. R. (2019). Chapter 5—Dysfunctional brain network organization in neurodevelopmental disorders. En B. C. Munsell, G. Wu, L. Bonilha, & P. J. Laurienti (Eds.), *Connectomics* (pp. 83-100). Academic Press. https://doi.org/10.1016/B978-0-12-813838-0.00005-4

Herweg, N. A., Solomon, E. A., & Kahana, M. J. (2020). Theta Oscillations in Human Memory. *Trends in Cognitive Sciences*, *24*(3), 208-227. https://doi.org/10.1016/j.tics.2019.12.006

Heuvel, M. P., & Sporns, O. (2013). Network hubs in the human brain. *Trends in Cognitive Sciences*, *17*(12), 683-696.

Heuvel, M. I. van den, Turk, E., Manning, J. H., Hect, J., Hernandez-Andrade, E., Hassan, S. S., Romero, R., van den Heuvel, M. P, & Thomason, M. E. (2018). Hubs in the human fetal brain network. *Developmental Cognitive Neuroscience*, *30*. https://doi.org/10.1016/j.dcn.2018.02.001

Hilger, K., Ekman, M., Fiebach, C. J., & Basten, U. (2017a). Efficient hubs in the intelligent brain: Nodal efficiency of hub regions in the salience network is associated with general intelligence. *Intelligence*, *60*, 10-25. https://doi.org/10.1016/j.intell.2016.11.001

Hilger, K., Ekman, M., Fiebach, C. J., & Basten, U. (2017b). Intelligence is associated with the modular structure of intrinsic brain networks. *Scientific Reports*, *7*(1). https://doi.org/10.1038/s41598-017-15795-7

Hill, A. T., Clark, G. M., Bigelow, F. J., Lum, J. A. G., & Enticott, P. G. (2022). Periodic and aperiodic neural activity displays age-dependent changes across early-to-middle childhood. *Developmental Cognitive Neuroscience*, *54*, 101076. https://doi.org/10.1016/j.dcn.2022.101076

Hofstee, M., Huijding, J., Cuevas, K., & Deković, M. (2022). Self-regulation and frontal EEG alpha activity during infancy and early childhood: A multilevel meta-analysis. *Developmental Science*, *25*(6), e13298. https://doi.org/10.1111/desc.13298

Holmboe, K., Bonneville-Roussy, A., Csibra, G., & Johnson, M. H. (2018). Longitudinal development of attention and inhibitory control during the first year of life. *Developmental Science*, *21*(6). https://doi.org/10.1111/desc.12690

Holmboe, K., Fearon, R. M. P., Csibra, G., Tucker, L. A., & Johnson, M. H. (2008). Freeze-Frame: A new infant inhibition task and its relation to frontal cortex tasks during infancy and early childhood. *Journal of*

Experimental Child Psychology, *100*(2), 89-114. https://doi.org/10.1016/j.jecp.2007.09.004

Holmboe, K., Larkman, C., de Klerk, C., Simpson, A., Bell, M. A., Patton, L., Christodoulou, C., & Dvergsdal, H. (2021). The early childhood inhibitory touchscreen task: A new measure of response inhibition in toddlerhood and across the lifespan. *PLOS ONE*, *16*(12), e0260695. https://doi.org/10.1371/journal.pone.0260695

Honey, C. J., Sporns, O., Cammoun, L., Gigandet, X., Thiran, J. P., Meuli, R., & Hagmann, P. (2009). Predicting human resting-state functional connectivity from structural connectivity. *Proceedings of the National Academy of Sciences*, *106*(6), 2035-2040.

Hongwanishkul, D., Happaney, K. R., Lee, W. S. C., Zelazo, P. D., Wendy, S., Lee, C., & Lee, S. C. (2005). Developmental Neuropsychology Assessment of Hot and Cool Executive Function in Young Children: Age-Related Changes and Individual Differences. *Developmental Neuropsychology*, *28*(2), 617-644. https://doi.org/10.1207/s15326942dn2802

Howard, S. J., & Melhuish, E. (2017). An Early Years Toolbox for Assessing Early Executive Function, Language, Self-Regulation, and Social Development: Validity, Reliability, and Preliminary Norms. *Journal of Psychoeducational Assessment*, *35*(3), 255-275. https://doi.org/10.1177/0734282916633009

Hu, D. K., Goetz, P. W., To, P. D., Garner, C., Magers, A. L., Skora, C., Tran, N., Yuen, T., Hussain, S. A., Shrey, D. W., & Lopour, B. A. (2022). Evolution of Cortical Functional Networks in Healthy Infants. *Frontiers in Network Physiology*, *2*, 893826. https://doi.org/10.3389/fnetp.2022.893826

Hughes, C., & Ensor, R. (2005). Executive Function and Theory of Mind in 2 Year Olds: A Family Affair? *Developmental Neuropsychology*, *28*(2), 645-668. https://doi.org/10.1207/s15326942dn2802_5

Hwang, K., Hallquist, M. N., & Luna, B. (2013). The development of hub architecture in the human functional brain network. *Cerebral Cortex*, *23*(10), 2380-2393. https://doi.org/10.1093/cercor/bhs227

Immink, M. A., Cross, Z. R., Chatburn, A., Baumeister, J., Schlesewsky, M., & Bornkessel-Schlesewsky, I. (2021). Resting-state aperiodic neural dynamics predict individual differences in visuomotor performance

and learning. *Human Movement Science*, *78*. https://doi.org/10.1016/j.humov.2021.102829

Ito, S., Stuphorn, V., Brown, J. W., & Schall, J. D. (2003). Performance Monitoring by the Anterior Cingulate Cortex During Saccade Countermanding. *Science*, *302*(5642), 120-122. https://doi.org/10.1126/science.1087847

Jahangiri, M., Kazemnejad, A., Goldfeld, K. S., Daneshpour, M. S., Mostafaei, S., Khalili, D., Moghadas, M. R., & Akbarzadeh, M. (2023). A wide range of missing imputation approaches in longitudinal data: A simulation study and real data analysis. *BMC Medical Research Methodology*, *23*(1), 161. https://doi.org/10.1186/s12874-023-01968-8

Jensen, O., & Mazaheri, A. (2010). Shaping Functional Architecture by Oscillatory Alpha Activity: Gating by Inhibition. *Frontiers in Human Neuroscience*, *4*. https://doi.org/10.3389/fnhum.2010.00186

Jentzsch, I., & Dudschig, C. (2009). Short Article: Why do we slow down after an error? Mechanisms underlying the effects of posterror slowing. *Quarterly Journal of Experimental Psychology*, *62*(2), 209-218. https://doi.org/10.1080/17470210802240655

Jing, H., Gilchrist, J. M., Badger, T. M., & Pivik, R. T. (2010). A longitudinal study of differences in electroencephalographic activity among breastfed, milk formula-fed, and soy formula-fed infants during the first year of life. *Early Human Development*, *86*(2), 119-125. https://doi.org/10.1016/j.earlhumdev.2010.02.001

Johansson, M., Forssman, L., & Bohlin, G. (2014). Individual differences in 10-month-olds' performance on the A-not-B task. *Scandinavian Journal of Psychology*, *55*(2), 130-135.

Johansson, M., Marciszko, C., Brocki, K., & Bohlin, G. (2016). Individual Differences in Early Executive Functions: A Longitudinal Study from 12 to 36 Months. *Infant and Child Development*, *25*(6), 533-549. https://doi.org/10.1002/icd.1952

Johnson, A., Bathelt, J., Akarca, D., & Astle, D. E. (2021). Far and wide: Associations between childhood socio-economic status and brain connectomics. *Developmental Cognitive Neuroscience*, *48*. https://doi.org/10.1016/j.dcn.2020.100888

References

Johnson, E. L., Yin, Q., O'Hara, N. B., Tang, L., Jeong, J. W., Asano, E., & Ofen, N. (2022). Dissociable oscillatory theta signatures of memory formation in the developing brain. *Current Biology*, *32*(7), 1457-1469.

Johnson, M. H. (2011). Interactive Specialization: A domain-general framework for human functional brain development? *Developmental Cognitive Neuroscience*, *1*(1), 7-21. https://doi.org/10.1016/j.dcn.2010.07.003

Johnson, M. H., & Haan, M. (2015). *Developmental Cognitive Neuroscience* (4th ed.). Wiley Blackwell.

Johnson, M. H., Posner, M. I., & Rothbart, M. K. (1991). Components of visual orienting in early infancy: Contingency learning, anticipatory looking, and disengaging. *Journal of Cognitive Neuroscience*, *3*(4), 335-344. https://doi.org/10.1162/jocn.1991.3.4.335

Johnson, S. B., Riis, J. L., & Noble, K. G. (2016). State of the art review: Poverty and the developing brain. *Pediatrics*, *137*(4). https://doi.org/10.1542/peds.2015-3075

Johnstone, S. J., Pleffer, C. B., Barry, R. J., Clarke, A. R., & Smith, J. L. (2005). Development of Inhibitory Processing During the Go/NoGo Task. *Journal of Psychophysiology*, *19*(1), 11-23. https://doi.org/10.1027/0269-8803.19.1.11

Jones, E. J. H., Goodwin, A., Orekhova, E., Charman, T., Dawson, G., Webb, S. J., & Johnson, M. H. (2020). Infant EEG theta modulation predicts childhood intelligence. *Sci. Rep*, *101*(10), 1-10. https://doi.org/10.1038/s41598-020-67687-y

Jones, L. B., Rothbart, M. K., & Posner, M. I. (2003). Development of executive attention in preschool children. *Developmental Science*, *6*(5), 498-504. https://doi.org/10.1111/1467-7687.00307

Jones, S. R. (2016). When brain rhythms aren't 'rhythmic': Implication for their mechanisms and meaning. *Current Opinion in Neurobiology*, *40*, 72-80. https://doi.org/10.1016/j.conb.2016.06.010

Jung, R. E., & Haier, R. J. (2007). The Parieto-Frontal Integration Theory (P-FIT) of intelligence: Converging neuroimaging evidence. *Behavioral and Brain Sciences*, *30*(2), 135-154. https://doi.org/10.1017/S0140525X07001185

Kam, J. W. Y., Lin, J. J., Solbakk, A.-K., Endestad, T., Larsson, P. G., & Knight, R. T. (2019). Default network and frontoparietal control network theta

connectivity supports internal attention. *Nature Human Behaviour*, *3*(12), 1263-1270. https://doi.org/10.1038/s41562-019-0717-0

Karalunas, S. L., Ostlund, B. D., Alperin, B. R., Figuracion, M., Gustaffson, H., Deming, E. M., Foti, D., Antovich, D., Dude, J., Nigg, J., & Sullivan, E. (2021). Aperiodic exponent of the EEG power spectrum can be reliably measured in early development and predicts ADHD risk. *Dev. Psychobiol*. https://doi.org/10.1002/dev.22228

Karama, S., Colom, R., Johnson, W., Deary, I. J., Haier, R., Waber, D. P., Lepage, C., Ganjavi, H., Jung, R., & Evans, A. C. (2011). Cortical thickness correlates of specific cognitive performance accounted for by the general factor of intelligence in healthy children aged 6 to 18. *NeuroImage*, *55*(4), 1443-1453. https://doi.org/10.1016/j.neuroimage.2011.01.016

Kavčič, A., Demšar, J., Georgiev, D., Bon, J., & Soltirovska-Šalamon, A. (2023). Age related changes and sex related differences of functional brain networks in childhood: A high-density EEG study. *Clinical Neurophysiology*, *150*, 216-226. https://doi.org/10.1016/j.clinph.2023.03.357

Keller, A. S., Pines, A. R., Shanmugan, S., Sydnor, V. J., Cui, Z., Bertolero, M. A., Barzilay, R., Alexander-Bloch, A. F., Byington, N., Chen, A., Conan, G. M., Davatzikos, C., Feczko, E., Hendrickson, T. J., Houghton, A., Larsen, B., Li, H., Miranda-Dominguez, O., Roalf, D. R., … Satterthwaite, T. D. (2023). Personalized functional brain network topography is associated with individual differences in youth cognition. *Nature Communications*, *14*(1), 8411. https://doi.org/10.1038/s41467-023-44087-0

Keller, A. S., Sydnor, V. J., Pines, A., Fair, D. A., Bassett, D. S., & Satterthwaite, T. D. (2022). Hierarchical functional system development supports executive function. En *Trends in Cognitive Sciences*.

Klimesch, W. (1999). EEG alpha and theta oscillations reflect cognitive and memory performance: A review and analysis. *Brain Research Reviews*, *29*(2-3), 169-195. https://doi.org/10.1016/S0165-0173(98)00056-3

Klimesch, W. (2012). Alpha-band oscillations, attention, and controlled access to stored information. *Trends in Cognitive Sciences*, *16*(12), 606-617. https://doi.org/10.1016/j.tics.2012.10.007

References

Klimesch, W., Sauseng, P., & Hanslmayr, S. (2007). EEG alpha oscillations: The inhibition–timing hypothesis. *Brain Research Reviews*, *53*(1), 63-88.

Kloo, D., & Sodian, B. (2017). The developmental stability of inhibition from 2 to 5 years. *British Journal of Developmental Psychology*, *35*(4), 582-595. https://doi.org/10.1111/bjdp.12197

Knickmeyer, R. C. (2008). A structural MRI study of human brain development from birth to 2 years. *J. Neurosci*, *28*, 12176-12182.

Knyazev, G. G., Savostyanov, A. N., Bocharov, A. V., Slobodskaya, H. R., Bairova, N. B., Tamozhnikov, S. S., & Stepanova, V. V. (2017). Effortful control and resting state networks: A longitudinal EEG study. *Neuroscience*, *346*, 365-381. https://doi.org/10.1016/j.neuroscience.2017.01.031

Koch, I., Frings, C., & Schuch, S. (2018). Explaining response-repetition effects in task switching: Evidence from switching cue modality suggests episodic binding and response inhibition. *Psychological Research*, *82*(3), 570-579. https://doi.org/10.1007/s00426-017-0847-9

Kochanska, G., Murray, K. T., & Harlan, E. T. (2000). Effortful control in early childhood: Continuity and change, antecedents, and implications for social development. *Developmental Psychology*, *36*(2), 220-232. https://doi.org/10.1037/0012-1649.36.2.220

Konrad, K., & Eickhoff, S. B. (2010). Is the ADHD brain wired differently? A review on structural and functional connectivity in attention deficit hyperactivity disorder. *Human Brain Mapping*, *31*(6), 904-916. https://doi.org/10.1002/hbm.21058

Köster, M., Brzozowska, A., Bánki, A., Tünte, M., Ward, E. K., & Hoehl, S. (2023). Rhythmic visual stimulation as a window into early brain development: A systematic review. *Developmental Cognitive Neuroscience*, *64*, 101315. https://doi.org/10.1016/j.dcn.2023.101315

Köster, M., & Gruber, T. (2022). Rhythms of human attention and memory: An embedded process perspective. *Frontiers in Human Neuroscience*, *16*, 905837. https://doi.org/10.3389/fnhum.2022.905837

Köster, M., Langeloh, M., & Hoehl, S. (2019). Visually entrained theta oscillations increase for unexpected events in the infant brain. *Psychological Science*, *30*(11), 1656-1663.

References

Köster, M., Langeloh, M., Michel, C., & Hoehl, S. (2021). Young infants process prediction errors at the theta rhythm. *NeuroImage*, *236*, 118074.

Kovacs, A. M., & Mehler, J. (2009). Cognitive gains in 7-month-old bilingual infants. *Proceedings of the National Academy of Sciences*, *106*(16), 6556-6560. https://doi.org/10.1073/pnas.0811323106

Krienen, F. M., Yeo, B. T. T., & Buckner, R. L. (2014). Reconfigurable task-dependent functional coupling modes cluster around a core functional architecture. *Philosophical Transactions of the Royal Society B: Biological Sciences*, *369*(1653), 20130526. https://doi.org/10.1098/rstb.2013.0526

Kruschwitz, J. D., Waller, L., Daedelow, L. S., Walter, H., & Veer, I. M. (2018). General, crystallized and fluid intelligence are not associated with functional global network efficiency: A replication study with the human connectome project 1200 data set. *NeuroImage*, *171*, 323-331. https://doi.org/10.1016/j.neuroimage.2018.01.018

Kwon, M.-K., Setoodehnia, M., Baek, J., Luck, S. J., & Oakes, L. M. (2016). The development of visual search in infancy: Attention to faces versus salience. *Developmental Psychology*, *52*(4), 537-555. https://doi.org/10.1037/dev0000080

Lakatos, P., Gross, J., & Thut, G. (2019). A New Unifying Account of the Roles of Neuronal Entrainment. *Current Biology*, *29*(18), R890-R905. https://doi.org/10.1016/j.cub.2019.07.075

Lakatos, P., Karmos, G., Mehta, A. D., Ulbert, I., & Schroeder, C. E. (2008). Entrainment of Neuronal Oscillations as a Mechanism of Attentional Selection. *Science*, *320*(5872), 110-113. https://doi.org/10.1126/science.1154735

Lammertink, F., Heuvel, M. P., Hermans, E. J., Dudink, J., Tataranno, M. L., Benders, M. J., & Vinkers, C. H. (2022). Early-life stress exposure and large-scale covariance brain networks in extremely preterm-born infants. *Translational Psychiatry*, *12*(1), 256.

Langer, N., Pedroni, A., Gianotti, L. R. R., Hänggi, J., Knoch, D., & Jäncke, L. (2012). Functional brain network efficiency predicts intelligence. *Human Brain Mapping*, *33*(6), 1393-1406. https://doi.org/10.1002/hbm.21297

References

Langeslag, S. J. E., Schmidt, M., Ghassabian, A., Jaddoe, V. W., Hofman, A., Lugt, A. V. D., Verhulst, F. C., Tiemeier, H., & White, T. J. H. (2013). *Functional Connectivity between Parietal and Frontal Brain Regions and Intelligence in Young Children: The Generation R Study*. *3307*, 3299-3307. https://doi.org/10.1002/hbm.22143

Larsson, H., Chang, Z., D'Onofrio, B. M., & Lichtenstein, P. (2014). The heritability of clinically diagnosed attention deficit hyperactivity disorder across the lifespan. *Psychological Medicine*, *44*(10), 2223-2229. https://doi.org/10.1017/S0033291713002493

Latora, V., & Marchiori, M. (2001). Efficient behavior of small-world networks. *Physical Review Letters*, *87*(19), 198701.

Lawson, K. R., & Ruff, H. A. (2004). Early attention and negative emotionality predict later cognitive and behaviournal function. *International Journal of Behavioral Development*, *28*(2), 157-165. https://doi.org/10.1080/01650250344000361

Leach, S. C., Morales, S., Bowers, M. E., Buzzell, G. A., Debnath, R., Beall, D., & Fox, N. A. (2020). Adjusting ADJUST: Optimizing the ADJUST algorithm for pediatric data using geodesic nets. *Psychophysiology*, *57*(8). https://doi.org/10.1111/psyp.13566

Leno, V. C., Pickles, A., Noordt, S., Huberty, S., Desjardins, J., Webb, S. J., & Team, B. A. S. I. S. (2021). 12-Month peak alpha frequency is a correlate but not a longitudinal predictor of non-verbal cognitive abilities in infants at low and high risk for autism spectrum disorder. *Developmental Cognitive Neuroscience*, *48*, 100938.

Lin, P., Sun, J., Yu, G., Wu, Y., Yang, Y., Liang, M., & Liu, X. (2014). Global and local brain network reorganization in attention-deficit/hyperactivity disorder. *Brain Imaging and Behavior*, *8*(4), 558-569. https://doi.org/10.1007/s11682-013-9279-3

Lo, S. L. (2018). A meta-analytic review of the event-related potentials (ERN and N2) in childhood and adolescence: Providing a developmental perspective on the conflict monitoring theory. *Developmental Review*, *48*(November 2016), 82-112. https://doi.org/10.1016/j.dr.2018.03.005

Logan, G. D., & Cowan, W. B. (1984). *On the Ability to Inhibit Thought and Action: A Theory of an Act of Control*.

Lüdecke, D., Ben-Shachar, M., Patil, I., Waggoner, P., & Makowski, D. (2021). performance: An R Package for Assessment, Comparison and Testing

of Statistical Models. *Journal of Open Source Software*, *6*(60), 3139. https://doi.org/10.21105/joss.03139

Lui, K. Y., Hendry, A., Fiske, A., Dvergsdal, H., & Holmboe, K. (2021). Associations between touchscreen exposure and hot and cool inhibitory control in 10-month-old infants. *Infant Behavior and Development*, *65*, 101649.

Lundqvist, M., Rose, J., Herman, P., Brincat, S. L., Buschman, T. J., & Miller, E. K. (2016). Gamma and beta bursts underlie working memory. *Neuron*, *90*(1), 152-164.

MacNeill, L. A., Ram, N., Bell, M. A., Fox, N. A., & Pérez-Edgar, K. (2018). Trajectories of Infants' Biobehavioral Development: Timing and Rate of A-Not-B Performance Gains and EEG Maturation. *Child Development*, *89*(3), 711-724. https://doi.org/10.1111/cdev.13022

Maguire, M. J., & Schneider, J. M. (2019). Socioeconomic status related differences in resting state EEG activity correspond to differences in vocabulary and working memory in grade school. *Brain and Cognition*. https://doi.org/10.1016/j.bandc.2019.103619

Marcovitch, S., Clearfield, M. W., Swingler, M., Calkins, S. D., & Bell, M. A. (2016). Attentional Predictors of 5-month-olds' Performance on a Looking A-not-B Task. *Infant and Child Development*, *25*(4), 233-246. https://doi.org/10.1002/icd.1931

Marcovitch, S., & Zelazo, P. D. (1999). The A-Not-B Error: Results from a Logistic Meta-Analysis. *Child Development*, *70*(6), 1297-1313. https://doi.org/10.1111/1467-8624.00095

Marek, S., & Dosenbach, N. U. F. (2018). The frontoparietal network: Function, electrophysiology, and importance of individual precision mapping. *Dialogues in Clinical Neuroscience*, *20*(2), 133-140. https://doi.org/10.31887/DCNS.2018.20.2/smarek

Marek, S., Hwang, K., Foran, W., Hallquist, M. N., & Luna, B. (2015). The Contribution of Network Organization and Integration to the Development of Cognitive Control. *PLoS Biology*, *13*(12). https://doi.org/10.1371/journal.pbio.1002328

Markant, J., & Amso, D. (2016). The Development of Selective Attention Orienting is an Agent of Change in Learning and Memory Efficacy. *Infancy*, *21*(2), 154-176. https://doi.org/10.1111/infa.12100

References

Marshall, P. J., Bar-Haim, Y., & Fox, N. A. (2002). Development of the EEG from 5 months to 4 years of age. *Clinical Neurophysiology*, *113*(8), 1199-1208. https://doi.org/10.1016/S1388-2457(02)00163-3

Marshall, P. J., & Fox, N. A. (2004). A comparison of the electroencephalogram between institutionalized and community children in Romania. *Journal of Cognitive Neuroscience*, *16*(8), 1327-1338.

Matta, T. H., Flournoy, J. C., & Byrne, M. L. (2018). Making an unknown unknown a known unknown: Missing data in longitudinal neuroimaging studies. *Developmental Cognitive Neuroscience*, *33*, 83-98. https://doi.org/10.1016/j.dcn.2017.10.001

McSweeney, M., Morales, S., Valadez, E. A., Buzzell, G. A., & Fox, N. A. (2021). Longitudinal age- and sex-related change in background aperiodic activity during early adolescence. *Developmental Cognitive Neuroscience*, *52*, 101035. https://doi.org/10.1016/j.dcn.2021.101035

Mehnert, J., Akhrif, A., Telkemeyer, S., Rossi, S., Schmitz, C. H., Steinbrink, J., Wartenburger, I., Obrig, H., & Neufang, S. (2013). Developmental changes in brain activation and functional connectivity during response inhibition in the early childhood brain. *Brain and Development*, *35*(10), 894-904. https://doi.org/10.1016/j.braindev.2012.11.006

Mierau, A., Klimesch, W., & Lefebvre, J. (2017). State-dependent alpha peak frequency shifts: Experimental evidence, potential mechanisms and functional implications. *Neuroscience*, *360*, 146-154. https://doi.org/10.1016/j.neuroscience.2017.07.037

Miller, D. J. (2012). Prolonged myelination in human neocortical evolution. *Proc. Natl Acad. Sci. USA*, *109*, 16480-16485.

Miller, K. J., Sorensen, L. B., Ojemann, J. G., & Den Nijs, M. (2009). Power-Law Scaling in the Brain Surface Electric Potential. *PLoS Computational Biology*, *5*(12), e1000609. https://doi.org/10.1371/journal.pcbi.1000609

Miller, S. E., & Marcovitch, S. (2015). Examining executive function in the second year of life: Coherence, stability, and relations to joint attention and language. *Developmental Psychology*, *51*(1), 101-114. https://doi.org/10.1037/a0038359

References

Miskovic, V., Ma, X., Chou, C. A., Fan, M., Owens, M., Sayama, H., & Gibb, B. E. (2015). Developmental changes in spontaneous electrocortical activity and network organization from early to late childhood. *NeuroImage*, *118*, 237-247. https://doi.org/10.1016/j.neuroimage.2015.06.013

Mitra, A., Snyder, A. Z., Tagliazucchi, E., Laufs, H., Elison, J., Emerson, R. W., Shen, M. D., Wolff, J. J., Botteron, K. N., Dager, S., Estes, A. M., Evans, A. C., Gerig, G., Hazlett, H. C., Paterson, S. J., Schultz, R. T., Styner, M. A., Zwaigenbaum, L., Chappell, C., … Raichle, M. (2017). Resting-state fMRI in sleeping infants more closely resembles adult sleep than adult wakefulness. *PLoS ONE*, *12*(11). https://doi.org/10.1371/journal.pone.0188122

Miyake, A., & Friedman, N. P. (2012). The nature and organization of individual differences in executive functions: Four general conclusions. *Current Directions in Psychological Science*, *21*(1), 8-14.

Moffitt, T. E., Arseneault, L., Belsky, D., Dickson, N., Hancox, R. J., Harrington, H., Houts, R., Poulton, R., Roberts, B. W., Ross, S., Sears, M. R., Thomson, W. M., & Caspi, A. (2011). A gradient of childhood self-control predicts health, wealth, and public safety. *Proceedings of the National Academy of Sciences of the United States of America*, *108*(7), 2693-2698. https://doi.org/10.1073/pnas.1010076108

Morasch, K. C., & Bell, M. A. (2011). The role of inhibitory control in behavioral and physiological expressions of toddler executive function. *Journal of Experimental Child Psychology*, *108*(3), 593-606.

Moyano, S., Conejero, Á., Fernández, M., Serrano, F., & Rueda, M. R. (2022). Development of visual attention control in early childhood: Associations with temperament and home environment. *Frontiers in Psychology*, *13*. https://doi.org/10.3389/fpsyg.2022.1069478

Moyano, S., Rico-Picó, J., Conejero, Á., Hoyo, Á., Ballesteros-Duperón, M. D. L. Á., & Rueda, M. R. (2023). Influence of the environment on the early development of attentional control. *Infant Behavior and Development*, *71*, 101842. https://doi.org/10.1016/j.infbeh.2023.101842

Muldoon, S. F., Bridgeford, E. W., & Bassett, D. S. (2016). Small-world propensity and weighted brain networks. *Scientific Reports*, *6*(1), 22057.

References

Munakata, Y., Snyder, H. R., & Chatham, C. H. (2012). Developing Cognitive Control: Three Key Transitions. *Current Directions in Psychological Science*, *21*(2), 71-77. https://doi.org/10.1177/0963721412436807

Musso, M. F., Cómbita, L. M., Cascallar, E. C., & Rueda, M. R. (2022). Modeling the Contribution of Genetic Variation to Cognitive Gains Following Training with a Machine Learning Approach. *Mind, Brain, and Education*, *16*(4), 300-317. https://doi.org/10.1111/mbe.12336

Muthukrishnan, S. P., Soni, S., & Sharma, R. (2020). Brain Networks Communicate Through Theta Oscillations to Encode High Load in a Visuospatial Working Memory Task: An EEG Connectivity Study. *Brain Topography*, *33*(1), 75-85. https://doi.org/10.1007/s10548-019-00739-3

Nakagawa, A., & Sukigara, M. (2013). Individual differences in disengagement of fixation and temperament: Longitudinal research on toddlers. *Infant Behavior and Development*, *36*(4), 728-735. https://doi.org/10.1016/j.infbeh.2013.08.001

Nakagawa, A., & Sukigara, M. (2019). Early development of attentional disengagement and phasic alertness. *Infant Behavior and Development*. https://doi.org/10.1016/j.infbeh.2019.02.004

Nakagawa, S., Johnson, P. C., & Schielzeth, H. (2017). The coefficient of determination R2 and intra-class correlation coefficient from generalized linear mixed-effects models revisited and expanded. *Journal of the Royal Society Interface*, *14*(134), 20170213. https://doi.org/10.1098/rsif.2017.0213

Newman, M. E. (2006). Modularity and community structure in networks. *Proceedings of the National Academy of Sciences*, *103*(23), 8577-8582.

Nguyen, T., Reisner, S., Lueger, A., Wass, S. V., Hoehl, S., & Markova, G. (2023). Sing to me, baby: Infants show neural tracking and rhythmic movements to live and dynamic maternal singing. *Developmental Cognitive Neuroscience*, *64*, 101313. https://doi.org/10.1016/j.dcn.2023.101313

Nitzl, C., Roldan, J. L., & Cepeda, G. (2016). Mediation analysis in partial least squares path modeling: Helping researchers discuss more sophisticated models. *Industrial Management & Data Systems*, *116*(9), 1849-1864. https://doi.org/10.1108/IMDS-07-2015-0302

References

Noble, K. G., Houston, S. M., Kan, E., & Sowell, E. R. (2012). Neural correlates of socioeconomic status in the developing human brain. *Developmental Science*, *15*(4), 516-527. https://doi.org/10.1111/j.1467-7687.2012.01147.x

Nolan, H., Whelan, R., & Reilly, R. B. (2010). FASTER: Fully Automated Statistical Thresholding for EEG artifact Rejection. *Journal of Neuroscience Methods*, *192*(1), 152-162. https://doi.org/10.1016/j.jneumeth.2010.07.015

Nolte, G., Bai, O., Wheaton, L., Mari, Z., Vorbach, S., & Hallett, M. (2004). Identifying true brain interaction from EEG data using the imaginary part of coherency. *Clinical Neurophysiology*, *115*(10), 2292-2307.

Norcia, A. M., & Tyler, C. W. (1984). Temporal frequency limits for stereoscopic apparent motion processes. *Vision Research*, *24*(5), 395-401. https://doi.org/10.1016/0042-6989(84)90037-3

Norcia, A. M., Tyler, C. W., & Homer, R. D. (1978). *High Visual Contrast Sensitivity in the Young Human Infant*. *1*.

Obleser, J., & Kayser, C. (2019). Neural Entrainment and Attentional Selection in the Listening Brain. *Trends in Cognitive Sciences*, *23*(11), 913-926. https://doi.org/10.1016/j.tics.2019.08.004

Oehrn, C. R., Hanslmayr, S., Fell, J., Deuker, L., Kremers, N. A., Do Lam, A. T., Elger, C. E., & Axmacher, N. (2014). Neural Communication Patterns Underlying Conflict Detection, Resolution, and Adaptation. *Journal of Neuroscience*, *34*(31), 10438-10452. https://doi.org/10.1523/JNEUROSCI.3099-13.2014

Oldham, S., & Fornito, A. (2019). The development of brain network hubs. *Developmental Cognitive Neuroscience*, *36*, 100607. https://doi.org/10.1016/j.dcn.2018.12.005

Omidvarnia, A., Fransson, P., Metsäranta, M., & Vanhatalo, S. (2014). Functional bimodality in the brain networks of preterm and term human newborns. *Cerebral Cortex*, *24*(10), 2657-2668. https://doi.org/10.1093/cercor/bht120

Oostenveld, R., Fries, P., Maris, E., & Schoffelen, J.-M. (2011). FieldTrip: Open Source Software for Advanced Analysis of MEG, EEG, and Invasive Electrophysiological Data. *Computational Intelligence and Neuroscience*, *2011*, 1-9. https://doi.org/10.1155/2011/156869

References

Orekhova, E. V., Stroganova, T. A., & Posikera, I. N. (1999). Theta synchronization during sustained anticipatory attention in infants over the second half of the first year of life. *International Journal of Psychophysiology*, *32*(2), 151-172. https://doi.org/10.1016/S0167-8760(99)00011-2

Orekhova, E. V., Stroganova, T. A., & Posikera, I. N. (2001). Alpha activity as an index of cortical inhibition during sustained internally controlled attention in infants. *Clinical Neurophysiology*. https://doi.org/10.1016/S1388-2457(01)00502-8

Orekhova, E. V., Stroganova, T. A., Posikera, I. N., & Elam, M. (2006). EEG theta rhythm in infants and preschool children. *Clinical Neurophysiology*. https://doi.org/10.1016/j.clinph.2005.12.027

Ostlund, B. D., Alperin, B. R., Drew, T., & Karalunas, S. L. (2021). Behavioral and cognitive correlates of the aperiodic (1/f-like) exponent of the EEG power spectrum in adolescents with and without ADHD. *Dev. Cogn. Neurosci*, *48*, 100931. https://doi.org/10.1016/J.DCN.2021.100931

Ostlund, B., Donoghue, T., Anaya, B., Gunther, K. E., Karalunas, S. L., Voytek, B., & Pérez-Edgar, K. E. (2022). Spectral parameterization for studying neurodevelopment: How and why. *Developmental Cognitive Neuroscience*, *54*, 101073. https://doi.org/10.1016/j.dcn.2022.101073

Otero, G. A. (1997). Poverty, cultural disadvantage and brain development: A study of pre-school children in Mexico Q. En *Electroencephalography and clinical Neurophysiology* (Vol. 102, pp. 512-516).

Otero, G. A., Pliego-Rivero, F. B., Fernández, T., & Ricardo, J. (2003). EEG development in children with sociocultural disadvantages: A follow-up study. *Clinical Neurophysiology*, *114*(10), 1918-1925. https://doi.org/10.1016/S1388-2457(03)00173-1

Ouyang, M., Dubois, J., Yu, Q., Mukherjee, P., & Huang, H. (2019). Delineation of early brain development from fetuses to infants with diffusion MRI and beyond. *NeuroImage*, *185*, 836-850. https://doi.org/10.1016/j.neuroimage.2018.04.017

Paavonen, E. J., Saarenpää-Heikkilä, O., Morales-Munoz, I., Virta, M., Häkälä, N., Pölkki, P., Kylliäinen, A., Karlsson, H., Paunio, T., & Karlsson, L. (2020). Normal sleep development in infants: Findings from two large birth cohorts. *Sleep Medicine*, *69*, 145-154. https://doi.org/10.1016/j.sleep.2020.01.009

References

Palva, S., & Palva, J. M. (2011). Functional Roles of Alpha-Band Phase Synchronization in Local and Large-Scale Cortical Networks. *Frontiers in Psychology*, *2*. https://doi.org/10.3389/fpsyg.2011.00204

Pamplona, G. S. P., Santos Neto, G. S., Rosset, S. R. E., Rogers, B. P., & Salmon, C. E. G. (2015). Analyzing the association between functional connectivity of the brain and intellectual performance. *Frontiers in Human Neuroscience*, *9*. https://doi.org/10.3389/fnhum.2015.00061

Papageorgiou, K. A., Smith, T. J., Wu, R., Johnson, M. H., Kirkham, N. Z., & Ronald, A. (2014). Individual Differences in Infant Fixation Duration Relate to Attention and Behavioral Control in Childhood. *Psychological Science*, *25*(7), 1371-1379. https://doi.org/10.1177/0956797614531295

Pathania, A., Euler, M. J., Clark, M., Cowan, R. L., Duff, K., & Lohse, K. R. (2022). Resting EEG spectral slopes are associated with age-related differences in information processing speed. *Biological Psychology*, *168*, 108261. https://doi.org/10.1016/j.biopsycho.2022.108261

Perica, M. I., Calabro, F. J., Larsen, B., Foran, W., Yushmanov, V. E., Hetherington, H., Tervo-Clemmens, B., Moon, C.-H., & Luna, B. (2022). Development of frontal GABA and glutamate supports excitation/inhibition balance from adolescence into adulthood. *Progress in Neurobiology*, *219*, 102370. https://doi.org/10.1016/j.pneurobio.2022.102370

Perone, S., & Gartstein, M. A. (2019). Mapping cortical rhythms to infant behavioral tendencies via baseline EEG and parent-report. *Developmental Psychobiology*, *61*(6), 815-823. https://doi.org/10.1002/dev.21867

Perone, S., Palanisamy, J., & Carlson, S. M. (2018). Age-related change in brain rhythms from early to middle childhood: Links to executive function. *Developmental Science*, *21*(6), 1-15. https://doi.org/10.1111/desc.12691

Petersen, I. T., Hoyniak, C. P., McQuillan, M. E., Bates, J. E., & Staples, A. D. (2016). Measuring the development of inhibitory control: The challenge of heterotypic continuity. *Developmental Review*, *40*, 25-71.

Petersen, S. E., & Posner, M. I. (2012). The attention system of the human brain: 20 years after. *Annual Review of Neuroscience*, *35*(1), 73-89. https://doi.org/10.1146/annurev-neuro-062111-150525

References

Petrill, S. A., Pike, A., Price, T., & Plomin, R. (2004). Chaos in the home and socioeconomic status are associated with cognitive development in early childhood: Environmental mediators identified in a genetic design. *Intelligence*, *32*(5), 445-460. https://doi.org/10.1016/j.intell.2004.06.010

Pierce, L. J., Reilly, E., & Nelson, C. A. (2020). Associations between Maternal Stress, Early Language Behaviors, and Infant Electroencephalography during the First Year of Life. *Journal of Child Language*. https://doi.org/10.1017/S0305000920000501

Pires, L., Leitão, J., Guerrini, C., & Simões, M. R. (2014). Event-Related Brain Potentials in the Study of Inhibition: Cognitive Control, Source Localization and Age-Related Modulations. *Neuropsychology Review*, *24*(4), 461-490. https://doi.org/10.1007/s11065-014-9275-4

Plebanek, D. J., & Sloutsky, V. M. (2019). Selective attention, filtering, and the development of working memory. *Developmental Science*, *22*(1), e12727. https://doi.org/10.1111/desc.12727

Posner, M. I., & Petersen, S. E. (1990). The attention system of the human brain. *Annual Review of Psychology*, *13*, 25-42. https://doi.org/10.1007/s11069-007-9150-1

Posner, M. I., Rothbart, M. K., Sheese, B. E., & Voelker, P. (2014). Developing Attention: Behavioral and Brain Mechanisms. *Advances in Neuroscience*, 1-9. https://doi.org/10.1155/2014/405094

Power, J. D., Fair, D. A., Schlaggar, B. L., & Petersen, S. E. (2010). The Development of Human Functional Brain Networks. *Neuron*, *67*(5), 735-748. https://doi.org/10.1016/j.neuron.2010.08.017

Power, J., IJzendoorn, M., Lewis, A. J., Chen, W., & Galbally, M. (2021). Maternal perinatal depression and child executive function: A systematic review and meta-analysis. *Journal of Affective Disorders*, *291*, 218-234. https://doi.org/10.1016/j.jad.2021.05.003

Qiu, A., Mori, S., & Miller, M. I. (2015). Diffusion Tensor Imaging for Understanding Brain Development in Early Life. *Annual Review of Psychology*, *66*(1). https://doi.org/10.1146/annurev-psych-010814-015340

Quinn, A. J., Van Ede, F., Brookes, M. J., Heideman, S. G., Nowak, M., Seedat, Z. A., Vidaurre, D., Zich, C., Nobre, A. C., & Woolrich, M. W. (2019). Unpacking Transient Event Dynamics in Electrophysiological Power

References

Spectra. *Brain Topography*, *32*(6), 1020-1034. https://doi.org/10.1007/s10548-019-00745-5

R Core Team. (2022). *R: A Language and Environment for Statistical Computing* [Software]. R Foundation for Statistical Computing.

Raja, V. (2021). Resonance and radical embodiment. *Synthese*, *199*(S1), 113-141. https://doi.org/10.1007/s11229-020-02610-6

Rayson, H., Debnath, R., Alavizadeh, S., Fox, N., Ferrari, P. F., & Bonaiuto, J. J. (2022). Detection and analysis of cortical beta bursts in developmental EEG data. *Developmental Cognitive Neuroscience*, *54*, 101069. https://doi.org/10.1016/j.dcn.2022.101069

Rayson, H., Szul, M. J., El-Khoueiry, P., Debnath, R., Gautier-Martins, M., Ferrari, P. F., Fox, N., & Bonaiuto, J. J. (2023). Bursting with Potential: How Sensorimotor Beta Bursts Develop from Infancy to Adulthood. *The Journal of Neuroscience*, *43*(49), 8487-8503. https://doi.org/10.1523/JNEUROSCI.0886-23.2023

Reineberg, A. E., & Banich, M. T. (2016). Functional connectivity at rest is sensitive to individual differences in executive function: A network analysis. *Human Brain Mapping*, *37*(8). https://doi.org/10.1002/hbm.23219

Richards, J. E. (1985). The development of sustained visual attention in infants from 14 to 26 weeks of age. *Psychophysiology*, *22*(4), 409-416. https://doi.org/10.1111/j.1469-8986.1985.tb01625.x

Rico-Picó, J., Hoyo, Á., Guerra, S., Conejero, Á., & Rueda, M. R. (2021). Behavioral and brain dynamics of executive control in relation to children's fluid intelligence. *Intelligence*, *84*, 101513. https://doi.org/10.1016/j.intell.2020.101513

Rico-Picó, J., Moyano, S., Conejero, Á., Hoyo, Á., Ballesteros-Duperón, M. Á., & Rueda, M. R. (2023). Early development of electrophysiological activity: Contribution of periodic and aperiodic components of the EEG signal. *Psychophysiology*, e14360. https://doi.org/10.1111/psyp.14360

Righi, G., Tierney, A. L., Tager-Flusberg, H., & Nelson, C. A. (2014). Functional connectivity in the first year of life in infants at risk for autism spectrum disorder: An EEG study. *PLoS ONE*, *9*(8). https://doi.org/10.1371/journal.pone.0105176

References

Robertson, M. M., Furlong, S., Voytek, B., Donoghue, T., Boettiger, C. A., & Sheridan, M. A. (2019). EEG power spectral slope differs by ADHD status and stimulant medication exposure in early childhood. *Journal of Neurophysiology*, *122*(6), 2427-2437. https://doi.org/10.1152/jn.00388.2019

Robertson, S. S., Watamura, S. E., & Wilbourn, M. P. (2012). Attentional dynamics of infant visual foraging. *Proceedings of the National Academy of Sciences*, *109*(28), 11460-11464. https://doi.org/10.1073/pnas.1203482109

Rohart, F., Gautier, B., Singh, A., & Lê Cao, K.-A. (2017). mixOmics: An R package for 'omics feature selection and multiple data integration. *PLOS Computational Biology*, *13*(11), e1005752. https://doi.org/10.1371/journal.pcbi.1005752

Rothbart, M. K., Ellis, L. K., Rueda, M. R., & Posner, M. I. (2003). Developing Mechanisms of Temperamental Effortful Control. *Journal of Personality*, *71*(6), 1113-1143. https://doi.org/10.1111/1467-6494.7106009

RStudio Team. (2020). *RStudio: Integrated Development for R* [Software]. RStudio.

Rubinov, M., & Sporns, O. (2010). Complex network measures of brain connectivity: Uses and interpretations. *NeuroImage*, *52*(3), 1059-1069. https://doi.org/10.1016/j.neuroimage.2009.10.003

Rueda, M. R., Fan, J., McCandliss, B. D., Halparin, J. D., Gruber, D. B., Lercari, L. P., & Posner, M. I. (2004). Development of attentional networks in childhood. *Neuropsychologia*, *42*(8), 1029-1040. https://doi.org/10.1016/j.neuropsychologia.2003.12.012

Rueda, M. R., Moyano, S., & Rico-Picó, J. (2021). Attention: The grounds of self-regulated cognition. *Wiley Interdisciplinary Reviews: Cognitive Science*, 1582. https://doi.org/10.1002/wcs.1582

Rueda, M. R., Pozuelos, J. P., & Cómbita, L. M. (2015). Cognitive neuroscience of attention: From brain mechanisms to individual differences in efficiency. *AIMS Neuroscience*, *2*(4), 183-202. https://doi.org/10.3934/Neuroscience.2015.4.183

Ruff, H. A., & Lawson, K. R. (1990). Development of Sustained, Focused Attention in Young Children During Free Play. *Developmental Psychology*, *26*(1), 85-93. https://doi.org/10.1037/0012-1649.26.1.85

References

Saby, J. N., & Marshall, P. J. (2012). The Utility of EEG Band Power Analysis in the Study of Infancy and Early Childhood. *Developmental Neuropsychology*, *37*(3), 253-273. https://doi.org/10.1080/87565641.2011.614663

Sadaghiani, S., & Kleinschmidt, A. (2016). Brain Networks and α-Oscillations: Structural and Functional Foundations of Cognitive Control. *Trends in Cognitive Sciences*, *20*(11), 805-817. https://doi.org/10.1016/j.tics.2016.09.004

Sadaghiani, S., Scheeringa, R., Lehongre, K., Morillon, B., Giraud, A.-L., D'Esposito, M., & Kleinschmidt, A. (2012). Alpha-Band Phase Synchrony Is Related to Activity in the Fronto-Parietal Adaptive Control Network. *The Journal of Neuroscience*, *32*(41), 14305-14310. https://doi.org/10.1523/JNEUROSCI.1358-12.2012

Salvador, R., Suckling, J., Schwarzbauer, C., & Bullmore, E. (2005). Undirected graphs of frequency-dependent functional connectivity in whole brain networks. *Philosophical Transactions of the Royal Society B: Biological Sciences*, *360*(1457), 937-946.

Samaha, J., & Cohen, M. X. (2022). Power spectrum slope confounds estimation of instantaneous oscillatory frequency. *NeuroImage*, *250*, 118929. https://doi.org/10.1016/j.neuroimage.2022.118929

Sauseng, P., Griesmayr, B., Freunberger, R., & Klimesch, W. (2010). Control mechanisms in working memory: A possible function of EEG theta oscillations. *Neuroscience & Biobehavioral Reviews*, *34*(7), 1015-1022. https://doi.org/10.1016/j.neubiorev.2009.12.006

Sauseng, P., Klimesch, W., Schabus, M., & Doppelmayr, M. (2005). Fronto-parietal EEG coherence in theta and upper alpha reflect central executive functions of working memory. *International Journal of Psychophysiology*, *57*(2), 97-103. https://doi.org/10.1016/j.ijpsycho.2005.03.018

Sauseng, P., Klimesch, W., Stadler, W., Schabus, M., Doppelmayr, M., Hanslmayr, S., Gruber, W. R., & Birbaumer, N. (2005). A shift of visual spatial attention is selectively associated with human EEG alpha activity. *European Journal of Neuroscience*, *22*(11), 2917-2926. https://doi.org/10.1111/j.1460-9568.2005.04482.x

Schaworonkow, N., & Voytek, B. (2021). Longitudinal changes in aperiodic and periodic activity in electrophysiological recordings in the first

seven months of life. *Developmental Cognitive Neuroscience*, *47*, 100895. https://doi.org/10.1016/j.dcn.2020.100895

Schultz, D. H., & Cole, M. W. (2016). Higher Intelligence Is Associated with Less Task-Related Brain Network Reconfiguration. *The Journal of Neuroscience*, *36*(33), 8551-8561. https://doi.org/10.1523/JNEUROSCI.0358-16.2016

Segalowitz, S. J., & Davies, P. L. (2004). Charting the maturation of the frontal lobe: An electrophysiological strategy. *Brain and Cognition*, *55*(1), 116-133. https://doi.org/10.1016/S0278-2626(03)00283-5

Senoussi, M., Verbeke, P., Desender, K., Loof, E., Talsma, D., & Verguts, T. (2022). Theta oscillations shift towards optimal frequency for cognitive control. *Nature Human Behaviour*, 1-14.

Shafto, C. L., Conway, C. M., Field, S. L., & Houston, D. M. (2012). Visual Sequence Learning in Infancy: Domain-General and Domain-Specific Associations With Language. *Infancy*, *17*(3), 247-271. https://doi.org/10.1111/j.1532-7078.2011.00085.x

Sheese, B. E., Rothbart, M. K., Posner, M. I., White, L. K., & Fraundorf, S. H. (2008). Executive attention and self-regulation in infancy. *Infant Behavior and Development*, *31*(3), 501-510. https://doi.org/10.1016/j.infbeh.2008.02.001

Shinya, Y., Kawai, M., Niwa, F., Kanakogi, Y., Imafuku, M., & Myowa, M. (2022). Cognitive flexibility in 12-month-old preterm and term infants is associated with neurobehavioural development in 18-month-olds. *Scientific Reports*, *12*(1). https://doi.org/10.1038/s41598-021-04194-8

Shrey, D. W., McManus, O. K., Rajaraman, R., Ombao, H., Hussain, S. A., & Lopour, B. A. (2018). Strength and stability of EEG functional connectivity predict treatment response in infants with epileptic spasms. *Clinical Neurophysiology*, *129*(10), 2137-2148.

Shrout, P. E., & Bolger, N. (2002). Mediation in experimental and nonexperimental studies: New procedures and recommendations. *Psychological Methods*, *7*(4), 422-445. https://doi.org/10.1037/1082-989X.7.4.422

Shuffrey, L. C., Pini, N., Potter, M., Springer, P., Lucchini, M., Rayport, Y., Sania, A., Firestein, M., Brink, L., Isler, J. R., Odendaal, H., & Fifer, W. P. (2022). Aperiodic electrophysiological activity in preterm infants is

linked to subsequent autism risk. *Developmental Psychobiology*, *64*(4), e22271. https://doi.org/10.1002/dev.22271

Shulman, G. L., McAvoy, M. P., Cowan, M. C., Astafiev, S. V., Tansy, A. P., d'Avossa, G., & Corbetta, M. (2003). Quantitative Analysis of Attention and Detection Signals During Visual Search. *Journal of Neurophysiology*, *90*(5), 3384-3397. https://doi.org/10.1152/jn.00343.2003

Siegler, R. S. (2007). Cognitive variability. *Developmental Science*, *10*(1), 104-109. https://doi.org/10.1111/j.1467-7687.2007.00571.x

Siqueiros Sanchez, M., Ronald, A., Mason, L., Jones, E. J. H., Bölte, S., & Falck-Ytter, T. (2021). Visual disengagement in young infants in relation to age, sex, SES, developmental level and adaptive functioning. *Infant Behavior and Development*, *63*(February). https://doi.org/10.1016/j.infbeh.2021.101555

Smit, D. J. A., Boersma, M., Schnack, H. G., Micheloyannis, S., Boomsma, D. I., Pol, H. E. H., Stam, C. J., & Geus, E. J. C. de. (2012). The brain matures with stronger functional connectivity and decreased randomness of its network. *PloS one*, *7*(5). https://doi.org/10.1371/journal.pone.0036896

Smit, D. J. A., Geus, E. J. C. D., Boersma, M., Boomsma, D. I., & Stam, C. J. (2016). Life-Span Development of Brain Network Integration Assessed with Phase Lag Index Connectivity and Minimum Spanning Tree Graphs. *Brain Connectivity*, *6*(4), 312-325. https://doi.org/10.1089/brain.2015.0359

Smith, J. R. (1938). The Electroencephalogram During Normal Infancy and Childhood: I. Rhythmic Activities Present in the Neonate and Their Subsequent Development. *The Pedagogical Seminary and Journal of Genetic Psychology*, *53*(2), 431-453. https://doi.org/10.1080/08856559.1938.10533820

Smith, R. J., Alipourjeddi, E., Garner, C., Maser, A. L., Shrey, D. W., & Lopour, B. A. (2021). Infant functional networks are modulated by state of consciousness and circadian rhythm. *Network Neuroscience*, 1-17. https://doi.org/10.1162/netn_a_00194

Smyser, C. D., Inder, T. E., Shimony, J. S., Hill, J. E., Degnan, A. J., Snyder, A. Z., & Neil, J. J. (2010). Longitudinal analysis of neural network

development in preterm infants. *Cerebral Cortex*, *20*(12), 2852-2862. https://doi.org/10.1093/cercor/bhq035

Spaak, E., De Lange, F. P., & Jensen, O. (2014). Local Entrainment of Alpha Oscillations by Visual Stimuli Causes Cyclic Modulation of Perception. *The Journal of Neuroscience*, *34*(10), 3536-3544. https://doi.org/10.1523/JNEUROSCI.4385-13.2014

Spadone, S., Penna, S. D., Sestieri, C., Betti, V., Tosoni, A., Perrucci, M. G., Romani, G. L., & Corbetta, M. (2015). Dynamic reorganization of human resting-state networks during visuospatial attention. *Proceedings of the National Academy of Sciences*. https://doi.org/10.1073/pnas.1415439112

Spiegel, J. A., Goodrich, J. M., Morris, B. M., Osborne, C. M., & Lonigan, C. J. (2021). Relations between executive functions and academic outcomes in elementary school children: A meta-analysis. *Psychological Bulletin*, *147*(4), 329.

St. John, A. M., Kao, K., Choksi, M., Liederman, J., Grieve, P. G., & Tarullo, A. R. (2016). Variation in infant EEG power across social and nonsocial contexts. *Journal of Experimental Child Psychology*, *152*, 106-122. https://doi.org/10.1016/j.jecp.2016.04.007

Stahl, A. E., & Feigenson, L. (2015). Observing the unexpected enhances infants' learning and exploration. *Science*, *348*(6230), 91-94. https://doi.org/10.1126/science.aaa3799

Stam, C. J., Nolte, G., & Daffertshofer, A. (2007). Phase lag index: Assessment of functional connectivity from multi channel EEG and MEG with diminished bias from common sources. *Human Brain Mapping*, *28*(11), 1178-1193. https://doi.org/10.1002/hbm.20346

Stechler, G., & Latz, E. (1966). Some observations on attention and arousal in the human infant. *Journal of the American Academy of Child Psychiatry*, *5*(3), 517-525. https://doi.org/10.1016/S0002-7138(09)62098-7

Stephens, R. L., Langworthy, B. W., Short, S. J., Girault, J. B., Styner, M. A., & Gilmore, J. H. (2020). White Matter Development from Birth to 6 Years of Age: A Longitudinal Study. En *Cerebral Cortex* (Vol. 30, Número ue 12). https://doi.org/10.1093/cercor/bhaa170

Stevens, A. A., Tappon, S. C., Garg, A., & Fair, D. A. (2012). Functional Brain Network Modularity Captures Inter- and Intra-Individual Variation

in Working Memory Capacity. *PLoS ONE*, *7*(1), e30468. https://doi.org/10.1371/journal.pone.0030468

Stevens, M. C., Calhoun, V. D., & Kiehl, K. A. (2005). Hemispheric differences in hemodynamics elicited by auditory oddball stimuli. *NeuroImage*, *26*(3), 782-792. https://doi.org/10.1016/j.neuroimage.2005.02.044

Stroganova, T. A., Orekhova, E. V., & Posikera, I. N. (1998). Externally and internally controlled attention in infants: An EEG study. *International Journal of Psychophysiology*. https://doi.org/10.1016/S0167-8760(98)00026-9

Stroganova, T. A., Orekhova, E. V., & Posikera, I. N. (1999). EEG alpha rhythm in infants. *Clinical Neurophysiology*, *110*(6), 997-1012. https://doi.org/10.1016/S1388-2457(98)00009-1

Swingler, M. M., Willoughby, M. T., & Calkins, S. D. (2011). EEG power and coherence during preschoolers' performance of an executive function battery. *Developmental Psychobiology*, *53*(8), 771-784. https://doi.org/10.1002/dev.20588

Tan, E., Tang, A., Debnath, R., Humphreys, K. L., Zeanah, C. H., Nelson, C. A., & Fox, N. A. (2023). Resting brain activity in early childhood predicts IQ at 18 years. *Developmental Cognitive Neuroscience*, *63*, 101287. https://doi.org/10.1016/j.dcn.2023.101287

Tang, A., Crawford, H., Morales, S., Degnan, K. A., Pine, D. S., & Fox, N. A. (2020). Infant behavioral inhibition predicts personality and social outcomes three decades later. *Proceedings of the National Academy of Sciences*, *117*(18), 9800-9807.

Tarullo, A. R., Obradović, J., Keehn, B., Rasheed, M. A., Siyal, S., Nelson, C. A., & Yousafzai, A. K. (2017). Gamma power in rural Pakistani children: Links to executive function and verbal ability. *Developmental Cognitive Neuroscience*, *26*, 1-8. https://doi.org/10.1016/j.dcn.2017.03.007

Taylor, A. B., & MacKinnon, D. P. (2012). Four applications of permutation methods to testing a single-mediator model. *Behavior Research Methods*, *44*(3), 806-844. https://doi.org/10.3758/s13428-011-0181-x

Thatcher, R. W., North, D. M., & Biver, C. J. (2008). Development of cortical connections as measured by EEG coherence and phase delays. *Human Brain Mapping*, *29*(12), 1400-1415. https://doi.org/10.1002/hbm.20474

Thompson, A., & Steinbeis, N. (2020). Sensitive periods in executive function development. *Current Opinion in Behavioral Sciences*, *36*, 98-105.

Thompson, P. M., Ge, T., Glahn, D. C., Jahanshad, N., & Nichols, T. E. (2013). Genetics of the connectome. *NeuroImage*, *80*, 475-488. https://doi.org/10.1016/j.neuroimage.2013.05.013

Tierney, A. L., Gabard-Durnam, L., Vogel-Farley, V., Tager-Flusberg, H., & Nelson, C. A. (2012). Developmental Trajectories of Resting EEG Power: An Endophenotype of Autism Spectrum Disorder. *PLoS ONE*, *7*(6), e39127. https://doi.org/10.1371/journal.pone.0039127

Tomasi, D., & Volkow, N. D. (2011). Functional connectivity hubs in the human brain. *Neuroimage*, *57*(3), 908-917.

Tooley, U. A., MacKey, A. P., Ciric, R., Ruparel, K., Moore, T. M., Gur, R. C., Gur, R. E., Satterthwaite, T. D., & Bassett, D. S. (2020). Associations between Neighborhood SES and Functional Brain Network Development. *Cerebral Cortex*, *30*(1), 1-19. https://doi.org/10.1093/cercor/bhz066

Tosoni, A., Capotosto, P., Baldassarre, A., Spadone, S., & Sestieri, C. (2023). Neuroimaging evidence supporting a dual-network architecture for the control of visuospatial attention in the human brain: A mini review. *Frontiers in Human Neuroscience*, *17*, 1250096. https://doi.org/10.3389/fnhum.2023.1250096

Tóth, B., Urbán, G., Háden, G. P., Márk, M., Török, M., Stam, C. J., & Winkler, I. (2017). Large-scale network organization of EEG functional connectivity in newborn infants. *Human Brain Mapping*, *38*(8), 4019-4033. https://doi.org/10.1002/hbm.23645

Troller-Renfree, S. V., Brito, N. H., Desai, P. M., Leon-Santos, A. G., Wiltshire, C. A., Motton, S. N., Meyer, J. S., Isler, J., Fifer, W. P., & Noble, K. G. (2020). Infants of mothers with higher physiological stress show alterations in brain function. *Developmental Science*, *23*(6). https://doi.org/10.1111/desc.12976

Troller-Renfree, S. V., Buzzell, G. A., Fox, N. A., & Troller-Renfree, S. (2019). Changes in working memory facilitate the transition from reactive to proactive cognitive control during childhood.

Troller-Renfree, S. V., Costanzo, M. A., Duncan, G. J., Magnuson, K., Gennetian, L. A., Yoshikawa, H., Halpern-Meekin, S., Fox, N. A., & Noble, K. G. (2022). The impact of a poverty reduction intervention

on infant brain activity. *Proceedings of the National Academy of Sciences*, *119*(5), e2115649119. https://doi.org/10.1073/pnas.2115649119

Tröndle, M., Popov, T., Dziemian, S., & Langer, N. (2022). Decomposing the role of alpha oscillations during brain maturation. *eLife*, *11*, e77571. https://doi.org/10.7554/eLife.77571

Tummeltshammer, K., & Amso, D. (2018). Top-down contextual knowledge guides visual attention in infancy. *Developmental Science*, *21*(4), e12599. https://doi.org/10.1111/desc.12599

Uddin, L. Q., Supekar, K. S., Ryali, S., & Menon, V. (2011). Dynamic reconfiguration of structural and functional connectivity across core neurocognitive brain networks with development. *Journal of Neuroscience*, *31*(50), 18578-18589. https://doi.org/10.1523/JNEUROSCI.4465-11.2011

Usher, M., Cohen, J. D., Servan-Schreiber, D., Rajkowski, J., & Aston-Jones, G. (1999). The Role of Locus Coeruleus in the Regulation of Cognitive Performance. *Science*, *283*(5401), 549-554. https://doi.org/10.1126/science.283.5401.549

Vaessen, M. J., Hofman, P. A., Tijssen, H. N., Aldenkamp, A. P., Jansen, J. F., & Backes, W. H. (2010). The effect and reproducibility of different clinical DTI gradient sets on small world brain connectivity measures. *Neuroimage*, *51*(3), 1106-1116.

Van Den Heuvel, M. I., Donkers, F. C. L., Winkler, I., Otte, R. A., & Van Den Bergh, B. R. H. (2015). Maternal mindfulness and anxiety during pregnancy affect infants' neural responses to sounds. *Social Cognitive and Affective Neuroscience*, *10*(3), 453-460. https://doi.org/10.1093/scan/nsu075

Van Den Heuvel, M. I., Henrichs, J., Donkers, F. C. L., & Van Den Bergh, B. R. H. (2018). Children prenatally exposed to maternal anxiety devote more attentional resources to neutral pictures. *Developmental Science*, *21*(4), e12612. https://doi.org/10.1111/desc.12612

Van Den Heuvel, M. P., Stam, C. J., Kahn, R. S., & Hulshoff Pol, H. E. (2009). Efficiency of Functional Brain Networks and Intellectual Performance. *Journal of Neuroscience*, *29*(23), 7619-7624. https://doi.org/10.1523/JNEUROSCI.1443-09.2009

Van Den Heuvel, M. P., Van Soelen, I. L. C., Stam, C. J., Kahn, R. S., Boomsma, D. I., & Hulshoff Pol, H. E. (2013). Genetic control of functional brain

network efficiency in children. *European Neuropsychopharmacology*, *23*(1), 19-23. https://doi.org/10.1016/j.euroneuro.2012.06.007

Van Der Velde, B., White, T., & Kemner, C. (2021). The emergence of a theta social brain network during infancy. *NeuroImage*, *240*, 118298. https://doi.org/10.1016/j.neuroimage.2021.118298

Van Noordt, S., Heffer, T., & Willoughby, T. (2022). A developmental examination of medial frontal theta dynamics and inhibitory control. *NeuroImage*, *246*, 118765. https://doi.org/10.1016/j.neuroimage.2021.118765

Vasung, L., Turk, E. A., Ferradal, S. L., Sutin, J., Stout, J. N., Ahtam, B., Lin, P. Y., & Grant, P. E. (2019). Exploring early human brain development with structural and physiological neuroimaging. *NeuroImage*, *187*. https://doi.org/10.1016/j.neuroimage.2018.07.041

Veer, I. M., Luyten, H., Mulder, H., Van Tuijl, C., & Sleegers, P. J. C. (2017). Selective attention relates to the development of executive functions in 2,5- to 3-year-olds: A longitudinal study. *Early Childhood Research Quarterly*, *41*, 84-94. https://doi.org/10.1016/j.ecresq.2017.06.005

Vértes, P. E., & Bullmore, E. T. (2015). Annual research review: Growth connectomics—The organization and reorganization of brain networks during normal and abnormal development. *Journal of Child Psychology and Psychiatry and Allied Disciplines*, *56*(3), 299-320. https://doi.org/10.1111/jcpp.12365

Vinck, M., Oostenveld, R., Van Wingerden, M., Battaglia, F., & Pennartz, C. M. A. (2011). An improved index of phase-synchronization for electrophysiological data in the presence of volume-conduction, noise and sample-size bias. *NeuroImage*, *55*(4), 1548-1565. https://doi.org/10.1016/j.neuroimage.2011.01.055

Vinck, M., Uran, C., Spyropoulos, G., Onorato, I., Broggini, A. C., Schneider, M., & Canales-Johnson, A. (2023). Principles of large-scale neural interactions. *Neuron*, *111*(7), 987-1002. https://doi.org/10.1016/j.neuron.2023.03.015

von Stein, A., & Sarnthein, J. (2000). Different frequencies for different scales of cortical integration: From local gamma to long range alphartheta synchronization. *Psychophysiology*, *38*, 301-313.

Voytek, B., & Knight, R. T. (2015). Dynamic Network Communication as a Unifying Neural Basis for Cognition, Development, Aging, and

Disease. *Biological Psychiatry*, *77*(12), 1089-1097. https://doi.org/10.1016/j.biopsych.2015.04.016

Voytek, B., Kramer, M. A., Case, J., Lepage, K. Q., Tempesta, Z. R., Knight, R. T., & Gazzaley, A. (2015). Age-Related Changes in 1/f Neural Electrophysiological Noise. *Journal of Neuroscience*, *35*(38), 13257-13265. https://doi.org/10.1523/JNEUROSCI.2332-14.2015

Wang, R., Liu, M., Cheng, X., Wu, Y., Hildebrandt, A., & Zhou, C. (2021). Segregation, integration, and balance of large-scale resting brain networks configure different cognitive abilities. *Proceedings of the National Academy of Sciences*, *118*(23), e2022288118. https://doi.org/10.1073/pnas.2022288118

Wang, T., Zhang, X., Li, A., Zhu, M., Liu, S., Qin, W., Li, J., Yu, C., Jiang, T., & Liu, B. (2017). Polygenic risk for five psychiatric disorders and cross-disorder and disorder-specific neural connectivity in two independent populations. *NeuroImage: Clinical*, *14*, 441-449. https://doi.org/10.1016/j.nicl.2017.02.011

Wang, X.J. (2010). Neurophysiological and Computational Principles of Cortical Rhythms in Cognition. *Physiological Reviews*, *90*(3), 1195-1268. https://doi.org/10.1152/physrev.00035.2008

Wass, S., Porayska-Pomsta, K., & Johnson, M. H. (2011). Training attentional control in infancy. *Current Biology*, *21*(18), 1543-1547. https://doi.org/10.1016/j.cub.2011.08.004

Wass, S., Noreika, V., Georgieva, S., Clackson, K., Brightman, L., Nutbrown, R., Covarrubias, L. S., & Leong, V. (2018). Parental neural responsivity to infants' visual attention: How mature brains influence immature brains during social interaction. *PLOS Biology*, *16*(12), e2006328. https://doi.org/10.1371/journal.pbio.2006328

Wass, S., Perapoch Amadó, M., & Ives, J. (2022). Oscillatory entrainment to our early social or physical environment and the emergence of volitional control. *Developmental Cognitive Neuroscience*, *54*, 101102. https://doi.org/10.1016/j.dcn.2022.101102

Watts, D. J., & Strogatz, S. H. (1998). *Collective dynamics of 'small-world' networks*. *393*.

Wen, X., Zhang, H., Li, G., Liu, M., Yin, W., Lin, W., Zhang, J., & Shen, D. (2019). First-year development of modules and hubs in infant brain

functional networks. *NeuroImage*. https://doi.org/10.1016/j.neuroimage.2018.10.019

Whedon, M., Perry, N. B., & Bell, M. A. (2020). Relations between frontal EEG maturation and inhibitory control in preschool in the prediction of children's early academic skills. *Brain and Cognition*, *146*. https://doi.org/10.1016/j.bandc.2020.105636.

Whedon, M., Perry, N. B., Calkins, S. D., & Bell, M. A. (2016). *Changes in Frontal EEG Coherence Across Infancy Predict Cognitive Abilities at Age 3: The Mediating Role of Attentional Control*. *52*(9), 1341-1352.

Wickham, H. (2016). Elegant Graphics for Data Analysis. *Springer-Verlag New York*.

Wickham, H., Averick, M., Bryan, J., Chang, W., McGowan, L., François, R., Grolemund, G., Hayes, A., Henry, L., Hester, J., Kuhn, M., Pedersen, T., Miller, E., Bache, S., Müller, K., Ooms, J., Robinson, D., Seidel, D., Spinu, V., … Yutani, H. (2019). Welcome to the Tidyverse. *Journal of Open Source Software*, *4*(43), 1686. https://doi.org/10.21105/joss.01686

Wilkinson, C. L., Pierce, L. J., Sideridis, G., Wade, M., & Nelson, C. A. (2023). Associations between EEG trajectories, family income, and cognitive abilities over the first two years of life. *Developmental Cognitive Neuroscience*, *61*, 101260. https://doi.org/10.1016/j.dcn.2023.101260

Wold, H. (1975). 11—Path Models with Latent Variables: The NIPALS Approach**NIPALS = Nonlinear Iterative PArtial Least Squares. En H. M. Blalock, A. Aganbegian, F. M. Borodkin, R. Boudon, & V. Capecchi (Eds.), *Quantitative Sociology* (pp. 307-357). Academic Press. https://doi.org/10.1016/B978-0-12-103950-9.50017-4

Wolfe, C. D., & Bell, M. A. (2004). Working memory and inhibitory control in early childhood: Contributions from physiology, temperament, and language. *Developmental Psychobiology: The Journal of the International Society for Developmental Psychobiology*, *44*(1), 68-83.

Woods, A. J., Göksun, T., Chatterjee, A., Zelonis, S., Mehta, A., & Smith, S. E. (2013). The development of organized visual search. *Acta Psychologica*, *143*(2), 191-199. https://doi.org/10.1016/j.actpsy.2013.03.008

Wu, G., Wang, Y., Mwansisya, T. E., Pu, W., Zhang, H., Liu, C., Yang, Q., Chen, E. Y. H., Xue, Z., Liu, Z., & Shan, B. (2014). Effective connectivity of the posterior cingulate and medial prefrontal cortices

relates to working memory impairment in schizophrenic and bipolar patients. *Schizophrenia Research*, *158*(1-3), 85-90. https://doi.org/10.1016/j.schres.2014.06.033

Wu, K., Taki, Y., Sato, K., Hashizume, H., Sassa, Y., Takeuchi, H., Thyreau, B., He, Y., Evans, A. C., Li, X., Kawashima, R., & Fukuda, H. (2013). Topological Organization of Functional Brain Networks in Healthy Children: Differences in Relation to Age, Sex, and Intelligence. *PLoS ONE*, *8*(2). https://doi.org/10.1371/journal.pone.0055347

Xie, W., Jensen, S. K. G., Wade, M., Kumar, S., Westerlund, A., Kakon, S. H., Haque, R., Petri, W. A., & Nelson, C. A. (2019). Growth faltering is associated with altered brain functional connectivity and cognitive outcomes in urban Bangladeshi children exposed to early adversity. *BMC Medicine*, *17*(1). https://doi.org/10.1186/s12916-019-1431-5

Xie, W., Mallin, B. M., & Richards, J. E. (2018). Development of infant sustained attention and its relation to EEG oscillations: An EEG and cortical source analysis study. *Developmental Science*, *21*(3). https://doi.org/10.1111/desc.12562

Xie, W., Mallin, B. M., & Richards, J. E. (2019). Development of brain functional connectivity and its relation to infant sustained attention in the first year of life. *Developmental Science*, *22*(1), e12703. https://doi.org/10.1111/desc.12703

Yeo, B. T., Krienen, F. M., Sepulcre, J., Sabuncu, M. R., Lashkari, D., Hollinshead, M., Roffman, J. L., Smoller, J. W., Zöllei, L., Polimeni, J. R., Fischl, B., Liu, H., & Buckner, R. L. (2011). The organization of the human cerebral cortex estimated by intrinsic functional connectivity. *Journal of Neurophysiology*, *106*(3), 1125-1165. https://doi.org/10.1152/jn.00338.2011

Yin, W., Chen, M. H., Hung, S. C., Baluyot, K. R., Li, T., & Lin, W. (2019). Brain functional development separates into three distinct time periods in the first two years of life. *NeuroImage*, *189*, 715-726. https://doi.org/10.1016/j.neuroimage.2019.01.025

Zakharov, I., Tabueva, A., Adamovich, T., Kovas, Y., & Malykh, S. (2020). Alpha Band Resting-State EEG Connectivity Is Associated With Non-verbal Intelligence. *Frontiers in Human Neuroscience*, *14*, 10. https://doi.org/10.3389/fnhum.2020.00010

References

Zelazo, P. D. (2015). Executive function: Reflection, iterative reprocessing, complexity, and the developing brain. *Developmental Review*, *38*, 55-68.

Zelazo, P. D. (2023). *The Development of Executive Function in Early Childhood*.

Zelazo, P. D., Frye, D., & Rapus, T. (1996). An Age Related Dissociation Between Knowing Rules and Using Them. *Cognitive Development*, *11*(1), 37-63. https://doi.org/10.1016/S0885-2014(96)90027-1

Zelazo, P. D., Müller, U., Frye, D., & Marcovitch, S. (2003). The Development of Executive Function in Early Childhood. *Monographs of the Society for Research in Child Development*, *68*(3), 1-137. https://doi.org/10.1111/j.1540-5834.2003.06803003.x

Zhao, T., Mishra, V., Jeon, T., Ouyang, M., Peng, Q., Chalak, L., Wisnowski, J. L., Heyne, R., Rollins, N., Shu, N., & Huang, H. (2019). Structural network maturation of the preterm human brain. *NeuroImage*, *185*. https://doi.org/10.1016/j.neuroimage.2018.06.047

Zhao, T., Xu, Y., & He, Y. (2019). Graph theoretical modeling of baby brain networks. *NeuroImage*, *185*, 711-727. https://doi.org/10.1016/j.neuroimage.2018.06.038

Zhao, W., Huang, L., Li, Y., Zhang, Q., Chen, X., Fu, W., Du, B., Deng, X., Ji, F., Xiang, Y., Wang, C., Li, X., Dong, Q., Chen, C., Jaeggi, S. M., & Li, J. (2020). Evidence for the contribution of *COMT* gene Val158/108Met polymorphism (rs4680) to working memory training-related prefrontal plasticity. *Brain and Behavior*, *10*(2), e01523. https://doi.org/10.1002/brb3.1523

Zich, C., Quinn, A. J., Mardell, L. C., Ward, N. S., & Bestmann, S. (2020). Dissecting Transient Burst Events. *Trends in Cognitive Sciences*, *24*(10), 784-788. https://doi.org/10.1016/j.tics.2020.07.004

Appendix

Appendix of Chapter 2

We evaluated several aspects of the children's environment using questionnaires that allowed us to collect information regarding the time spent by parents, schooling, socioeconomic status, and maternal health.

A2.1. Time Spent with the Children

Most of the families in the study had the following structure: mother, father, and infants with one sibling. Only in a handful of families (6-mo. n = 11, 11.70%; 16-mo. n = 10, 11,36%), the uncles/aunts or grandparents lived with the main family nucleus, or the children lived alone with their mothers (n = 1). At the beginning of the study ($M_{siblings}$ = .55, $SD_{siblings}$ = .79), most of the infants were only child (n = 54, 57.45%), followed by having an older sibling (n = 33, 35,10%), and only 7 families had more than two child (3 children n = 3, 4 children n = 3, 5 children n = 1) sons/daughters apart from the infant in the study. The pattern in the third session ($M_{siblings}$ = .63, $SD_{siblings}$ = .75) was like the earlier one, with 39.53% of the infants being only child (n = 17) and 51.16% having one sibling (n = 22). However, in the last session ($M_{siblings}$ = .96, $SD_{siblings}$ = .81), families with two children were the majority (n = 36, 64.28%), followed by families with only one child (n = 13, 23.21%).

The time spent by children (Fig. A2.1) was unevenly distributed, independently of the session. At six months, 88.8% (n = 111) of the mothers spent more than six hours per day with their child, a percentage that diminished to 70.32% (n = 64) and 69.64% (n = 39) at 16- and 36-months sessions, respectively. Furthermore, 9.6% (n = 12), 20.88% (n = 19), and 25% (n = 14) of mothers spent between four and six hours per day with their children at 6, 16, and 36 months, respectively. In contrast, fathers' distribution of care time was more even across all sessions. When the infants were 6-mo., 21.95% (n = 27) of the fathers had children between two and four hours a day, while 29.27% (n = 36) and 36.59% (n = 45) spent between four and six hours and more than six hours a day, respectively. The results were similar at 16 months (6h+ n = 36, 4h – 6h n = 33, 2h – 4h n = 17, 0h – 2h n = 5) and 36 months (6h+ n = 16, 4h – 6h n = 18, 2h – 4h n = 16, 0h – 2h n = 6). Grandparents also played a

relevant role in the caregiving time spent with the children, with 42.74% spending more than 2h a day with them (6h+ n = 11, 4h – 6h n = 18, 2h – 4h n = 24, 0h – 2h n = 71) at 6 months. This increased in the third session (6h+ n = 27, 4h – 6h n = 13, 2h – 4h n = 19, 0h – 2h n = 33) but in the fourth session grandparents reduced the time spent, with 78.6% spending less than 2h with their grandsons/granddaughters (6h+ n = 3, 4h – 6h n = 2, 2h – 4h n = 7, 0h – 2h n = 44).

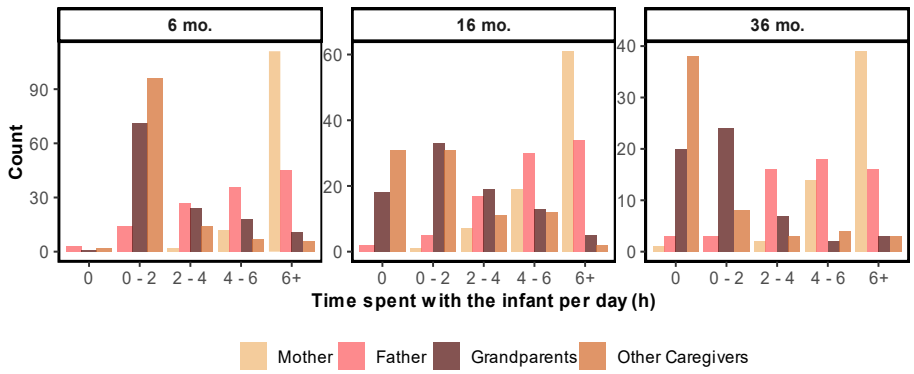

Fig. A2.1. Time spent with the children divided by the caregiver.

A2.2. Socioeconomic indicators

Parents were asked about their professional occupation, income, and educational level at 6 months session (Fig. A2.2). We also collected information about occupation and income in the 16-mo. session. We considered education level on a Likert scale ranging from 0 (no study) to 6 (postgraduate study). Occupation was manually coded based on the National Classification of Occupations (CNO-11) of the National Institute of Statistics of Spain (INE). It can vary from zero (unemployed) to nine (high rank related to management). Additionally, the income-to-need ratio was calculated. This results from dividing the family's annual net income by the poverty line, according to the INE data for families with the same demographic composition. Smaller values in the income-to-need ratio represent less economic power, with values under one meaning an income below poverty for a given family structure.

The education levels of fathers and mothers were skewed towards high educative levels. With regards to mothers, 68% had a superior education (master/PhD, n = 26; bachelor's degree, n = 33; superior degree/technical degree, n = 26), 25.6% had at least a basic technical education (FP1, n = 20), or had a medium technical degree (n = 12). Only 6.4% of the mothers did not complete the basic studies. Regarding fathers, 51.61% had a superior education: technical degree (18.54%), bachelor's degree (16.94%), or master's or PhD degree (16.13%). Approximately 13% of the fathers did not complete basic studies (n = 16), 25.80% had basic technical education, and 9.68% completed high school.

In relation to income, our six-month sample had an average income-to-need ratio of 1.37 (SD = 0.67), with 35% of the participants being under the poverty line. At 16 months of age, the mean income-to-need ratio was 1.72 (SD = 0.79), with 20% of the participants below the poverty threshold.

With respect to maternal occupation, 37.85% and 28.57% of the mothers were unemployed at the 6- and 16-months sessions, respectively. The 52.85% had scores over 5 in the CEO11 scale in the first session (i.e., administrative, technician, scientific, and teachers), which increased to 68.88% in the third session. Approximately 10% of the fathers were unemployed in the first and third sessions. Over 20% of the fathers worked in bars and restaurants, and approximately 40% had administrative, technician, or professor jobs independent of the session.

A2.2. Early Childhood Schooling

Of all the samples, only 23.89% of infants went to kindergarten when they were 6 months-old (n = 27, M_{age} = 6.21, SD_{age} = 1.85), which increased to 71.58% in the third (n = 68, M_{age} = 9.76, SD_{age} = 4.06) and 82.76% in the fourth (n = 48, M_{age} = 13.11, SD_{age} = 7.12) sessions. Some children went to kindergarten intermittently because of the COVID-19 pandemic.

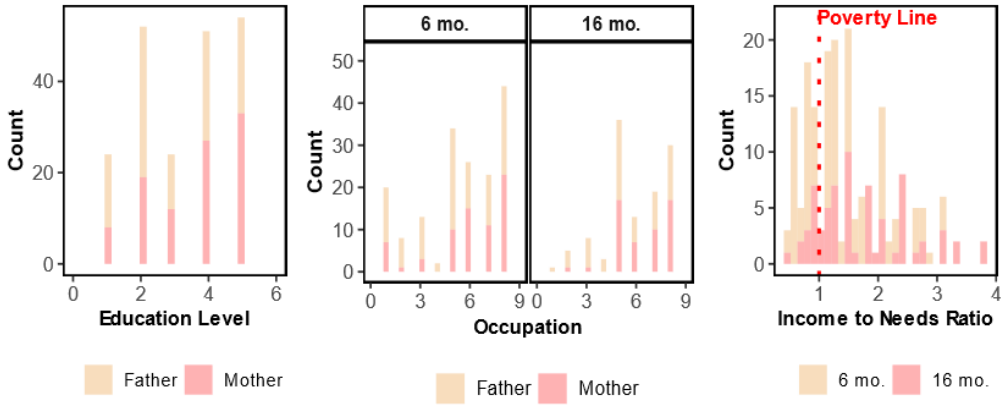

Fig. A2.2. Socioeconomic indicators of the families included in the study. The figure displays the number of fathers and mothers or family units in the income-to-needs ratio by category in education, occupation, and income-to-needs ratio. It shows the information divided by the session.

A2.2. Maternal Mental Health

We evaluated the mothers' mental health (Fig. A2.3) using the Spanish version of the Beck Depression Inventory II (BDI-II; Beck et al., 1996). The BDI-II is a 21-item self-reported inventory that asks, in this case, how mothers felt in the previous two weeks with respect depressive symptoms. Responses range from 0 to 3 on a Likert scale. In our sample, the inventory showed good internal consistency (6 months: α = .88; 16 months: α = 90, 36 months: α = .87). In the first session, the mothers were not depressed on average (M = 10.74, SD = 7.40), with 74.04% (n = 94) below the range of mild depression. However, 17 (12.98%), 12 (9.16%), and 5 (3.81%) mothers had scores within the ranges of mild, moderate, and severe depression, respectively. The pattern was similar when the children were 16 or 36 months old. In the third session, maternal depression (M = 11.29, SD = 7.73) did not reach a clinical value for 55 mothers (78,57%); however, 15 mothers (mild depression, n = 4; moderate depression, n = 7; severe depression, n = 4) had punctuation within the clinical range (21.42%). In the fourth session (M = 8.84, SD = 6.04), 75.51% (n = 37) fell below the threshold for clinical depression, while 9 (18.8%) and 3 (6.12%) mothers had scores within the ranges of mild and moderate depression, respectively.

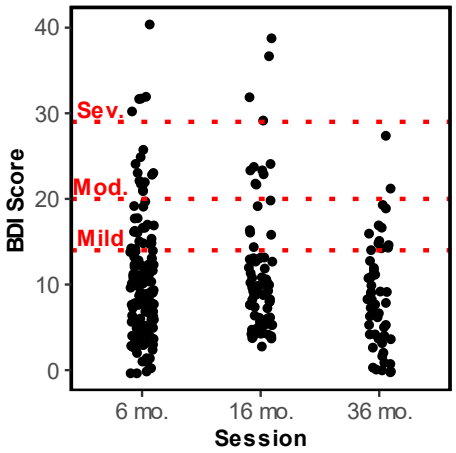

Fig. A2.3. Maternal depression scores by session. The figure displays the BDI-II scores for each mother. The thresholds were based on the Spanish scale of the BDI-II adaptation.

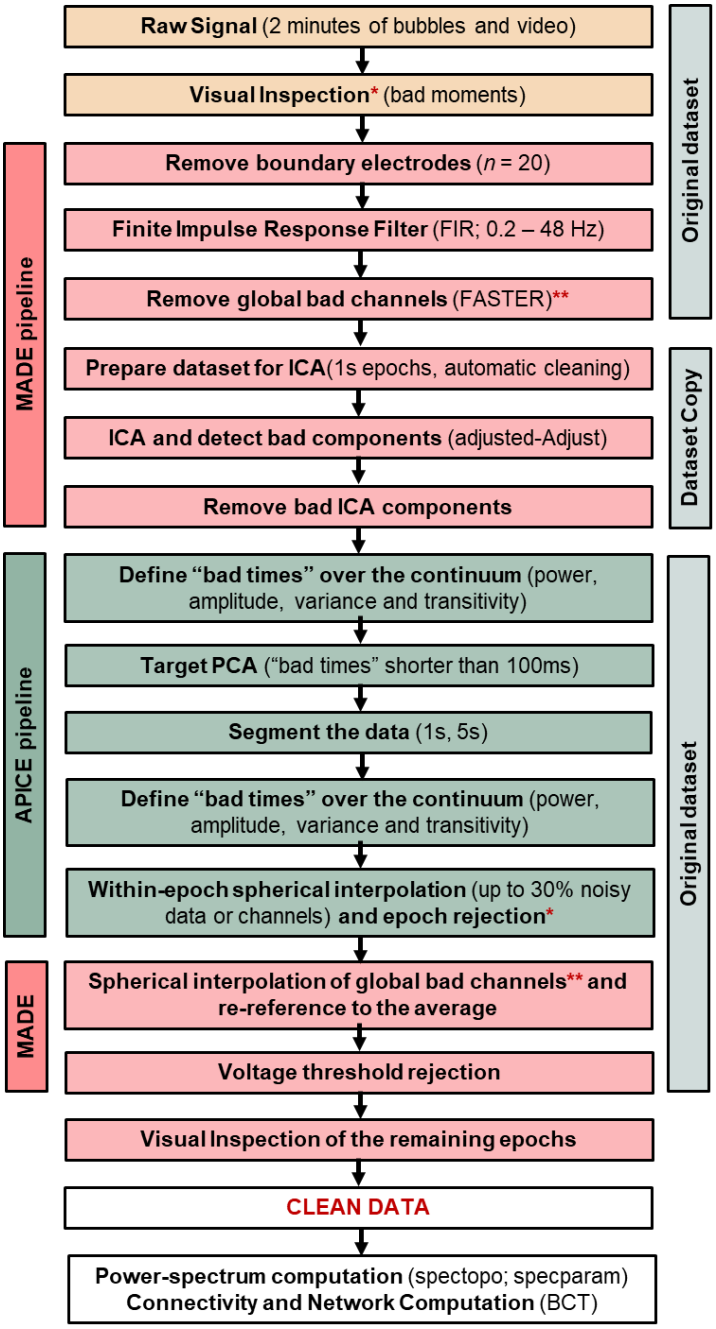

Fig. A2.4. Pipeline of the EEG preprocessing. The figure shows all the steps conducted sequentially. The pipeline from employed in each preprocessing step is filled with different colors: red (MADE), green (APICE).

Appendix of Chapter 3A

Table A3A.1

Goodness of fit of the power specparam toolbox divided by cluster.

Session	Sex	Goodness of Fit (R^2)				% Electrodes			
		C	*Fr*	*O*	*P*	*C*	*Fr*	*O*	*P*
6-mo.	*F*	99.42 (0.79)	98.26 (2.19)	99.61 (0.43)	99.45 (0.75)	0.01 (0.1)	0.05 (0.21)	0 (0.03)	0.01 (0.08)
	M	99.39 (0.85)	98.09 (2.35)	99.6 (0.47)	99.37 (0.94)	0.01 (0.1)	0.07 (0.25)	0.01 (0.09)	0.01 (0.11)
9-mo.	*F*	99.53 (0.59)	98.54 (2.31)	99.67 (0.34)	99.46 (0.89)	0.01 (0.11)	0.03 (0.18)	0 (0.04)	0 (0.05)
	M	99.08 (2.34)	97.74 (3.06)	99.66 (0.3)	99.28 (1.19)	0.01 (0.09)	0.03 (0.18)	0.01 (0.08)	0 (0.06)
16-mo.	*F*	99.52 (0.6)	98.84 (1.44)	99.68 (0.22)	99.58 (0.51)	0.01 (0.11)	0.04 (0.19)	0 (0)	0.01 (0.1)
	M	99.5 (0.47)	99.01 (1.29)	99.68 (0.3)	99.46 (0.68)	0.02 (0.13)	0.06 (0.23)	0.01 (0.09)	0.01 (0.08)
36-mo.	*F*	99.53 (0.49)	99.08 (1.69)	99.64 (0.38)	99.52 (0.49)	0.01 (0.12)	0.02 (0.14)	0.01 (0.1)	0.01 (0.09)
	M	99.6 (0.46)	99.13 (1.74)	99.71 (0.37)	99.62 (0.41)	0.02 (0.15)	0.04 (0.21)	0.01 (0.11)	0.02 (0.13)

Note. F = Female, M = Male, C = Central, Fr = Frontal, O = Occipital, P = Parietal. The table displays the mean (standard deviation) of the goodness of fit and the percentage of electrodes removed because they did not have the required $R^2 > .95$.

Table A3A.2

Oscillatory power per cluster, band, and session age.

Band	Sex	6-mo.				9-mo.				16-mo.				36-mo.			
		O	*P*	*C*	*Fr*	*O*	*P*	*C*	*Fr*	*O*	*P*	*C*	*Fr*	*O*	*P*	*C*	*Fr*
T	*F*	2.61	2.58	2.08	2.05	2.23	2.43	2.31	2.39	1.94	2.49	2.29	2.41	1.03	1.22	1.45	1.69
		(1.46)	(1.62)	(1.46)	(1.62)	(1.2)	(1.63)	(1.57)	(1.69)	(1.28)	(1.59)	(1.5)	(1.53)	(1.02)	(1.46)	(1.65)	(1.41)
	M	2.77	2.81	2.3	2.44	2.91	2.94	2.45	2.79	1.82	2.32	2.4	2.43	1.05	1.42	1.71	1.62
		(1.35)	(1.32)	(1.25)	(1.49)	(1.53)	(1.54)	(1.52)	(1.7)	(1.63)	(1.49)	(1.39)	(1.35)	(1.08)	(1.17)	(1.24)	(1.21)
A	*F*	3.65	4.05	4.33	2.44	5.51	5.29	5.72	3.53	7.41	7.3	7.64	5.25	6.07	6.53	7.35	5.37
		(2.15)	(2.92)	(2.91)	(2.62)	(2.02)	(2.59)	(3)	(2.52)	(2.55)	(3.15)	(2.76)	(2.39)	(2.55)	(2.69)	(3.21)	(2.54)
	M	2.82	2.77	3.12	1.72	4.57	4.2	4.4	2.4	6.02	5.32	6.44	3.91	5.7	5.88	6.87	4.89
		(1.92)	(2.47)	(2.8)	(2.77)	(2.85)	(3.18)	(3.78)	(3.05)	(2.84)	(2.97)	(3.41)	(3.17)	(2.86)	(3.41)	(3.89)	(3.28)
B	*F*	0.98	1.41	1.41	2.76	0.76	1.18	1.24	2.18	0.68	0.98	1.18	1.66	0.96	0.97	1.16	1.38
		(1.62)	(2.16)	(1.9)	(3.33)	(1.23)	(1.86)	(1.62)	(2.76)	(1.03)	(1.44)	(1.51)	(2.15)	(1.01)	(1.25)	(1.49)	(1.9)
	M	1.2	1.57	1.62	2.57	1.13	1.54	1.98	3.16	0.71	1.07	1.49	2.03	0.79	0.77	0.84	1.25
		(1.92)	(2.33)	(2.18)	(3.02)	(1.83)	(2.22)	(2.46)	(3.82)	(1.49)	(1.68)	(1.79)	(2.32)	(1.03)	(1.2)	(1.24)	(1.76)

Note. F = Female, M = Male, T = Theta, A = Alpha, B = Beta, O = Occipital, P = Parietal, C = Central, Fr = Frontal. The table displays the mean (standard deviation).

Table A3A.3

Des Relative power per cluster, band, and session age.

Band	Sex	6-mo.				9-mo.				16-mo.				36-mo.			
		O	*P*	*C*	*Fr*	*O*	*P*	*C*	*Fr*	*O*	*P*	*C*	*Fr*	*O*	*P*	*C*	*Fr*
T	*F*	15.56	15.68	15.77	15.4	15.08	15.24	15.55	15.32	14.8	14.95	15.15	15	14.36	14.38	14.69	14.56
		(0.78)	(0.97)	(0.94)	(1.07)	(0.55)	(0.8)	(0.85)	(0.95)	(0.7)	(0.84)	(0.91)	(0.95)	(0.48)	(0.71)	(0.84)	(0.71)
	M	15.73	15.91	16	15.64	15.52	15.63	15.71	15.48	14.94	15.13	15.44	15.3	14.43	14.58	14.98	14.66
		(0.72)	(0.8)	(0.84)	(0.95)	(0.65)	(0.77)	(0.85)	(1)	(0.6)	(0.72)	(0.8)	(0.77)	(0.56)	(0.66)	(0.79)	(0.71)
A	*F*	16.72	16.96	17.27	16.26	18.24	18.28	18.67	17.63	20.25	20.26	20.65	19.55	20.01	20.26	20.71	19.74
		(2.45)	(2.57)	(2.58)	(2.51)	(2.21)	(2.32)	(2.3)	(2.23)	(1.07)	(1.29)	(1.27)	(1.15)	(1.23)	(1.33)	(1.49)	(1.26)
	M	16.68	16.71	17.02	16.32	18.04	17.99	18.22	17.24	19.56	19.31	19.89	18.75	19.89	20.03	20.55	19.58
		(2.44)	(2.48)	(2.65)	(2.65)	(1.99)	(2.17)	(2.4)	(2.11)	(1.52)	(1.67)	(1.98)	(1.85)	(1.39)	(1.58)	(1.74)	(1.53)
B	*F*	35.76	35.36	34.47	36.67	36.11	36.08	34.82	36.7	35.91	36.05	35.1	36.86	37.01	36.75	35.39	37.15
		(1.71)	(2.17)	(2.23)	(2.8)	(1.26)	(1.95)	(1.82)	(2.22)	(1.24)	(1.79)	(2.01)	(2.11)	(1.43)	(1.81)	(1.93)	(1.86)
	M	35.63	35.31	34.49	36.45	35.81	35.82	35.16	37.18	35.94	36.24	34.89	36.61	37.02	36.69	35	37.04
		(1.47)	(2.12)	(2.16)	(2.52)	(1.21)	(2)	(2.09)	(2.46)	(1.25)	(1.97)	(1.91)	(1.87)	(1.47)	(1.95)	(1.97)	(1.75)

Note. F = Female, M = Male, A = Alpha, B = Beta, T = Theta, O = Occipital, P = Parietal, C = Central, Fr = Frontal. The table displays the mean (standard deviation)

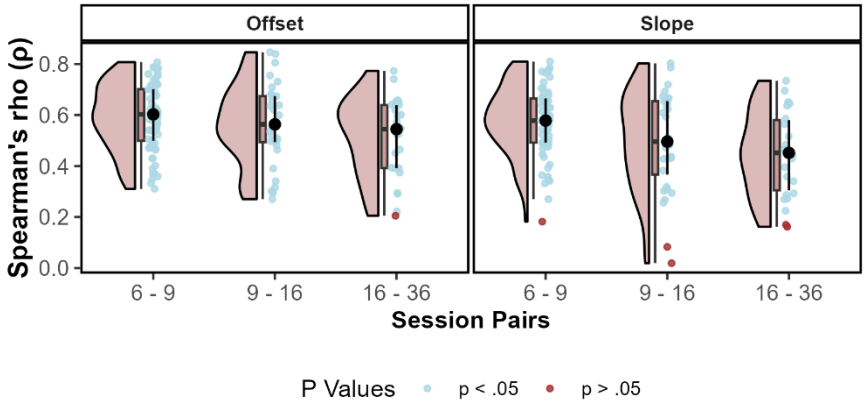

Fig. A3A.1. Within-participant spatial stability. The figure displays Spearman's rank correlation values when the aperiodic components of each electrode were individually correlated between sessions for each participant. Colors represent p-values.

Table A3A.4

Within-participant spatial stability of the aperiodic components.

	6 to 9-mo.		**9 to 16-mo.**		**16 to 36-mo.**	
	r_s	%	r_s	%	r_s	%
Offset	0.52 (0.16) [0.21 - 0.77]	0.96 (0.2)	0.59 (0.13) [0.3 - 0.8]	1 (0)	0.56 (0.16) [0.27 - 0.8]	1 (0)
Exponent	0.45 (0.17) [0.16 - 0.73]	0.92 (0.27)	0.58 (0.14) [0.2 - 0.8]	0.99 (0.12)	0.49 (0.19) [0.02 - 0.8]	0.94 (0.25)

Note. The table shows the mean Spearman's rank correlation found when the topological distribution aperiodic component properties were correlated in different sessions individually, and the percentage (%) of occasions where the correlation was significant. It shows the mean (SD) [min – max].

Table A3A.5

Within-participant spatial stability in the relative and oscillatory power.

	Band	6 to 9-mo.		9 to 16-mo.		16 to 36-mo.	
		r_s	%	r_s	%	r_s	%
Osc.	*T*	0.2 (0.17) [-0.31 -0.57]	0.2 (0.17)	0.22 (0.21) [-0.41 - 0.58]	0.22 (0.21)	0.2 (0.21) [-0.26 - 0.66]	0.2 (0.21)
	A	0.51 (0.17) [-0.16 - 0.81]	0.51 (0.17)	0.54 (0.18) [0.01 - 0.79]	0.54 (0.18)	0.48 (0.2) [-0.03 -0.77]	0.48 (0.2)
	B	0.22 (0.16) [-0.23 - 0.55]	0.22 (0.16)	0.18 (0.17) [-0.21 - 0.53]	0.18 (0.17)	0.05 (0.17) [-0.3 - 0.46]	0.05 (0.17)
Rel.	*T*	0.44 (0.15) [0.1 - 0.76]	0.44 (0.15)	0.39 (0.17) [-0.08 - 0.67]	0.39 (0.17)	0.38 (0.15) [0.04 - 0.69]	0.38 (0.15)
	A	0.56 (0.17) [-0.09 - 0.81]	0.56 (0.17)	0.6 (0.14) [0.31 - 0.81]	0.6 (0.14)	0.52 (0.16) [0.15 - 0.82]	0.52 (0.16)
	B	0.61 (0.13) [0.22 - 0.83]	0.61 (0.13)	0.58 (0.12) [0.39 - 0.82]	0.58 (0.12)	0.5 (0.17) [0.08 - 0.71]	0.5 (0.17)

Note. The table shows mean Spearman's rank correlation found when the topological distribution aperiodic components properties was correlated in different sessions individually and the percentage (%) of occasions where the correlation was significant. It shows the mean (SD) [min – max].

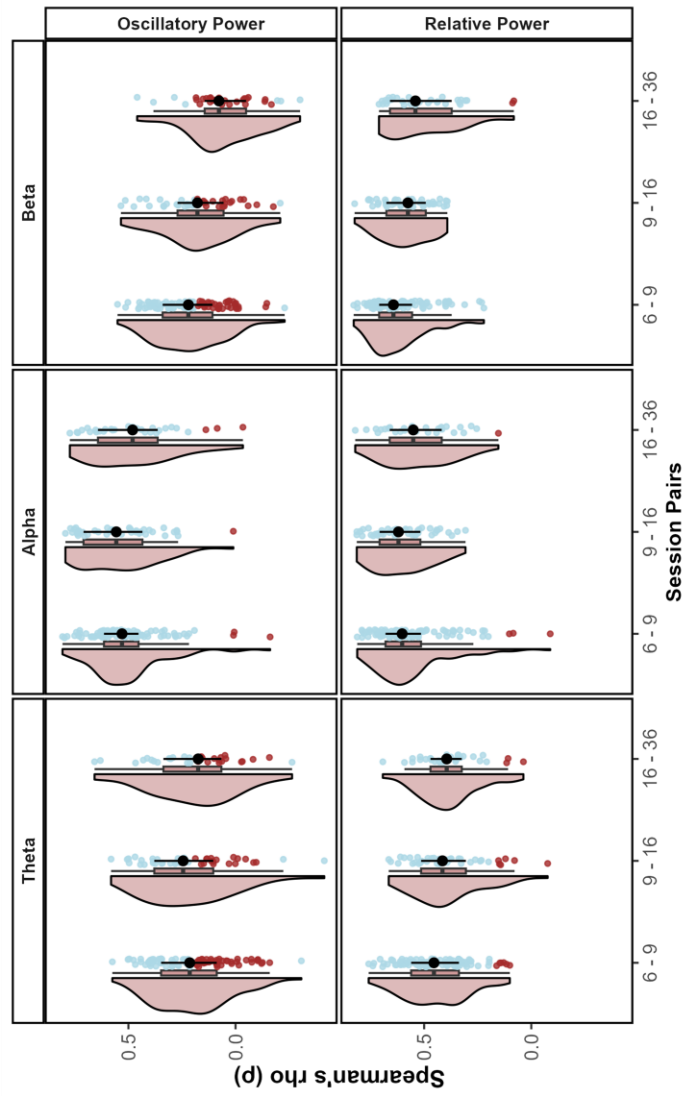

Fig. A3A.2 Within-participant spatial stability in the relative and oscillatory power. The figure displays the Spearman's rank correlation values when the power measures of each electrode were correlated between session individually for each participant and divided by frequency bands. Colors represent the p values.

A3A. Burst and Rhythms Development

Although the distinction between oscillatory and aperiodic activity isolates the activity above the decaying 1/*f* background curve, the lack of a peak in the power spectrum does not represent the absence of oscillatory activity (Jones, 2016). Regarding brain activity, we must consider that it is both tonic (i.e., sustained or rhythmic) and transient (bursty; Zich et al., 2020). The latter is especially present in the case of the beta and gamma bands (Cole & Voytek, 2017; Jones, 2016). Considering this, it is not necessary to increase the amplitude to augment the energy, as a longer and/or higher number of bursts would result in the same pattern in power-spectrum decomposition (Ede et al., 2018). Thus, there are several possible explanations for the maturation of the brain power in each band.

Only a handful of studies, apart from the classic qualitative ones (e.g., Smith, 1936), have explored burst property changes, mostly in the alpha band. Alpha band bursts increase in number with age, which parallels the larger percentage of infants with a clear alpha peak when they grow (Schaworonkow & Voytek, 2021). By 12 months of life (Rayson et al., 2022), alpha activity is self-predictable, indicating sustained or rhythmic activity. In a recent study, Rayson et al. (2023) found age-related changes in burst beta activity. Therefore, it is possible that the changes found in the alpha band are derived from changes either in bursts or rhythmic properties, whereas the pattern found in the theta and beta bands may differ because they are not sustained oscillations.

The objective of this appendix was to clarify whether the results found in Chapter 3A were derived from changes in burst (vs. rhythmic) activity in the alpha band and compare them to the theta and beta bands. We decomposed the signal by employing lagged coherence (Fransen et al. 2013) and studied the burst properties (duration, amplitude, and number) using the p-episode method. First, we explored the differences in oscillatory power between peak and non-peak electrodes and then traced the developmental changes of burst and rhythmic properties over time. We expected a transition from burst to rhythmic in the alpha band, which would be represented by an increment in lagged coherence. In contrast, we hypothesized that theta and

beta bands would be mostly transient (i.e., low lag-coherence beyond the second cycle).

RA3A. Method

RA3A.1. Burst properties and rhythmicity of the EEG power

The sample was identical to that included in the main test in Chapter 3A. To determine whether the oscillatory power had bursty or rhythmic properties, we followed the guidance proposed by Rayson et al. (2022) using the FieldTrip toolbox (2018).

We employed lagged coherence to explore the rhythmicity of the signal. It has a similar rationale to coherence; however, instead of applying over electrode pairs, it tries to predict the activity of the same electrode at further time points. To this end, it decomposes the signal using an FFT, extracts the phase values, and tests whether the current phase is related to the following phases. The lagged coherence can be defined as follows (Fransen et al., 2015):

(4)

$$\lambda(\mathrm{k}) = \left| \frac{\sum_{\mathrm{n}=1}^{\mathrm{N}-1} \mathcal{F}(x_{\mathrm{n}})_{\mathrm{k}} \mathcal{F}(x_{\mathrm{n}+1})_{\mathrm{k}}^{\mathrm{H}}}{\sqrt{(\sum_{\mathrm{n}=1}^{\mathrm{N}-1} |\mathcal{F}(x_{\mathrm{n}})_{\mathrm{k}}|^2)(\sum_{\mathrm{n}=1}^{\mathrm{N}-1} |\mathcal{F}(x_{\mathrm{n}+1})_{\mathrm{k}}|^2)}} \right|$$

where lagged coherence $\lambda(\mathrm{k})$ over a frequency k is computed based on the FFT transformation $\mathcal{F}(x_{\mathrm{n}})$ of the signal comparing it to over oscillatory cycles ($\boldsymbol{x}_{\mathrm{n+1}}$) from $n = 1\ldots$, N lags.

According to the lagged coherence measure, rhythmic oscillations must be self-predictable over several lags (e.g., lags > 2.5). In contrast, if the lagged coherence is high during one cycle, it is considered a burst activity. We computed the lagged coherence from 2 to 20 Hz in .2 Hz steps from 1 to 5 lags in .1 increment, as in previous experiments (Rayson et al., 2022).

To explore the burst properties of the frequency bands, we employed the so-called "p-episode" method (Lundqvist et al. 2016). This method

computes the amplitude envelope of the power using a two-pass Hilbert filter, thereby narrowing the signal to the frequency band of interest. Once obtained the amplitude of a given band in each epoch, the "p-episode" method creates thresholds based on the standard deviation over the median amplitude of every epoch. To determine the best threshold for each child, the number of bursts found in each segment was correlated with the mean amplitude of that epoch using Spearman's rank correlation. The selected threshold was the one that maximized the correlation between the number of bursts and the amplitude of the epoch. Once we obtained the final threshold, it was applied to all epochs to detect the burst and extract their amplitude, duration, and average number of bursts per epoch.

RA3A. Results

To determine whether oscillatory activity presented burst and/or rhythmicity properties (i.e., lag coherence), we conducted a linear mixed model diving the sample in those channels with a peak detected by the *Spectparam* toolbox versus those that did not have a clear peak (within-subject variability) in the 6-mo. session. We selected this session because the infants had a larger percentage of electrodes without a peak. We also correlated the percentage of channels with an oscillatory peak with the remaining variables (burst amplitude, burst duration, number of bursts, and lagged coherence). We focused on burst properties in the alpha and theta bands. Furthermore, we explored lagged coherence up to the third and a half lag in the alpha band, but not in the other bands, as they did not display sustained activity (Fig. RA3A.1). In addition, in this section, we did not analyze the beta band because it does not exhibit a clear peak in the power spectrum. However, we studied the beta trajectory in burst properties.

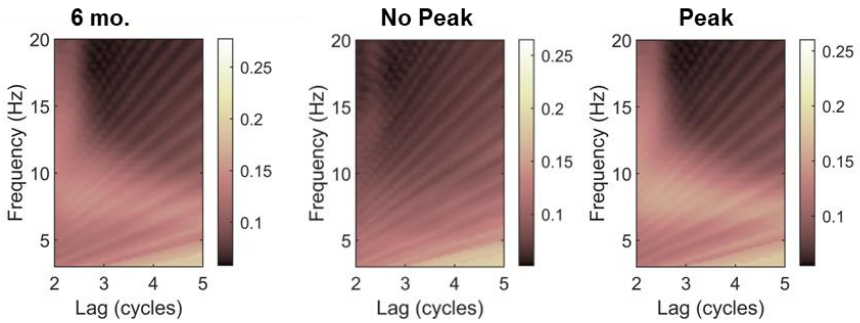

Fig. RA3A.1. Lagged coherence values at 6-mo. The figure represents the lagged coherence at 6-mo. sessions from 3 to 20 Hz in 2 to 5 lags on average and divided into electrodes that presented (vs. did not have) an alpha peak.

As a control measurement, we assessed whether the channels that presented oscillatory peaks differed in oscillatory power. In both alpha (β = 2.83, $t(65.92) = 19.21$, $p < .001$, 95% CI = [2.53 – 3.12]) and theta (β = 1.02, $t(114.53) = 15.66$, $p < .001$, 95% CI = [0.89 – 1.15]) bands, the oscillatory power had a higher amplitude when the toolbox detected a peak.

In the case of the alpha band, the channels that presented a clear peak had longer ($\beta = 0.02$, $t(82.45) = 5.60$, $p < .001$, 95% CI = [0.02 – 0.03]) and ampler bursts (β = 1.06, $t(79.00) = 10.95$, $p < .001$, 95% CI = [0.87 – 1.26]), but fewer bursts on average per epoch ($\beta = -0.13$, $t(92.87) = -2.59$, $p = .011$, 95% CI = [-0.23 – -0.03]). In addition, channels with a clear peak had larger lagged coherence ($\beta = 0.02$, $t(76.70) = 5.63$, $p < .001$, 95% CI = [0.01 – 0.02]; Fig. RA3A.2 and Fig. RA3A.3, and Table RA3A.1).

With respect to the theta band, the electrodes with an oscillatory peak did not differ in the number of bursts on average per epoch ($t < 1$), but the bursts had a larger amplitude ($\beta = 0.38$, $t(115.44) = 2.33$, $p = .021$, 95% CI = [0.06 – 0.70]) and were longer (β = 0.02, $t(115.63) = 5.18$, $p < .001$, 95% CI = [0.01 – 0.02]). See Table RA3A.1.

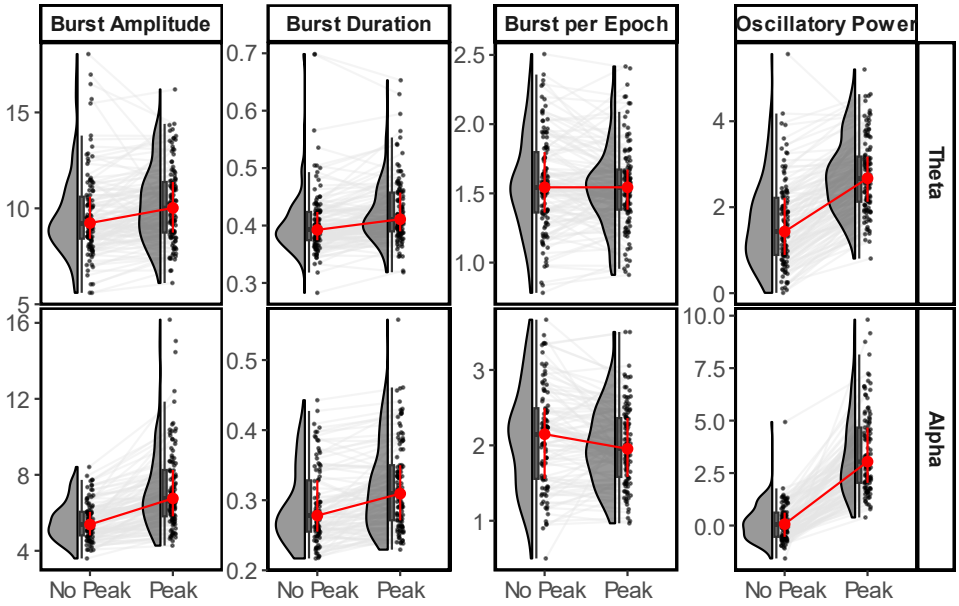

Fig. RA3A.2 Burst properties in the theta and alpha at 6-mo. The gray line represents the individual trajectory, whereas the red line represents the average trajectory.

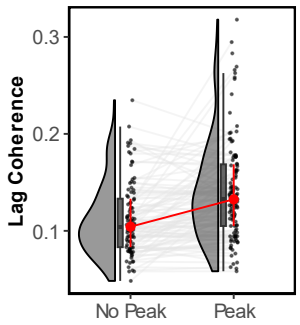

Fig. RA3A.3. Lagged coherence in the alpha band at 6-mo. The figure displays the lagged coherence divided by electrodes that had or did not have a clear peak. Grey lines correspond to the individual trajectory, while the red line stands for the average trajectory.

Table. RA3A.1

Descriptive statistics of burst and lagged coherence properties in electrodes with and without an oscillatory peak at 6-mo.

Band	Sex	Osc. Power		Burst						LagCoh	
				Amplitude		*Number*		*Duration*			
		NP	P	NP	P	NP	P	NP	P	NP	P
Alpha	*F*	0.03 (1.13)	4.36 (2.73)	5.39 (1.58)	8.17 (3.49)	2.26 (1.31)	1.88 (1.04)	0.29 (0.08)	0.34 (0.11)	0.12 (0.06)	0.16 (0.09)
	M	0.04 (1.2)	3.88 (2.55)	5.23 (1.36)	7.37 (2.63)	2.23 (1.29)	2.02 (1.09)	0.28 (0.08)	0.32 (0.09)	0.1 (0.04)	0.14 (0.08)
Theta	*F*	1.31 (1.3)	2.87 (1.23)	9.37 (3.17)	10.47 (3.46)	1.56 (0.81)	1.51 (0.76)	0.4 (0.1)	0.43 (0.11)	0.13 (0.05)	0.13 (0.05)
	M	1.49 (1.26)	2.85 (1.23)	9.41 (2.96)	10.38 (3.29)	1.69 (0.83)	1.58 (0.76)	0.4 (0.1)	0.42 (0.11)	0.13 (0.05)	0.14 (0.06)

Note. The table displays the mean (standard deviation). F = Female, M = Male, Osc. = Oscillatory, NP = No peak, P = Peak, LagCoh = Lagged Coherence.

We explored the relationship between the burst properties, lagged coherence, and the presence (or absence) of a peak in the power spectrum. To this end, we first determined whether the oscillatory activity of theta and alpha bands could discern if a channel had an oscillatory peak over the power spectrum. We employed a binomial linear (5000 permutations) mixed model to assess the prediction of the presence (1) or absence (0) of a peak based on oscillatory power, including the participant as a random intercept. We divided the dataset into two sub-datasets: *a training dataset* (80% of the data) and *a testing dataset* (20% of the data) to determine the relationship and validity of the models. Given that the percentages of alpha and theta were superior to chance (i.e., 50% of the electrodes), we downsampled the datasets to contain the same number of electrodes with and without a peak.

Binominal models determined that alpha oscillatory power could be predicted accurately if an electrode had an oscillatory peak (M = .96, SD < .01; M_{AUC} = .89, SD_{AUC} < .01). This also occurred in the theta band, where the model accurately predicted the presence/absence of theta peaks (M_{ACC} = .86, SD_{ACC} = .01; M_{AUC} = .78, SD_{AUC} = .01). Therefore, we used oscillatory power as a proxy for the peak and tested both the spatial and within-participant relationships using Spearman's rank correlation.

Correlation analysis revealed that the larger the oscillatory power in the alpha band, the longer and larger the amplitude alpha burst, and the higher the values in the lagged coherence of the infants (r_s = [.57 – .92], p < .001), but they also displayed a lower number of bursts per epoch on average (r_s = -.33, p < .001, 95% CI = [-.45 – -.11]). Regarding the theta band, infants with more oscillatory power also had a greater amplitude in the bursts and an increased duration (r_s = [.20, .68], ps < .05), but no other significant correlations (see Table RA3A.2).

Regarding the spatial distribution (Fig. RA3A.4, and Table RA3A.2), alpha oscillatory power was positively related to the amplitude of the signal, burst duration, and lagged coherence values (r_s = [.52 – .62], all ps < .001) but negatively related to the number of bursts per epoch (r_s = -.34, p < .001). In the case of the theta band, oscillatory power was positively related to burst amplitude (r_s = .71, p < .001) and duration (r_s = .6, p < .091), but not to the number of bursts per epoch on average (r_s = -.08, p > .05).

Table RA3A.2

Correlations between individual values of oscillatory power and lagged coherence and burst properties in the alpha and theta bands.

	Band	Bursts			Lagged Coherence
		Amp.	*Duration*	*Number*	
Within Participant	*Theta*	0.69*** [0.65 - 0.72]	0.22* [0.16 - 0.28]	-0.03 [-0.09 - 0.04]	-
	Alpha	0.84*** [0.82 - 0.86]	0.58*** [0.54 - 0.62]	-0.33*** [-0.38 - - 0.27]	0.65*** [0.61 - 0.69]
Spatial Correlation	*Theta*	0.71*** [0.67 - 0.74]	0.49*** [0.44 - 0.54]	-0.08 [-0.15 - - 0.02]	-
	Alpha	0.52*** [0.47 - 0.57]	0.62*** [0.58 - 0.66]	-0.34*** [-0.39 - - 0.28]	0.61*** [0.56 - 0.65]

Note. The table displays the Spearman's rank correlation [95% CI] coefficient between the lagged coherence/burst properties and oscillatory power. Confidence intervals were computed using 1000 bootstrap replicates.

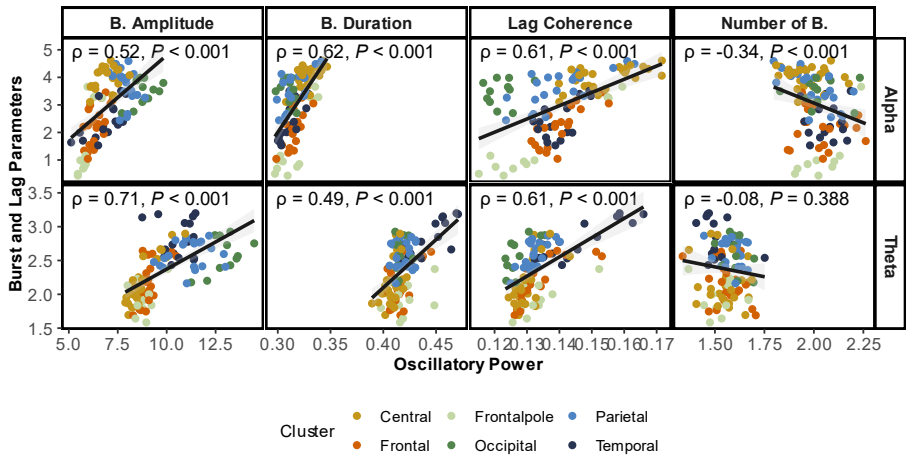

Fig. RA3A.4. Spatial correlation between oscillatory power and burst and rhythmic properties at 6-mo. The figure displays the correlation between the alpha and theta band oscillatory power and burst and lagged coherence. Each dot represents an electrode, and its color represents the cluster to which it belongs.

Finally, we evaluated the development of these variables by conducting a linear mixed model for bust properties and lagged coherence (only in the alpha band). The descriptive statistics of the development of these parameters are presented in Table RA3A.3 and RA3A.4.

Theta band

The theta band (Fig. RA3A5), burst amplitude (marginal r^2 = .34, conditional r^2 = .73) increased between the sessions with a negative quadratic effect (time: β = 2.38, t(669.91) = 7.84, p < .001, 95% CI = [1.78 – 2.97]; time squared: β = -1, t(678.10) = -8.97, p < .001, 95% CI = [-1.2 – -0.78]). The frontal cluster had a larger increase than the central area (β = 0.68, t(691.92) = 4.03, p < .001, 95% CI = [0.32 – 0.93]), but no other interactions were significant (all ts < 2). The occipital cluster had a larger amplitude than the other clusters (all zs > 6.67, all ps < .001), while the parietal cluster had a higher amplitude than the central and frontal areas (all zs > 11.69, all ps < .001), and the frontal cluster displayed ampler bursts than the central area cluster (z = 6.67, p < .001).

The model exploring the duration of theta bursts (marginal r^2 = .02, conditional r^2 = .57) showed that the duration of theta bursts decreased over time (β = -0.01, t(44.99) = -2.47, p = .017, 95% CI = [-0.02 – 0.00]). In contrast, the average number of bursts per epoch included time (marginal r^2 = .00, conditional r^2 = .38), but it was not significant (t < 1).

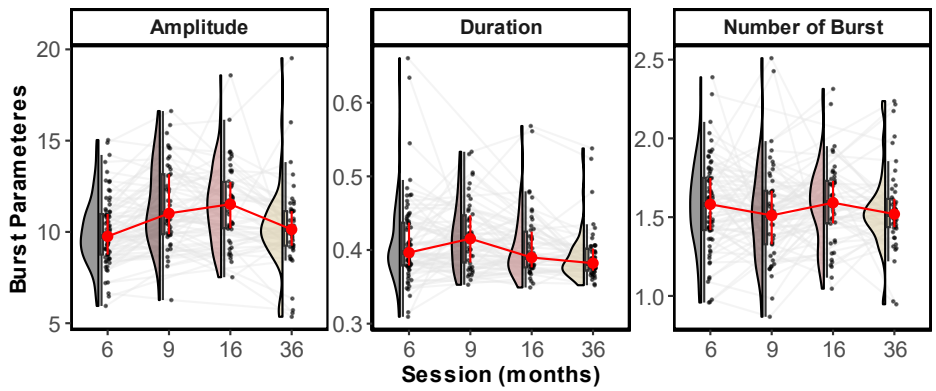

Fig. RA3A.5. Burst property development in theta band. The figure displays the individual values of amplitude, duration (milliseconds), and number of bursts (avg. per epoch) per session. The gray lines represent the individual trajectories, and the red line represents the average trajectory.

Alpha band

In relation to the alpha band, lagged coherence (marginal r^2 = .05, conditional r^2 = .79) increased between sessions but with a reduction in the growth rate in later months (time: β = 0.06, t(223.95) = 6.16, p < .001, 95% CI = [0.04 – 0.08]; time squared: β = -0.02, t(628.86) = -6.49, p < .001, 95% CI = [-0.03 – -0.02]). The frontal cluster had less lagged coherence than the central cluster (z = -5.64, p < .001), but it did not differ in relation to the parietal and occipital clusters (all z < 2.53, all ps > .06). The central cluster had a larger lagged coherence than the parietal and occipital clusters (all zs > 3.11, all ps < .01), and the lagged coherence was higher in the parietal area than in the occipital area (z = 4.72, p < .001). See Fig. RA3A.6.

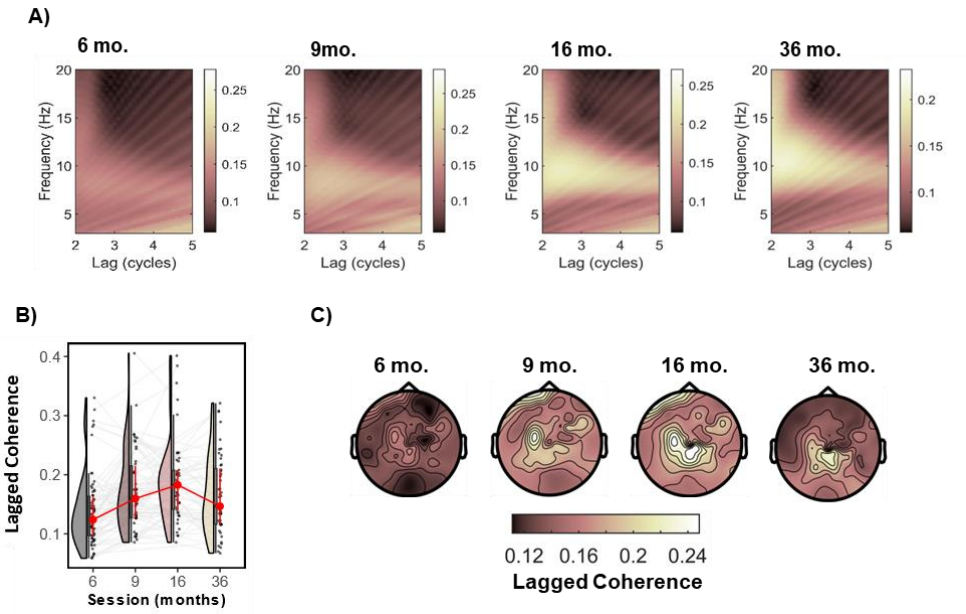

Fig. RA3A.6. Lagged coherence development. (A) Lagged coherence development over the average of clusters. (B) The development of alpha-lagged coherence (avg. Three-and-a-half cycles). The gray lines represent the individual trajectories, and the red line represents the average trajectories. (C). Topological development of lagged coherence (three-and-a-half cycles) in the alpha band.

Table RA3A.3

Alpha lagged coherence development.

Sex	6mo.	9mo.	16mo.	36mo.
Female	0.15 (0.09)	0.18 (0.1)	0.2 (0.1)	0.18 (0.09)
Male	0.12 (0.07)	0.17 (0.09)	0.18 (0.09)	0.16 (0.09)

Note. The table displays the mean (standard deviation) of the average values over three lags and all clusters included in the analysis.

Alpha (Fig. RA3A.7) burst amplitude (marginal r^2 = .24, conditional r^2 = .79) increased between 6 and 36 months of life (time: β = 4.70, t(313.63) = 12.49, p < .001, 95% CI = [3.96 – 5.44]) but slowed down in later months (time squared: β = -1.61, t(689.88) = -12.38, p < .001, 95% CI = [-1.87, -1.36]). In addition, the frontal (β = 0.45, t(650.94) = 2.81, p = .003, 95% CI = [0.14 – 0.77]) and occipital (β = 0.36, t(650.94) = 2.25, p = .025, 95% CI = [0.05 – 0.68]) areas increased the burst amplitude change in comparison to the central cluster, but the parietal area did not differ (t < 2). Regarding the area effect, the frontal area had a lower burst amplitude than the rest of the clusters (*all* zs < -3.49, all ps < .001), while the occipital area had a larger burst amplitude (*all* zs > 10.96, all ps < .001). Furthermore, the parietal area had a greater amplitude than the central cluster (z = 9.87, p < .001).

When it comes to burst duration (marginal r^2 = .08, conditional r^2 = .71), the duration of the burst decreased over time (time: β = -0.04, t(198.07) = -4.93, p < .001, 95% CI = [-0.06 – -0.02]), slowing down this trajectory over the sessions (time squared: β = 0.01, t(405.37) = 2.97, p = .003, 95% CI = [0.00 – 0.01]). The frontal cluster had a shorter alpha burst than the central and parietal clusters (all zs < -3.55, all ps < .001) but did not differ when compared to the occipital cluster (z < 2). The central area had a larger burst than the occipital area (z = 4.41, p < .001) with no differences from the parietal area (z = 2.32, p = .09). Finally, the parietal and occipital areas did not vary (z = 2.09, p = .16). The average number of bursts per epoch in the alpha band (marginal r^2 = .03, conditional r^2 = .54) increased during this period (time: β = 0.29, t(455.60) = 3.56, p < .001, 95% CI = [0.14 – 0.44]), with a negative quadratic effect (time squared: β = -0.08, t(580.31) = -2.63, p < .008, 95% CI = [-0.13 – -0.02]).

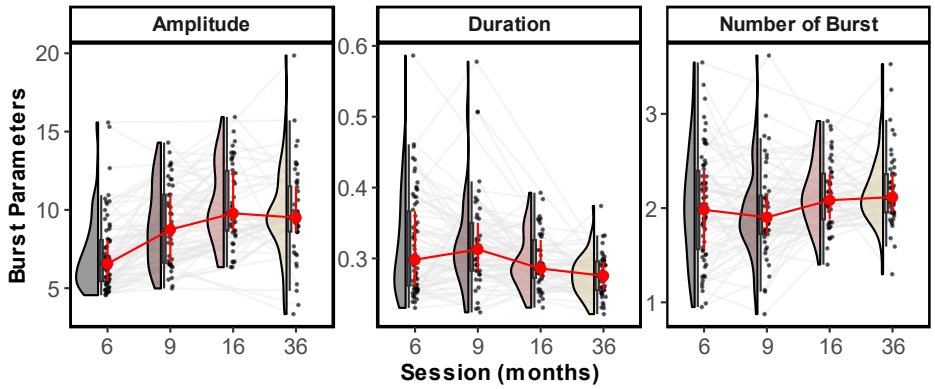

Fig. RA3A.7. Burst property development in alpha band. The figure displays the individual values of amplitude, duration (milliseconds), and number of bursts (avg. per epoch) per session. The gray lines represent the individual trajectories, and the red line represents the average trajectory.

Beta band

As beta band activity is usually transient, we only analyzed the amplitude of the burst. The amplitude of the beta burst (marginal r^2 = .46, conditional r^2 = .77) increased between sessions (time: β = 1.77, t(636.72) = 14.22, p < .001, 95% CI = [1.53 – 2.01]), reducing its change over time (time squared: β = -0.59, t(696.29) = -12.83, p < .001, 95% CI = [-0.68 – -0.50]). All clusters had larger increases than the central area (β = [.27–.44], t(703.14) = [4.27 – 4.36], p < .001, 95% CI = [0.14 – 0.56]. In addition, the central cluster displayed a lower amplitude than the rest of the areas (all zs < − 16.44, all ps < .001), while the occipital cluster had a larger amplitude than the other clusters (all zs > 11.93, all ps < .001). There was no difference between the parietal and frontal clusters (z = 2.08, p = .16).

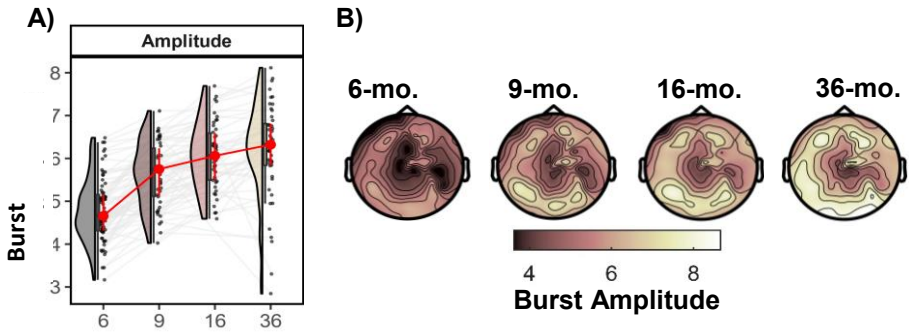

Fig. RA3A.8. Burst amplitude development in the beta band. (A) Mean trajectory of the burst amplitude. The gray lines represent individual trajectories, and the red line represents the average trajectory. (B) Topological development of the beta burst amplitude.

Table RA3A.4

Descriptive statistics of burst properties in each session and frequency band.

Session	Sex	Theta			Alpha			Beta
		Amp.	*NB*	*Dur*	*Amp.*	*NB*	*Dur*	*Amp.*
6-mo.	*F*	9.87 (3.39)	1.54 (0.79)	0.41 (0.1)	7.62 (3.37)	1.93 (1.08)	0.34 (0.11)	0.08 (0.02)
	M	10.3 (3.12)	1.61 (0.78)	0.41 (0.11)	6.66 (2.45)	2.13 (1.21)	0.3 (0.09)	0.08 (0.02)
9-mo.	*F*	11.26 (3.58)	1.52 (0.76)	0.42 (0.1)	9.39 (3.36)	1.93 (1.01)	0.33 (0.1)	0.08 (0.02)
	M	11.75 (3.73)	1.54 (0.77)	0.42 (0.11)	8.72 (3.56)	2 (1.15)	0.32 (0.1)	0.09 (0.02)
16-mo.	*F*	11.25 (3.44)	1.61 (0.8)	0.4 (0.1)	10.71 (3.69)	2.13 (1.08)	0.29 (0.08)	0.08 (0.02)
	M	11.95 (3.8)	1.56 (0.75)	0.41 (0.1)	10.01 (3.64)	2.17 (1.06)	0.3 (0.08)	0.08 (0.02)
36-mo.	*F*	10.21 (3.82)	1.59 (0.79)	0.39 (0.1)	9.8 (3.68)	2.28 (1.19)	0.28 (0.06)	0.08 (0.02)
	M	10.33 (3.12)	1.51 (0.67)	0.39 (0.08)	9.87 (3.98)	2.11 (0.94)	0.28 (0.06)	0.08 (0.01)

Note. F = Female, M = Male, Amp = Amp. = Amplitude. NB = Number of bursts, Dur. = Duration. The table shows the mean (standard deviation) per session and sex.

RA3A.3 Discussion

In this appendix, we aimed to explore the distinction between rhythmic and phasic oscillatory activity in the theta, beta, and alpha bands. We explored the rhythmicity of the signal with lagged coherence and its burst properties. In general, our results found that only alpha was rhythmic, and that its rhythmicity gradually appeared with age. Other frequency bands did not present a clear pattern of rhythmic activity but changed the burst properties over time.

The maturation processes underlying the oscillatory changes vary depending on the frequency band. At 6-mo., electrodes that had a peak, either in alpha or theta, had larger burst amplitudes and longer burst durations. However, only the alpha band was self-predictable over time, which was lower in channels that did not have a peak. This suggests the presence of sustained activity in the alpha band in infants as young as 6-mo. Importantly, the spatial distribution of oscillatory alpha and lagged coherence reinforced the co-occurrence of these phenomena, as the topology differed. This is probably due to two mechanisms involved in the manifestation of alpha power, one sustained over the central and parietal electrodes and one tonic over the rest of the areas.

Finally, the developmental trajectories of burst and lagged coherence coincided with the oscillatory power in the alpha band, but the theta and beta bands differed. That is, the lagged coherence and burst amplitude increased in the alpha band, while the theta and beta burst amplitudes increased over time; however, oscillatory activity did not vary or was reduced. The main difference compared to alpha is that those bursts were less present and had no sustained activity, according to the lagged coherence graphics. Therefore, even after removing the aperiodic background, the power spectrum may not be able to extract the underlying oscillatory activity of the theta and beta bands. It should be noted that we evaluated the duration (in milliseconds), but we did not adjust for the peak frequency. As shown in chapter 3A, the peak frequency in both theta and alpha increases with age. Thus, it is possible that the reduction in burst duration is an artifact caused by the changing properties.

Appendix of Chapter 3A

Several authors have claimed the relevance of considering the signal non-stationary to unveil oscillatory activity (e.g., Cole and Voytek, 2017). There are several mechanisms that might cause the appearance of a peak in the power spectrum, including increasing the burst amplitude, burst duration, and number of bursts per epoch (Zich et al., 2020). Thus, any of these parameters can explain the appearance (versus absence) of the peak over the power spectrum. In the case of alpha, we found that its oscillatory power relies on rhythmicity and burst activity, which is consistent with the development of alpha burst and the presence of alpha rhythm by 12 months of life (Rayson et al., 2002; Schaworonkow and Voytek, 2021). In addition, our results are consistent with those of Rayson et al. (2022), who showed that beta has burst activity independent of the presence of a peak in the power spectrum, indicating that more fine-grained approaches are needed to capture oscillatory activity, as has been seen previously in adults.

Appendix of Chapter 3B

Table A3B.1

Socio-economic information of the sample included in development of functional networks analysis.

Sex	Education		Occupation		I2N	SES
	Mother	*Father*	*Mother*	*Father*		
Female	4.59	3.83	4.51	5.46	1.44	0.26
	(1.54)	(1.76)	(3.39)	(2.67)	(0.73)	(0.7)
Male	4.43	4.06	3.81	4.86	1.37	0.1
	(1.4)	(1.75)	(3.27)	(2.84)	(0.77)	(0.72)

Note. The descriptives were extracted from the first session, as we found a large stability in the parameters and the session with the most answered questionnaires. I2N = Income to needs ratio; SES = Socioeconomic Status Index.

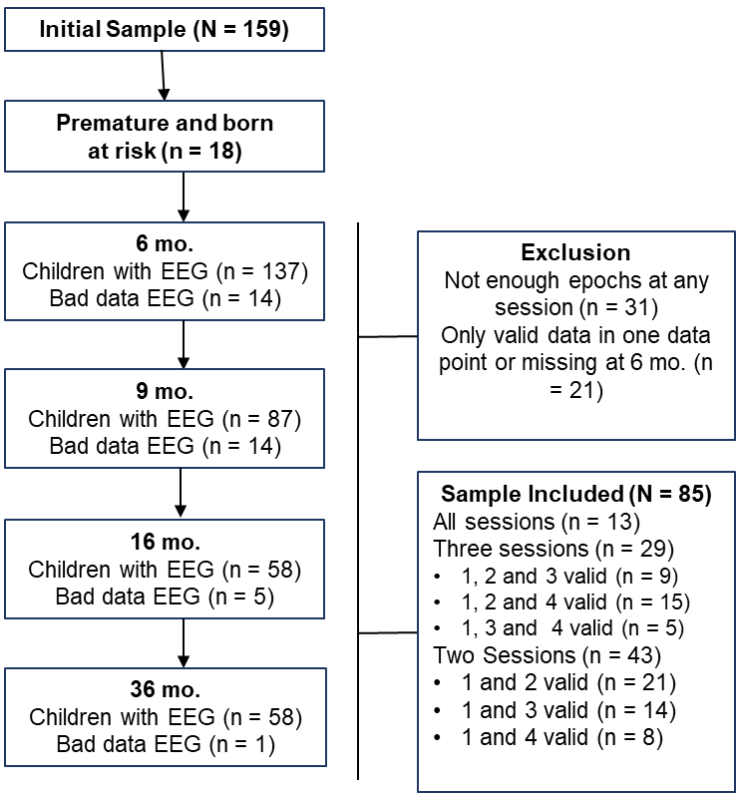

Fig. A3B.1. Diagram of participants included in the longitudinal analysis exploring network development.

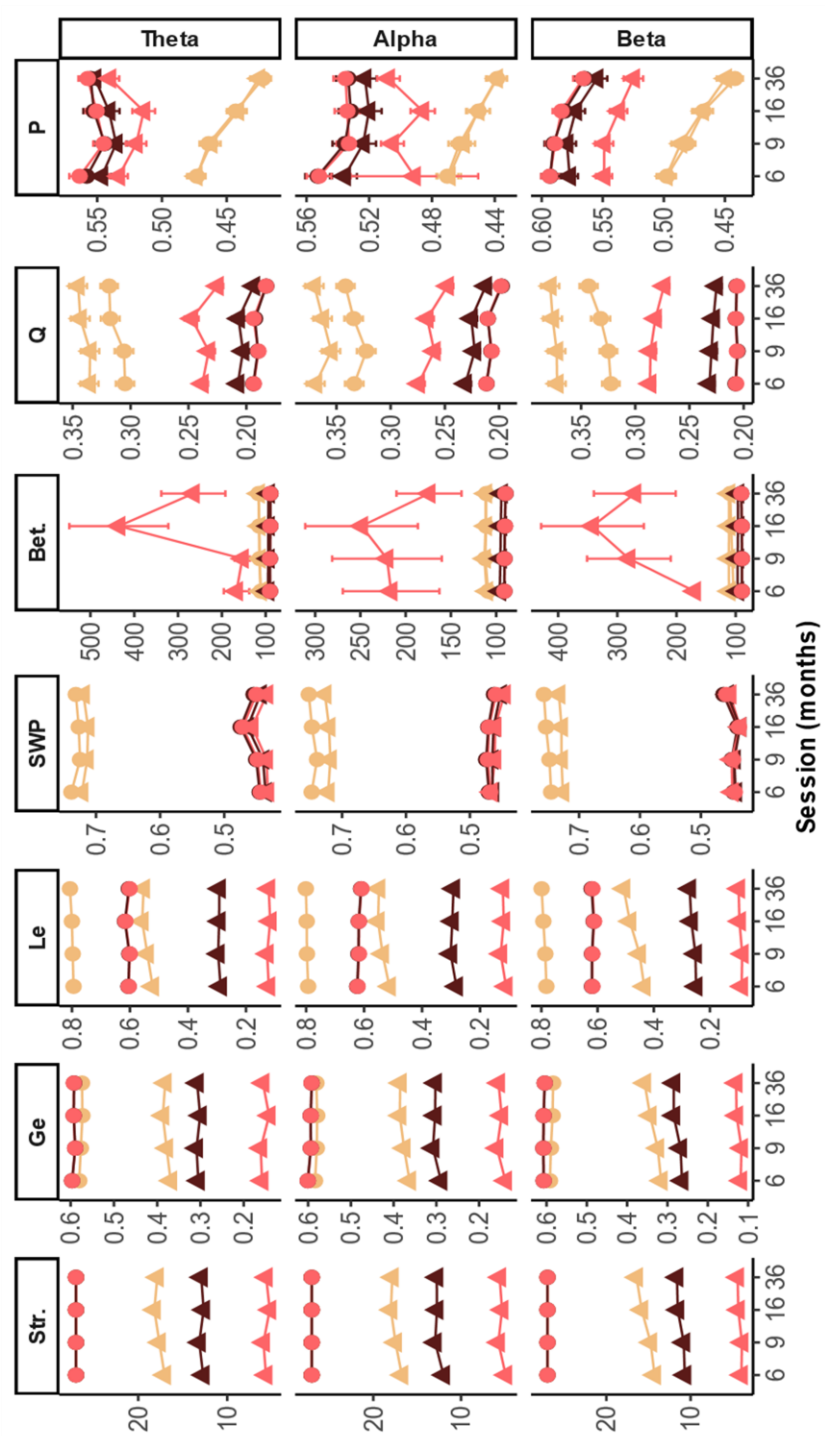

Fig. A3B.2. Descriptive representation of multiverse network trajectories. The figure displays the strength (Str.) of the top connections and their topological properties. Ge = Global Efficiency, Le = Local Efficiency, Bet. = Betweenness centrality, Q = Modularity, P = Participation coefficient. It shows the mean per age, band, connectivity measure, and edge type. The error bars correspond to the standard error.

Table A3B.2.

Descriptive statistics of the iCoh weighted (density: .25) network for each session and band. It displays the mean (SD) for global efficiency (Geff), local efficiency (Leff), and betweenness centrality (max. Centrality), and small-world propensity score (SPW).

	Theta				Alpha				Beta			
	6-mo.	*9-mo.*	*16-mo.*	*36-mo.*	*6-mo.*	*9-mo.*	*16-mo.*	*36-mo.*	*6-mo.*	*9-mo.*	*16-mo.*	*36-mo*
Geff.	0.37 (0.02)	0.38 (0.02)	0.39 (0.02)	0.39 (0.02)	0.37 (0.02)	0.38 (0.02)	0.39 (0.02)	0.39 (0.02)	0.32 (0.02)	0.33 (0.02)	0.35 (0.02)	0.36 (0.02)
Leff.	0.52 (0.04)	0.54 (0.04)	0.56 (0.04)	0.55 (0.03)	0.51 (0.04)	0.53 (0.03)	0.55 (0.04)	0.55 (0.04)	0.43 (0.04)	0.44 (0.04)	0.48 (0.04)	0.50 (0.04)
Bet.	123.05 (6.3)	130.44 (7.92)	130.09 (8.72)	151.85 (8.72)	118.88 (4.67)	122.37 (5.78)	130.33 (7.36)	144.7 (8.12)	114.9 (4.29)	112.66 (4.29)	121.76 (5.9)	141.16 (6.88)
SWP	0.72 (0.02)	0.71 (0.03)	0.71 (0.03)	0.72 (0.04)	0.72 (0.01)	0.72 (0.02)	0.72 (0.02)	0.73 (0.03)	0.73 (0.02)	0.73 (0.02)	0.73 (0.02)	0.73 (0.03)

Table A3B.3.

Descriptive statistics of the iCoh weighted (density: .25) network for each session, band, and sex. It displays the mean (SD) for Newman's Q modularity (Q) and the participation coefficient (P).

	Theta				Alpha				Beta			
	6-mo.	*9-mo..*	*16-mo.*	*36-mo.*	*6-mo.*	*9-mo.*	*16-mo.*	*36-mo.*	*6-mo.*	*9-mo.*	*16-mo.*	*36-mo.*
Q	0.32 (0.03)	0.32 (0.03)	0.33 (0.03)	0.33 (0.03)	0.35 (0.02)	0.34 (0.03)	0.34 (0.03)	0.35 (0.04)	0.35 (0.02)	0.35 (0.02)	0.36 (0.03)	0.36 (0.03)
P	0.49 (0.05)	0.48 (0.04)	0.46 (0.05)	0.43 (0.05)	0.49 (0.04)	0.48 (0.04)	0.48 (0.04)	0.46 (0.05)	0.52 (0.04)	0.51 (0.04)	0.49 (0.04)	0.47 (0.05)

Table A3B.4

Within-participant spatial stability in the functional networks' properties.

	Band	6- to 9-mo.		9- to 16-mo.		16- to 36-mo.	
		r_s	%	r_s	%	r_s	%
Bet	*Alpha*	0.2 (0.11) [-0.02 - 0.42]	0.57	0.22 (0.13) [-0.01 - 0.49]	0.62	0.17 (0.11) [-0.07 - 0.34]	0.42
	Beta	0.17 (0.11) [-0.07 - 0.46]	0.46	0.17 (0.11) [-0.1 - 0.39]	0.45	0.15 (0.09) [-0.06 - 0.35]	0.33
	Theta	0.21 (0.13) [-0.07 - 0.49]	0.6	0.24 (0.14) [-0.04 - 0.58]	0.66	0.13 (0.12) [-0.05 - 0.37]	0.29
Leff	*Alpha*	0.3 (0.16) [-0.09 - 0.64]	0.76	0.33 (0.15) [-0.06 - 0.62]	0.83	0.22 (0.15) [-0.01 - 0.53]	0.54
	Beta	0.27 (0.13) [-0.09 - 0.51]	0.7	0.27 (0.13) [0.09 - 0.54]	0.69	0.16 (0.12) [-0.07 - 0.39]	0.42
	Theta	0.32 (0.13) [0.04 - 0.59]	0.86	0.33 (0.15) [0 - 0.65]	0.83	0.19 (0.13) [-0.01 - 0.42]	0.42
P	*Alpha*	0.29 (0.18) [-0.15 - 0.63]	0.78	0.33 (0.19) [-0.13 - 0.69]	0.83	0.21 (0.18) [-0.12 - 0.45]	0.62
	Beta	0.33 (0.18) [-0.31 - 0.65]	0.79	0.37 (0.19) [0.03 - 0.7]	0.83	0.32 (0.2) [-0.18 - 0.59]	0.79
	Theta	0.34 (0.16) [-0.17 - 0.66]	0.84	0.28 (0.18) [-0.14 - 0.72]	0.76	0.21 (0.18) [-0.12 - 0.49]	0.54
L	*Alpha*	0.59 (0.16) [0.12 - 0.88]	0.98	0.65 (0.14) [0.33 - 0.87]	1	0.56 (0.11) [0.4 - 0.82]	1
	Beta	0.49 (0.17) [0.01 - 0.78]	0.97	0.52 (0.15) [0.1 - 0.77]	0.97	0.56 (0.18) [0.04 - 0.79]	0.96
	Theta	0.7 (0.15) [0.22 - 0.88]	1	0.71 (0.16) [0.19 - 0.9]	1	0.69 (0.09) [0.4 - 0.84]	1
Str.	*Alpha*	0.59 (0.15) [0.08 - 0.84]	0.98	0.65 (0.13) [0.35 - 0.86]	1	0.54 (0.12) [0.33 - 0.83]	1
	Beta	0.47 (0.16) [0.09 - 0.75]	0.97	0.48 (0.15) [0.1 - 0.74]	0.97	0.53 (0.16) [0.04 - 0.74]	0.96
	Theta	0.69 (0.14) [0.11 - 0.87]	0.98	0.7 (0.17) [0.09 - 0.89]	0.97	0.66 (0.08) [0.4 - 0.78]	1

Note. The table displays the average correlation (rs) found when the topological distribution of the graph network properties was correlated in different sessions individually and the percentage (%) of occasions where the correlation was significant. It shows the mean (SD) [min – max]. As the number of participants with valid session pair information varied, the number of correlations also varied. 6 to 9-mo. N = 63, 9 to 16-mo. N = 29, 16 to 36-mo. N = 24. Bet = Betweenness centrality. Leff = Local Efficiency. P = Participation coefficient. PL = Path length. Str. = Strength.

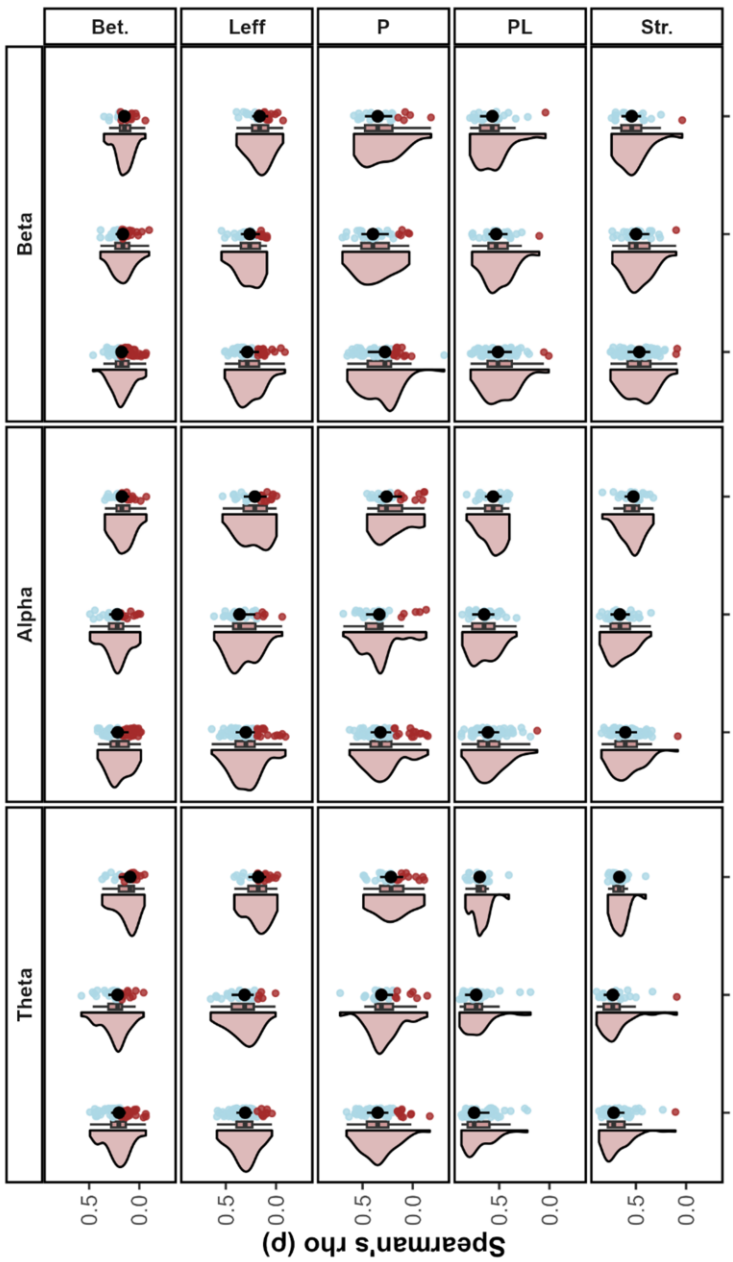

Fig. A3B.3. Distribution of Spearman's rho values in within-participant spatial stability for each variable, band, and pair of sessions. The figure displays Spearman's rank correlation values when the network measures of each electrode were individually correlated between sessions for each participant and divided by frequency bands. Colors represent p-values. Bet. = Betweenness, Leff = Local Efficiency, P = Participation Coefficient, PL = Path Length, Str. = Strength.

Table A3B.5

Within-participants stability in the functional network properties.

	Waves	Theta	Alpha	Beta
Geff	*6-mo. - 9-mo.*	0.21 [0.13 - 0.29]	0.34** [0.26 - 0.42]	0.3* [0.22 - 0.38]
	9-mo. – 16-mo.	0.14 [0 - 0.26]	0.33 [0.21 - 0.45]	0.15 [0.02 - 0.28]
	16-mo. – 36-mo.	0.3 [0.16 - 0.43]	0.46* [0.34 - 0.57]	0.38 [0.24 - 0.5]
Str.	*6-mo. - 9-mo.*	0.21 [0.12 - 0.29]	0.34** [0.26 - 0.41]	0.31* [0.23 - 0.38]
	9-mo. – 16-mo.	0.19 [0.06 - 0.31]	0.3 [0.18 - 0.42]	0.02 [-0.11 - 0.15]
	16-mo. – 36-mo.	0.28 [0.14 - 0.41]	0.45* [0.32 - 0.56]	0.4 [0.27 - 0.52]
Leff	*6-mo. - 9-mo.*	0.17 [0.09 - 0.26]	0.3* [0.22 - 0.38]	0.28* [0.2 - 0.36]
	9-mo. – 16-mo.	0.13 [0 - 0.25]	0.24 [0.11 - 0.36]	0.1 [-0.03 - 0.23]
	16-mo. – 36-mo.	0.27 [0.13 - 0.4]	0.42* [0.29 - 0.53]	0.38 [0.24 - 0.49]
Bet.	*6-mo. - 9-mo.*	0.28* [0.2 - 0.36]	0.21 [0.13 - 0.29]	0.13 [0.05 - 0.22]
	9-mo. – 16-mo.	-0.03 [-0.16 - 0.1]	0.37 [0.25 - 0.47]	0.14 [0.01 - 0.27]
	16-mo. – 36-mo.	0.11 [-0.04 - 0.25]	0.37 [0.24 - 0.49]	-0.03 [-0.18 - 0.11]
SWP	*6-mo. - 9-mo.*	0.23 [0.14 - 0.31]	0.04 [-0.05 - 0.12]	0.28* [0.2 - 0.36]
	9-mo. – 16-mo.	0.19 [0.06 - 0.32]	0.28 [0.16 - 0.4]	0.06 [-0.07 - 0.19]
	16-mo. – 36-mo.	-0.09 [-0.23 - 0.06]	0.49* [0.38 - 0.6]	0.18 [0.04 - 0.32]

Note. The table displays Spearman's rank correlation results [95% CI]. Bet = Betweenness centrality. Leff = Local Efficiency. SWP = Small-World Propensity score5tt; Geff = Global efficiency. The correlations had different sample: 6 to nine months. N = 63, 9 to 16-mo. N = 29, 16 to 36-mo. N = 24. The confidence intervals were computed with 1000 bootstraps. ** $p < .01$; * $p < .05$

Table A3B.5. Continuation

	Waves	Theta	Alpha	Beta
P	*6-mo. - 9-mo.*	0.12 [0.03 - 0.2]	-0.06 [-0.15 - 0.03]	0.03 [-0.06 - 0.11]
	9-mo. – 16-mo.	0.03 [-0.1 - 0.16]	0.16 [0.03 - 0.29]	0.2 [0.07 - 0.32]
	16-mo. – 36-mo.	-0.06 [-0.21 - 0.08]	0.23 [0.09 - 0.37]	-0.1 [-0.24 - 0.05]
Q	*6-mo. - 9-mo.*	0.36** [0.28 - 0.43]	-0.01 [-0.1 - 0.07]	0.32* [0.24 - 0.39]
	9-mo. – 16-mo.	0.14 [0.01 - 0.27]	0.33 [0.21 - 0.44]	0.18 [0.05 - 0.3]
	16-mo. – 36-mo.	0.02 [-0.13 - 0.16]	-0.18 [-0.32 - -0.04]	0.37 [0.24 - 0.49]

Note: The table displays Spearman's rank correlation results [95% CI]. P = Participation Coefficient. Q = Modularity. The correlations had different sample: 6 to nine months. N = 63, 9 to 16-mo. N = 29, 16 to 36-mo. N = 24. The confidence intervals were computed with 1000 bootstraps. ** $p < .01$; * $p < .05$

Appendix of Chapter 4

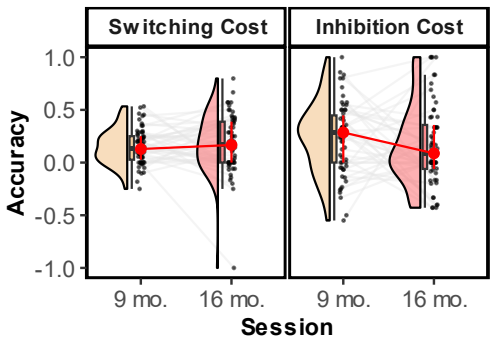

Fig. A4.1. Development of switching and inhibition cost indices in the ECITT. The figure displays individual values (dots), and the gray lines represent each participant's trajectory.

Table A4.1

Multiple linear regression models predicting Inhibitory Switch at 16-mo. based on performance at 9-mo.

	Overall Model			Regression Parameters			
Variable	*df*	r^2	*F*	*B (SE)*	*95% CI*	*β*	*z*
Model	3, 68	.09	10.97**	-	-	-	-
PNS	-	-	-	**0.94 (0.27)**	**[0.41 1.43]**	**.61**	**3.49*** **
PS	-	-	-	**-1.59 (0.59)**	**[-2.74 -.43]**	**-.48**	**-2.70****
IS	**-**	**-**	**-**	**0.41 (0.16)**	**[0.09 0.72]**	**.33**	**2.55***

Note. The regression model included FIML to account for missing data (N = 74). The beta and CI estimates were computed using 5000 bootstraps. PNS = Prepotent Non-Switch accuracy; PS = Prepotent Switch accuracy; IS = Inhibitory Switch accuracy; SE = Switching Effect index; IE = Inhibitory Effect index. ** p < .01.

Table A4.2

Spearman rho correlations between session age (in days) and performance on the ECITT task.

	PNS	PS	IS	SE	IE
9-mo.	.004 [-.25 .26]	-.03 [-.30 .22]	-.09 [-.33 .16]	.03 [-.23 .20]	.06 [-.18 .28]
16-mo.	.07 [-.21 .31]	.14 [-.12 .37]	.06 [-.19 .31]	-.10 [-.34 .15]	.04 [-.24 .30]

Note. The correlations were within age and included all infants with valid data at that age. The sample sizes were 60 (32 male) at 9 months and 60 (29 men) at 16 months. Confidence intervals were extracted from 5000 bootstrap replicates. *PNS* = Prepotent Non-Switch accuracy; PS = Prepotent Switch accuracy; IS = Inhibitory Switch accuracy; SE = Switching Effect index; IE = Inhibitory Effect index.

Table A4.3

Descriptive statistics of the Bee-Attentive Task after the commission of an error or a hit.

Sex	Go								NoGo			
	High				*Low*				*High*		*Low*	
	Acc.		*RT*		*Acc.*		*RT*					
	Error	Hit	Error	Hit	Error	Hit	Error	Hit	Error	Hit	Error	Hit
F	0.92	0.95	2156	2167.5	0.91	0.96	1917	1824	0.47	0.81	0.63	0.81
	(0.27)	(0.23)	(1281.49)	(1014.25)	(0.29)	(0.19)	(1221.64)	(964.78)	(0.5)	(0.39)	(0.49)	(0.39)
M	0.94	0.97	2139	1992	0.94	0.98	1959	1727	0.46	0.76	0.34	0.76
	(0.24)	(0.18)	(1228.56)	(1015.35)	(0.25)	(0.14)	(1306.04)	(964.64)	(0.5)	(0.43)	(0.48)	(0.43)

Note. F = Female, M = Male. The table displays the mean (standard deviation).

Table A4.4

Descriptive statistics of the accuracy in the Bee-Attentive Task per block and trial type.

Trial Type		Sex	Block Number					
			1	*2*	*3*	*4*	*5*	*6*
Go	*High*	F	0.93 (0.25)	0.96 (0.19)	0.95 (0.21)	0.91 (0.28)	0.94 (0.24)	0.96 (0.2)
		M	0.94 (0.24)	0.97 (0.17)	0.98 (0.12)	0.96 (0.21)	0.96 (0.19)	0.97 (0.17)
	Low	F	0.96 (0.19)	0.96 (0.19)	0.96 (0.18)	0.94 (0.24)	0.95 (0.22)	0.95 (0.21)
		M	0.97 (0.17)	0.98 (0.12)	0.97 (0.17)	0.99 (0.11)	0.96 (0.19)	0.97 (0.17)
NoGo	*High*	F	0.76 (0.43)	0.78 (0.42)	0.72 (0.45)	0.75 (0.43)	0.85 (0.36)	0.78 (0.42)
		M	0.68 (0.47)	0.63 (0.49)	0.68 (0.47)	0.75 (0.43)	0.75 (0.44)	0.86 (0.35)
	Low	F	0.76 (0.43)	0.78 (0.42)	0.71 (0.46)	0.87 (0.33)	0.91 (0.29)	0.82 (0.39)
		M	0.72 (0.45)	0.7 (0.46)	0.63 (0.49)	0.79 (0.41)	0.79 (0.41)	0.78 (0.42)

Note. F = Female, M = Male. The table displays the mean (standard deviation).

Table A4.5.

Descriptive statistics of the RT in the Bee-Attentive Task per block and trial type.

Load	Sex	Block Number					
		1	*2*	*3*	*4*	*5*	*6*
High	*F*	2537 (1114.36)	2196 (1187)	2034.5 (977.82)	1972.5 (963.62)	2178 (931.12)	2076 (961.63)
	M	2204.5 (1209.48)	1975.5 (1045.4)	2074 (1025.88)	2099 (890.49)	1834 (1041.61)	1781.5 (979.99)
Low	*F*	1969.5 (998.94)	1951 (1054.95)	1773 (1100.46)	1649 (825.49)	1788 (968.21)	1722.5 (935.63)
	M	1943 (1138.46)	1700 (870.36)	1687 (1000.38)	1819.5 (1089.87)	1579 (949.03)	1684 (890.84)

Note. F = Female, M = Male. The table displays the mean (standard deviation).

Table A4.6.

Descriptive statistics of ECITT and Bee Attentive tasks included in the correlation analysis.

Sex	*n*	ECITT (16-mo.)			Bee Attentive (36-mo.)					
		IS	PNS	PS	*ACC*		RT	RT SD	SAE	RT Cost
					Go	NoGo				
F	18	0.61 (0.35)	0.95 (0.09)	0.8 (0.26)	0.97 (0.03)	0.68 (0.3)	1902.94 (405.16)	922.98 (278.47)	433.76 (584.75)	285.03 (272.12)
M	25	0.53 (0.28)	0.92 (0.1)	0.63 (0.18)	0.95 (0.05)	0.75 (0.27)	2026.3 (621.8)	976.6 (294.13)	431.14 (760.74)	346.08 (301.85)

Note. F = Female, Male, IS = Inhibitory Switch, PNS = Prepotent Non-Switch, PS = Prepotent Switch, SAE = Slowing After Error. The table shows the mean values (standard deviation).

A4.1. ECITT original indices

To determine whether the results employed in this study differed when used the original variables previous ECITT studies, we analyzed the data computing the variables as Hendry et al. (2021). The indices were accuracy in the prepotent and inhibitory trials, without differentiating between the switching and non-switching positions. In addition, we compared the accuracy between switching and non-switching trials, regardless of whether the trial preceded the switch. Finally, we evaluated the Inhibitory Index, which was computed by subtracting the inhibitory trial hits from the prepotent trial hits and inverting punctuation.

SR1. Development and Stability

The analysis plan was identical to that used in the main text. In other words, a linear mixed model estimating missing data with the Type of Trial × Time to estimate the development and a linear mixed model regression between the performance to compute the stability of the measures of the ECITT. Descriptions of the performance and stability are depicted in Tables RA4.1 and RA4.2, respectively. In addition, refer to Figs. RA4.1 and RA4.2.

Regarding the development of inhibitory vs. prepotent trial accuracy (marginal R^2 = .35; conditional R^2 = .46), prepotent trials were more accurate than inhibitory trials in general (β = 0.32, $t(211) = 8.73$, $p < .001$, 95% CI = [0.25 – 0.40]) without a significant main effect of Time ($t < 2$) or an interaction effect ($t < 1$). However, when we differentiated between prepotent and inhibitory trials, we found no increment in the prepotent trials (marginal R^2 = .03; conditional R^2 = .22; $t < 2$) but a positive increase in inhibitory trial accuracy (marginal R^2 = .03; conditional R^2 = .49; β = 0.15, $t(104) = 2$, $p = .048$, 95% CI = [0.01 – 0.30]). Regarding switch accuracy (marginal R^2 = .45; conditional R^2 = .55), the trials that required location change had worse performance (β = -0.27, $t(211) = -9.97$, $p < .001$, 95% CI = [-0.32 – -0.22]), and older the children performed better in general (β = 0.11, $t(211) = 2.18$, $p = .030$, 95% CI = [0.01 – 0.20]), without a significant interaction ($t < 1$). Nevertheless, when we exploratorily tested the development separately, the non-switch trials increased the accuracy between sessions (marginal R^2 = .07; conditional R^2 = .12; β = 0.10, $t(105) = 2.94$, $p = .004$, 95% CI = [0.03 – 0.17]), but it was not

significant in the switch trials ($t < 2$). Finally, the inhibitory cost index did not vary over time ($t < 1$).

The stability between sessions was computed only in terms of accuracy in the switch, non-switch, and inhibitory trials, plus the inhibitory cost index, as the accuracy in the prepotent trial model did not converge. Accuracy in the switch (adj $R^2 = .16$; $\beta = 0.52$, $F(1,73) = 3.78$, $p < .001$, 95% CI = [0.28 – 0.88]) and inhibitory trials (adj $R^2 = .16$; $\beta = 0.49$, $F(1,73) = 3.49$, $p < .001$, 95% CI = [0.23 – 0.83]) at 9-mo. was a significant predictor of 16-mo. performance. This was not observed for other variables (all Fs < 1).

Table RA4.1.

Mean (standard deviation) performance on the ECITT task at 9 and 16 months of age using the original indices.

Session	Accuracy				IC
	Prpt.	*Inhb.*	*Switch*	*Non-Switch*	
9-mo.	0.83 (0.11)	0.50 (0.28)	0.59 (0.19)	0.86 (0.11)	-0.29 (0.42)
16-mo.	0.87 (0.11)	0.56 (0.30)	0.62 (0.22)	0.92 (0.10)	-0.30 (0.33)

The sample size included in the linear mixed model was the same as in the main text (74), considering the missing data. The table displays the mean (standard deviation) for direct accuracy and the computed indexes.

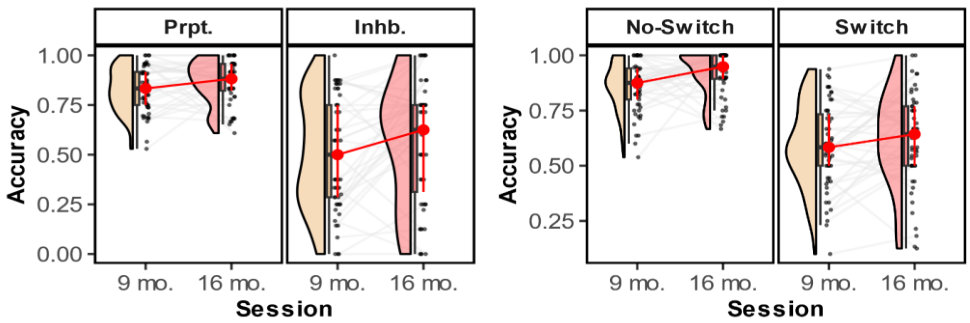

Fig. RA4.1. Development of ECITT performance based on the original indices. This figure shows age-related changes in the accuracy of the prepotent (Prpt.), and inhibitory (Inhb.) trials. Additionally, it shows the accuracy in the switch (vs. non-switch) trials. Each dot represents a participant, and the gray line indicates the individual trajectory.

Table RA4.2.

Linear regression models predicting the ECITT performance at 16-mo. based on 9-mo. results employing the original indices.

Variable	Overall Model			Regression Parameters			
	df	r^2	*F*	*B (SE)*	*95% CI*	*β*	*z*
Inhb.	**1, 73**	**0.24**	**9.02****	**0.53 (0.15)**	**[0.23 0.83]**	**0.48**	**3.49*****
Switch	**1, 73**	**0.27**	**9.87****	**0.58 (0.15)**	**[0.28 0.88]**	**0.52**	**3.78****
Non-Switch	1, 73	<0.01	<1	0.04 (0.15)	[-0.25 0.34]	0.05	0.27
IC	1, 73	<0.01	<1	-0.02 (0.13)	[-0.29 0.24]	-0.03	-0.16

Note. The regression model included FIML to account for missing data ($N = 74$). Inhb. = inhibitory trial accuracy, switch = switching trial accuracy, non-switch = non-switch trial accuracy, IC = inhibitory cost. Beta and CI estimates were computed using 5000 bootstraps. *** $p < .001$. ** $p < .01$.

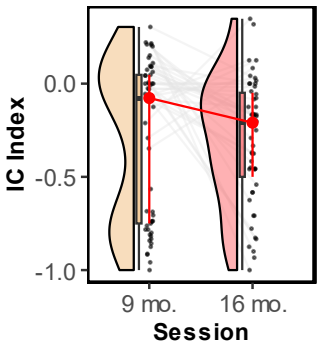

Fig. RA4.2. Inhibitory cost development according to the original index. Each dot represents a participant and gray lines represent individual trajectories.

Appendix of Chapter 5A

Table A5A.1

Descriptive statistics of the goodness of fit (R^2) and percentage of electrodes were included in the analysis.

Sessions		Sex	R^2			Electrodes Included %		
			F	*O*	*P*	*F*	*O*	*P*
Concurrent	*9-mo.*	*F*	99.11 (0.93)	99.71 (0.25)	99.58 (0.58)	0.97 (0.18)	1 (0)	0.99 (0.07)
		M	98.55 (1.19)	99.62 (0.36)	99.39 (0.75)	0.88 (0.33)	1 (0)	0.98 (0.13)
	16-mo.	*F*	99.02 (1.03)	99.66 (0.31)	99.59 (0.43)	0.98 (0.14)	1 (0)	1 (0)
		M	99.11 (0.96)	99.71 (0.2)	99.47 (0.67)	0.98 (0.14)	1 (0)	1 (0)
Longitudinal		*F*	98.87 (1.08)	99.63 (0.34)	99.41 (0.72)	0.91 (0.28)	1 (0)	0.98 (0.14)
		M	98.76 (1.1)	99.67 (0.29)	99.42 (0.72)	0.88 (0.32)	1 (0)	0.98 (0.13)

Note. As the values of R^2 were proximal to 1, we multiplied its value by 100 to obtain more detailed information. F = Female, M = Male. F = Frontal, O = Occipital, P = Parietal. Data are presented as mean (standard deviation).

Table A5A.2

Descriptives of the oscillatory and aperiodic EEG parameters of the participants included in the regression models predicting ECITT performance.

Session	N	Oscillatory Power		Peak Frequency (Hz)		Aperiodic Exponent
		Theta	*Alpha*	*Theta*	*Alpha*	
9-mo.	52	2.58 (1.72)	3.48 (2.82)	4.30 (0.48)	7.09 (0.79)	1.82 (0.26)
16-mo.	37	2.50 (1.44)	4.67 (2.87)	4.41 (0.42)	7.92 (0.63)	1.81 (0.23)

Note. The participants in the table are all infants who are included in the three regressions. The table displays the mean (SD) of the oscillatory power, peak frequency, and aperiodic exponent divided by the session.

Table A5A.3

Descriptives of the ECITT performance of the participants included in the regression models between the EEG and ECITT

Session	N	PS	PNS	IS
9-mo.	52	0.68 (0.24)	0.84 (0.12)	0.43 (0.27)
16-mo.	37	0.71 (0.23)	0.92 (0.1)	0.53 (0.33)

Note. The participants in the table are all infants who are included in the three regressions. The table shows the mean values (SD).

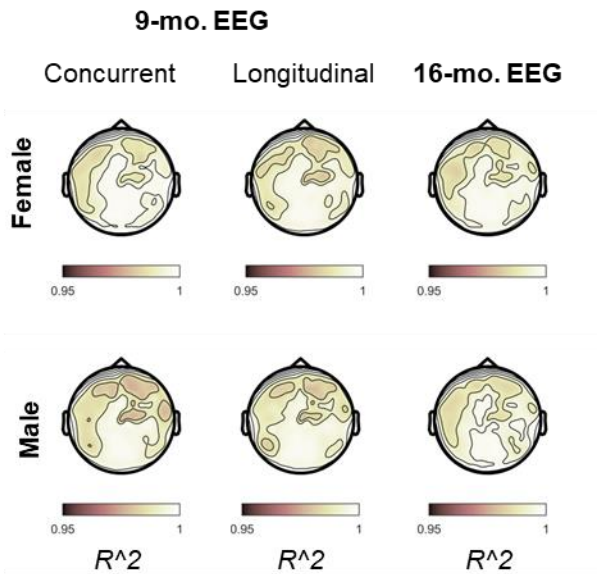

Fig. A5A.1. Topographical representation of the goodness of fit in the participants included in the analysis relating EEG and ECITT task. The figure shows R^2 provided by the *spectparam* toolbox after excluding the electrodes with poor fit ($R^2 < .95$).

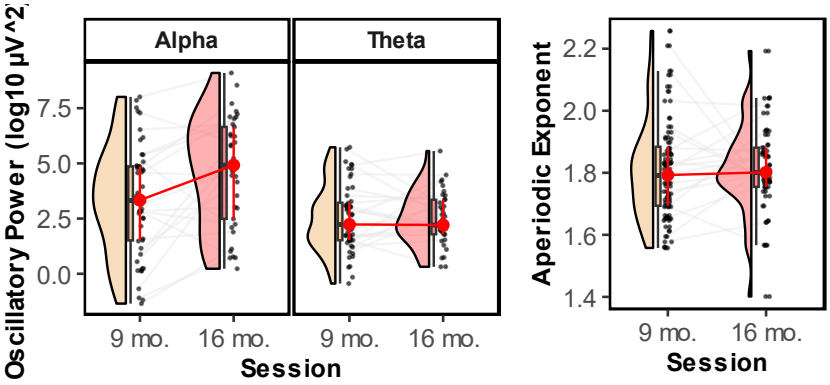

Fig. A5A.2. Descriptive figure of oscillatory and aperiodic parameters included in the regression analysis predicting ECITT performance. The figure displays the oscillatory power in the alpha and theta bands for each participant (dots) and its individual trajectory in case they had been included in the regression analysis in both sessions (gray line).

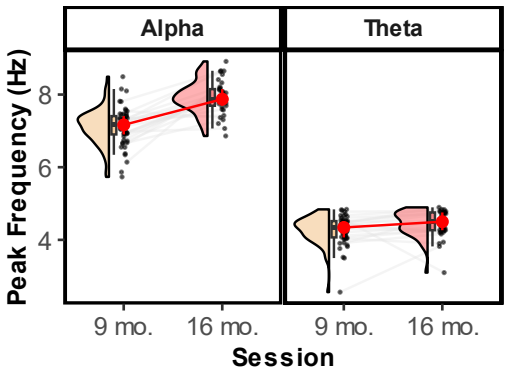

Fig. A5A.3. Descriptive figure of the peak frequency of alpha and theta bands included in the regression analysis predicting ECITT performance. The figure displays the peak frequency per band for each participant (dots) and its individual trajectory in case they had been included the regression analysis at both session (grey line).

Sex	Frontal	Occipital	Parietal
Female	99.36 (0.38)	99.65 (0.23)	99.54 (0.21)
Male	99.42 (0.42)	99.74 (0.17)	99.63 (0.15)

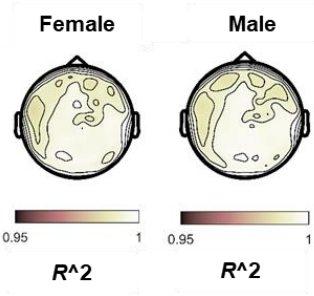

Fig. A5A.4. Topographical representation of the goodness of fit in the participants included in the analysis related to EEG and Bee-Attentive task. The figure shows the R^2 provided by the *Spectparam* toolbox after excluding the electrodes with poor fit ($R^2 < .95$). The table shows the average (standard deviation) per cluster.

Table A5A.4

Descriptive statistics of the oscillatory and aperiodic EEG parameters of the participants included in the regression models predicting Bee-Attentive performance at 36-mo.

		Variable	*M* (*SD*)
EEG	*Alpha*	Oscillatory Power	5.23 (2.8)
		Frequency	8.49 (0.47)
	Theta	Oscillatory Power	1.7 (1.01)
		Frequency	4.54 (0.31)
	-	Aperiodic Exponent	1.73 (0.13)
Bee-Attentive	*Acc.*	Go	0.95 (0.06)
		NoGo	0.73 (0.29)
	RT	Go	1935.94 (525.01)
		SD	932.67 (270.74)
		Cost	265.67 (285.03)

Appendix of Chapter 5B

	M (SD)
IS	0.49 (0.31)
PNS	0.91 (0.1)
PS	0.7 (0.24)

Table A5B.1
Descriptives of the ECITT performance at 16-mo. of the participants included in the PLS analysis.

Table A5B.2
Descriptives of the network parameters divided by cluster and frequency band of the participants included in the PLS predicting ECITT performance.

Band	**Session**	**Clustering**			**Path Length**		
		Fr.	*Fp.*	*P*	*Fr.*	*Fp.*	*P*
Theta	*6-mo.*	0.41 (0.04)	0.45 (0.07)	0.39 (0.04)	2.85 (0.23)	3.06 (0.37)	3.02 (0.18)
	9-mo.	0.42 (0.04)	0.45 (0.05)	0.4 (0.04)	2.76 (0.17)	2.88 (0.28)	2.92 (0.15)
	16-mo.	0.43 (0.04)	0.46 (0.06)	0.41 (0.05)	2.77 (0.18)	2.9 (0.28)	2.92 (0.15)
Alpha	*6-mo.*	0.41 (0.06)	0.44 (0.06)	0.36 (0.04)	2.95 (0.25)	3.11 (0.36)	3.12 (0.21)
	9-mo.	0.43 (0.04)	0.46 (0.06)	0.38 (0.04)	2.77 (0.2)	2.99 (0.33)	2.96 (0.16)
	16-mo.	0.42 (0.04)	0.45 (0.05)	0.38 (0.04)	2.81 (0.21)	2.97 (0.34)	2.96 (0.17)

Note. Fr. = Frontal, Fp. = Frontal pole, P = Parietal. The table below shows the mean (standard deviation)

		M (SD)
Accuracy	Go	0.96 (0.05)
	No Go	0.65 (0.32)
RT	Median	2235.66 (523.65)
	SD	959.9 (284.06)
	Cost	252.13 (317.8)

Table A5B.3
Descriptives of the Bee-Attentive performance at 36-mo. in the participants included in the PLS analysis.

Table A5B.4
Descriptives of network parameters divided by cluster and frequency band of the participants included in the PLS analysis predicting Bee-Attentive performance.

Band	**Session**	**Clustering**			**Path Length**		
		Fr.	*Fp.*	*P*	*Fr.*	*Fp.*	*P*
Theta	*6-mo.*	0.41 (0.04)	0.45 (0.08)	0.38 (0.04)	2.86 (0.21)	3.05 (0.34)	2.99 (0.19)
	9-mo.	0.42 (0.04)	0.45 (0.07)	0.4 (0.04)	2.75 (0.2)	2.94 (0.35)	2.93 (0.19)
	16-mo.	0.43 (0.04)	0.47 (0.05)	0.41 (0.04)	2.75 (0.16)	2.86 (0.25)	2.91 (0.16)
	36-mo.	0.43 (0.04)	0.46 (0.05)	0.41 (0.04)	2.73 (0.19)	2.87 (0.26)	2.94 (0.21)
Alpha	*6-mo.*	0.41 (0.05)	0.44 (0.05)	0.36 (0.04)	2.92 (0.24)	3.05 (0.31)	3.11 (0.21)
	9-mo.	0.43 (0.05)	0.48 (0.05)	0.38 (0.05)	2.8 (0.22)	2.99 (0.35)	2.98 (0.17)
	16-mo.	0.43 (0.04)	0.46 (0.06)	0.39 (0.04)	2.79 (0.18)	2.92 (0.24)	2.94 (0.15)
	36-mo.	0.42 (0.04)	0.45 (0.05)	0.39 (0.04)	2.77 (0.18)	2.89 (0.28)	2.9 (0.2)

Note. Fr. = Frontal, Fp. = Frontal pole, P = Parietal. The table below shows the mean values (standard deviations).

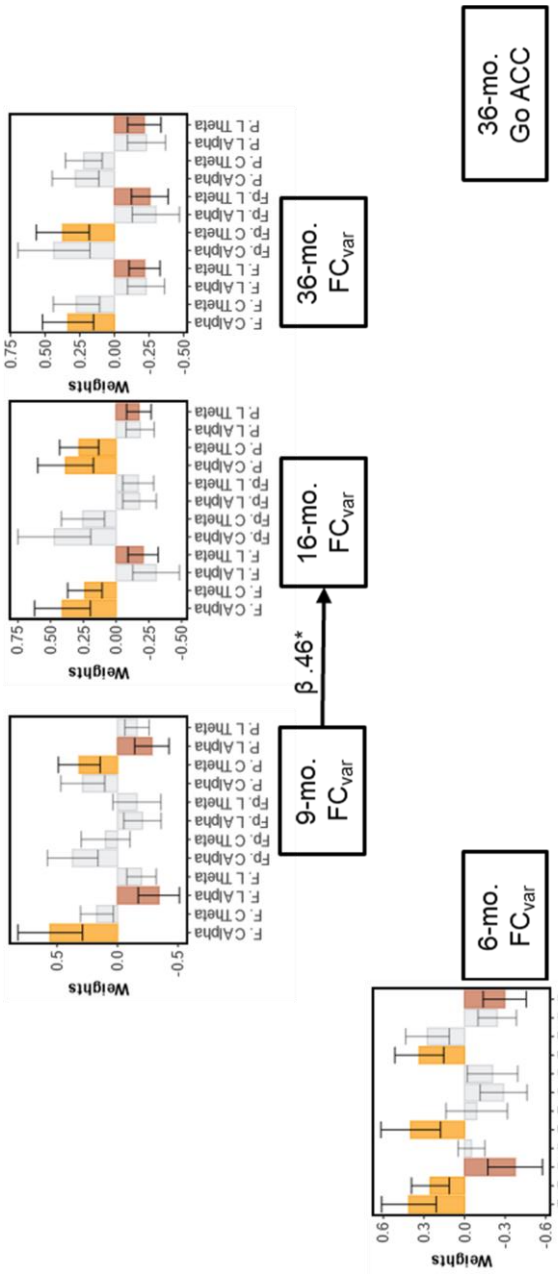

Fig. A5B.1. PLS analysis predicting Go Accuracy performance from functional network properties. The figure displays the significant path after permutation testing and indirect paths between Go Accuracy and FC_{var}. Colored weights stand for the reliable factor loadings (yellow = clustering, orange = path length), while gray represent non-reliable factor loadings. F = Frontal, Fp. = frontal pole, P = Parietal, L = Path Length, C = Clustering Coefficient. * $p < .05$.

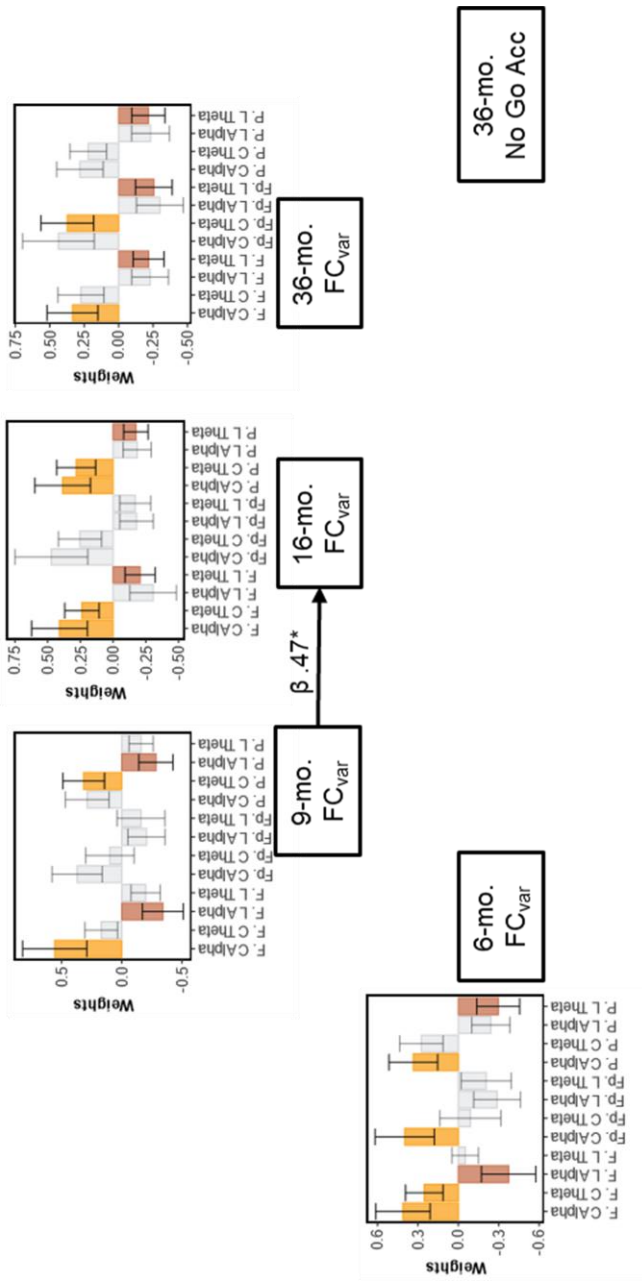

Fig. A5B.2. PLS analysis predicting No-Go Accuracy performance from functional network properties. The figure displays the significant path after permutation testing and indirect paths between No-Go Accuracy and FC_{var}. colored weights stand for the reliable factor loadings (yellow = clustering, orange = path length), while gray represent non-reliable factor loadings. F = Frontal, Fp. = frontal pole, P = Parietal, L = Path Length, C = Clustering Coefficient. * $p < .05$.

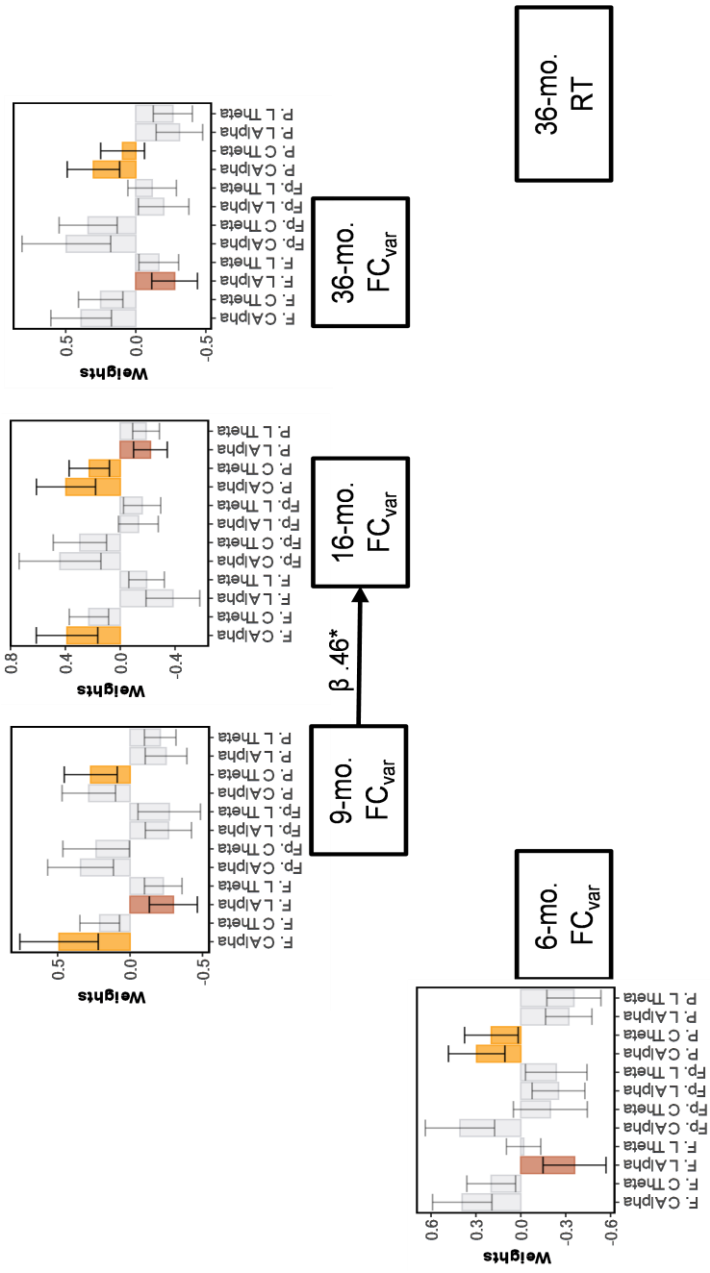

Fig. A5B.3. PLS analysis predicting median RT performance from functional network properties. The figure displays the significant path after permutation testing and indirect paths between median RT and FC_{var}. Colored weights stand for the reliable factor loadings (yellow = clustering, orange = path length), while gray represent non-reliable factor loadings. F = Frontal, Fp. = frontal pole, P = Parietal, L = Path Length, C = Clustering Coefficient. * $p < .05$.

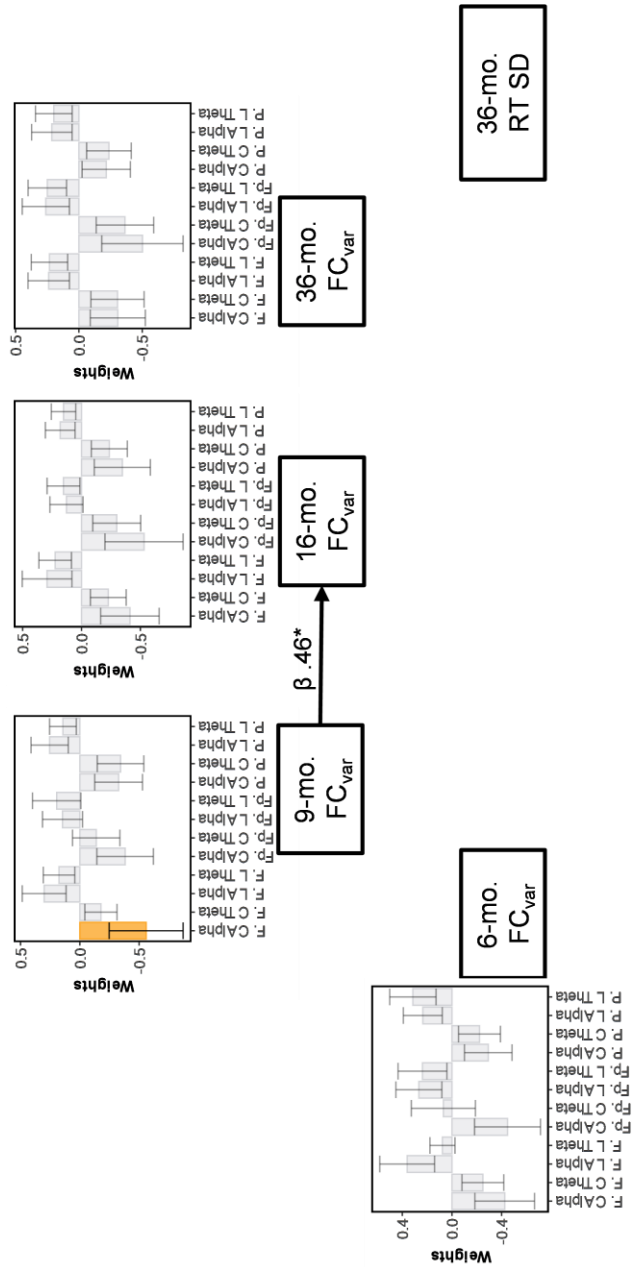

Fig. A5B.4. PLS analysis predicting RT SD performance from functional network properties. The figure displays the significant path after permutation testing and indirect paths between RT SD and FC$_{var}$. Colored weights stand for the reliable factor loadings (yellow = clustering, orange = path length), while gray represent non-reliable factor loadings. F = Frontal, Fp. = frontal pole, P = Parietal, L = Path Length, C = Clustering Coefficient. * $p < .05$.

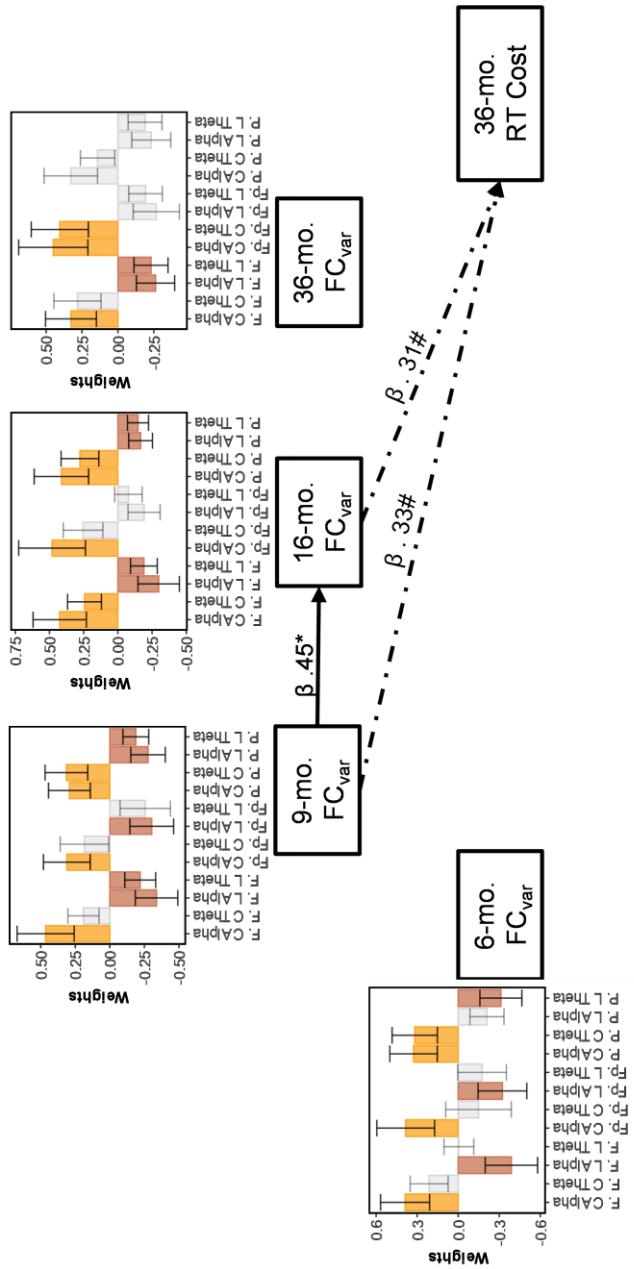

Fig. A5B.5. PLS analysis predicting RT cost from functional network properties. The figure displays the significant path after permutation testing and indirect paths between RT cost and FCvar. Colored weights stand for the reliable factor loadings (yellow = clustering, orange = path length), while gray represent non-reliable factor loadings. F = Frontal, Fp. = frontal pole, P = Parietal, L = Path Length, C = Clustering Coefficient. * p < .05, # p < .10.